

The conformal bootstrap: Theory, numerical techniques, and applications

David Poland

*Department of Physics, Yale University,
217 Prospect St., New Haven, Connecticut 06511, USA*

Slava Rychkov

*Institut des Hautes Études Scientifiques, Bures-sur-Yvette, France
and Laboratoire de physique théorique, Département de physique de l'ENS,
École normale supérieure, PSL University, Sorbonne Universités,
UPMC Univ. Paris 06, CNRS, 75005 Paris, France*

Alessandro Vichi

Institute of Physics, École Polytechnique Fédérale de Lausanne, Switzerland

 (published 11 January 2019)

Conformal field theories have been long known to describe the fascinating universal physics of scale invariant critical points. They describe continuous phase transitions in fluids, magnets, and numerous other materials, while at the same time sit at the heart of our modern understanding of quantum field theory. For decades it has been a dream to study these intricate strongly coupled theories nonperturbatively using symmetries and other consistency conditions. This idea, called the conformal bootstrap, saw some successes in two dimensions but it is only in the last ten years that it has been fully realized in three, four, and other dimensions of interest. This renaissance has been possible due to both significant analytical progress in understanding how to set up the bootstrap equations and the development of numerical techniques for finding or constraining their solutions. These developments have led to a number of groundbreaking results, including world-record determinations of critical exponents and correlation function coefficients in the Ising and $O(N)$ models in three dimensions. This article will review these exciting developments for newcomers to the bootstrap, giving an introduction to conformal field theories and the theory of conformal blocks, describing numerical techniques for the bootstrap based on convex optimization, and summarizing in detail their applications to fixed points in three and four dimensions with no or minimal supersymmetry.

DOI: [10.1103/RevModPhys.91.015002](https://doi.org/10.1103/RevModPhys.91.015002)

CONTENTS

I. Introduction	2	5. Rational approximation of conformal blocks and their derivatives	16
A. Outline	3	6. Shadow formalism	17
II. Conformal Bootstrap: Informal Overview	3	7. Spinning conformal blocks	18
A. Universality and the role of microscopic input	5	G. Global symmetry	19
III. Conformal Field Theory Techniques in d Dimensions	6	H. Conserved local currents	20
A. Conformal transformations	6	1. Stress tensor	20
B. Operators: Primaries and descendants	6	2. Global symmetry currents	21
C. Correlation functions	7	I. Crossing relations	21
1. 2pt functions	8	1. Explicit solutions to crossing	22
2. 3pt functions	8	IV. Numerical Methods	23
3. 4pt functions	9	A. Convex optimization and linear programming	23
4. Conformal frames	9	1. Continuous primal simplex algorithm	24
D. Operator product expansion	9	B. Semidefinite programming	25
E. Constraints from unitarity	10	1. Mixed correlators	25
1. Unitarity bounds	10	2. Polynomial approximations	26
2. OPE coefficients	11	C. Bounds and allowed regions	26
3. Averaged null energy condition	11	D. Spectrum extraction	27
F. Conformal blocks	12	1. Flow method	27
1. The Casimir equation	13	2. Truncation method	28
2. Radial expansion for conformal blocks	14	V. Applications in $d = 3$	28
3. Recursion relation from the Casimir equation	15	A. Bounds on critical versus multicritical behavior	29
4. Recursion relation from analytic structure	15	B. \mathbb{Z}_2 global symmetry	29

1. General results	29
2. Critical Ising model	31
3. Spectrum extraction and rearrangement	33
4. Why kink? Why island?	34
5. Non-Gaussianity	35
6. Boundary and defect bootstrap, nontrivial geometries, off criticality	35
C. $O(N)$ global symmetry	36
1. General results	36
2. Critical $O(N)$ model	37
3. $O(2)$ global symmetry	37
4. $O(3)$ global symmetry	38
D. CFTs with fermion operators	39
1. Models	39
2. General results	40
3. Gross-Neveu-Yukawa models	40
E. QED ₃	42
1. Monopole bootstrap for QED ₃	42
2. Bosonic QED ₃ and deconfined quantum critical points	44
3. Aside: Constraints on symmetry enhancement	45
4. Back to deconfined criticality: Is the transition second order?	45
F. Current and stress-tensor bootstrap	46
G. Future targets	49
1. Multifield Landau-Ginzburg models	49
2. Projective space models	49
3. Non-Abelian gauge and Chern-Simons matter theories	50
4. Other models	50
VI. Applications in $d = 4$	50
A. General results	50
B. Applications to the hierarchy problem	52
C. Constraints on the QCD ₄ conformal window	53
VII. Applications to Superconformal Theories	55
A. Theories with 4D $\mathcal{N} = 1$ supersymmetry	55
1. Bounds without global symmetries	56
2. Bounds with global symmetries	57
B. Theories with 3D $\mathcal{N} = 2$ supersymmetry	58
VIII. Applications to Nonunitary Models	59
IX. Other Applications	59
X. Outlook	61
Acknowledgments	62
Appendix: Embedding Formalism	62
References	63

I. INTRODUCTION

For most physical systems, the first step to qualitative understanding is to identify their characteristic scales (length, energy, etc.), through which everything else can be expressed via approximate dimensional analysis. However, there exist theories for which this familiar approach does not work and which are therefore harder to understand intuitively. These are scale invariant theories, which by definition look the same at all distances and energies and hence do not possess any characteristic scales.

Scale invariant theories are important in physics, because they arise naturally in the theory of critical phenomena. One experimental manifestation of scale invariance in critical phenomena is critical opalescence, first observed near the critical point of CO₂ by Andrews (1869) and interpreted as a

sign of density fluctuations occurring over many distance scales by Smoluchowski (1908). The exact solution of the two-dimensional (2D) Ising model by Onsager (1944) also made it possible to see the emergence of scale invariance at the ferromagnet-paramagnet critical point. Nowadays it is understood that all critical points are described by scale invariant theories. This has been incorporated into Wilson's renormalization group (RG) theory of phase transitions, introduced by Wilson and Kogut (1974) and Wilson (1983), according to which continuous phase transitions are described by the fixed points of RG flows and are therefore scale invariant.

Formally, scale invariance is expressed as invariance under a rescaling (dilatation) of all coordinates by a uniform factor $x \rightarrow \lambda x$. Another interesting class of transformations of space is *conformal transformations*, defined as transformations preserving angles. Thus conformal transformations are required to look locally at each point as a rotation accompanied by a dilatation, although the rescaling factor can be x dependent. Conformal transformations have been studied by mathematicians since the 19th century (Monge, 1850). They first entered into physics when Bateman (1910) and Cunningham (1910) showed that Maxwell's equations are conformally invariant (they are also trivially scale invariant because of the masslessness of the photon).¹

With conformal invariance being thus a natural extension of scale invariance, one may wonder if scale invariant theories describing critical points in fact possess full conformal invariance. That this should be the case was first conjectured by Polyakov (1970). Since then several theoretical arguments have been given for why scale invariance should generically imply conformal invariance.² By now it is understood that most physically relevant scale invariant theories are conformally invariant and hence referred to as “conformal field theories” (CFTs).

In addition to their role in the theory of critical phenomena, CFTs are also extremely important for the study of quantum field theories (QFTs). For this discussion QFTs may be Euclidean d -dimensional field theories, relevant for statistical physics, or field theories in Lorentzian signature, which are relevant for high-energy physics and quantum condensed matter.³ From the modern perspective, large classes of QFTs can be seen as RG flows which emerge from one CFT (called the UV fixed point) at short distances and flow to either another nontrivial CFT (called the IR fixed point) or a massive phase at long distances.⁴ In this sense CFTs can be called signposts in the space of general QFTs. The quest to classify and solve CFTs is a major goal of modern theoretical physics.

¹ See Kastrup (2008) for the early history of conformal transformations.

² See Polchinski (1988) and references therein as well as the recent review by Nakayama (2015b). The question is subtle because in fact rare examples of scale invariant and not conformally invariant theories do exist (Riva and Cardy, 2005), although it is fully understood how they evade the general expectation.

³ In this review the space dimension d denotes the total number of coordinate dimensions, including time if one works in Lorentzian signature.

⁴ Some QFTs cannot be viewed as coming from a CFT in the UV, for example, RG flows involving 3D gauge fields.

The study of CFTs was initiated in the late 1960s, focusing mostly on formal properties of these theories.⁵ This early work was done in general dimension d , where the group of conformal transformations is finite dimensional, while it is infinite dimensional in $d = 2$ where any holomorphic map gives rise to a conformal transformation. The importance of this special case was realized by [Belavin, Polyakov, and Zamolodchikov \(1984\)](#). Using the infinite-dimensional conformal symmetry, they solved the 2D minimal models—an infinite sequence of CFTs describing the critical points of the 2D Ising model and other lattice models such as the three-state Potts model.

Of course many 2D models can be exactly solved directly on the lattice ([Baxter, 1989](#)), starting with the Onsager solution of the 2D Ising model. The approach of [Belavin, Polyakov, and Zamolodchikov \(1984\)](#) was different in that it allowed for a solution of critical theories using the constraints of conformal symmetry alone, with minimal or no microscopic input. The crucial idea to find these solutions was the conformal bootstrap, first described by [Ferrara, Grillo, and Gatto \(1973\)](#) and [Polyakov \(1974\)](#). The conformal bootstrap combines conformal invariance with the existence of the operator product expansion (OPE), another powerful concept going back to [Wilson \(1969\)](#) and [Kadanoff \(1969\)](#). This leads to mathematical consistency conditions on the CFT parameters, which were enough to solve the 2D minimal models.

Following these developments, CFT has become an indispensable tool in the theory of 2D critical phenomena.⁶ On the other hand, applications of the conformal bootstrap in higher dimensions lagged behind. For example, 3D continuous phase transitions are traditionally studied using the RG by starting from a microscopic action and looking for a fixed point. Often the 3D fixed point of interest is strongly coupled, requiring one to deform the theory artificially in order to do perturbation theory in a small parameter with the large- N expansion [see, e.g., [Moshe and Zinn-Justin \(2003\)](#) for a review] and the ϵ expansion ([Wilson and Fisher, 1972](#)) being two prime examples. While these theoretical approaches have undoubtedly scored some success in describing the experimental data, one may wonder what a fully nonperturbative approach such as the conformal bootstrap has to say about this problem.

A period of renewed interest in the conformal bootstrap started following [Rattazzi *et al.* \(2008\)](#). This work proposed a numerical method, based on linear programming, which made it possible to extract concrete predictions from the conformal bootstrap equations. The method was applicable in higher dimensions (as well as in 2D). Also, an advantage of the method was that rigorous predictions could be extracted

⁵We do not attempt here a full historical account. Early pioneering contributions included [Mack and Salam \(1969\)](#), [Polyakov \(1970, 1974\)](#), [Ferrara, Grillo, and Gatto \(1971, 1973\)](#), [Migdal \(1971\)](#), [Parisi \(1972\)](#), [Ferrara *et al.* \(1972, 1974\)](#), [Ferrara, Gatto, and Grillo \(1974, 1975\)](#), [Dobrev *et al.* \(1977\)](#), and [Mack \(1977c\)](#).

⁶Many excellent 2D CFT reviews include [Cardy \(1990\)](#), [Ginsparg \(1990\)](#), [Di Francesco, Mathieu, and Senechal \(1997\)](#), and [Henkel \(1999\)](#).

without having to fully solve the equations.⁷ Since then the method was greatly improved and many interesting results were obtained, mostly for conformal field theories in 3D and 4D, but also in other dimensions. One flagship result of this line of research is the world's most precise determination of the critical exponents of the critical 3D Ising model [see [Kos *et al.* \(2016\)](#) for the current world-record results]. Our purpose is to review these developments focusing on applications to the most interesting 3D and 4D CFTs considered so far, as well as to give an overview of the theoretical and numerical techniques which proved useful for these applications.

A. Outline

Because of the overwhelming number of results in various incarnations of the conformal bootstrap, our review will necessarily be limited in scope. Let us briefly outline the topics that we will cover. We begin in Sec. II with an informal overview of the conformal bootstrap. Section III provides a concise introduction to the conformal field theory techniques that are needed to set up the bootstrap in d dimensions. We follow in Sec. IV with an overview of the various numerical methods that have been employed in studies of the bootstrap. Sections V and VI review results obtained from applying these methods to 3D and 4D CFTs. Section VII reviews results obtained with the stronger assumptions of 4D $\mathcal{N} = 1$ or 3D $\mathcal{N} = 2$ superconformal symmetry. We comment on applications to nonunitary models in Sec. VIII. Notably absent from our main review are CFTs in other dimensions (e.g., $d = 2$ or $d > 4$), CFTs with extended supersymmetry, analytical progress in the bootstrap, logarithmic and nonrelativistic CFTs, and other related topics. We finish with a brief overview of progress in these related lines of research in Sec. IX and give some concluding words in Sec. X.

II. CONFORMAL BOOTSTRAP: INFORMAL OVERVIEW

In this section we will give a brief outline of the conformal bootstrap approach to critical phenomena in d dimensions. We will be rather informal in this section, while in the subsequent sections the same material will be treated in more depth and at a higher level of rigor. For another short introduction to these matters, see [Poland and Simmons-Duffin \(2016\)](#). For longer pedagogical introductions see [Rychkov \(2016b\)](#) and [Simmons-Duffin \(2017b\)](#).

As a simple physical setup where these methods would be applicable, we can consider a statistical physics system in d spatial dimensions which is (a) in thermodynamic equilibrium and (b) at a temperature corresponding to a continuous phase transition (so that the correlation length is infinite). Suppose that we are interested in equal-time correlation functions of some local quantities characterizing this system:

$$\langle \mathcal{O}_1(x_1) \cdots \mathcal{O}_n(x_n) \rangle, \quad (1)$$

where x_i are positions in \mathbb{R}^d . For example, one can think of the 3D Ising model at the critical point with $\mathcal{O}_i(x)$ the local

⁷Such full solutions in $d > 2$ are still beyond reach except in very special cases; see Sec. III.I.1.

magnetization, local energy density, etc. In general, the $\mathcal{O}_i(x)$ are called local operators.

We are interested in the behavior of the correlators (1) at distances large compared to any microscopic (such as lattice) scale a . According to Wilson's RG theory, continuous phase transitions are fixed points of RG flows, which means that the long-distance behavior of Eq. (1) will have scale invariance (as well as rotation and translation invariance). Using scale invariance, we can formally extend the long-distance behavior of these correlators from distances $|x_i - x_j| \gg a$ to arbitrary short distances. In what follows we work in the so-defined *continuous limit* theory, which is exactly scale invariant at all distances from 0 to ∞ .⁸

As discussed in the Introduction, we expect that the critical theory is also conformally invariant (i.e., a CFT). This means that for any conformal transformation of d -dimensional space $x \rightarrow x'$ (see Sec. III.A for the definition), Eq. (1) is related to the same correlation function evaluated at points x'_1, \dots, x'_n . This invariance property (or covariance) of correlation functions is expressed as a transformation rule for local operators, in the next section appearing in Eq. (16). For scalar operators, we have

$$\mathcal{O}(x') = \Omega(x)^{-\Delta_{\mathcal{O}}} \mathcal{O}(x), \quad (2)$$

where $\Omega(x) = |\partial x'/\partial x|^{1/d}$ is the x -dependent scale factor of the conformal transformation, and $\Delta_{\mathcal{O}}$ is a fixed parameter characterizing the operator \mathcal{O} , called its *scaling dimension*.⁹

Polyakov (1970) noticed that invariance under Eq. (2) strongly restricts two-point (2pt) and three-point (3pt) correlation functions. The 2pt function is nonzero only for identical operators and can be normalized to 1:

$$\langle \mathcal{O}_i(x_1) \mathcal{O}_j(x_2) \rangle = \delta_{ij} |x_1 - x_2|^{-2\Delta_i}, \quad (3)$$

while the 3pt function is fixed up to a numerical coefficient:

$$\langle \mathcal{O}_1(x_1) \mathcal{O}_2(x_2) \mathcal{O}_3(x_3) \rangle = \frac{\lambda_{123}}{|x_{12}|^{h_{123}} |x_{13}|^{h_{132}} |x_{23}|^{h_{231}}}, \quad (4)$$

where $x_{ij} \equiv x_i - x_j$ and $h_{ijk} \equiv \Delta_i + \Delta_j - \Delta_k$. Similar equations hold for operators with indices; see Sec. III.C.

The set of numerical parameters Δ_i and λ_{ijk} appearing in Eqs. (3) and (4) is called the *CFT data*. It turns out that the CFT data determine not only 2pt and 3pt functions, but are also sufficient to compute all local observables in CFTs in flat space, by which we mean all correlation functions of local operators, including four-point (4pt) and higher-order correlation functions.¹⁰

⁸However, in this paper we will not consider behavior of correlators at coincident points.

⁹To be precise, such transformation rules hold for *primary* local operators, a subtlety which will not play a role in this informal discussion.

¹⁰It should be mentioned that CFTs also possess nonlocal observables in addition to the local ones, which are not necessarily determined by the OPE data. For example, one can probe a CFT by extended operators, such as boundaries or defects, or put it in a space of nontrivial geometry or topology. In this review we will focus on the local observables, although the bootstrap philosophy can also be useful in the study of some nonlocal observables; see Sec. V.B.6 for boundaries and defects and Sec. IX for the modular bootstrap.

To see this, one uses the OPE, which says that we can replace the insertion of two nearby local operators inside a correlation function by a series of single local operators:

$$\mathcal{O}_i(x_1) \mathcal{O}_j(x_2) = \sum_k f_{ijk} \mathcal{O}_k(y). \quad (5)$$

The coefficients of the series f_{ijk} may and will depend on the relative positions of the operators \mathcal{O}_i , \mathcal{O}_j , \mathcal{O}_k , and on their quantum numbers. Crucially, however, these coefficients are not supposed to depend on which other operators appear in the correlation function, as long as they are sufficiently far away from x_1 , x_2 , and y . The precise criterion in the CFT context will be given in Eq. (7).

Notice the freedom in where we put operators appearing on the right-hand side (rhs) of the OPE: we can choose $y = (1/2)(x_1 + x_2)$, $y = x_1$, or any other point nearby. Different choices of y can be related by Taylor expanding \mathcal{O}_k , and thus can be compensated by changing the coefficients of derivatives of \mathcal{O}_k in the OPE. In what follows we will group the operator \mathcal{O}_k together with all its derivatives, formally thinking of f_{ijk} as an infinite power series in ∂_y .

There are two things that make OPE in conformal field theories more powerful than in a generic QFT. First, compatibility of the OPE with conformal invariance determines the functions f_{ijk} up to a numerical prefactor, coinciding with the 3pt function coefficient λ_{ijk} (for this reason it is also called an OPE coefficient):

$$f_{ijk}(x_1, x_2, y, \partial_y) = \lambda_{ijk} \hat{f}_{ijk}(x_1, x_2, y, \partial_y). \quad (6)$$

The reduced functions \hat{f}_{ijk} depend only on the operator dimensions Δ_i , Δ_j , Δ_k , the spins of these operators (which are kept implicit in this informal discussion), and on the space dimension d .¹¹

Secondly, the OPE in conformal theories has a finite radius of convergence, which is determined by the distance to the next operator insertions. For example, in the correlator of Eq. (8) given later, the OPE will converge if

$$|x_1 - y|, \quad |x_2 - y| < \min_{i=3, \dots, n} |x_i - y|, \quad (7)$$

i.e., if there exists a sphere centered at y and separating x_1 and x_2 from any other operator insertion.

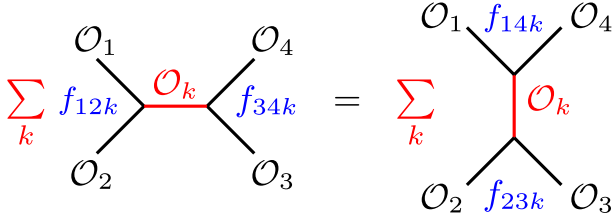
Because of these two reasons we can compute any correlation function recursively using the OPE, provided that we know the CFT data. For example, suppose we want to compute the n -point function

$$\langle \mathcal{O}_1(x_1) \mathcal{O}_2(x_2) \mathcal{O}_3(x_3) \cdots \mathcal{O}_n(x_n) \rangle. \quad (8)$$

Applying the OPE to $\mathcal{O}_1(x_1) \mathcal{O}_2(x_2)$, we reduce this correlator to a sum of correlators containing $n - 1$ operators

$$\langle \mathcal{O}_k(y) \mathcal{O}_3(x_3) \cdots \mathcal{O}_n(x_n) \rangle. \quad (9)$$

¹¹Note that here we are assuming the normalization in Eq. (3).

FIG. 1. The crossing relation for the 4pt function $\langle \mathcal{O}_1 \mathcal{O}_2 \mathcal{O}_3 \mathcal{O}_4 \rangle$.

Proceeding in this way, we will eventually get down to 2pt functions, which are determined by the CFT data. The only parameters which will enter this computation are the operator positions and quantum numbers, the CFT data, and the space dimension d .¹²

Consider now the case of a 4pt function [Eq. (8) with $n = 4$] and compute it in two different ways. The first way is to apply the OPE to the pairs of operators $\mathcal{O}_1 \mathcal{O}_2$ and $\mathcal{O}_3 \mathcal{O}_4$. This reduces the 4pt function to an infinite sum of 2pt functions of operators which appear in these OPEs. A second way is to apply the OPE to the pairs $\mathcal{O}_1 \mathcal{O}_4$ and $\mathcal{O}_2 \mathcal{O}_3$. Since we are dealing with the same 4pt function, the two expansions must agree in their overlapping regions of convergence. This *crossing relation* represents a consistency condition on the CFT data and is illustrated in Fig. 1.

The main idea of the conformal bootstrap is that by imposing the crossing relation, we should be able to significantly winnow down the set of all possible CFT data. In the subsequent sections of this review, we will see how the crossing relation can be written in a mathematically manageable form, and how numerical algorithms can be applied to extract from it concrete constraints.

Ideally, if we impose crossing relations for all 4pt functions of the theory, we will be left with the CFT data corresponding to the actually existing critical theories. In practice, it has so far been possible to impose crossing relations on only a handful of 4pt functions at a time. However, we will see that even this limited procedure produces nontrivial constraints, which are in some cases surprisingly strong.

A. Universality and the role of microscopic input

A fundamental concept in the theory of critical phenomena is universality: all continuous phase transitions can be grouped into universality classes which share the same critical exponents. This is neatly explained in Wilson's RG theory: two phase transitions will fall into the same universality class if they are described by the same fixed point. On the other hand, the conformal bootstrap provides a different perspective on the same phenomenon: each universality class corresponds to a different CFT, with a different set of CFT data.

These two points of view are clearly complementary, and it is important to establish the correspondence between them. Consider, for example, the critical exponents. In RG theory they can be related to the eigenvalues λ^{y_i} of the RG

¹²Note that although the presented scheme solves the problem of computing n -point functions in principle, it is not trivial to do in practice. For 4pt functions, the necessary techniques will be presented in Sec. III.F.

transformation linearized around the fixed point, where $\lambda > 1$ is the RG rescaling factor. As is well known, these eigenvalues are simply related to the scaling dimensions of the local operators $y_i = d - \Delta_i$. Thus, information about the critical exponents can be easily extracted from CFT data, and agreement of their values between an RG fixed point and a CFT may give us confidence that the two describe the same critical universality class.

There are however three more fundamental structural characteristics which can be used to identify universality classes, even before considering the numerical values of critical exponents. These characteristics may not be sufficient to uniquely classify the different CFTs, but they will give us a convenient starting point.

(1) *The global (or internal) symmetry group:* It can be discrete, as for the \mathbb{Z}_2 symmetry of the Ising model, or continuous, as for the $O(N)$ models. In RG studies, the global symmetry group is specified by considering an RG flow in the space of microscopic theories described by an action possessing a given symmetry. The global symmetry group for a CFT is the same group G as for the corresponding RG fixed point, although it is specified in a different way: by demanding that each local operator transform in an irreducible representation of G and that OPE coefficients respect this symmetry structure.

We note in passing that unlike the global symmetry, the presence of a *gauge symmetry* in a microscopic description does not manifest itself in the conformal bootstrap, because physically observable local CFT operators are gauge invariant.¹³

(2) *The number of relevant singlet scalars:* The number of scalar operators which are relevant (i.e., have dimension $\Delta_i < d$) and transform as singlets under the global symmetry determines whether the universality class has critical as opposed to multicritical behavior. This will be discussed in more detail in Sec. V.A. Here it suffices to note that this number is easy to identify from both the RG and CFT perspectives.

(3) *Unitarity:* Unitarity is of course a required property when quantum mechanics is involved, which is the case for theories of interest to high-energy physics and quantum condensed matter. Many universality classes of interest to statistical physics also happen to be unitary.¹⁴ Importantly, the existence of unitarity can be established at the microscopic scale and is then inherited by the RG fixed point. In the CFT description, unitarity is imposed via lower bounds on the operator dimensions and reality constraints on the OPE coefficients; see Sec. III.E.

Finally, let us comment on the OPE coefficients λ_{ijk} . From the CFT point of view, they are an integral part of the CFT data on par with the scaling dimensions. In the conformal bootstrap approach, the crossing relation involves both λ_{ijk} and Δ_i .

¹³Gauge symmetries can make themselves known more indirectly, through anomaly coefficients which show up in the correlation functions of local operators or the existence of higher-form symmetries.

¹⁴In statistical physics, the role of unitarity is played by its Euclidean counterpart called reflection positivity.

In the examples presented, when we are able to determine the Δ_i 's to some accuracy [as for the 3D Ising and the $O(N)$ models], we can typically determine the λ_{ijk} 's to a comparable accuracy. This can be contrasted with the RG approach, where the OPE coefficients do not appear to play such a fundamental role, and they have received relatively little attention.

III. CONFORMAL FIELD THEORY TECHNIQUES IN d DIMENSIONS

In this section we review the theory techniques that form the backbone of the conformal bootstrap. These include conformal symmetry, operators and their correlation functions, unitarity and reflection positivity, conformal blocks, and the way they enter crossing relations (also in the presence of global symmetries).

A. Conformal transformations

The content of this section is standard textbook material. We mention only a few fundamental results and set up our conventions. For more details see, e.g., Rychkov (2016b) and Simmons-Duffin (2017b).¹⁵

We consider CFTs in flat Euclidean or Lorentzian space with coordinates x^μ and metric $\eta_{\mu\nu}$.¹⁶ Conformal transformations are diffeomorphisms $x \rightarrow x'$ which locally look like a rotation $\Lambda^\mu_\nu(x)$ combined with a rescaling $\Omega(x) \geq 0$ (also called a dilatation), which means that the Jacobian takes the form

$$\frac{\partial x'^\mu}{\partial x^\nu} = \Omega(x)\Lambda^\mu_\nu(x), \quad \eta_{\rho\sigma}\Lambda^\rho_\mu(x)\Lambda^\sigma_\nu(x) = \eta_{\mu\nu}. \quad (10)$$

Alternatively, the same condition can be expressed by saying that the transformation preserves angles or that it leaves the metric invariant up to an overall factor.

In any dimension $d \geq 3$,¹⁷ the case of primary interest for this review, a theorem of Liouville says that any conformal transformation can be obtained by composing four types of basic transformations: translations and rotations (which by themselves form the Poincaré group and have $\Omega = 1$), dilatations $x'^\mu = \Omega x^\mu$ with Ω a constant, and inversions $x'^\mu = x^\mu/x^2$ which have $\Omega(x) = 1/x^2$.¹⁸

The resulting conformal group is a Lie group of dimension $(d+1)(d+2)/2$. Its special role in physics and mathematics

¹⁵Other expository sources about CFTs in $d > 2$ dimensions containing material of interest to this review are Ferrara, Gatto, and Grillo (1973), Cardy (1987), Fradkin and Palchik (1996), Di Francesco, Mathieu, and Senechal (1997), Qualls (2015a), and Osborn (2018).

¹⁶Set $\eta_{\mu\nu} \rightarrow \delta_{\mu\nu}$ if interested uniquely in the Euclidean signature.

¹⁷See footnote 3.

¹⁸As is well known, the 2D case is special. The group of 2D conformal transformations is infinite dimensional, since any holomorphic function $f(z)$ with $z = x_1 + ix_2$ defines a conformal transformation $z' = f(z)$. This case has been subject to intense study (see footnote 6), and it will be mostly left out of this review except for a few comments in Sec. IX.

is explained by the fact that it is actually the largest nontrivial subgroup of diffeomorphisms of \mathbb{R}^d .

The inversion belongs to the component of the conformal group which is disconnected from the identity, but by composing an inversion, translation, and a second inversion we can define special conformal transformations (SCTs), also called conformal boosts, given by

$$x'^\mu = \frac{x^\mu - b^\mu x^2}{1 - 2x \cdot b + b^2 x^2}, \quad \Omega(x) = 1 - 2x \cdot b + b^2 x^2, \quad (11)$$

where $b^\mu \in \mathbb{R}^d$ is an arbitrary constant vector.

The conformal algebra generators can be obtained by considering the infinitesimal versions of the above-mentioned transformations. We denote by $M_{\mu\nu}$ and P_μ the usual Poincaré generators, D the dilatation generator, and K_μ the generators of SCTs. Their nonzero commutation relations are¹⁹

$$\begin{aligned} [M_{\mu\nu}, M_{\rho\sigma}] &= \eta_{\nu\rho}M_{\mu\sigma} - \eta_{\mu\rho}M_{\nu\sigma} + \eta_{\nu\sigma}M_{\rho\mu} - \eta_{\mu\sigma}M_{\rho\nu}, \\ [M_{\mu\nu}, P_\rho] &= \eta_{\nu\rho}P_\mu - \eta_{\mu\rho}P_\nu, \\ [M_{\mu\nu}, K_\rho] &= \eta_{\nu\rho}K_\mu - \eta_{\mu\rho}K_\nu, \\ [D, P_\mu] &= P_\mu, \\ [D, K_\mu] &= -K_\mu, \\ [K_\mu, P_\nu] &= 2\eta_{\mu\nu}D - 2M_{\mu\nu}. \end{aligned} \quad (12)$$

In Euclidean signature, the conformal algebra is isomorphic to the algebra of $SO(d+1, 1)$.²⁰ This is shown by the mapping

$$\begin{aligned} \mathcal{J}_{d+1\mu} &= (P_\mu - K_\mu)/2, & \mathcal{J}_{d+2\mu} &= (P_\mu + K_\mu)/2, \\ \mathcal{J}_{\mu\nu} &= M_{\mu\nu}, & \mathcal{J}_{d+1d+2} &= D, \end{aligned} \quad (13)$$

which satisfies the $SO(d+1, 1)$ commutation relations

$$[\mathcal{J}_{AB}, \mathcal{J}_{CD}] = \eta_{BC}\mathcal{J}_{AD} - \eta_{AC}\mathcal{J}_{BD} + \eta_{BD}\mathcal{J}_{CA} - \eta_{AD}\mathcal{J}_{CB}, \quad (14)$$

where η_{AB} is the Lorentzian metric on $\mathbb{R}^{d+1, 1}$.

B. Operators: Primaries and descendants

Our main objects of study will be correlation functions of local operators. Conformal symmetry places constraints on these correlators, expressed as covariance properties when the operators are transformed in a certain way. Our goal here will be to present these transformations, the form of which is determined by representation theory of the conformal group.

Following Mack and Salam (1969), we can restrict to operators inserted at $x = 0$, since the transformation properties at any other point can be obtained by applying a translation

$$\mathcal{O}(x) = e^{x^\mu P_\mu} \mathcal{O}(0) e^{-x^\mu P_\mu}, \quad (15)$$

¹⁹We follow the conventions of Simmons-Duffin (2017b).

²⁰In Lorentzian signature it is $SO(d, 2)$.

and the commutation relations of Eq. (12). Then we have only to specify the action of the stabilizer group of the origin, generated by $M_{\mu\nu}$, D , and K_μ . We will assume that $\mathcal{O}(0) \equiv \mathcal{O}_{\Delta,r}^{\mathbf{i}}(0)$ forms a finite-dimensional irreducible representation (irrep) r of the rotation group (with indices \mathbf{i}) and is characterized by the dilatation eigenvalue Δ , called its scaling dimension:

$$\begin{aligned} [D, \mathcal{O}_{\Delta,r}^{\mathbf{i}}(0)] &= \Delta \mathcal{O}_{\Delta,r}^{\mathbf{i}}(0), \\ [M_{\mu\nu}, \mathcal{O}_{\Delta,r}^{\mathbf{i}}(0)] &= (R_{\mu\nu})^{\mathbf{j}}_{\mathbf{i}} \mathcal{O}_{\Delta,r}^{\mathbf{j}}(0). \end{aligned} \quad (16)$$

Here $R_{\mu\nu}$ are generators of the representation r of $SO(d)$ [or its double cover $Spin(d)$ for spinor representations].

According to the conformal algebra in Eq. (12), the generators P_μ and K_μ act as raising and lowering operators for D , generating what we call the conformal multiplet of \mathcal{O} . In physically interesting theories the spectrum of the dilatation operator is real and bounded from below,²¹ so the conformal multiplet must contain an operator of lowest dimension. Without loss of generality we assume that $\mathcal{O}(0)$ is this lowest operator, so that

$$[K_\mu, \mathcal{O}_{\Delta,r}^{\mathbf{i}}(0)] = 0. \quad (17)$$

An operator satisfying this condition is called the *primary operator* of the conformal multiplet.²² All other operators in the multiplet are called descendants and are obtained from the primary by acting $n \geq 1$ times with P_μ , which means that they are simply its derivatives.²³

Equations (16) define the main quantum numbers characterizing the operator: its scaling dimension Δ and its irrep r under the rotation group. In practice it is important to know the transformation rules of an operator $\mathcal{O}(x)$ under general infinitesimal or finite conformal transformations and for any x . These rules can be determined uniquely from Eqs. (15), (16), and (17). Infinitesimal transformations take the form of first-order differential operators; see, e.g., Rychkov (2016b) (Sec. III.1.2). Here we will just give the explicit form for the finite transformations in terms of the parameters of Eq. (10):

$$\mathcal{O}_{\Delta,r}^{\mathbf{i}}(x') = \mathcal{F}^{\mathbf{i}}_{\mathbf{j}} \mathcal{O}_{\Delta,r}^{\mathbf{j}}(x), \quad \mathcal{F} = \frac{1}{\Omega(x)^\Delta} \mathcal{R}[\Lambda_\nu^\mu(x)], \quad (18)$$

where $\mathcal{R}[\Lambda_\nu^\mu(x)]$ is the matrix representing the finite rotation $\Lambda_\nu^\mu(x)$ in the representation r .²⁴ This equation generalizes Eq. (2) for scalar operators.²⁵

²¹As discussed in Sec. III.E, in unitary theories this property can be shown rigorously.

²²This is called a quasiprimary in the context of 2D CFTs.

²³Explicitly $[P_\mu, \mathcal{O}_{\Delta,r}^{\mathbf{i}}(x)] = \partial_\mu \mathcal{O}_{\Delta,r}^{\mathbf{i}}(x)$. Often n is called the level of the descendant.

²⁴If r is a spinorial representation then Λ_ν^μ specifies \mathcal{R} only up to a sign, and this sign has to be chosen consistently for all operators in a correlator.

²⁵Although we write the left-hand side (lhs) as \mathcal{O}' (as is customary), it is important to remember that \mathcal{O} and \mathcal{O}' represent the same operator.

The scaling dimensions of primary operators comprise the spectrum of the theory. In $d \geq 3$, the spectrum is typically discrete.²⁶ Discreteness of the spectrum follows, e.g., from the requirement of a well-defined thermal partition function (Simmons-Duffin, 2017b).

C. Correlation functions

Consider now a correlation function of n primaries:

$$\mathcal{G}^{\mathbf{i}_1 \cdots \mathbf{i}_n}(x_i) = \langle \mathcal{O}_{\Delta_1 r_1}^{\mathbf{i}_1}(x_1) \cdots \mathcal{O}_{\Delta_n r_n}^{\mathbf{i}_n}(x_n) \rangle. \quad (19)$$

For our purposes we will need only to work at noncoincident points and will not be concerned with possible delta-function-like “contact terms,” which play no role in the numerical conformal bootstrap.

Equation (18) implies that this correlator transforms covariantly under the conformal group. Operationally, for any conformal transformation $x \rightarrow x'$, correlators at points x'_j and x_j are related by

$$\mathcal{G}^{\mathbf{i}_1 \cdots \mathbf{i}_n}(x'_j) = \mathcal{F}^{(1)\mathbf{i}_1}_{\mathbf{j}_1} \cdots \mathcal{F}^{(n)\mathbf{i}_n}_{\mathbf{j}_n} \mathcal{G}^{\mathbf{j}_1 \cdots \mathbf{j}_n}(x_j). \quad (20)$$

While covariance under translations, rotations, and dilatations is straightforward to understand, it is less intuitive for SCTs, since they act nonlinearly on x .

One can classify the most general form of the correlator satisfying Eq. (20). This problem has been addressed using different techniques over the years, starting with Polyakov (1970).²⁷ Two modern efficient methods to obtain such results are the embedding formalism of Costa *et al.* (2011b) reviewed in the Appendix, and the conformal frame approach described in Sec. III.C.4; see Osborn and Petkou (1994) and Kravchuk and Simmons-Duffin (2018a).

We will now state results for the most frequently occurring cases $n = 2, 3$, and 4 . We will focus on scalars \mathcal{O}_Δ as well as operators $\mathcal{O}_{\Delta,\ell}$ transforming in the rank ℓ traceless symmetric representation of $SO(d)$. For the latter we will introduce an auxiliary polarization vector ζ_μ and consider the contraction

$$\mathcal{O}_{\Delta,\ell}(x, \zeta) = \zeta_{\mu_1} \cdots \zeta_{\mu_\ell} \mathcal{O}_{\Delta,\ell}^{\mu_1 \cdots \mu_\ell}(x). \quad (21)$$

The components of the operator itself can be recovered by differentiating in ζ .²⁸

²⁶The only exceptions known to us have been discussed by Levy and Oz (2018). They are nonunitary.

²⁷General 3pt functions in 4D were first worked out by Mack (1977b).

²⁸This is called the index free notation; see, e.g., Dobrev *et al.* (1976) and Costa *et al.* (2011b). Often one imposes $\zeta^2 = 0$, which sets to zero the “traces” in, e.g., Eq. (22), but we will not do this here. Index free notation can be generalized to mixed-symmetry tensors and fermions; see e.g., Giombi, Prakash, and Yin (2013), Simmons-Duffin (2014a), Li and Stergiou (2014), Costa and Hansen (2015), and Iliesiu *et al.* (2016a).

1. 2pt functions

It follows from Eq. (20) that the 2pt function of two operators $\mathcal{O}_{\Delta_1, r_1}$ and $\mathcal{O}_{\Delta_2, r_2}$ vanishes unless $\Delta_1 = \Delta_2$ and $r_1 = r_2^{\dagger}$.²⁹ As a consequence, for every physical operator $\mathcal{O}_{\Delta, r}$, one can identify an operator $\mathcal{O}_{\Delta, r^{\dagger}}$ which transforms in the conjugate representation.³⁰

Further, one can almost always work in a basis of operators such that \mathcal{O} has a nonzero 2pt function only with \mathcal{O}^{\dagger} , which is usually stated as “the 2pt function is diagonal.”³¹ For example, this is always possible in unitary theories. For operators in real $SO(d)$ representations $r^{\dagger} = r$, like traceless symmetric tensors, we can choose a real operator basis so that $\mathcal{O}^{\dagger} = \mathcal{O}$.

Specializing to traceless symmetric tensors, the 2pt function takes the form³²

$$\langle \mathcal{O}_{\Delta, \ell}(x_1, \zeta_1) \mathcal{O}_{\Delta, \ell}(x_2, \zeta_2) \rangle = \frac{[I_{\mu\nu}(x_{12}) \zeta_1^\mu \zeta_2^\nu]^\ell - \text{traces}}{(x_{12}^2)^\Delta},$$

$$I_{\mu\nu}(x) = \eta_{\mu\nu} - 2x_\mu x_\nu / x^2, \quad (22)$$

where $x_{ij} \equiv x_i - x_j$, and “traces” are terms proportional to ζ_1^2, ζ_2^2 , which are uniquely fixed by the tracelessness of $\mathcal{O}_{\Delta, \ell}$. This generalizes Eq. (3) for scalars. It is customary to normalize such 2pt functions to unity, with exceptions being conserved currents and the stress tensor; see Sec. III.H. The nontrivial part of the correlator is its numerator, which specifies the dependence on the operator indices. We refer to such numerators as “tensor structures.”

If the CFT contains a global symmetry, operators are grouped into global symmetry multiplets π . In this case Eq. (22) still applies to the individual components of the multiplets, with appropriate modifications.³³ We discuss the consequences of global symmetries further in Sec. III.G.

2. 3pt functions

Next we turn to 3pt functions, focusing on the case where the first two operators are scalars. Then it turns out that the

²⁹ Here the \dagger means complex conjugation in Lorentzian signature or taking the dual reflected representation in Euclidean signature, where reflected means replacing generators $R_{1\nu}$ by $-R_{1\nu}$. In 3D all representations are real, so the requirement $r_1 = r_2^{\dagger}$ reduces to $r_1 = r_2$, while in 4D if $r_1 = (\ell, \bar{\ell})$ then $r_2 = (\bar{\ell}, \ell)$.

³⁰ The precise action of Hermitian conjugation on Hilbert space operators depends on the signature and choice of quantization surface. For a detailed discussion see Simmons-Duffin (2017b).

³¹ Examples of nonunitary conformal theories in which the 2pt functions cannot be so diagonalized occur in logarithmic CFTs; see, e.g., Hogervorst, Paulos, and Vichi (2017). We will not consider them in this review.

³² For the purposes of this review, it is sufficient to consider correlation functions in Euclidean signature. Most equations can also be used in Lorentzian signature, provided that all points are spacelike separated. For timelike separation one needs modifications, such as an $i\epsilon$ prescription, which we will not discuss.

³³ If π is a complex representation, then it is not convenient to use the real operator basis. The nonzero 2pt function will then be between \mathcal{O} and \mathcal{O}^{\dagger} transforming in $\bar{\pi}$.

third operator can only be a traceless symmetric tensor. Generalizing Eq. (4) for three scalars, the 3pt function takes the form (Mack, 1977b)

$$\begin{aligned} &\langle \mathcal{O}_{\Delta_1}(x_1) \mathcal{O}_{\Delta_2}(x_2) \mathcal{O}_{\Delta_3, \ell}(x_3, \zeta) \rangle \\ &= \lambda_{123} [(Z_{123}^\mu \zeta_\mu)^\ell - \text{traces}] \mathbf{K}_3, \end{aligned} \quad (23)$$

where $\mathbf{K}_3 = \mathbf{K}_3(\Delta_i, x_i)$ is given by

$$\mathbf{K}_3 = \frac{1}{(x_{12}^2)^{(h_{123}+\ell)/2} (x_{13}^2)^{(h_{132}-\ell)/2} (x_{23}^2)^{(h_{231}-\ell)/2}}, \quad (24)$$

$h_{ijk} \equiv \Delta_i + \Delta_j - \Delta_k$, and

$$Z_{123}^\mu = \frac{x_{13}^\mu}{x_{13}^2} - \frac{x_{23}^\mu}{x_{23}^2}.$$

This 3pt function is unique up to the overall coefficient λ_{123} . Notice that as defined,

$$\lambda_{123} = (-1)^\ell \lambda_{213}, \quad (25)$$

while if $\ell = 0$ we can exchange any pair of fields and λ_{123} is fully symmetric. The normalization of these coefficients is unambiguous, since the operators are assumed to be unit normalized according to Eq. (22). Together with the spectrum, the λ 's constitute the CFT data, which distinguish one CFT from another, as discussed in Sec. II.

In unitary theories, the CFT data must satisfy a set of general well-understood constraints; see Sec. III.E. Significantly more nontrivial constraints on the CFT data come from the crossing relations to be discussed in Sec. III.I.

For operators in three general $SO(d)$ representations, the 3pt functions take a form more complicated than Eq. (23). They are also in general not unique, although for any three representations there is at most a finite-dimensional space of allowed tensor structures. The problem of their construction has been completely solved in the most physically important cases of $d = 3$ (Costa *et al.*, 2011b; Iliesiu *et al.*, 2016a) and $d = 4$ (Elkhidir, Karateev, and Serone, 2015). For general d there are partial results, e.g., Costa *et al.* (2011b) for 3pt functions of traceless symmetric tensors, Costa *et al.* (2016a) for traceless mixed-symmetry tensors, and Kravchuk and Simmons-Duffin (2018a) for a general approach to classifying the structures.

3. 4pt functions

Finally let us consider 4pt functions, which as mentioned in Sec. II play a fundamental role in the conformal bootstrap. Focusing here on the case of scalars, the 4pt function must take the general form

$$\langle \mathcal{O}_{\Delta_1}(x_1) \mathcal{O}_{\Delta_2}(x_2) \mathcal{O}_{\Delta_3}(x_3) \mathcal{O}_{\Delta_4}(x_4) \rangle = g(u, v) \mathbf{K}_4. \quad (26)$$

The factor $\mathbf{K}_4 = \mathbf{K}_4(\Delta_i, x_i)$ is given by

$$\mathbf{K}_4 = \frac{1}{(x_{12}^2)^{(\Delta_1+\Delta_2)/2} (x_{34}^2)^{(\Delta_3+\Delta_4)/2}} \left(\frac{x_{24}^2}{x_{14}^2} \right)^{\Delta_{12}/2} \left(\frac{x_{14}^2}{x_{13}^2} \right)^{\Delta_{34}/2}, \quad (27)$$

where $\Delta_{ij} \equiv \Delta_i - \Delta_j$. This factor by itself transforms under conformal transformations as prescribed by Eq. (20). The remaining part of the correlator $g(u, v)$ must be a function of two cross ratios u and v :

$$u = \frac{x_{12}^2 x_{34}^2}{x_{13}^2 x_{24}^2}, \quad v = \frac{x_{14}^2 x_{23}^2}{x_{13}^2 x_{24}^2}, \quad (28)$$

which are invariant under all conformal transformations.

While no further information about $g(u, v)$ can be obtained from conformal invariance alone, it can in fact be computed in terms of the CFT data using additional tools such as the OPE and conformal blocks. This will be discussed in Secs. III.D and III.F.

4. Conformal frames

Here we give a more group theoretical intuition of the number of degrees of freedom contained in a given correlator, and, in particular, of why conformal invariance fixes 2pt and 3pt functions up to a few constants, but allows arbitrariness in 4pt functions.

Given a set of n points, we can make use of conformal transformations to arrange them in convenient configurations. For instance, given three arbitrary points we can find a conformal transformation which maps them to $x_{1,2,3} = 0, \hat{e}, \infty$, where \hat{e} is a fixed unit vector.

For four points, we can first find a conformal transformation fixing three of them as above and then rotate around the axis to put the fourth point into a fixed plane (we assume that $d \geq 2$). The resulting configuration can be parametrized in Euclidean signature as $(\mathbf{0} \equiv \mathbf{0}_{d-2})^{34}$

$$\begin{aligned} x_1 &= (0, 0, \mathbf{0}), & x_2 &= (\sigma, \tau, \mathbf{0}), \\ x_3 &= (1, 0, \mathbf{0}), & x_4 &= (\infty, 0, \mathbf{0}). \end{aligned} \quad (29)$$

It is customary to define (see Fig. 2)

$$z = \sigma + i\tau, \quad \bar{z} = \sigma - i\tau, \quad (30)$$

which are complex conjugate variables if we are working in the Euclidean signature.³⁵ The conformal cross ratios can be expressed in terms of z and \bar{z} as

$$u = z\bar{z}, \quad v = (1-z)(1-\bar{z}). \quad (31)$$

A choice of points x_i , as in Eq. (29), is called a *conformal frame*. It can be thought of as a gauge fixing of most or all of the conformal symmetry. By construction, any coordinate configuration can be reduced to the conformal frame form. Therefore, the knowledge of a correlation function in the conformal frame is sufficient to reconstruct it at any other point through its covariance properties (Osborn and Petkou, 1994). The functional forms of 2pt and 3pt functions are fixed because their conformal frames do not contain any free parameters. The 4pt conformal frame (29) has two real parameters, explaining the

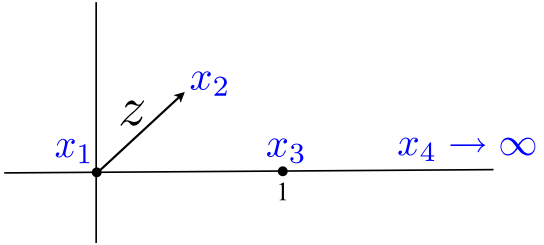


FIG. 2. A conformal frame defining the z coordinate. From Hogervorst and Rychkov, 2013.

functional freedom of the conformal 4pt function. See Sec. III.F.2 for another frequently used conformal frame.

Conformal frames provide a way to construct conformal correlators which is sometimes more convenient than the embedding formalism described in the Appendix. This method can also be used to classify the allowed tensor structures. An important role is then played by the stabilizer group, defined as the set of conformal transformations leaving the conformal frame configuration invariant. It is $SO(d-1)$ for 3pt functions and $SO(d-2)$ for 4pt functions. One classifies tensor structures invariant under the stabilizer group, and each of them lifts to an independent conformally invariant tensor structure (Kravchuk and Simmons-Duffin, 2018a). This method is particularly useful when dealing with 4pt functions of tensor operators: it does not overcount tensor structures, which may happen in the embedding formalism unless special care is taken.

D. Operator product expansion

Our point of view on the origin and the role of the OPE in CFT is the one pedagogically reviewed by Rychkov (2016b) and Simmons-Duffin (2017b). Here we present the main logic and set some conventions.

The key idea is that of radial quantization, which says that we can represent Euclidean CFT correlation functions as scalar products of states $\langle \Psi_{\text{out}} | \Psi_{\text{in}} \rangle$ which live on a sphere of radius R . The state $|\Psi_{\text{in}}\rangle$ is generated by operators in the interior of the sphere, while $\langle \Psi_{\text{out}} |$ by those in the exterior. Once we replace the interior operators by the state $|\Psi_{\text{in}}\rangle$, in a scale invariant theory we can scale the radius of the sphere to zero. Thus any state $|\Psi_{\text{in}}\rangle$ can be expanded in a basis of local operators inserted at the center of the sphere. This is called the state-operator correspondence.

The OPE, written schematically in Eq. (5), is just the special case of the above when there are two operators at points x_1 and x_2 inside the sphere centered at y . We also see the origin of the OPE convergence criterion (7), since we need to have a separating sphere to start the argument.³⁶

As discussed in Sec. II, the next step is to group primaries and descendants in the OPE and to impose the constraints of conformal invariance. This gives the “conformal OPE”:

$$\mathcal{O}_{\Delta_i}(x_1) \mathcal{O}_{\Delta_j}(x_2) = \sum_k \lambda_{ijk} \hat{f}_{ijk}(x_1, x_2, y, \partial_y) \mathcal{O}_{\Delta_k}(y). \quad (32)$$

³⁴We define $\mathcal{O}(\infty)$ by taking the limit of $|x_4|^{2\Delta_0} \mathcal{O}(x_4)$ as $x_4 \rightarrow \infty$, which yields a finite value for the correlation function.

³⁵Note that we can analytically continue to the Lorentzian via $\tau \rightarrow it$, and then z and \bar{z} become independent real variables, but this does not play a role in this review.

³⁶See Pappadopulo *et al.* (2012) for a detailed discussion of OPE convergence in CFT.

The differential operator \hat{f}_{ijk} is fixed by conformal invariance. It can be determined by demanding that the conformal OPE reproduce the 3pt function $\langle \mathcal{O}_{\Delta_i}(x_1) \mathcal{O}_{\Delta_j}(x_2) \mathcal{O}_{\Delta_k}^\dagger(x_3) \rangle$, whose form is by itself fixed by conformal invariance up to the constants λ_{ijk} .

Any $SO(d)$ [or $Spin(d)$] index which the operators \mathcal{O}_{Δ_i} may have are left implicit in Eq. (32). Depending on their representations, there may be several allowed 3pt function tensor structures, and then each structure comes with its own OPE coefficient and a corresponding conformally invariant differential operator \hat{f}_{ijk} . In the most frequently occurring case where \mathcal{O}_{Δ_i} and \mathcal{O}_{Δ_j} are scalars and $\mathcal{O}_{\Delta_k,\ell}$ a spin- ℓ traceless symmetric tensor there is just one OPE coefficient.

While it is important to know that the conformal OPE exists and converges, it turns out that in practice one rarely needs its full explicit form.³⁷ For example, conformal block computations can be organized in ways that avoid explicit knowledge of the full OPE; see Sec. III.F. For this reason, one frequently writes only the “leading OPE,” i.e., the primary term.

For example, in the case of two scalars and a traceless symmetric tensor, the leading OPE has the form (specializing to $x_1 = x$, $x_2 = y = 0$)

$$\mathcal{O}_{\Delta_i}(x) \mathcal{O}_{\Delta_j}(0) \supset \lambda_{ijk} \frac{x^{\mu_1} \cdots x^{\mu_\ell}}{(x^2)^{(h_{ijk}+\ell)/2}} \mathcal{O}_{\Delta_k,\ell}^{\mu_1 \cdots \mu_\ell}(0) + \cdots \quad (33)$$

This reproduces the leading asymptotics of the 3pt function (23) in the limit $x \rightarrow 0$ with x_3 fixed, including the normalization, provided that the 2pt function of $\mathcal{O}_{\Delta_k,\ell}$ is unit normalized as in Eq. (22). Occasionally we will schematically write such a leading OPE as $\mathcal{O}_{\Delta_i} \times \mathcal{O}_{\Delta_j} \supset \mathcal{O}_{\Delta_k,\ell}$, but the form (33) should always be understood.

As explained in Sec. II, any n -point function can be computed from the CFT data by repeated application of the OPE. The 4pt function case, of primary importance for the bootstrap, will be discussed in Sec. III.F.

E. Constraints from unitarity

Here we review the notion of a unitary CFT, focusing on the constraints on CFT data arising for such theories which make the bootstrap especially powerful.

Unitary CFTs can be considered in both Lorentzian and Euclidean signature. They are characterized in the latter by a property called reflection positivity.³⁸ On the other hand, non-unitary CFTs are generally expected to make sense only in Euclidean signature. They will be discussed briefly in Sec. VIII.

Unitary theories allow for quantization in a Hilbert space with a positive-definite norm. In the quantization by planes normally used in Euclidean QFT, an “in” state $|\Psi\rangle$ is generated by n local operators \mathcal{O}_i inserted in the half-space $x_1 < 0$, and an “out” state $\langle\Psi|$ is generated by reflected operators \mathcal{O}_i^\dagger ,

³⁷For some cases when the explicit conformal OPE has been worked out, see Ferrara, Grillo, and Gatto (1971), Ferrara, Gatto, and Grillo (1973), Mack (1977b), and Dolan and Osborn (2001).

³⁸We often abuse terminology and refer to “reflection positivity” as “unitarity” in the context of Euclidean CFTs or when the signature is ambiguous.

inserted at $x_1 > 0$ at mirror-symmetric positions.³⁹ Unitarity implies that the norm $\langle\Psi|\Psi\rangle$ must be non-negative. This norm is just a $2n$ -point function in a particular kinematic configuration, and its positivity is called Osterwalder-Schrader reflection positivity.

Analogously, in the radial quantization usually used for CFTs, an in state $|\Psi\rangle$ is generated by local operators \mathcal{O}_i inserted at positions x_i inside the unit sphere ($i = 1, \dots, n$), and a conjugate out state $\langle\Psi|$ is generated by operators \mathcal{O}_i^\dagger inserted at positions related by an inversion transformation $x'_i = x_i/x^2$. The norm $\langle\Psi|\Psi\rangle$, which is just an inversion-symmetric $2n$ -point function, must be non-negative, a property we call “inversion positivity.”⁴⁰ In CFTs, both forms of positivity are equivalent,⁴¹ and they are both useful depending on circumstances.

1. Unitarity bounds

We already get a simple and powerful constraint by considering radial quantization states $|\Psi\rangle$ produced by a local operator \mathcal{O} acting at the origin. In this case the conjugate operator is inserted at infinity. For a primary \mathcal{O} we recover that its 2pt function must have positive normalization and hence can be normalized to 1 as in Eq. (22). Additional constraints arise from considering descendants of \mathcal{O} . The conformal algebra computes the norms of descendants as polynomials in the primary dimension Δ . Imposing that all descendants have a non-negative norm gives a lower bound on Δ . This “unitarity bound” depends on the representation r of $SO(d)$ (or its double cover for spinor representations) in which the primary transforms.^{42,43}

³⁹For reflected tensor operators, each tensor component is multiplied by a factor $\Theta = (-1)^{N_\perp}$, where N_\perp is the number of tensor indices perpendicular to the reflection plane.

⁴⁰If the \mathcal{O}_i are not scalars, their indices at the inverted positions are contracted with the $I_{\mu\nu}$ tensors defined in Eq. (22), as in Simmons-Duffin (2017b), Eq. (110).

⁴¹By a conformal transformation, radial quantization may be mapped onto a “North-South quantization,” relating inversion positivity to the usual reflection positivity (Rychkov, 2016b).

⁴²Standard CFT references are Ferrara, Gatto, and Grillo (1974), Mack (1977a), and Minwalla (1998). An early physics reference is Evans (1967). In the mathematics literature, these bounds were derived by Jantzen (1977), although the relevance of this work for physics was realized only recently (Penedones, Trevisani, and Yamazaki, 2016; Yamazaki, 2016). See also Rychkov (2016b) and Simmons-Duffin (2017b) for a review. Unitarity bounds can be equivalently derived by studying the positivity of the Fourier transform of the 2pt function analytically continued to Lorentzian signature (the Wightman function). See Ferrara, Gatto, and Grillo (1974), Mack (1977a) (in the sufficiency part of the argument), as well as Grinstein, Intriligator, and Rothstein (2008) for a recent exposition emphasizing physics.

⁴³In Lorentzian signature, operators satisfying the unitarity bounds correspond to the unitary representations of the universal covering group of the Lorentzian conformal group $SO(d, 2)$ having positive energy. Note that in Euclidean signature operators satisfying the unitarity bounds have no relation to the representation of the Euclidean conformal group $SO(d+1, 1)$ which are unitary in the usual mathematical sense of the term. This is already clear from looking at the principal series unitary representations of $SO(d+1, 1)$ which have complex scaling dimensions $d/2 + i\mathbb{R}$.

In 3D, the representation r is labeled by a half integer j , with $j = \ell$ for traceless symmetric spin- ℓ tensors. The unitarity bounds are

$$\begin{aligned} d=3: \Delta &\geq 1/2 & (\text{scalar}, j=0), \\ &\Delta \geq 1 & (\text{smallest spinor}, j=1/2), \\ &\Delta \geq j+1 & (j > 1/2). \end{aligned} \quad (34)$$

In 4D, we can label the representation r by two integers $(\ell, \bar{\ell})$, with traceless symmetric spin- ℓ tensors having $\ell = \bar{\ell}$.⁴⁴ The unitarity bounds then read

$$\begin{aligned} d=4: \Delta &\geq 1 & (\text{scalar}, \ell = \bar{\ell} = 0), \\ &\Delta \geq \frac{1}{2}\ell + 1 & (\ell > 0, \bar{\ell} = 0), \\ &\Delta \geq \frac{1}{2}(\ell + \bar{\ell}) + 2 & (\ell \bar{\ell} \neq 0). \end{aligned} \quad (35)$$

For the 5D and 6D unitarity bounds, see [Minwalla \(1998\)](#). For some representations occurring in all dimensions the unitarity bounds can be written in a dimension-independent form as follows:

$$\begin{aligned} \Delta &\geq \frac{1}{2}(d-2) & (\text{scalar}), \\ \Delta &\geq \frac{1}{2}(d-1) & (\text{smallest spinor}), \\ \Delta &\geq \ell + d - 2 & (\text{traceless symmetric, spin } \ell \geq 1). \end{aligned} \quad (36)$$

As a final comment, in the physics literature the unitarity bounds are often derived by imposing positivity of the descendant norms on the first (and the second, for scalars) level. It is a nontrivial fact that no further constraints arise from higher levels. See [Bourget and Troost \(2018\)](#), Tables 3 and 5, for a review of rigorous mathematical results for unitary bounds in any d .

2. OPE coefficients

Unitarity also gives reality constraints on OPE coefficients of real operators. Consider the 3pt function (23) between two scalars and a traceless symmetric tensor, assuming all three operators are real. Then the 3pt function coefficient must be real:

$$\lambda_{123} \in \mathbb{R}. \quad (37)$$

To argue this, we can consider a 6pt function $\langle \mathcal{O}_1 \mathcal{O}_2 (\Theta \mathcal{O}_3) \mathcal{O}_3 \mathcal{O}_2 \mathcal{O}_1 \rangle$, with the operators arranged mirror symmetrically against a plane into two compact groups positioned a large distance from each other (see Fig. 3). Here Θ is the reflection factor mentioned in footnote 39. Reflection positivity implies that this 6pt function should be real and positive.⁴⁵ On the other hand, by cluster decomposition this 6pt function is equal to the product of two distant 3pt functions, which is easily seen to be λ_{123}^2 times a positive

⁴⁴It is also common in the literature to label by half integers $j = \ell/2$ and $\bar{j} = \bar{\ell}/2$.

⁴⁵For this argument we are using the standard Osterwalder-Schrader reflection positivity and not the inversion positivity.



FIG. 3. The positivity of the 6pt function implies reality of the 3pt function coefficient λ_{123} ; see the text.

number. As a result Eq. (37) follows. We stress that this conclusion holds for both even and odd ℓ .⁴⁶

It was important for this argument that the tensor structure entering Eq. (23) was parity invariant (i.e., it did not involve the ϵ tensor). This argument can be generalized to OPE coefficients for general 3pt tensor structures. The OPE coefficients of tensor structures must be purely imaginary or real depending on whether they involve the ϵ tensor or not. One must similarly be careful with OPE coefficients involving spinors.

Consider now the 4pt function $\langle \mathcal{O}_2 \mathcal{O}_1 \mathcal{O}_1 \mathcal{O}_2 \rangle$, where \mathcal{O}_1 and \mathcal{O}_2 are real scalars and the point configuration is reflection symmetric or inversion symmetric. This 4pt function should be non-negative as a basic consequence of unitarity, and Eq. (37) implies that a more nuanced statement is true: the individual contribution of every primary \mathcal{O} to this 4pt function is non-negative; see Eq. (43). This can be generalized to external operators in general $SO(d)$ [or $Spin(d)$] representations, including the case when there are multiple 3pt function tensor structures.

To summarize, the unitarity bounds say that the CFT Hilbert space has a positive-definite norm, and the OPE coefficient reality constraints say that the OPE preserves this positive-definite structure. If the CFT data satisfy both of these constraints, we are guaranteed that the CFT will be unitary. The bootstrap obtains further constraints on CFT data by combining unitarity with crossing relations.

3. Averaged null energy condition

In a QFT in Lorentzian signature, we can consider the integral of the stress-tensor component T_{++} along a light ray: the lightlike direction x^+ with all other coordinates fixed to zero. The averaged null energy condition (ANEC) says that this light-ray operator has a non-negative expectation value in any state:⁴⁷

⁴⁶In essence we argued that the complex conjugate of a 3pt function is equal to the 3pt function of conjugate fields at reflected positions. This for general n -point functions is sometimes taken as an additional axiom for unitary theories, encoded by the equation $\mathcal{O}(\tau, \mathbf{x})^\dagger = \mathcal{O}^\dagger(-\tau, \mathbf{x})$ valid in Euclidean quantization by planes. Upon analytic continuation to Lorentzian signature, this leads to commutativity of operators at spacelike separation, used to prove reality of OPE coefficients in [Rattazzi et al. \(2008\)](#). Our 6pt argument shows that this axiom is not independent but follows from reflection positivity and cluster decomposition.

⁴⁷Such conditions were first introduced in general relativity, with integration along a null geodesic, in connection with singularity theorems and wormholes. Here we focus on the ANEC in flat space, first discussed by [Klinkhammer \(1991\)](#).

$$\langle \Phi | \int_{-\infty}^{\infty} dx^+ T_{++} | \Phi \rangle \geq 0. \quad (38)$$

The ANEC should hold in any unitary QFT. Two general proofs of the ANEC were given recently, one via quantum information (Faulkner *et al.*, 2016), and one by causality (Hartman, Kundu, and Tajdini, 2017).⁴⁸ Specializing to CFTs, the causality argument makes it clear that the ANEC is not an extra assumption but follows from other CFT axioms such as unitarity, the OPE, and crossing relations for correlation functions involving $T_{\mu\nu}$.⁴⁹ Note, however, that any results following from the ANEC will require the existence of a local stress-tensor operator.

Choosing $|\Phi\rangle$ in Eq. (38) to be generated by a local operator \mathcal{O} acting on the vacuum, the ANEC leads to positivity constraints on 3pt functions $\langle \mathcal{O} T_{\mu\nu} \mathcal{O} \rangle$ called “conformal collider bounds” (Hofman and Maldacena, 2008).⁵⁰

Recently, Cordova and Diab (2018) used the ANEC to argue that primaries of high chirality (large $|\ell - \bar{\ell}|$) in unitary 4D CFTs should satisfy unitarity bounds stronger than Eq. (35). From partial checks for $\bar{\ell} = 0, 1$, they conjecture the general bound (assuming $\ell \geq \bar{\ell}$)

$$\Delta \geq \ell. \quad (39)$$

If $\bar{\ell} = 0$ this becomes stronger than Eq. (35) for $\ell > 2$ and for $\ell > \bar{\ell} + 4$ otherwise. This can be viewed as a CFT strengthening of the theorem of Weinberg and Witten (1980).

F. Conformal blocks

Conformal blocks are of capital importance for the bootstrap. Their theory was initiated in the 1970s (Ferrara *et al.*, 1972, 1974; Ferrara, Gatto, and Grillo, 1975), with further advances in the early 2000s (Dolan and Osborn, 2001, 2004) which were crucial for the bootstrap revival. Recently it experienced further rapid developments, and here we review its current state.

Consider a 4pt function of four primary *scalar* operators $\phi_i(x_i)$ with $i = 1, \dots, 4$ (see Sec. III.F.7 for the general case of external operators with spin). As mentioned in Sec. II, this 4pt function can be computed by applying the OPE of Eq. (5) to

⁴⁸ See also Kravchuk and Simmons-Duffin (2018b) for a recent discussion of light-ray operators in Lorentzian CFTs and an alternative proof of the ANEC.

⁴⁹ This is also suggested by the fact that bounds following from the ANEC can be reproduced in the numerical bootstrap; see Sec. V.F.

⁵⁰ Conformal collider bounds in general dimensions for states created by the stress tensor or global symmetry currents were obtained by Buchel *et al.* (2010) and Chowdhury *et al.* (2013). A proof of these bounds independent from the ANEC was given by Hofman *et al.* (2016); see also Hartman, Jain, and Kundu (2016a, 2016b). Other generalizations of these bounds have been explored by Li, Meltzer, and Poland (2016a), Komargodski, Kulaxizi *et al.* (2017), Chowdhury, David, and Prakash (2017a), Cordova, Maldacena, and Turciaci (2017), Meltzer and Perlmutter (2017), and Cordova and Diab (2018). Sum rules involving the same coefficients were also recently presented by Witczak-Krempa (2015), Chowdhury, David, and Prakash (2017b), Chowdhury (2017), and Gillioz, Lu, and Luty (2017, 2018).

two pairs of fields. For definiteness we fix here the pairing $\phi_1(x_1)\phi_2(x_2)$ and $\phi_3(x_3)\phi_4(x_4)$. This is referred to as “the (12)-(34) OPE channel” to distinguish it from other pairings which will play a role when we discuss crossing. This gives an expansion

$$\langle \phi_1(x_1)\phi_2(x_2)\phi_3(x_3)\phi_4(x_4) \rangle = \sum_{\mathcal{O}} \lambda_{12\mathcal{O}} \lambda_{34\mathcal{O}} W_{\mathcal{O}}, \quad (40)$$

where $W_{\mathcal{O}} \equiv W_{\mathcal{O}}(x_i)$ are the *conformal partial waves* (CPWs) given by

$$W_{\mathcal{O}} = \hat{f}_{12\mathcal{O}}(x_1, x_2, y, \partial_y) \hat{f}_{34\mathcal{O}}(x_3, x_4, y', \partial_{y'}) \langle \mathcal{O}(y)\mathcal{O}(y') \rangle. \quad (41)$$

Since the 2pt function is diagonal, the summation is over the same operator \mathcal{O} in both OPEs. It follows from conformal invariance of the OPE that each CPW transforms under the conformal transformations in the same way as the 4pt function itself; see, e.g., Costa *et al.* (2011a). It is then conventional to split off the factor K_4 defined in Eq. (27), so that we finally have

$$W_{\mathcal{O}} = g_{\Delta_{\mathcal{O}}, \ell_{\mathcal{O}}}^{\Delta_{12}, \Delta_{34}}(u, v) K_4, \quad (42)$$

where $g_{\Delta_{\mathcal{O}}, \ell_{\mathcal{O}}}^{\Delta_{12}, \Delta_{34}}(u, v)$ is called the *conformal block*.⁵¹ It represents the contribution of a primary \mathcal{O} and all of its descendants to the 4pt function. As shown, it depends on the dimension and spin of the exchanged traceless symmetric primary \mathcal{O} , and also on the dimension differences Δ_{12}, Δ_{34} of the external scalars.⁵² Comparing with Eq. (26), we thus have

$$g(u, v) = \sum_{\mathcal{O}} \lambda_{12\mathcal{O}} \lambda_{34\mathcal{O}} g_{\Delta_{\mathcal{O}}, \ell_{\mathcal{O}}}^{\Delta_{12}, \Delta_{34}}(u, v). \quad (43)$$

Equations (40) and (43) are referred to as the CPW decomposition and the conformal block decomposition.

Let us briefly discuss the regions of convergence of the considered expansions. If one works in the z conformal frame of Eq. (29) in Euclidean signature, then Eq. (41) defining the CPWs converges for $|z| < 1$, and the conformal block decomposition (43) is also seen to converge in this region, at least if the theory is unitary (Pappadopulo *et al.*, 2012). While this is sufficient for many applications, a stronger convergence result can be established using the ρ frame; see Sec. III.F.2.

The above definition of conformal blocks via the conformal OPE is important in principle. In practice, there exist efficient approaches to compute the blocks which avoid needing explicit knowledge of the conformal OPE.⁵³ They will be described next.

⁵¹ We make a distinction between CPWs and conformal blocks following the conventions of Costa *et al.* (2011a). In part of the literature these two terms are used interchangeably.

⁵² Sometimes we omit the latter dependence, if it is clear from the context.

⁵³ However, see Dolan and Osborn (2001) and Fortin and Skiba (2016a, 2016b) for direct constructions using the conformal OPE.

1. The Casimir equation

Let us consider the following alternative representation of CPWs. In radial quantization, as mentioned in Sec. III.D, the above 4pt function is expressed as a scalar product of two states

$$\langle \phi_3(x_3)\phi_4(x_4)|\phi_1(x_1)\phi_2(x_2)\rangle \quad (44)$$

living on a sphere separating x_1, x_2 from x_3, x_4 . The CPW then corresponds to inserting an orthogonal projector $\mathcal{P}_{\Delta,\ell}$ onto the conformal multiplet of $\mathcal{O}_{\Delta,\ell}$:

$$\lambda_{12}\lambda_{34}\mathbf{W}_{\mathcal{O}} = \langle \phi_3(x_3)\phi_4(x_4)|\mathcal{P}_{\Delta,\ell}|\phi_1(x_1)\phi_2(x_2)\rangle. \quad (45)$$

For future reference, the projector can be written as

$$\mathcal{P}_{\Delta,\ell} = \sum_{\alpha,\beta=\mathcal{O},P\mathcal{O},PP\mathcal{O},\dots} |\alpha\rangle G^{\alpha\beta}\langle\beta|, \quad (46)$$

where $G_{\alpha\beta} = \langle\alpha|\beta\rangle$ is the Gram matrix of the multiplet and $G^{\alpha\beta}$ is its inverse.

Furthermore, consider the quadratic Casimir⁵⁴

$$\mathcal{C}_2 = \frac{1}{2}\mathcal{J}_{AB}\mathcal{J}^{BA}, \quad (47)$$

where \mathcal{J}_{AB} are the $SO(d+1,1)$ generators, Eq. (14). Insert this operator into Eq. (45) right after $\mathcal{P}_{\Delta,\ell}$. The resulting expression can be computed in two ways. When we act with \mathcal{C}_2 on the left we have

$$\mathcal{P}_{\Delta,\ell}\mathcal{C}_2 = C_{\Delta,\ell}\mathcal{P}_{\Delta,\ell}, \quad (48)$$

where $C_{\Delta,\ell}$ is the quadratic Casimir eigenvalue:

$$C_{\Delta,\ell} = \Delta(\Delta - d) + \ell(\ell + d - 2). \quad (49)$$

On the other hand, the action of \mathcal{C}_2 on the right can be computed using the representation of the conformal generators on primaries as first-order differential operators, mentioned in Sec. III.B. We conclude that the CPW, and hence the conformal block, satisfies a second-order partial differential equation.⁵⁵ The actual form of this “Casimir equation” is most conveniently found using the embedding formalism (Dolan and Osborn, 2004). In the z, \bar{z} coordinates of Eq. (31) it takes the form

$$\mathcal{D}g_{\Delta,\ell}^{\Delta_{12},\Delta_{34}}(z, \bar{z}) = C_{\Delta,\ell}g_{\Delta,\ell}^{\Delta_{12},\Delta_{34}}(z, \bar{z}), \quad (50)$$

where

⁵⁴The quartic Casimir operator $\mathcal{C}_4 = (1/2)\mathcal{J}_{AB}\mathcal{J}^{BC}\mathcal{J}_{CD}\mathcal{J}^{DA}$ has also proved useful in some conformal block studies (Dolan and Osborn, 2011; Hogervorst, Osborn, and Rychkov, 2013).

⁵⁵We followed the presentation of Simmons-Duffin (2017b), Sec. IX.3. The same conclusion can be reached using the OPE (Costa et al., 2011a).

$$\mathcal{D} = \mathcal{D}_z + \mathcal{D}_{\bar{z}} + 2(d-2)\frac{z\bar{z}}{z-\bar{z}}[(1-z)\partial_z - (1-\bar{z})\partial_{\bar{z}}],$$

$$\mathcal{D}_z = 2z^2(1-z)\partial_z^2 - (2 + \Delta_{34} - \Delta_{12})z^2\partial_z + \frac{\Delta_{12}\Delta_{34}}{2}z. \quad (51)$$

Moreover, the leading $z, \bar{z} \rightarrow 0$ behavior of the conformal block can be easily determined using the OPE, and this provides boundary conditions for Eq. (50). Considering the $x_{12}, x_{34} \rightarrow 0$ limit in Eq. (42) and using Eqs. (22) and (33), one obtains⁵⁶

$$g_{\Delta,\ell}^{\Delta_{12},\Delta_{34}}(z, \bar{z}) \underset{z, \bar{z} \rightarrow 0}{\sim} \mathcal{N}_{d,\ell}(z\bar{z})^{\Delta/2} \text{Geg}_{\ell}\left(\frac{z + \bar{z}}{2\sqrt{z\bar{z}}}\right), \quad (52)$$

where $\text{Geg}_{\ell}(x)$ is a Gegenbauer polynomial,

$$\text{Geg}_{\ell}(x) = C_{\ell}^{(d/2-1)}(x), \quad (53)$$

and the normalization factor $\mathcal{N}_{d,\ell}$ is given by⁵⁷

$$\mathcal{N}_{d,\ell} = \frac{\ell!}{(-2)^{\ell}(d/2-1)_{\ell}}. \quad (54)$$

We warn the reader that many different normalization choices can be found in the literature. Different conformal block normalizations correspond to different normalizations of OPE coefficients as compared with the one in Eq. (33). In this review we use this normalization unless mentioned otherwise. For the reader’s convenience, we have collected some other frequently used normalizations in Table I.

By solving Eq. (50) one can find conformal blocks for even d (Dolan and Osborn, 2004). They are expressed in terms of the basic function

$$k_{\beta}(x) = x^{\beta/2} {}_2F_1\left(\frac{\beta - \Delta_{12}}{2}, \frac{\beta + \Delta_{34}}{2}, \beta; x\right), \quad (55)$$

which satisfies

$$\mathcal{D}_x k_{\beta}(x) = \frac{1}{2}\beta(\beta - 2)k_{\beta}(x), \quad k_{\beta}(x) \underset{x \rightarrow 0}{\sim} x^{\beta/2}. \quad (56)$$

In the simplest case of $d = 2$, we have $\mathcal{D} = \mathcal{D}_z + \mathcal{D}_{\bar{z}}$, so the conformal blocks factorize. They take the form⁵⁸

$$\begin{aligned} d = 2: g_{\Delta,\ell}^{\Delta_{12},\Delta_{34}}(z, \bar{z}) &= \frac{1}{(-2)^{\ell}(1 + \delta_{\ell 0})} \\ &\times [k_{\Delta+\ell}(z)k_{\Delta-\ell}(\bar{z}) + z \leftrightarrow \bar{z}]. \end{aligned} \quad (57)$$

⁵⁶The limit is worked out carefully in, e.g., Dolan and Osborn (2001) or Costa et al. (2011a).

⁵⁷Here $(a)_n$ stands for the Pochhammer symbol.

⁵⁸A partial case of this result was first found in Ferrara, Gatto, and Grillo (1975) by another method. See also Osborn (2012) for general conformal blocks in 2D. Note that the 2D global conformal blocks discussed here should be distinguished from the Virasoro conformal blocks.

TABLE I. Summary of various conformal block normalizations $\mathcal{N}_{d,\ell}$, Eqs. (52) and (62), used in the literature.

$\mathcal{N}_{d,\ell}$	Reference
$\frac{\ell!}{(-2)^{\ell}(d/2-1)_{\ell}}$	Dolan and Osborn (2001, 2004), Rattazzi <i>et al.</i> (2008), Penedones, Trevisani, and Yamazaki (2016), this review
$\frac{\ell!}{(d-2)_{\ell}}$	Dolan and Osborn (2011); El-Showk <i>et al.</i> (2012, 2014b); Hogervorst and Rychkov (2013); JULIBOOTs, Paulos (2014b); Costa <i>et al.</i> (2016b); CBOOT, Ohtsuki (2016)
$\frac{(-1)^{\ell}\ell!}{4^{\Delta}(d/2-1)_{\ell}}$	Kos, Poland, and Simmons-Duffin (2014a); Kos <i>et al.</i> (2015b, 2016); Li, Meltzer, and Stergiou (2017); PYCFTBOOT, Behan (2017a)
$\frac{\ell!}{(d/2-1)_{\ell}}$	Poland, Simmons-Duffin, and Vichi (2012), Poland and Stergiou (2015)
$\frac{\ell!}{4^{\Delta}(d-2)_{\ell}}$	Kos, Poland, and Simmons-Duffin (2014b); MATHEMATICA notebook, Simmons-Duffin (2015b)
$\frac{(-1)^{\ell}\ell!}{(d/2-1)_{\ell}}$	Simmons-Duffin (2017c)

Results for higher even d can then be found using recursion relations relating blocks in d and $d+2$ dimensions (Dolan and Osborn, 2004). The important case of $d=4$ reads⁵⁹

$$d=4: g_{\Delta,\ell}^{\Delta_{12},\Delta_{34}}(z,\bar{z}) = \frac{1}{(-2)^{\ell}} \frac{z\bar{z}}{z-\bar{z}} [k_{\Delta+\ell}(z)k_{\Delta-\ell-2}(\bar{z}) - z \leftrightarrow \bar{z}]. \quad (58)$$

In odd d , general closed-form solutions of the Casimir equation are so far unavailable. Sometimes, one can get closed-form solutions along the “diagonal” $z=\bar{z}$, as, e.g., in $d=3$ for all equal external dimensions [Rychkov and Yvernay, 2016, see Eqs. (3.7)–(3.10)]. Other expressions along the diagonal, valid for any d , can be found in Hogervorst, Osborn, and Rychkov (2013). Using these results as a starting point, one can compute derivatives of conformal blocks orthogonal to the diagonal using the Casimir equation, by the Cauchy-Kovalevskaya method; see Sec. III.F.5. The knowledge of these derivatives is usually sufficient for numerical conformal bootstrap applications. Other techniques used to access the conformal blocks numerically will be discussed below.

Finally, let us mention that conformal blocks have simple transformation properties under the interchange of external operators $1 \leftrightarrow 2$ and $3 \leftrightarrow 4$ (Dolan and Osborn, 2001, 2011):

$$\begin{aligned} g_{\Delta,\ell}^{\Delta_{12},\Delta_{34}}(u/v, 1/v) &= (-1)^{\ell} v^{\Delta_{34}/2} g_{\Delta,\ell}^{-\Delta_{12},\Delta_{34}}(u, v) \\ &= (-1)^{\ell} v^{-\Delta_{12}/2} g_{\Delta,\ell}^{\Delta_{12},-\Delta_{34}}(u, v). \end{aligned} \quad (59)$$

This follows from the symmetry of the OPE under the same interchange. As a check, the explicit expressions in Eqs. (57) and (58) satisfy these relations.

⁵⁹This result was first found by Dolan and Osborn (2001) by resumming the OPE expansion.

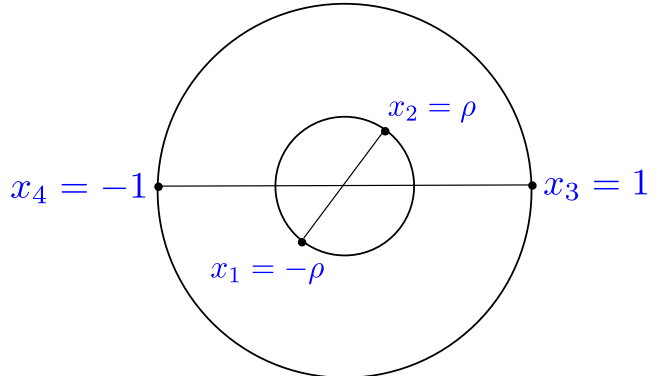


FIG. 4. A conformal frame defining the radial coordinate. From Hogervorst and Rychkov, 2013.

2. Radial expansion for conformal blocks

While closed-form expressions for conformal blocks in general d are unknown, there exist rapidly convergent power series expansions. Following Hogervorst and Rychkov (2013), we describe a particular conformal frame used to generate such expansions.

Starting from the conformal frame (29), we apply an additional conformal transformation which keeps the four points in the same 2-plane but moves them into a configuration symmetric around the origin as in Fig. 4. So the points $x_1 = -x_2$ are now on a circle of radius $r < 1$, while $x_3 = -x_4$ lie on the unit circle.

Let us call \mathbf{n} and \mathbf{n}' the unit vectors pointing to x_2 and x_3 and introduce the complex *radial coordinate* (Pappadopulo *et al.*, 2012)

$$\rho = re^{i\theta}, \quad \mathbf{n} \cdot \mathbf{n}' = \cos \theta = \eta, \quad (60)$$

which is related to the variable z in Eq. (30) via

$$\rho = \frac{z}{(1 - \sqrt{1-z^2})^2}, \quad z = \frac{4\rho}{(1+\rho)^2}.$$

See Hogervorst and Rychkov (2013) for why ρ is preferable to z for constructing rapidly convergent power series expansions for conformal blocks.

In this configuration, the 4pt function is interpreted as a matrix element between two radial quantization states: $|\phi_3(1, \mathbf{n}')\phi_4(1, -\mathbf{n}')|$ and $|\phi_1(r, -\mathbf{n})\phi_2(r, \mathbf{n})\rangle = r^D |\phi_1(1, -\mathbf{n})\phi_2(1, \mathbf{n})\rangle$. The factor r^D , with D the dilatation generator, takes care of the radial dependence.⁶⁰

Consider then the conformal partial wave given in Eq. (45). The conformal multiplet of the operator $\mathcal{O}_{\Delta,\ell}$ at level m contains descendants $|\Delta+m, j\rangle$ of spin j varying from $\max(0, \ell-m)$ to $\ell+m$. We need to know the matrix elements between these descendants and the above in and out states. Leaving aside the overall normalization of these matrix elements, their dependence on the unit vector \mathbf{n} must be proportional to the traceless symmetric tensor $(\mathbf{n}_{\mu_1} \cdots \mathbf{n}_{\mu_j} - \text{traces})$. Contracting two such tensors for \mathbf{n} and \mathbf{n}' gives, up to

⁶⁰ D plays the role of the Hamiltonian operator in radial quantization and $\log r$ is time.

a constant factor, the Gegenbauer polynomial $\text{Geg}_j(\mathbf{n} \cdot \mathbf{n}')$ from Eq. (53).

We conclude that the conformal block has a power series expansion of the form

$$g_{\Delta, \ell}^{\Delta_{12}, \Delta_{34}}(u, v) = r^\Delta \sum_{m=0}^{\infty} r^m \sum_j w(m, j) \text{Geg}_j(\eta), \quad (61)$$

where $w(m, j) \neq 0$ only for $\max(0, \ell - m) \leq j \leq \ell + m$. Using unitarity, one can also conclude that $w(m, j) \geq 0$ if Δ is above the unitarity bound and $\Delta_{12} = -\Delta_{34}$.

Since $z \sim 4\rho$ at small z , the OPE limit (52) becomes

$$g_{\Delta, \ell}^{\Delta_{12}, \Delta_{34}}(r, \eta) \underset{r \rightarrow 0}{\sim} \mathcal{N}_{d, \ell}(4r)^\Delta \text{Geg}_\ell(\eta), \quad (62)$$

which fixes $w(0, \ell) = \mathcal{N}_{d, \ell} 4^\Delta$. To find higher $w(m, j)$, one must determine the normalization of the descendant matrix elements and not just their dependence on \mathbf{n}, \mathbf{n}' . While in principle this can be done using conformal algebra, two more efficient techniques will be discussed later.

The expansion (61) converges for $|r| < 1$, showing that conformal blocks are smooth and real-analytic functions in this region.⁶¹ The conformal block decomposition (43) can be similarly argued to converge for $|r| < 1$.⁶² In terms of the z coordinate, this covers the whole complex plane minus the cut $(1, +\infty)$, improving the convergence result argued below Eq. (43) using the z frame.

3. Recursion relation from the Casimir equation

The first method to find the coefficients $w(m, j)$ is to substitute the expansion (61) into the Casimir equation. This gives rise to recurrence relations, obtained by Hogervorst and Rychkov (2013) and Costa *et al.* (2016b), which determine $w(m, j)$ for $m > 0$ starting from $w(0, \ell)$.

Namely, defining the functions $f_{m,j} \equiv r^m \text{Geg}_j(\eta)$, it is straightforward to show that any of the operators $\{r, \eta, \partial_r, \partial_\eta\}$ acting on these functions produces linear combinations of $f_{m \pm 1, j \pm 1}$. Similarly, the operator \mathcal{D} in Eq. (50), when written in radial coordinates, maps $f_{m,j}$ into a linear combination of $f_{m+\hat{m}, j+\hat{j}}$ functions with suitable shifts. Equation (50) then gives rise to a relation which can be economically written in the form (Costa *et al.*, 2016b)

$$\sum_{(\hat{m}, \hat{j}) \in \mathcal{S}} c(\hat{m}, \hat{j}) w(m + \hat{m}, j + \hat{j}) = 0, \quad (63)$$

where the set $\mathcal{S} = \{(0, 0), (-1, 1), (-1, -1), \dots\}$ contains 30 points, all of which but the first have $\hat{m} < 0$. The coefficients $c(\hat{m}, \hat{j})$ are known functions of the variables $\Delta_{12}, \Delta_{34}, \Delta, \ell, d, m$, and j (Costa *et al.*, 2016b, attached MATHEMATICA notebook). Using Eq. (63), the coefficient $w(m, j)$ can then be recursively expressed in terms of $w(m', j)$ with $m' < m$.

⁶¹An exception occurs at the origin because of the r^Δ factor.

⁶²This can be shown rigorously in unitary CFTs (Pappadopulo *et al.*, 2012). While there are no general results concerning the convergence of conformal block decomposition in nonunitary theories, it appears reasonable to assume that it remains convergent in the same region.

4. Recursion relation from analytic structure

The second method exploits the analytic structure in Δ to obtain a recursion relation for the conformal blocks. A similar approach was first applied by Zamolodchikov (1984, 1987) to the 2D Virasoro conformal blocks by considering them as meromorphic functions of the central charge c or of the scaling dimension Δ . For conformal blocks of external scalars in arbitrary d , this idea was introduced by Kos, Poland, and Simmons-Duffin (2014a, 2014b). It was formalized and extended to conformal blocks for external operators with spin in Penedones, Trevisani, and Yamazaki (2016). Here we explain the external scalar case.

Equations (45) and (46) provide a convenient starting point for discussing the analytic structure of a conformal block as a function of the exchanged primary dimension Δ . When Δ is above the unitarity bound, the Gram matrix $G_{\alpha\beta}(\Delta)$ is positive definite and invertible. However it turns out that for special values of $\Delta = \Delta_A^*$ at or below the unitarity bounds, the Gram matrix becomes degenerate in the sense that some states are null (i.e., have zero norm). The conformal block then develops a pole in $\Delta - \Delta_A^*$. Here we assume that there are only simple poles, as is true, for example, in odd d (see the end of this section for even d).

The crucial observation is that the residue of the pole is proportional to another conformal block:

$$g_{\Delta, \ell}^{\Delta_{12}, \Delta_{34}}(r, \eta) \sim \frac{R_A}{\Delta - \Delta_A^*} g_{\Delta_A, \ell_A}^{\Delta_{12}, \Delta_{34}}(r, \eta). \quad (64)$$

Namely, we identify the first descendant state $\mathcal{O}_A^{\text{null}}$ of \mathcal{O} which becomes null when $\Delta \rightarrow \Delta_A^*$. Let $\Delta_A = \Delta_A^* + n_A$ be its dimension in this limit and ℓ_A its spin. It can be shown that $\mathcal{O}_A^{\text{null}}$ is annihilated by K_μ when $\Delta \rightarrow \Delta_A^*$ and so can be thought of as both a descendant and a primary. Consider then a fictitious primary \mathcal{O}_A which has quantum numbers (Δ_A, ℓ_A) and which is unit normalized. It is the conformal block of such a primary, with standard normalization (62), that appears in the residue.

To be more precise, consider the rate with which $\mathcal{O}_A^{\text{null}}$ becomes null as $\Delta \rightarrow \Delta_A^*$:

$$\langle \mathcal{O}_A^{\text{null}} | \mathcal{O}_A^{\text{null}} \rangle \sim Q_A(\Delta - \Delta_A^*), \quad (65)$$

with Q_A some constant. When $\mathcal{O}_A^{\text{null}}$ becomes null, all of its descendants become null too, with the rate proportional to Eq. (65). Moreover, it can be shown that the Gram matrix in the submultiplet consisting of these descendants is equal to (65) times the (nonsingular) Gram matrix of the multiplet of \mathcal{O}_A , up to corrections of higher order in $\Delta - \Delta_A^*$. This explains why the residue in Eq. (64) involves the whole conformal block of \mathcal{O}_A .⁶³

⁶³The Casimir equation gives another argument for why the residue is a conformal block. Near the pole the Casimir equation for the block reduces to the Casimir equation for the residue (Rychkov, 2016a). The Casimir eigenvalue of the null descendant is the same as for the original block (since it is a descendant): $C_{\Delta_A, \ell} = C_{\Delta_A, \ell_A}$. Finally, the boundary condition at $r \rightarrow 0$ is consistent with the residue being the conformal block.

The coefficient R_A in Eq. (64) is a product of three factors:

$$R_A = M_A^{(L)} Q_A^{-1} M_A^{(R)}, \quad (66)$$

where Q_A is defined in Eq. (65), while $M_A^{(L)}$ and $M_A^{(R)}$ come from the 3pt functions $\langle \phi_3 \phi_4 | \mathcal{O}_A^{\text{null}} \rangle$ and $\langle \mathcal{O}_A^{\text{null}} | \phi_1 \phi_2 \rangle$.

Using information about the poles, we can now write a complete formula for the conformal block. It is convenient to define the regularized conformal block $h_{\Delta,\ell} \equiv h_{\Delta,\ell}^{\Delta_{12},\Delta_{34}}$ by removing a $(4r)^{\Delta}$ prefactor:

$$g_{\Delta,\ell}^{\Delta_{12},\Delta_{34}}(r, \eta) = (4r)^{\Delta} h_{\Delta,\ell}(r, \eta). \quad (67)$$

The function $h_{\Delta,\ell}$ has the same poles in Δ as $g_{\Delta,\ell}$. Moreover it is a meromorphic function of Δ and is therefore fully characterized by its poles and the value at infinity:

$$\begin{aligned} h_{\Delta,\ell}(r, \eta) &= h_{\infty,\ell}(r, \eta) \\ &+ \sum_A \frac{R_A}{\Delta - \Delta_A^*} (4r)^{n_A} h_{\Delta_A^* + n_A, \ell}(r, \eta). \end{aligned} \quad (68)$$

Detailed analysis shows that the poles occurring in this equation organize into one finite and two infinite sequences:

$$\begin{array}{cccc} A & \Delta_A^* & n_A & \ell_A \\ \text{I}_n (n \in \mathbb{N}) & 1 - \ell - n & n & \ell + n, \\ \text{II}_n (1 \leq n \leq \ell) & \ell + d - 1 - n & n & \ell - n, \\ \text{III}_n (n \in \mathbb{N}) & d/2 - n & 2n & \ell. \end{array} \quad (69)$$

Using this definition, it is easy to check that the residues of the poles themselves are nonsingular, except in even dimensions.

The $h_{\infty,\ell}$ term and the constants R_A are given by (Kos, Poland, and Simmons-Duffin, 2014a; Penedones, Trevisani, and Yamazaki, 2016)

$$\begin{aligned} h_{\infty,\ell}(r, \eta) &= \frac{(1 - r^2)^{1-d/2} \mathcal{N}_{d,\ell} \text{Geg}_{\ell}(\eta)}{(r^2 - 2\eta r + 1)^{(1-\Delta_{12}+\Delta_{34})/2} (r^2 + 2\eta r + 1)^{(1+\Delta_{12}-\Delta_{34})/2}}, \\ R_{\text{I}_n} &= \frac{-n(-2)^n}{(n!)^2} \left(\frac{\Delta_{12} + 1 - n}{2} \right)_n \left(\frac{\Delta_{34} + 1 - n}{2} \right)_n, \\ R_{\text{II}_n} &= \frac{-n\ell!}{(-2)^n (n!)^2 (\ell - n)!} \frac{(d + \ell - n - 2)_n}{(d/2 + \ell - n)_n (d/2 + \ell - n - 1)_n} \left(\frac{\Delta_{12} + 1 - n}{2} \right)_n \left(\frac{\Delta_{34} + 1 - n}{2} \right)_n, \\ R_{\text{III}_n} &= \frac{-n(-1)^n (d/2 - n - 1)_{2n}}{(n!)^2 (d/2 + \ell - n - 1)_{2n} (d/2 + \ell - n)_{2n}} \left(\frac{\Delta_{12} - d/2 - \ell - n + 2}{2} \right)_n \left(\frac{\Delta_{12} + d/2 + \ell - n}{2} \right)_n \\ &\times \left(\frac{\Delta_{34} - d/2 - \ell - n + 2}{2} \right)_n \left(\frac{\Delta_{34} + d/2 + \ell - n}{2} \right)_n. \end{aligned} \quad (70)$$

The key property of Eq. (68) is that each pole residue comes with a factor r^{n_A} . This means that it can be used as a recursion relation to generate the regularized conformal block as a power series in r . Indeed, suppose we want to compute $h_{\Delta,l}(r, \eta)$ up to $O(r^N)$. We use Eq. (68) keeping all poles with $n_A \leq N$ of which there are finitely many. The residues of these poles themselves are needed up to smaller order $O(r^{N-n_A})$, so we get a recursion relation. This is one of the most elegant and efficient currently known methods to compute the conformal blocks outside of even d .

The described recursion relation is adequate for computing conformal blocks in odd dimensions and also in generic d . It cannot be applied directly in even d , since some simple poles coalesce into double poles. This is not a problem, since even d conformal blocks are known in closed form. Alternatively, one can apply the recursion relation ϵ away from an even d and take the limit $\epsilon \rightarrow 0$ after the coefficients of the r expansion have been generated. This gives the correct result because the conformal blocks vary analytically with d .

5. Rational approximation of conformal blocks and their derivatives

We now describe how to construct rational approximations to conformal blocks and their derivatives at a given point (r_*, η_*) , which permit an efficient numerical evaluation of

these quantities as a function of Δ . This will play an important role in the numerical techniques described in Sec. IV. Our focus will be on rational approximations to scalar conformal blocks, but later in Sec. III.F.7 we also describe how they can be extended to blocks for external spinning operators.

A rational approximation for conformal block derivatives at a given point can be obtained by combining the radial expansion (61) and the recursion relation (68). It can be expressed in the form

$$\partial_r^m \partial_{\eta}^n g_{\Delta,\ell}(r_*, \eta_*) = (4r_*)^{\Delta} \left(\frac{P_N^{mn}(\Delta)}{Q_N(\Delta)} + O(r_*^{N-m}) \right). \quad (71)$$

Here Q_N is a polynomial made by the product of poles given in Eq. (69) up to order N ,

$$Q_N(\Delta) = \prod_{A=(\text{I},\text{II},\text{III})_n, n \leq N} (\Delta - \Delta_A^*), \quad (72)$$

and $P_N^{mn}(\Delta)$ is a polynomial with $\deg(P_N^{mn}) \leq \deg(Q_N) + m$. The approximation can be made arbitrarily precise by increasing N at the expense of increasing the order of the polynomials.

In numerical applications it is often desirable to keep the polynomial order relatively small while maintaining a precise

approximation. This can be accomplished using a trick introduced by Kos, Poland, and Simmons-Duffin (2014b), where one discards some number of poles but compensates by modifying the residues of the kept poles. For example, if one keeps n poles, one can choose their new residues by demanding that the first $n/2$ Δ derivatives match between the old and new functions at both the unitarity bound and $\Delta = \infty$.

An important property that will be exploited in Sec. IV is that the denominator $Q_N(N)$ is always positive in unitary theories. This follows from the fact that all the poles are at values of Δ below the unitarity bound.

The techniques introduced in the previous sections allow one to compute conformal blocks either in closed form or as a power series in the variable r . Starting from these expressions one can take a direct approach of first analytically computing the r expansion to order N , taking r, η derivatives of the resulting expression, and evaluating the result at the points r_*, η_* . The result can then be recombined to the form in Eq. (71). Since the crossing relations will be more simply written in z, \bar{z} coordinates, one then typically converts to z, \bar{z} derivatives at the corresponding points z_*, \bar{z}_* using a suitable transformation matrix. This approach, while somewhat inefficient at large N due to the need to compute the analytical dependence on η , has been successfully used in the literature, almost always at the crossing symmetric point $z_* = \bar{z}_* = 1/2$ which corresponds to $\eta_* = 1, r_* = 3 - 2\sqrt{2}$.

A somewhat more efficient algorithm is the following:

(i) Compute the r expansion to order N and take derivatives only along the radial direction $\eta = 1$ ($z = \bar{z}$) using the methods of either Sec. III.F.3 or III.F.4.⁶⁴

(ii) Convert to z, \bar{z} derivatives along the diagonal $z = \bar{z}$ using a suitable transformation matrix.

(iii) Use the Casimir equation to recursively compute derivatives in the transverse direction.

Let us briefly discuss the last step, also called the Cauchy-Kovalevskaya method. Consider the Casimir differential equation (50) and express it in the variables $a = z + \bar{z}, \sqrt{b} = (z - \bar{z})$. The radial direction corresponds to $b = 0$. Moreover, since conformal blocks are symmetric in $z \leftrightarrow \bar{z}$, their power series expansion away from the $z = \bar{z}$ line will contain only integer powers of b . Let us denote the $\partial_a^m \partial_b^n$ derivative of the conformal block evaluated at $z = \bar{z} = 1/2$ by $h_{m,n}$. From step (i) we know $h_{m,0}$ for any m . Then we can translate the Casimir equation into a recursion relation for $h_{m,n}$ (with $n > 0$) in terms of $h_{m,n}$ with lower values of n . This recursion relation was obtained by El-Showk *et al.* (2012), Appendix C for $\Delta_{12} = \Delta_{34} = 0$ and generalized by Behan (2017a), Eq. (2.17). It has the following general structure:

$$h_{m,n} = \sum_{m' \leq m-1} m(\dots) h_{m',n} \\ + \sum_{m' \leq m+2} [(\dots) h_{m',n-1} + (n-1)(\dots) h_{m',n-2}]. \quad (73)$$

⁶⁴In even dimensions one can start from the closed-form expression of Sec. III.F.1 evaluated at $\eta = 1$ and expand in r .

Since the Casimir equation is of second order, m' can take values only up to $m+2$. Also the recursion relation for $h_{0,n}$ involves only $h_{m',n'}$ with $n' < n$. Equation (73) is then all that we need to perform step (iii).

Finally, let us mention a few software packages that implement the efficient algorithms described in this section. Their functionality for solving convex optimization problems will be discussed in Sec. IV, so here we focus on how they compute conformal blocks.

A MATHEMATICA notebook by Simmons-Duffin (2015b) can be used for general scalar conformal blocks; at step (i) it implements the recursion relation from analytic structure discussed in Sec. III.F.4. It also implements the trick of shifting pole residues as already described.

Another MATHEMATICA notebook by Paulos (2014a) can also be used for general scalar conformal blocks. At step (i) it implements the recursion relation from the Casimir equation discussed in Sec. III.F.3. This notebook accompanies the JULIA package JULIBOOTS for bootstrap computations using linear programming (Paulos, 2014b).

A PYTHON package PYCFTBOOT (Behan, 2017a) and a SAGE package CBOOT (Ohtsuki, 2016) contain integrated functions that compute general scalar conformal block derivatives using the above procedure. These two packages are designed as front ends to the semidefinite program solver SDPB (Simmons-Duffin, 2015a).

6. Shadow formalism

Next we briefly review the shadow formalism, which was historically the very first technique to access the conformal blocks (Ferrara *et al.*, 1972), and it continues to play a role conceptually and also in explicit computations.

Suppose we want to compute the conformal block $g_{\Delta,\ell}$ of a primary operator $\mathcal{O}_{\Delta,\ell}$ in a scalar 4pt function $\langle \phi_1 \phi_2 \phi_3 \phi_4 \rangle$. Consider a primary “shadow operator” $\tilde{\mathcal{O}}_{d-\Delta,\ell}$ which has the same spin ℓ as \mathcal{O} and dimension $d - \Delta$. We stress that this operator is fictitious, it does not belong to the theory as a local operator, and, in particular, the fact that its dimension is below the unitarity bound is of no concern.

The starting point of the shadow formalism is the following integral:

$$U_{\Delta,\ell}(x_1, x_2, x_3, x_4) = \int d^d x \langle \phi_1(x_1) \phi_2(x_2) \mathcal{O}_{\Delta,\ell}^{\mu_1 \dots \mu_\ell}(x) \rangle \\ \times \langle \tilde{\mathcal{O}}_{d-\Delta,\ell;\mu_1 \dots \mu_\ell}(x) \phi_3(x_3) \phi_4(x_4) \rangle, \quad (74)$$

where under the integral sign we have a product of the conformal scalar-scalar-(spin- ℓ) 3pt functions in Eq. (23), with the spin- ℓ operators having dimensions Δ and $d - \Delta$.

The function $U_{\Delta,\ell}$ has two special properties. First, it conformally transforms in the same way as the 4pt function $\langle \phi_1(x_1) \phi_2(x_2) \phi_3(x_3) \phi_4(x_4) \rangle$. This is because the product (operator \times shadow) transforms as a dimension d primary scalar, which compensates for the Jacobian in the transformation of $d^d x$. Consequently we can write

$$U_{\Delta,\ell} = f_{\Delta,\ell}(u, v) \mathbf{K}_4, \quad (75)$$

where \mathbf{K}_4 is as in Eq. (40) and $f_{\Delta,\ell}(u, v)$ is some function of u and v .

Second, it is straightforward to see that $U_{\Delta,\ell}$ is an eigenfunction of the Casimir operator acting at x_1, x_2 , with eigenvalue $C_{\Delta,\ell}$. Since the latter property is also true for the CPW $W_{\mathcal{O}}$, it is tempting to identify $f_{\Delta,\ell}(u, v)$ in Eq. (75) with the conformal block (up to a proportionality factor). However, this is not quite true. The point is that the conformal blocks of the operator and of its shadow satisfy the same Casimir equation, since their Casimir eigenvalues coincide: $C_{\Delta,\ell} = C_{d-\Delta,\ell}$. For this reason $f_{\Delta,\ell}$ is a linear combination of the block $g_{\Delta,\ell}$ and of the shadow block $g_{d-\Delta,\ell}$; see Dolan and Osborn (2011), Eq. (3.25), for the precise relation.

From the practical viewpoint, the main advantage of the shadow formalism is that the integrand in Eq. (74) is quite easy to write. The downside is that the resulting conformal integrals are not always easy to evaluate, and that it is necessary to disentangle the contribution of a proper conformal block from the shadow one.

Efficient ways to deal with these problems were proposed by Simmons-Duffin (2014a). First of all, the integrals become much easier to evaluate when written using the embedding formalism. Second, to separate the block from the shadow one uses that they transform differently under a monodromy transformation

$$z \rightarrow e^{2\pi i} z, \quad \bar{z} = \text{fixed}, \quad (76)$$

$$g_{\Delta,\ell}(z, \bar{z}) \rightarrow e^{2\pi \Delta i} g_{\Delta,\ell}(z, \bar{z}). \quad (77)$$

The wanted conformal block is isolated via a *monodromy projector*, implemented as a proper choice of the integration contour in Eq. (74). This prescription allows one to extract integral expressions for generic conformal blocks in arbitrary d . In some cases the conformal integrals can be performed exactly, and the results match the known formulas from other techniques.

7. Spinning conformal blocks

Although in this review we mostly deal with scalar 4pt functions, the bootstrap has also been successfully applied to 4pt functions of operators with spin; see, e.g., Secs. V.D for $j = 1/2$ spinors and V.F for $\ell = 1, 2$ tensors in 3D. Here we review the theory of the associated conformal blocks, referred to as “spinning,” which present additional difficulties compared to the blocks of external scalars.

As in the scalar case, spinning conformal blocks correspond to the contribution of an entire conformal multiplet to a 4pt function. They are defined by

$$\begin{aligned} & \langle \mathcal{O}_3 \mathcal{O}_4 | P_{\Delta,r} | \mathcal{O}_1 \mathcal{O}_2 \rangle \\ &= \mathbf{K}_4 \sum_{a=1}^{n_3} \sum_{b=1}^{n'_3} \sum_{c=1}^{n_4} \lambda_{12\mathcal{O}^\dagger}^{(a)} \lambda_{34\mathcal{O}}^{(b)} \mathbf{T}_4^{(c)}(x_i, \zeta_i) \mathbf{G}_{c,\Delta,r}^{a,b}(\Delta_i, r_i, u, v). \end{aligned} \quad (78)$$

Here the external operators $\mathcal{O}_i = \mathcal{O}_{\Delta_i, r_i}(x_i, \zeta_i)$ are positioned at x_i and have their indices contracted with auxiliary

polarization vectors (or spinors) ζ_i . They transform in some general $SO(d)$ [or $Spin(d)$] representations r_i . On the other hand, $\mathcal{O}_{\Delta,r}$ is the exchanged operator (and $\mathcal{O}_{\Delta,r}^\dagger$ its conjugate, see the discussion in Sec. III.C.1), and $\mathcal{P}_{\Delta,r}$ is the projector onto its conformal multiplet similar to Eq. (46).

The prefactor \mathbf{K}_4 is as in Eq. (40); it captures the scaling properties of the 4pt function, leaving everything else dimensionless. Equation (78) also contains a sum over possible conformally invariant 4pt tensor structures $\mathbf{T}_4^{(c)}$ and a double sum over possible 3pt function structures

$$\begin{aligned} & \langle \mathcal{O}_{\Delta_1, r_1}(x_1, \zeta_1) \mathcal{O}_{\Delta_2, r_2}(x_2, \zeta_2) \mathcal{O}_{\Delta, r}^\dagger(x_3, \zeta_3) \rangle \\ &= \sum_{a=1}^{n_3} \lambda_{12\mathcal{O}^\dagger}^{(a)} \mathbf{T}_3^{(a)}(x_i, \zeta_i, \{\Delta_1, r_1\}, \{\Delta_2, r_2\}, \{\Delta, r\}), \end{aligned} \quad (79)$$

and similarly for n'_3 . Finally, the functions $\mathbf{G}_{c,\Delta,r}^{a,b}(\Delta_i, r_i, u, v)$ are the spinning conformal blocks.

According to the above definition, when r is not a real representation, both $\mathbf{G}_{c,\Delta,r}^{a,b}$ and $\mathbf{G}_{c,\Delta,r}^{a,b}$ have to be considered and generally both these blocks are nonzero. We will see a 4D example for $r = (\ell, \ell + p)$ later.

Spinning blocks can be computed by reducing them to “seed” blocks. Consider the simplest case when the exchanged primary is a traceless symmetric spin ℓ . To understand the reduction to seeds, the key observation is that the 3pt tensor structures (79) can be produced by differentiating the more elementary scalar-scalar (spin- ℓ) 3pt functions (23). Namely, Costa *et al.* (2011a) showed that there exist “spinning-up” differential operators $D_{r_1, r_2}^{(a)}$, depending on x_i and ζ_i , such that

$$\begin{aligned} & \mathbf{T}_3^{(a)}(x_i, \zeta_i, \{\Delta_1, r_1\}, \{\Delta_2, r_2\}, \{\Delta, r\}) \\ &= D_{r_1, r_2}^{(a)} \mathbf{T}_3(x_i, \zeta_i, \{\Delta'_1, 0\}, \{\Delta'_2, 0\}, \{\Delta, r\}), \end{aligned} \quad (80)$$

for a suitable basis of 3pt structures and choice of Δ'_i .⁶⁵ Note that in Eq. (80) the third point is not affected. Therefore, in the definition (78), the differential operators do not interfere with the sum over descendants in $\mathcal{P}_{\Delta,\ell}$. One concludes that the spinning blocks can be obtained by differentiating the scalar blocks:

$$\begin{aligned} & \mathbf{K}_4(\Delta_i) \sum_{c=1}^{n_4} \mathbf{T}_4^{(c)}(x_i, \zeta_i) \mathbf{G}_{c,\Delta,\ell}^{a,b}(\Delta_i, r_i, u, v) \\ &= D_{r_1, r_2}^{(a)} D_{r_3, r_4}^{(b)} \mathbf{K}_4(\Delta'_i) g_{\Delta,\ell}^{\Delta_{12}', \Delta_{34}'}(u, v), \end{aligned} \quad (81)$$

where $g_{\Delta,\ell}^{\Delta_{12}', \Delta_{34}'}(u, v)$ is the scalar conformal block discussed at length in the previous sections, referred to as a seed block in this situation.

In 3D, traceless symmetric tensors exhaust all bosonic $SO(d)$ representations, and therefore all bosonic spinning

⁶⁵In a generic basis of 3pt structures, e.g., one that would be naturally constructed using the embedding space or conformal frame formalisms, there would be a linear combination of terms like the rhs with different shifts.

blocks can be obtained from scalar seeds via Eq. (81).⁶⁶ The 3D spinning-up operators were also extended to external spinors and exchanged spin ℓ by Iliesiu *et al.* (2016a).

If a representation r does not couple to two scalars, its conformal block cannot be reduced to the scalar seed using this method. One therefore needs more seed blocks for such representations. As an example, consider the half-integer spin representations in 3D. The simplest pair of external operators to which they couple are a scalar ϕ and a Majorana fermion ψ . The corresponding conformal block $\langle \phi_3 \psi_4 | \mathcal{P}_{\Delta,j} | \phi_1 \psi_2 \rangle$ for half integer j can be taken as a seed. It was computed by Iliesiu *et al.* (2016b), using recursion relations as in Sec. III.F.4, making the list of 3D seeds complete.

A similar discussion holds in 4D. In this case the complete set of seed blocks corresponds to the representations $r = (\ell, \ell + p)$ and $(\ell + p, \ell)$ appearing in the 4pt function of two scalars, one $(p, 0)$ tensor, and one $(0, p)$ tensor:

$$\langle \phi_3(x_3) \mathcal{O}_{\Delta_4,(0,p)}(x_4) | \mathcal{P}_{\Delta,r} | \phi_1(x_1) \mathcal{O}_{\Delta_2,(p,0)}(x_2) \rangle. \quad (82)$$

All of these seeds were computed in closed form by Castedo Echeverri, Elkhidir *et al.* (2016), making use of the shadow formalism from Sec. III.F.6.

Once the seeds are known, a relation analogous to Eq. (81) allows one to relate any conformal block to a combination of seed blocks thorough a suitable set of spinning-up operators $D_{r_i, r_j}^{(a)}$. The latter can be nicely written in the embedding formalism discussed in the Appendix or one of its generalizations. The precise expressions can be found in Costa *et al.* (2011a) and Iliesiu *et al.* (2016b) in 3D or Echeverri *et al.* (2015) in 4D. In 4D there is also available a comprehensive MATHEMATICA package CFTS4D (Cuomo, Karateev, and Kravchuk, 2018) designed to facilitate general spinning 4D conformal block computations. Spinors and spinor-tensor correlators in arbitrary dimensions were instead studied by Isono (2017).

Let us briefly mention several other ideas which have proved useful when dealing with spinning blocks. Karateev, Kravchuk, and Simmons-Duffin (2018) introduced a more general class of “weight-shifting” operators which act on correlation functions. In addition to reproducing the spinning-up operators as a special case, they have a further interesting consequence: when acting on a conformal block these operators can change the $SO(d)$ [or $Spin(d)$] representation of the exchanged state by utilizing the $6j$ symbols of the conformal group. Through repetitive use of these operators, it is possible to express any conformal block, including the seeds, in terms of the scalar ones.⁶⁷ These methods also lead to efficient derivations of various recursion relations satisfied by the conformal blocks.

The Casimir recursion approach from Sec. III.F.3 was extended to arbitrary external bosonic operators by

⁶⁶Some explicitly worked out cases in 3D are for external operator pairs being (current)-(current) (Costa *et al.*, 2011a), scalar-(current or stress tensor) (Li, Meltzer, and Poland, 2016a), and (stress tensor)-(stress tensor) (Dymarsky *et al.*, 2018).

⁶⁷Explicit formulas expressing the seed blocks in 3D and 4D are provided by Karateev, Kravchuk, and Simmons-Duffin (2018).

Costa *et al.* (2016b). More recently, Kravchuk (2018) considered similar expansions for arbitrary external operators, and related the recursion relation coefficients to the $6j$ symbols of $Spin(d-1)$, which are known in closed form for arbitrary representations in $d = 3, 4$, and for representations entering the seed blocks in arbitrary d . He also discusses how to convert from the z to the ρ coordinate as is needed for practical applications.

The pole expansion of Sec. III.F.4 has also been generalized to spinning conformal blocks (Costa *et al.*, 2016b; Penedones, Trevisani, and Yamazaki, 2016). Although no closed-form expressions are known for the analogs of h_∞ and of the residues R_A in Eq. (68), these ingredients can sometimes be found by combining this approach with the spinning-up or weight-shifting operators as in Iliesiu *et al.* (2016b), Dymarsky *et al.* (2017), and Karateev, Kravchuk, and Simmons-Duffin (2018). Commuting these operators with the pole expansion sum, one obtains the expected pole expansion for spinning conformal blocks. By truncating the pole expansion, rational approximations similar to those considered in Sec. III.F.5 can then be constructed for each spinning block tensor structure.

Finally, the shadow block technique discussed in Sec. III.F.6 has been used to compute the conformal blocks appearing in 4pt function of two scalars and two identical conserved currents (Rejon-Barrera and Robbins, 2016).

G. Global symmetry

A majority of CFTs also possess a global symmetry group G , which acts on local operators in a way that commutes with conformal transformations.⁶⁸ The conformal multiplet is then characterized by an additional label: an irreducible G representation π in which the primary transforms. The cases of interest to physics are when G is a finite discrete group or compact Lie group, or a product thereof.

The correlator of n primaries will then be as discussed in Sec. III.C, times an extra factor which determines the dependence on indices in G representations. This extra factor is a $(\pi_1 \otimes \cdots \otimes \pi_n)^G$ tensor, i.e., a G -invariant tensor belonging to the tensor product representation.

By Schur’s lemma, the 2pt function can be nonzero only if $\pi_2 = \bar{\pi}_1$ are conjugate representations (or the same representation if self-conjugate), in which case its form is uniquely determined. The three typical cases of a real, pseudoreal, or complex representation are illustrated by the extra factors being δ_{ab} for $\pi_1 = \pi_2$ a fundamental of $SO(N)$, $i\epsilon_{ab}$ for $\pi_1 = \pi_2$ a fundamental of $SU(2)$, and δ_a^b for $\pi_1(\pi_2)$ (anti)fundamentals of $SU(N)$, $N > 2$.^{69,70}

The 3pt function can be nonzero only if $(\pi_1 \otimes \pi_2 \otimes \pi_3)^G$ is nonempty. This leads to selection rules. For example, if π_1 and

⁶⁸If the CFT arises as an IR fixed point of a gauge theory, we work only with gauge-invariant local operators. As mentioned in Sec. II.A, the gauge group does not enter into our considerations.

⁶⁹The indices of global symmetry representations will be denoted by either a, b, \dots or i, j, \dots depending on the situation.

⁷⁰In unitary CFTs, complex representations π necessarily occur in conjugate pairs, so it is natural to choose an operator basis so that $\mathcal{O}, \mathcal{O}^\dagger$ transform in $\pi, \bar{\pi}$.

π_2 are fundamentals of $SO(N)$, then π_3 can be either a singlet or a rank-2 traceless symmetric or antisymmetric $SO(N)$ tensor. The invariant tensors corresponding to these three possibilities can be readily written down (Rattazzi, Rychkov, and Vichi, 2011a).

Alternatively one can think in terms of the OPE: $\langle \mathcal{O}_{\pi_1} \mathcal{O}_{\pi_2} \mathcal{O}_{\pi_3} \rangle$ is nonzero if $\mathcal{O}_{\bar{\pi}_3}^\dagger$ appears in the OPE $\mathcal{O}_{\pi_1} \times \mathcal{O}_{\pi_2}$. The global symmetry structure is given by the Clebsch-Gordan coefficient for $\bar{\pi}_3$ in $\pi_1 \otimes \pi_2$. Note that the tensor product $\pi_1 \otimes \pi_2$ may include several copies of a given representation, in which case there may be several different invariant tensors possible in the 3pt function. This is similar to how conformal tensor structures for 3pt functions of primaries are in general nonunique.

The 4pt functions are proportional to nonzero tensors appearing in $(\pi_1 \otimes \pi_2 \otimes \pi_3 \otimes \pi_4)^G$. In a CPW decomposition such as Eq. (40), individual CPWs will be proportional to the invariant 4pt tensors obtained by contracting the 3pt tensors from $(\pi_1 \otimes \pi_2 \otimes \pi)^G$ and $(\pi_3 \otimes \pi_4 \otimes \bar{\pi})^G$, where π is the exchanged representation. By basic group theory (decomposing $\pi_1 \otimes \pi_2$ and $\pi_3 \otimes \pi_4$ into irreducibles and applying Schur's lemma), it is easy to see that any 4pt invariant tensor can be obtained in this way for an appropriate choice of π .

Another interesting possibility for additional symmetry is supersymmetry, in which case the conformal group is enhanced to a superconformal group, primary operators are grouped into supersymmetry multiplets, and conformal blocks are enhanced to superconformal blocks. Later in Sec. VII we will describe in more detail some of the consequences of superconformal symmetry for the bootstrap.

H. Conserved local currents

Next we turn to the conserved currents associated with conformal or global symmetries. Such currents are supposed to exist at the IR fixed points of RG flows starting from a microscopic Lagrangian or from a lattice model with finite-range interactions.⁷¹

1. Stress tensor

In the axiomatic approach considered here, a local CFT is simply defined as a CFT having a local conserved stress-tensor operator $T_{\mu\nu}$. In the operator classification, $T_{\mu\nu}$ is a traceless symmetric spin-2 primary of scaling dimension d .⁷²

In local CFTs, the conformal algebra generators (12) are obtained by integrating the stress tensor against a vector field $\epsilon_\nu^J(x)$, describing the corresponding infinitesimal conformal

⁷¹In a classical or weakly coupled quantum local field theory, the existence of local conserved currents follows from Noether's theorem. We are not aware of a general Noether's theorem for strongly coupled theories and lattice models. The existence of local conserved currents in these cases remains a physically motivated assumption, taken for granted in most of the literature. For an intuitive argument for the existence of a local stress tensor using the RG, see Cardy (1996), Sec. 11.3.

⁷²Conformal invariance allows one to consistently impose conservation of the stress tensor. In technical language, the divergence of the dimension d traceless symmetric spin-2 primary is a null descendant and can be set to zero.

transformation, over a surface Σ surrounding the origin. Thus we have

$$\mathcal{J} = - \int_{\Sigma} dS_\mu \epsilon_\nu^J(x) T^{\mu\nu}(x), \quad (83)$$

which is independent of the shape of Σ . See Simmons-Duffin (2017b) for a detailed review of this way of introducing the conformal algebra.⁷³ In particular, the dilatation generator D is given by Eq. (83) with $\epsilon_\nu^D = x_\nu$.

It is conventional to normalize the stress tensor via Eq. (83). Namely, inserting the above surface operator in any correlator should have the effect of replacing the operator at the origin by $[\mathcal{J}, \mathcal{O}(0)]$, assuming the other operators are outside of the region enclosed by Σ . This constraint is called an (integrated) Ward identity.

A frequently occurring case is to consider the 3pt function $\langle \mathcal{O}(0) T_{\mu\nu}(x) \mathcal{O}(y) \rangle$ which by the Ward identity should reduce to $\langle [\mathcal{J}, \mathcal{O}(0)] \mathcal{O}(y) \rangle$ after integration. Since $[\mathcal{J}, \mathcal{O}(0)]$ is known, this provides constraints on the coefficients of various tensor structures in the 3pt function.

These constraints should be imposed in addition to constraints from conservation of $T_{\mu\nu}$. Vanishing of the divergence is automatic for 2pt functions, while in general it must be imposed on 3pt functions containing $T_{\mu\nu}$, placing constraints on the allowed tensor structures. Such constraints are not independent if the other operators are scalars, but become nontrivial if they have spin; see Osborn and Petkou (1994) and Costa *et al.* (2011b).⁷⁴

In particular, when $\mathcal{O} = \phi$ is a scalar, there is just one tensor structure. Using the Ward identity, e.g., for $\mathcal{J} = D$ one fixes the OPE coefficient completely. In the notation of Eq. (23) we have (Osborn and Petkou, 1994)

$$\begin{aligned} \langle \phi(x_1) \phi(x_2) T(x_3, \zeta) \rangle &= \lambda_{\phi\phi T} [(Z_{123} \cdot \zeta)^2 - \frac{1}{2} \zeta^2] \mathbf{K}_3, \\ \lambda_{\phi\phi T} &= - \frac{d \Delta_\phi}{(d-1) S_d}, \quad S_d = \frac{2\pi^{d/2}}{\Gamma(d/2)}. \end{aligned} \quad (84)$$

⁷³However, it should be stressed that there are physically interesting theories which satisfy all CFT axioms except for the existence of the local stress tensor. Examples include defect and boundary CFTs (see Sec. V.B.6 and footnote 109), and critical points of models with long-range interactions; see, e.g., Paulos *et al.* (2016) and Behan *et al.* (2017a, 2017b).

⁷⁴Some important cases are when \mathcal{O} is a conserved spin-1 vector or the stress tensor itself. In both of these cases there are several tensor structures allowed by conformal invariance and conservation and only one independent Ward identity; see Osborn and Petkou (1994) and Dymarsky *et al.* (2017, 2018). Ward identity constraints on 3pt functions $\langle \psi T \bar{\psi} \rangle$ with ψ a fermion were studied in 3D by Iliesiu *et al.* (2016a) and in 4D by Elkhidir and Karateev (2017). In these cases there are two independent tensor structures allowed by conservation, and their coefficients can both be fixed by considering the Ward identity for D as well as for P_μ or $M_{\mu\nu}$.

It can also be shown that the stress tensor does not couple to two scalars of unequal dimension, as the 3pt function structure (23) is then incompatible with conservation.

Since we normalize via Eq. (83), the stress-tensor 2pt function will not be unit normalized but will contain a constant C_T called the central charge⁷⁵:

$$\langle T(x_1, \zeta_1)T(x_2, \zeta_2) \rangle = \frac{C_T(\zeta_1 \cdot I \cdot \zeta_2)^2 - (1/d)\zeta_1^2\zeta_2^2}{S_d^2(x_{12}^2)^d}. \quad (85)$$

A similar convention will be set below for conserved spin-1 currents, while the rest of primaries are kept unit normalized.

In the normalization equations (84) and (85), the contribution of the stress tensor to 4pt functions of scalars is given by⁷⁶

$$\begin{aligned} \langle \phi(x_1)\phi(x_2)\phi'(x_3)\phi'(x_4) \rangle &\supset p_{d,2}g_{d,2}^{0,0}(u, v)\mathbf{K}_4, \\ p_{d,2} = \lambda_{\phi\phi T}\lambda_{\phi'\phi' T} \frac{S_d^2}{C_T} &= \frac{d^2}{(d-1)^2} \frac{\Delta_\phi\Delta_{\phi'}}{C_T}. \end{aligned} \quad (86)$$

As usual, the conformal block is normalized according to Eq. (52). This constraint can play an important role in bootstrap analyses involving multiple 4pt functions, as it implies that the stress tensor contributes to different 4pt functions in a correlated way.

While outside of 2D there is no analog of the “c theorem” (Zamolodchikov, 1986) for C_T ,⁷⁷ the central charge typically scales with the number of degrees of freedom. This is illustrated by the values of the central charge of a free theory containing n_ϕ scalars, n_ψ Dirac fermions, and n_A gauge vectors (in 4D only), given by (Osborn and Petkou, 1994)

$$C_T = \frac{d}{d-1}n_\phi + 2^{\lfloor d/2 \rfloor - 1}dn_\psi + 16\delta_{d,4}n_A. \quad (87)$$

2. Global symmetry currents

The case of a continuous global symmetry in a local CFT is analogous. In this case there are conserved spin-1 currents J_μ^A which transform in the adjoint representation of G and have scaling dimension $d-1$. Global symmetry generators are obtained by integrating J_μ^A over a surface, which defines a normalization for the current and leads to Ward identities.

For concreteness, consider scalar operator ϕ_i with generators $(T^A)_i^j$ transforming in some representations r of G as well as $\phi^{\dagger j}$ transforming in \bar{r} . We assume that the scalar 2pt function is unit normalized, $\langle \phi_i \phi^{\dagger j} \rangle \propto \delta_i^j$, as discussed in

⁷⁵This corresponds to one of the central charge definitions in $d=2$. Note, however, that in $d>2$ there is no known analog of the Virasoro algebra interpretation of the central charge.

⁷⁶This is easy to find by rescaling $T_{\mu\nu}$ to match the normalization in Eq. (22).

⁷⁷Instead, it is known that in 3D the sphere free energy satisfies an “F theorem” [see Jafferis *et al.* (2011), Klebanov, Pufu, and Safdi (2011), and Casini and Huerta (2012)], while in 4D the a anomaly coefficient satisfies an “a theorem” [see Cardy (1988), Osborn (1989), Jack and Osborn (1990), Komargodski and Schwimmer (2011), and Komargodski (2012)].

Sec. III.G. The generators of the global symmetry transformations are then $Q^A = -i \int_\Sigma dS^\mu J_\mu^A$ and the associated Ward identity requires $[Q^A, \phi_i] = -(T^A)_i^j \phi_j$. The 3pt function with J^A is then fixed to be (Osborn and Petkou, 1994; Poland and Simmons-Duffin, 2011)

$$\langle \phi_i(x_1)\phi^{\dagger j}(x_2)J^A(x_3, \zeta) \rangle = -\frac{i}{S_d}(T^A)_i^j[Z_{123} \cdot \zeta]\mathbf{K}_3. \quad (88)$$

In this normalization one can define a *current central charge* C_J by

$$\langle J^A(x_1, \zeta_1)J^B(x_2, \zeta_2) \rangle = \tau^{AB} \frac{C_J \zeta_1 \cdot I \cdot \zeta_2}{S_d^2 (x_{12}^2)^{d-1}}, \quad (89)$$

where $\tau^{AB} = \text{Tr}[T^A T^B]$.

In the end, rescaling J_μ^A to match the normalization of Eq. (22), the contribution of a spin-1 conserved current to the scalar 4pt function is

$$\begin{aligned} \langle \phi_i(x_1)\phi^{\dagger j}(x_2)\phi_k(x_3)\phi^{\dagger l}(x_4) \rangle &\supset -\frac{\mathcal{T}_{ik}^{jl}}{C_J} g_{d-1,1}(u, v)\mathbf{K}_4, \\ \mathcal{T}_{ik}^{jl} &= (\tau^{-1})_{AB}(T^A)_i^j(T^B)_k^l. \end{aligned} \quad (90)$$

Note that τ^{AB} in Eq. (89), $(T^A)_i^j$ in Eq. (88), and \mathcal{T}_{ik}^{jl} are examples of 2pt, 3pt, and 4pt G -invariant tensors as discussed in Sec. III.G.

For example, if ϕ is a complex scalar charged under a $U(1)$ with charge 1, then $\mathcal{T}_{ik}^{jl} = \mathcal{T} = 1$. In the case in which ϕ_i is in the fundamental representation of $SU(N)$ or $SO(N)$ (where $\bar{r} = r$) we have instead

$$\mathcal{T}_{ik}^{jl} = \delta_i^l \delta_k^j - \frac{1}{N} \delta_i^j \delta_k^l \quad [G = SU(N)], \quad (91)$$

$$\mathcal{T}_{ijkl} = \frac{1}{2}(\delta_{il}\delta_{kj} - \delta_{ik}\delta_{jl}) \quad [G = SO(N)]. \quad (92)$$

A note about normalization is in order: once the generators T^A are chosen, the Ward identity fixes the normalization of J^A and determines C_J according to our definition. Clearly, if we use a different generator normalization, then the value of C_J would be modified accordingly. Moreover, once Eq. (88) is established, the Ward identity fixes the normalization of any other generator in any other representation.

Finally, it should be mentioned that while free theories contain higher-spin conserved currents, there exist no-go theorems showing that interacting CFTs in $d \geq 3$ dimensions do not have conserved currents of spin $\ell \geq 3$; see Maldacena and Zhiboedov (2013) and Alba and Diab (2016). This can be thought of as a CFT analog of the Coleman-Mandula theorem for S matrices.

I. Crossing relations

The main idea of the conformal bootstrap is to constrain CFT data by using the crossing relations for 4pt functions; see Fig. 1. Crossing relations are usually analyzed in the conformal frame of Fig. 2. Consider the 4pt function of scalar

operators in this frame and expand it into conformal blocks in the (12)-(34) and in the (32)-(14) OPE channels, referred to as the s and t channels. The two channels are obtained by interchanging points 1 and 3, which transforms $z \rightarrow 1 - z$. Taking into account the value of the \mathbf{K}_4 factor in both channels, and equating the two CPW decompositions, we get the crossing relation

$$\begin{aligned} & \sum_{\mathcal{O}} \lambda_{12\mathcal{O}} \lambda_{34\mathcal{O}} \frac{g_{\Delta_{\mathcal{O}}, \ell_{\mathcal{O}}}^{\Delta_{12}, \Delta_{34}}(z, \bar{z})}{(z\bar{z})^{(\Delta_1 + \Delta_2)/2}} \\ &= \sum_{\mathcal{O}'} \lambda_{32\mathcal{O}'} \lambda_{14\mathcal{O}'} \frac{g_{\Delta_{\mathcal{O}'}, \ell_{\mathcal{O}'}}^{\Delta_{32}, \Delta_{14}}(1-z, 1-\bar{z})}{[(1-z)(1-\bar{z})]^{(\Delta_3 + \Delta_2)/2}}. \end{aligned} \quad (93)$$

Here the sums run over the operators \mathcal{O} and \mathcal{O}' which appear in the OPE in the two channels.

One frequently occurring special case is a 4pt function of identical scalars $\langle \sigma\sigma\sigma\sigma \rangle$. Then the crossing relation simplifies because $\mathcal{O} = \mathcal{O}'$ and also because we get squares of the OPE coefficients $\lambda_{\sigma\sigma\mathcal{O}}$. It is customary to write it as

$$\sum_{\mathcal{O}} \lambda_{\sigma\sigma\mathcal{O}}^2 F_{\Delta_{\mathcal{O}}, \ell_{\mathcal{O}}}^{\Delta_{\sigma}}(z, \bar{z}) = 0, \quad (94)$$

where

$$\begin{aligned} F_{\Delta_{\mathcal{O}}}^{\Delta_{\sigma}}(z, \bar{z}) &= [(1-z)(1-\bar{z})]^{\Delta_{\sigma}} g_{\Delta_{\mathcal{O}}, \ell_{\mathcal{O}}}^{0,0}(z, \bar{z}) \\ &\quad - (z\bar{z})^{\Delta_{\sigma}} g_{\Delta_{\mathcal{O}}, \ell_{\mathcal{O}}}^{0,0}(1-z, 1-\bar{z}). \end{aligned} \quad (95)$$

Among the operators \mathcal{O} which appear in Eq. (94), a special role is played by the identity operator and (in local CFTs) by the stress tensor, because these are two operators of known dimension whose OPE coefficients are nonzero. In particular, the identity operator appears with the coefficient $\lambda_{\sigma\sigma 1} = 1$. By studying the $z \rightarrow 0$ limit of the crossing relation, it is easy to show analytically that there should be infinitely many further operators with nonzero $\lambda_{\sigma\sigma\mathcal{O}}$ (Rattazzi *et al.*, 2008). We will see later what can be learned about these operators using numerical methods.

Going back to the general case (93), it is similarly convenient to rewrite it as follows (Kos, Poland, and Simmons-Duffin, 2014a). We introduce the functions

$$\begin{aligned} F_{\pm, \Delta, \ell}^{ij, kl}(z, \bar{z}) &= [(1-z)(1-\bar{z})]^{(\Delta_k + \Delta_j)/2} g_{\Delta, \ell}^{\Delta_{ij}, \Delta_{kl}}(z, \bar{z}) \\ &\pm (z\bar{z})^{(\Delta_k + \Delta_j)/2} g_{\Delta, \ell}^{\Delta_{ij}, \Delta_{kl}}(1-z, 1-\bar{z}), \end{aligned} \quad (96)$$

which are symmetric or antisymmetric under $z \rightarrow 1-z$, $\bar{z} \rightarrow 1-\bar{z}$. We then take the sums and differences of Eq. (93) with the same equation with z, \bar{z} replaced by $1-z, 1-\bar{z}$. Then Eq. (93) is equivalent to the following pair of equations:

$$\begin{aligned} & \sum_{\mathcal{O}} \lambda_{12\mathcal{O}} \lambda_{34\mathcal{O}} F_{\mp, \Delta_{\mathcal{O}}, \ell_{\mathcal{O}}}^{12, 34}(z, \bar{z}) \\ & \pm \sum_{\mathcal{O}'} \lambda_{32\mathcal{O}'} \lambda_{14\mathcal{O}'} F_{\mp, \Delta_{\mathcal{O}'}, \ell_{\mathcal{O}'}}^{32, 14}(z, \bar{z}) = 0. \end{aligned} \quad (97)$$

If all operators are equal, the lower sign case is trivial, and the upper sign reduces to the single correlator crossing relation (94).

Crossing relations can be imposed at any point z, \bar{z} where both the s and t channels converge. From the discussion in Sec. III.F.2, this is the plane of all complex z minus cuts along $(1, +\infty)$ where the s channel diverges and $(-\infty, 0)$ where the t channel diverges. As we will see in Sec. IV.A, the standard choice in numerical studies is to impose crossing in a Taylor expansion around the point $z = \bar{z} = 1/2$, which is well inside this region.

There is also a third u -channel OPE (13)-(24). The u channel is typically not considered in the numerical bootstrap, because it is not convergent at $z = \bar{z} = 1/2$.⁷⁸ For four identical external scalars, the u channel is automatically satisfied if the s - t channel crossing relation holds (Poland and Simmons-Duffin, 2011). For nonidentical external operators, the u channel is important. To impose the u -channel crossing relation, one changes the conformal frame by interchanging the positions of operators 1 and 2 (Rattazzi, Rychkov, and Vichi, 2011a). The u channel in the original frame becomes the t channel in the new frame, and crossing can be imposed around $z = \bar{z} = 1/2$. The s -channel CPW decomposition in the new frame differs only by signs of all odd-spin terms because of Eq. (25).

In the case when the CFT has a global symmetry G , the crossing relations were formalized by Rattazzi, Rychkov, and Vichi (2011a). Consider a 4pt function of scalar operators transforming in G representations π_i . The exchanged operators \mathcal{O}_{π} then transform in representations π appearing in the tensor product decompositions of $\pi_i \otimes \pi_j$. Each term in the s - and t -channel CPW decompositions comes multiplied with a tensor structure obtained by contracting two 3pt G -invariant tensors, as described in Sec. III.G. We represent it by a vector \vec{V}_{π} in the space of 4pt G -invariant tensors $(\pi_1 \otimes \pi_2 \otimes \pi_3 \otimes \pi_4)^G$. (Anti)symmetrizing under $z \rightarrow 1-z$, $\bar{z} \rightarrow 1-\bar{z}$, the crossing relation takes form (97), with every term multiplied by the corresponding vector \vec{V}_{π} . It is thus a constraint in the space of vector functions. As an explicit example, crossing relations of 4pt functions $\langle \phi_a \phi_b \phi_c \phi_f \rangle$ and $\langle \phi_a \phi^{\dagger b} \phi_c \phi^{\dagger f} \rangle$ for ϕ_a a fundamental of $SO(N)$ or $SU(N)$ were found in Rattazzi, Rychkov, and Vichi (2011a).

A similar vector structure arises when analyzing 4pt functions of operators with Lorentz spin, with the conformally invariant 4pt tensors $\mathbf{T}_4^{(c)}$ in Eq. (78) playing the role of the G -invariant 4pt tensors in the case of global symmetry. General crossing relations involving both global symmetry and Lorentz indices were formalized by Kos, Poland, and Simmons-Duffin (2014a).

1. Explicit solutions to crossing

Many nontrivial 2D CFTs have exact solutions (e.g., the minimal models), and the conformal block decompositions of their 4pt functions provide explicit solutions to crossing relations. Here we will discuss a few explicit solutions to

⁷⁸Although it can be considered when crossing relations are analyzed around another point, e.g., $u = v = 1$ (Li, 2017).

crossing known in $d > 2$. Their existence is important, even though as we will see they come from theories which are not physically the most interesting ones. For example, it is common to check the numerical algorithms against the known explicit solutions to exclude coding errors, before proceeding to study more physically interesting solutions numerically.

Essentially all explicit solutions in $d > 2$ are provided by scale invariant “Gaussian theories,” i.e., theories coming from a quadratic action written in terms of a fundamental field and not having any massive parameter.⁷⁹ The correlation functions of such theories are generated by Wick’s theorem from the basic 2pt function of the fundamental field. The simplest examples are the massless free scalar and massless free fermion theory, which are conformally invariant in any d , and the free Abelian gauge theory, conformally invariant in $d = 4$. In 4D, explicit conformal block decompositions of 4pt scalar correlation functions $\langle \mathcal{O} \mathcal{O} \mathcal{O} \mathcal{O} \rangle$ in these theories (for $\mathcal{O} = \phi, \phi^2, \bar{\psi}\psi, F_{\mu\nu}^2$) were obtained by Dolan and Osborn (2001).

Another class of Gaussian theories are mean field theories (MFTs), also called generalized free fields (Heemskerk *et al.*, 2009; El-Showk and Papadodimas, 2012, Sec. 4). Correlation functions in these theories have the same disconnected structure generated by Wick’s theorem as in the above-mentioned free theories. The only difference is that the scaling dimension of the fundamental field, fixed to a particular value in free theories, becomes a free parameter in MFT.⁸⁰ For example, we can consider the MFT of a scalar field ϕ of arbitrary dimension Δ_ϕ . Such a MFT is unitary as long as Δ_ϕ satisfies the unitarity bound and reduces to the free massless scalar for $\Delta_\phi = (d - 2)/2$. Just as for the usual free theories, the full space of operators in MFTs can be classified by considering normal-ordered products of the fundamental field and its derivatives.⁸¹ For example, there is an operator ϕ^2 which has dimension $2\Delta_\phi$.

Although relatively trivial and nonlocal, MFTs satisfy most CFT axioms (except for the existence of a local stress tensor). As we will see later, they frequently fall inside regions allowed by the bootstrap bounds, so it helps to be familiar with them. Explicit conformal block decompositions of MFT 4pt functions containing scalars were obtained by Heemskerk *et al.* (2009) for $d = 2, 4$ and by Fitzpatrick and Kaplan in general d .

⁷⁹The only exceptions known to us are the “fishnet theories”—nonunitary biscalar field theories integrable in the large- N limit (Gürdoğan and Kazakov, 2016). Recently some conformally invariant 4pt functions and their conformal block decompositions were computed in such theories in 4D (Grabner *et al.*, 2018), and in their nonlocal generalizations to arbitrary d (Kazakov and Olivucci, 2018).

⁸⁰This structure naturally emerges in large- N CFTs as a consequence of large- N factorization. This is particularly transparent in CFTs with holographic duals, since MFT correlation functions are generated by free massive fields in AdS_{d+1} and the arbitrary scaling dimension is determined by the mass.

⁸¹The OPE $\phi \times \phi$ contains only operators of the schematic form $\phi(\partial^2)^n \partial^\ell \phi$, which have spin ℓ and dimension $2\Delta_\phi + 2n + \ell$.

IV. NUMERICAL METHODS

A. Convex optimization and linear programming

The CFT crossing relations describe a continuously infinite number of constraints on the CFT data parametrized by the cross ratios. In order to study the crossing relations numerically one must discretize this set of constraints. Starting with the results of Rattazzi *et al.* (2008), the common approach adopted in numerical studies is to Taylor expand the crossing relations around a point in cross-ratio space, typically taken to be the symmetric configuration $u = v = 1/4$ or equivalently $z = \bar{z} = 1/2$. If one takes derivatives only up to a certain order Λ , then one obtains a finite set of constraints.

Before proceeding, let us highlight the fact that a number of other choices could be made here, e.g., evaluating the crossing equations at different values of the cross ratios, Taylor expanding around other points, integrating the crossing equations, etc.⁸² Here we focus on the approach of Taylor expanding around the symmetric configuration since it works well in practice and is the most common approach in the literature. One justification for this choice of the expansion point is that it makes both the direct and the crossed channel in the conformal block expansion to converge maximally fast (Pappadopulo *et al.*, 2012). However, it is by no means obvious that it is the most efficient way to discretize the crossing relations.

In the case of a single 4pt function of identical scalars $\langle \sigma \sigma \sigma \sigma \rangle$, the resulting constraints take the form

$$0 = \sum_{\mathcal{O}} \lambda_{\sigma\sigma\mathcal{O}}^2 \vec{F}_{\Delta_{\mathcal{O}}, \ell_{\mathcal{O}}}^{\Delta_\sigma}, \quad (98)$$

where $\vec{F}_{\Delta_{\mathcal{O}}, \ell_{\mathcal{O}}}^{\Delta_\sigma}$ can be thought of as a vector with components

$$(\vec{F}_{\Delta_{\mathcal{O}}, \ell_{\mathcal{O}}}^{\Delta_\sigma})^{mn} = \partial_z^m \partial_{\bar{z}}^n F_{\Delta_{\mathcal{O}}, \ell_{\mathcal{O}}}^{\Delta_\sigma}(z, \bar{z})|_{z=\bar{z}=1/2}, \quad (99)$$

where we take derivatives of the functions (95) and keep components up to a cutoff $m + n \leq \Lambda$.⁸³ This computation will thus involve derivatives of conformal blocks up to some finite order.

Computing the vectors $\vec{F}_{\Delta, \ell}^{\Delta_\sigma}$ constitutes a nontrivial preliminary step for analyzing Eq. (98). This step is handled starting from one of the many exact or approximate expressions for conformal blocks discussed in Sec. III.F. The state-of-the-art approach is to use the rational approximation, see Sec. III.F.5, where available software packages are also described. This approach gives rise to approximate expressions which reproduce $\vec{F}_{\Delta, \ell}^{\Delta_\sigma}$ with any desired precision. These expressions can be efficiently evaluated “on the fly,” as needed in the continuous simplex algorithm from Sec. IV.A.1.

⁸²Some of these alternative ideas have been explored by Hogervorst and Rychkov (2013), Sec. 4.2, Castedo Echeverri, Harling, and Serone (2016), Li (2017), Mazac (2017), and Mazac and Paulos (2018).

⁸³Since the functions (95) are odd under $z \rightarrow 1 - z, \bar{z} \rightarrow 1 - z$, only components with $m + n$ odd lead to nontrivial equations.

They can also be used as an input to the semidefinite programming methods described in Sec. IV.B.

We now proceed to describe strategies on how to decide if Eq. (98) has solutions, i.e., if there exists some choice of the exchanged CFT spectrum $\{\Delta_{\mathcal{O}}, \ell_{\mathcal{O}}\}$ and OPE coefficients $\lambda_{\sigma\sigma\mathcal{O}}$ which makes it satisfied. First, let us remark that Eq. (98) is a set of linear equations in $\lambda_{\sigma\sigma\mathcal{O}}^2$. This is at the heart of both the linear programming approaches described in this section as well as the extremal functional and truncation methods described later. In particular, if one has a candidate CFT spectrum for operators appearing in $\sigma \times \sigma$ but does not know the OPE coefficients, one can straightforwardly solve a linear algebra problem to find the coefficients.

In unitary (or reflection positive) CFTs, Eq. (98) states that a sum of vectors must add to zero with *positive* coefficients, due to $\lambda_{\sigma\sigma\mathcal{O}}$ necessarily being real. For some choices of the CFT spectrum $\{\Delta_{\mathcal{O}}, \ell_{\mathcal{O}}\}$ this is not possible, as illustrated in Fig. 5. When it is not possible one can identify a separating plane α through the origin such that all vectors point to one side of the plane.⁸⁴

This observation forms the basis for the first numerical strategy of analyzing the crossing relation (Rattazzi *et al.*, 2008): input some assumption about the CFT spectrum (e.g., a gap in the scalar spectrum with all other operators satisfying unitarity bounds) and numerically search for a separating plane α . Equivalently we can say that we are applying a linear functional $\sum_{mn} \alpha_{mn} \partial_z^m \partial_{\bar{z}}^n [\cdot] |_{z=\bar{z}=1/2}$ to the crossing relations and checking if it is possible to derive a contradiction. Concretely, one can look for a vector $\vec{\alpha}$ such that the scalar product is strictly positive on at least one operator whose OPE coefficient is nonzero (this may be the identity, the stress tensor, or any other operator that we assume appears in the OPE):

$$\vec{\alpha} \cdot \vec{F}_{\Delta_{\mathcal{O}^*}, \ell_{\mathcal{O}^*}}^{\Delta_\sigma} > 0, \quad (100)$$

while it is non-negative for all other $\{\Delta_{\mathcal{O}}, \ell_{\mathcal{O}}\}$ allowed by our assumptions:

$$\vec{\alpha} \cdot \vec{F}_{\Delta_{\mathcal{O}}, \ell_{\mathcal{O}}}^{\Delta_\sigma} \geq 0. \quad (101)$$

Each inequality $\vec{\alpha} \cdot \vec{F}_{\Delta_{\mathcal{O}}, \ell_{\mathcal{O}}}^{\Delta_\sigma} \geq 0$ identifies a half-space and their intersection carves out a convex cone.

There is still one issue before the vector $\vec{\alpha}$ can be searched for numerically—*a priori* there are an infinite number of allowed vectors labeled by all $\{\Delta_{\mathcal{O}}, \ell_{\mathcal{O}}\}$. The first numerical bootstrap studies⁸⁵ employed a discretization approach: namely, they discretized the set $\{\Delta_{\mathcal{O}}, \ell_{\mathcal{O}}\}$ using some small spacing between allowed dimensions so that there are a finite number of linear inequalities satisfied by a finite number of unknown coefficients $\vec{\alpha}$. Then the problem becomes a standard

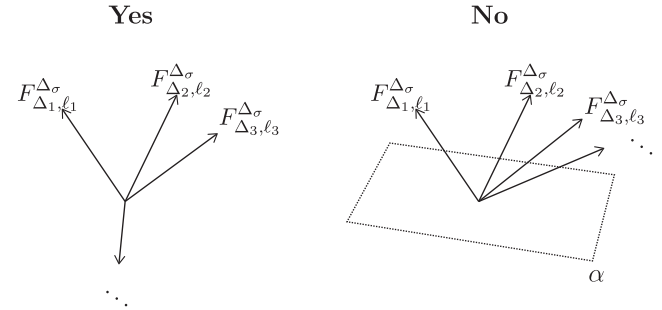


FIG. 5. Left: A case where vectors can sum to zero with positive coefficients. Right: A case where vectors cannot sum to zero with positive coefficients and there exists a separating plane α such that all vectors point on one side of the plane. From Poland and Simmons-Duffin, 2016.

linear programming problem and can be solved using standard algorithms. These include simplex algorithms, where one moves from vertex to vertex on the edge of the feasible region, or interior point algorithms, where one instead traverses the interior of the feasible region. Software packages that have been used in the past for this purpose are MATHEMATICA, the GNU LINEAR PROGRAMMING KIT (GLPK), and the IBM ILOG CPLEX OPTIMIZER. This discretization approach is currently considered to be obsolete, although it retains pedagogical value. More efficient approaches avoiding discretization will be discussed next.

One can slightly modify the problem in order to place bounds on OPE coefficients (Caracciolo and Rychkov, 2010). By isolating one particular contribution \mathcal{O}^* and again applying a functional $\vec{\alpha}$ one rewrites the equation as

$$\lambda_{\sigma\sigma\mathcal{O}^*}^2 \vec{\alpha} \cdot \vec{F}_{\Delta_{\mathcal{O}^*}, \ell_{\mathcal{O}^*}}^{\Delta_\sigma} = -\vec{\alpha} \cdot \vec{F}_{0,0}^{\Delta_\sigma} - \sum_{\mathcal{O}} \lambda_{\sigma\sigma\mathcal{O}}^2 \vec{\alpha} \cdot \vec{F}_{\Delta_{\mathcal{O}}, \ell_{\mathcal{O}}}^{\Delta_\sigma}. \quad (102)$$

Then by imposing the normalization condition $\vec{\alpha} \cdot \vec{F}_{\Delta_{\mathcal{O}^*}, \ell_{\mathcal{O}^*}}^{\Delta_\sigma} = 1$ and the positivity constraints $\vec{\alpha} \cdot \vec{F}_{\Delta_{\mathcal{O}}, \ell_{\mathcal{O}}}^{\Delta_\sigma} \geq 0$ one obtains the upper bound $\lambda_{\sigma\sigma\mathcal{O}^*}^2 \leq -\vec{\alpha} \cdot \vec{F}_{0,0}^{\Delta_\sigma}$. The strongest upper bound is obtained by minimizing $-\vec{\alpha} \cdot \vec{F}_{0,0}^{\Delta_\sigma}$, which yields an optimization problem that can be solved with linear programming algorithms, adopting the above-mentioned discretization approach or other methods discussed next. Alternatively, one can also seek lower bounds by instead imposing $\vec{\alpha} \cdot \vec{F}_{\Delta_{\mathcal{O}}, \ell_{\mathcal{O}}}^{\Delta_\sigma} \leq 0$ and maximizing $-\vec{\alpha} \cdot \vec{F}_{0,0}^{\Delta_\sigma}$ (Poland, Simmons-Duffin, and Vichi, 2012). However, in general it is not possible to obtain lower bounds on OPE coefficients unless the operator \mathcal{O}^* is isolated in the allowed spectrum, since one could always imagine that \mathcal{O}^* has a zero OPE coefficient but operators infinitesimally close to it have nonzero coefficients.

1. Continuous primal simplex algorithm

Instead of looking for a vector $\vec{\alpha}$ with the desired positivity properties, an alternate strategy is to search directly for a set of vectors $\{\vec{F}_{\Delta_{\mathcal{O}}, \ell_{\mathcal{O}}}^{\Delta_\sigma}\}$ appearing in Eq. (98), subject to the positivity conditions $\lambda_{\sigma\sigma\mathcal{O}}^2 \geq 0$. This search can be viewed as a “primal” formulation of the linear program, whereas the

⁸⁴Some vectors may point in the plane but at least one must point outside of it.

⁸⁵See Rattazzi *et al.* (2008), Rychkov and Vichi (2009), Caracciolo and Rychkov (2010), Poland and Simmons-Duffin (2011), Rattazzi, Rychkov, and Vichi (2011a, 2011b), Vichi (2011, 2012), and El-Showk *et al.* (2012).

search for $\vec{\alpha}$ described above can be viewed as the related “dual” problem. Note that in this formulation there are a continuously infinite number of possible vectors $\vec{F}_{\Delta_{\mathcal{O}, \ell_{\mathcal{O}}}}^{\Delta_{\sigma}}$ in the search space. El-Showk *et al.* (2014b) developed a modification of Dantzig’s simplex algorithm in order to handle such a continuous search space.⁸⁶ The essential idea is to use Newton’s method at each step of the algorithm to identify a vector to add, which is optimal over some continuous interval of scaling dimensions $[\Delta_{\min}, \Delta_{\max}]$ and discrete set of spins $[0, \ell_{\max}]$. For reasons explained by El-Showk *et al.* (2014b), it is necessary to perform computations at a precision higher than machine precision. This continuous simplex algorithm is one of two state-of-the art methods for the conformal bootstrap, the other one being the semidefinite programming method described below. Three implementations of this algorithm are available: a C++ code SIPSOLVER (Simmons-Duffin, 2014b) and a PYTHON/CYTHON code (El-Showk and Rychkov, 2014) which were used for the computations in El-Showk *et al.* (2014b), as well as a JULIA package JULIBOOTS (Paulos, 2014b).

B. Semidefinite programming

While the linear programming techniques previously described are adequate for crossing relations of single 4pt functions (possibly charged under some global symmetry), they are more difficult to adapt for systems of crossing relations containing multiple operators. The reason is that the resulting crossing relations for mixed correlators are no longer linear in the positive squares of OPE coefficients.⁸⁷ The same issue arises when considering 4pt functions of spinning operators, where multiple 3pt function tensor structures exist. In these situations one can phrase the optimization problem needed to obtain bounds using the language of semidefinite programming rather than linear programming (Kos, Poland, and Simmons-Duffin, 2014a).⁸⁸

Another use of semidefinite programming (Poland, Simmons-Duffin, and Vichi, 2012) is to avoid needing to discretize and impose a cutoff on the exchanged operator dimensions appearing in the positivity constraints such as $\vec{\alpha} \cdot \vec{F}_{\Delta_{\mathcal{O}, \ell_{\mathcal{O}}}} \geq 0$. In this section, we will describe both of these uses of semidefinite programming, as well as how they can be combined.

In most applications to the bootstrap, it has proven necessary for numerical stability to solve the semidefinite programs described below at a precision higher than machine precision. The first numerical studies made use of the software SDPA-GMP (Nakata, 2010) [a variant of SDPA (Yamashita *et al.*, 2010)] for this purpose. The state of the art is an efficient software package SDPB, described by Simmons-Duffin

⁸⁶Such linear programming problems are called “continuous” or “semi-infinite” (Reemtsen and Görner, 1998).

⁸⁷However, they can be made linear at the expense of introducing additional continuous parameters (El-Showk and Paulos, 2018). This observation has not yet been implemented and it is not known how it would perform in practice.

⁸⁸For a related problem of multiple internal symmetry coupling structures see Rattazzi, Rychkov, and Vichi (2011a).

(2015a), which improves on the SDPA’s primal-dual interior point algorithm primarily by taking advantage of matrix block structure and parallelization.⁸⁹ In order to set up the problems so that they can be solved by SDPB, recent studies have typically used either MATHEMATICA notebooks, or the interfaces PYCFTBOOT (Behan, 2017a) or CBOOT (Ohtsuki, 2016).

1. Mixed correlators

We illustrate the use of semidefinite programming for mixed correlators with a simple example. Consider a system of 4pt functions containing two operators σ and ϵ , where σ is odd under a \mathbb{Z}_2 symmetry and ϵ is even. The resulting system of crossing relations for $\langle \sigma\sigma\sigma\sigma \rangle$, $\langle \sigma\sigma\epsilon\epsilon \rangle$, and $\langle \epsilon\epsilon\epsilon\epsilon \rangle$ takes the form (Kos, Poland, and Simmons-Duffin, 2014a)

$$0 = \sum_{\mathcal{O}^+} (\lambda_{\sigma\sigma\mathcal{O}} \lambda_{\epsilon\epsilon\mathcal{O}}) \vec{V}_{+, \Delta, \ell} \begin{pmatrix} \lambda_{\sigma\sigma\mathcal{O}} \\ \lambda_{\epsilon\epsilon\mathcal{O}} \end{pmatrix} + \sum_{\mathcal{O}^-} \lambda_{\sigma\epsilon\mathcal{O}}^2 \vec{V}_{-, \Delta, \ell}, \quad (103)$$

where the components of the vectors $\vec{V}_{\pm, \Delta, \ell}$ run over five independent crossing relations,⁹⁰ \mathcal{O}_{\pm} denote operators even or odd under \mathbb{Z}_2 symmetry, and each $\vec{V}_{+, \Delta, \ell}$ is a 5-vector of 2×2 matrices:

$$\vec{V}_{-, \Delta, \ell} = \begin{pmatrix} 0 \\ 0 \\ F_{-, \Delta, \ell}^{\sigma\epsilon, \sigma\epsilon}(z, \bar{z}) \\ (-1)^{\ell} F_{-, \Delta, \ell}^{\epsilon\sigma, \sigma\epsilon}(z, \bar{z}) \\ -(-1)^{\ell} F_{+, \Delta, \ell}^{\epsilon\sigma, \sigma\epsilon}(z, \bar{z}) \end{pmatrix},$$

$$\vec{V}_{+, \Delta, \ell} = \begin{pmatrix} F_{-, \Delta, \ell}^{\sigma\sigma, \sigma\sigma}(z, \bar{z}) & 0 \\ 0 & 0 \\ 0 & 0 \\ 0 & F_{-, \Delta, \ell}^{\epsilon\epsilon, \epsilon\epsilon}(z, \bar{z}) \\ \begin{pmatrix} 0 & 0 \\ 0 & 0 \end{pmatrix} \\ \begin{pmatrix} 0 & \frac{1}{2} F_{-, \Delta, \ell}^{\sigma\sigma, \epsilon\epsilon}(z, \bar{z}) \\ \frac{1}{2} F_{-, \Delta, \ell}^{\sigma\sigma, \epsilon\epsilon}(z, \bar{z}) & 0 \end{pmatrix} \\ \begin{pmatrix} 0 & \frac{1}{2} F_{+, \Delta, \ell}^{\sigma\sigma, \epsilon\epsilon}(z, \bar{z}) \\ \frac{1}{2} F_{+, \Delta, \ell}^{\sigma\sigma, \epsilon\epsilon}(z, \bar{z}) & 0 \end{pmatrix} \end{pmatrix}. \quad (104)$$

The appearing functions $F_{\pm, \Delta, \ell}^{ij, kl}$ are given in Eq. (96). One can then look for bounds by making some assumption about the spectrum and searching for a functional $\vec{\alpha} = \sum_{mn} \vec{\alpha}_{mn} \partial_z^m \partial_{\bar{z}}^n [\cdot] |_{z=\bar{z}=1/2}$ satisfying the properties

⁸⁹Further development of SDPB is being carried out within the Simons Collaboration on the nonperturbative bootstrap (<http://bootstrapcollaboration.com/>), and this package will likely remain at the forefront of the numerical bootstrap studies in the coming years.

⁹⁰In this section we are using vector notation to describe the vector of crossing relations rather than derivatives.

$$(1 \ 1) \vec{\alpha} \cdot \vec{V}_{+,0,0} \begin{pmatrix} 1 \\ 1 \end{pmatrix} > 0,$$

$$\vec{\alpha} \cdot \vec{V}_{+,\Delta,\ell} \geq 0 \quad \text{for all } \mathbb{Z}_2\text{-even operators with } \ell \text{ even,}$$

$$\vec{\alpha} \cdot \vec{V}_{-,\Delta,\ell} \geq 0 \quad \text{for all } \mathbb{Z}_2\text{-odd operators.} \quad (105)$$

The novel feature is now that $\vec{\alpha} \cdot \vec{V}_{+,\Delta,\ell} \geq 0$ must be a *positive semidefinite* 2×2 matrix, which makes the search in Eq. (105) a semidefinite programming problem. A similar structure appears for more general systems of mixed or spinning correlators, where if an exchanged operator has N OPE coefficients appearing in the system then the needed positivity condition will be phrased in terms of positive semidefinite $N \times N$ matrices.

2. Polynomial approximations

A different use of semidefinite programming, relevant for either single correlators or mixed correlators, is to avoid any discretization of the exchanged operator dimensions (Poland, Simmons-Duffin, and Vichi, 2012). We first explain the idea for single correlators, where one imposes inequalities of the form

$$\sum_{mn} \alpha_{mn} \partial_z^m \partial_{\bar{z}}^n F_{\Delta,\ell}^{\Delta_\sigma}(z, \bar{z})|_{z=\bar{z}=1/2} \geq 0. \quad (106)$$

Because of the pole expansion of the conformal blocks described in Sec. III.F.4, if one keeps a finite number of poles, then by reorganizing $h_{\Delta,\ell}$ into a rational function of Δ , such derivatives can be rewritten in the form (see Sec. III.F.5)

$$\partial_z^m \partial_{\bar{z}}^n F_{\Delta,\ell}^{\Delta_\sigma}(z, \bar{z})|_{z=\bar{z}=1/2} \approx \chi_\ell(\Delta) P_\ell^{mn}(\Delta), \quad (107)$$

where $P_\ell^{mn}(\Delta)$ is a polynomial in Δ , and $\chi_\ell(\Delta)$ is a positive function for all Δ and ℓ satisfying the unitarity bounds. The degree of the polynomial depends on the number of poles kept in the expansion of the conformal block. Then one simply needs to impose the polynomial inequalities

$$\sum_{mn} \alpha_{mn} P_\ell^{mn}(\Delta_\ell^{\min} + x) \geq 0 \quad (108)$$

for all $x \geq 0$, where the minimum dimension at each spin Δ_ℓ^{\min} depends on the assumptions being made.

Such inequalities for polynomials can be rewritten in terms of positive semidefinite matrices following a theorem of Hilbert (1888). The relevant theorem states that any polynomial $P(x)$ that is non-negative on the interval $[0, \infty)$ can be written in the form

$$P(x) = a(x) + xb(x), \quad (109)$$

where $a(x)$ and $b(x)$ are sums of squares of polynomials. Such sums of squares can in turn always be expressed in the form

$$a(x) = \text{Tr}[A Q_{d_1}(x)], \quad b(x) = \text{Tr}[B Q_{d_2}(x)], \quad (110)$$

where $Q_d(x) \equiv [x]_d [x]_d^T$ is a matrix built out of the monomials $[x]_d = (1, x, \dots, x^d)^T$, $d_1 = \lfloor \frac{1}{2} \deg P \rfloor$, $d_2 = \lfloor \frac{1}{2} (\deg P - 1) \rfloor$, and A and B are some positive semidefinite matrices.

With this rewriting, one needs to search for coefficients α_{mn} and positive semidefinite matrices A_ℓ , $B_\ell \geq 0$ such that

$$\sum_{mn} \alpha_{mn} P_\ell^{mn}(\Delta_\ell^{\min} + x) = \text{Tr}[A_\ell Q_{d_1}(x)] + x \text{Tr}[B_\ell Q_{d_2}(x)]. \quad (111)$$

In practice one must also impose a cutoff on the set of included spins $0 \leq \ell \leq \ell_{\max}$. This search, combined with a normalization condition such as $\vec{\alpha} \cdot \vec{F}_{0,0}^{\Delta_\sigma} = 1$, is now in the form of a semidefinite programming problem.

As explained in detail by Kos, Poland, and Simmons-Duffin (2014a), this idea can also be applied to systems of mixed or spinning correlators where exchanged operators have multiple OPE coefficients appearing in the system. In those cases, after truncating the conformal block pole expansions one imposes constraints of the form

$$\sum_{mn} \vec{\alpha}_{mn} \cdot \begin{pmatrix} \vec{P}_\ell^{(11;mn)}(\Delta) & \dots & \vec{P}_\ell^{(1N;mn)}(\Delta) \\ \vdots & \ddots & \vdots \\ \vec{P}_\ell^{(N1;mn)}(\Delta) & \dots & \vec{P}_\ell^{(NN;mn)}(\Delta) \end{pmatrix} \geq 0$$

for $\Delta \geq \Delta_\ell^{\min}$. (112)

Again there is a theorem that such positive semidefinite matrix polynomials can always be written as sums of squares of matrix polynomials. A consequence, worked out by Kos, Poland, and Simmons-Duffin (2014a), is that each entry can be written as

$$\sum_{mn} \vec{\alpha}_{mn} \cdot \vec{P}_\ell^{(ij;mn)}(\Delta_\ell^{\min} + x) = \text{Tr}[A_\ell^{ij} Q_{d_1}(x)] + x \text{Tr}[B_\ell^{ij} Q_{d_2}(x)] \quad (113)$$

in terms of positive semidefinite matrices $A_\ell^{ij}, B_\ell^{ij} \geq 0$, and the problem is again phrased as a semidefinite programming problem.

C. Bounds and allowed regions

The algorithms described in the previous sections can be used to establish if a given point in the space of CFT data, parametrized by the dimensions of external operators and by assumptions on the exchanged spectrum, belongs to the region allowed by crossing and unitarity. Since the exchanged spectrum contains infinitely many operators, there are infinitely many assumptions one can test. The art of the numerical bootstrap is to choose an interesting assumption, and then to delineate as precisely as possible the allowed region corresponding to this assumption.

As we will see in the next sections, one of the most frequently asked questions is the following: given an OPE $\mathcal{O} \times \mathcal{O}$, derive an upper bound Δ_{\max} on the dimension of the first operator appearing in this OPE having specified

transformation properties under $SO(d)$ (and eventually under a global symmetry G),⁹¹ assuming that other operator dimensions are allowed to take any values allowed by unitarity. One can answer this question, for instance, as a function of $\Delta_{\mathcal{O}}$. This defines an allowed region with a boundary $\Delta_{\max}(\Delta_{\mathcal{O}})$. Similarly, when one obtains an upper (or lower) bound on an OPE coefficient as discussed in Sec. IV.A, this represents the boundary of an allowed region. These boundaries give us a view into the intricate underlying geometry of the space of CFT data allowed by crossing and unitarity.

D. Spectrum extraction

A point in the allowed region (see Sec. IV.C) is specified by external operator dimensions and by a handful of other numbers characterizing the assumptions, such as gaps on the exchanged operator spectrum. Once we ascertained that a point belongs to the allowed region, in some cases it is important to be able to go one step further and to extract an explicit solution to crossing, i.e., the whole spectrum of exchanged operator dimensions and their OPE coefficients. The precise way of doing this depends on which algorithm one uses. An important point is that we expect this solution to be nonunique inside the allowed region, but it should generically become unique on its boundary, as we will now explain.

The spectrum extraction is simplest in the primal simplex method; see Sec. IV.A.1. In this case the spectrum is encoded directly in the set of basic vectors and is available in each step of the algorithm.

In the dual formulation of the linear programming method, one does not have access to the spectrum strictly inside the allowed region. However, one can extract a solution to crossing symmetry from the limiting functional when one approaches a boundary of this region, by extremizing either an operator dimension or OPE coefficient. This is called the *extremal functional method*, introduced by [Poland and Simmons-Duffin \(2011\)](#) and [El-Showk and Paulos \(2013\)](#).

Namely, when approaching the boundary from the disallowed region, the system is on the verge of no longer allowing a separating plane, and the vector on which we require strict positivity is degenerating into the plane. In the case of a single crossing relation where we have imposed strict positivity on the identity operator, as we approach a dimension boundary we can find a vector $\vec{\alpha}$ such that $\vec{\alpha} \cdot \vec{F}_{0,0}^{\Delta_{\sigma}} \rightarrow 0$, together with the sum rule

$$0 = \sum_{\mathcal{O}} \lambda_{\sigma\sigma\mathcal{O}}^2 \vec{\alpha} \cdot \vec{F}_{\Delta_{\mathcal{O}},\ell_{\mathcal{O}}}^{\Delta_{\sigma}}, \quad (114)$$

where $\vec{\alpha} \cdot \vec{F}_{\Delta_{\mathcal{O}},\ell_{\mathcal{O}}}^{\Delta_{\sigma}} \geq 0$ for all other possible (nonidentity) operators in the spectrum. One obtains a similar condition from the OPE coefficient bound in Eq. (102) if one sets the OPE coefficient to its extremal value $\lambda_{\sigma\sigma\mathcal{O}^*}^2 = -\vec{\alpha} \cdot \vec{F}_{0,0}^{\Delta_{\sigma}}$.

In fact, it is easy to see that in order for these sums to hold along the boundary of the allowed region, it is necessary either for $\lambda_{\sigma\sigma\mathcal{O}}^2$ to be zero or for $\vec{\alpha} \cdot \vec{F}_{\Delta_{\mathcal{O}},\ell_{\mathcal{O}}}^{\Delta_{\sigma}}$ to be zero. Thus, the zeros of $\vec{\alpha} \cdot \vec{F}_{\Delta_{\mathcal{O}},\ell_{\mathcal{O}}}^{\Delta_{\sigma}}$ tell us the scaling dimensions and spins at which the OPE coefficients are allowed to be nonzero. The resulting *extremal spectrum* is generically unique ([El-Showk and Paulos, 2013](#)).

In the above-mentioned primal simplex method, the extremal spectrum is reached from within the allowed region and is encoded in the set of basic vectors that remain after the algorithm terminates. That this should agree with the dual approach via extremal functionals is guaranteed by the strong duality of linear programs.

The extremal functional method for extracting the spectrum is also applicable when using semidefinite programming. In this case the extremal functional is constructed in the dual formulation.⁹² Once the extremal spectrum is known, it is straightforward to reconstruct the OPE coefficients of the exchanged operators by either directly solving the bootstrap equations after inputting the extremal spectrum or extracting them from the primal solution of the primal-dual algorithm. [Simmons-Duffin \(2017c\)](#) gave a precise algorithm for doing this using functionals output by SDPB, realized in a PYTHON code ([Simmons-Duffin, 2016a](#)).

An important open question is to understand which CFTs are described by spectra which are extremal with respect to some extremization condition. As we will see in subsequent sections, empirically this seems to be the case for a variety of interesting CFTs including the 3D Ising and $O(N)$ models. Although it is not currently understood why it should be so, some speculations are given in Sec. V.B.3.

1. Flow method

An interesting idea was proposed by [El-Showk and Paulos \(2018\)](#), where given one extremal solution one can efficiently “flow” along the boundary to reconstruct nearby extremal solutions. The idea is to perturb the extremal spectrum and then impose that the perturbed spectrum is also extremal using Eq. (114) as well as the tangency conditions $\vec{\alpha} \cdot (\partial_{\Delta_{\mathcal{O}}} \vec{F}_{\Delta_{\mathcal{O}},\ell_{\mathcal{O}}}^{\Delta_{\sigma}})$. By linearizing perturbations of these conditions, the search for a nearby extremal spectrum (or a more precise extremal spectrum) can be efficiently solved using Newton’s method. This approach then avoids the use of convex optimization after

⁹¹In particular, the existence of a bound with $\Delta_{\max} < \infty$ provides a proof that such an operator exists. See [Rattazzi *et al.* \(2008\)](#) and [Simmons-Duffin \(2017b\)](#), Sec. 10.5, for intuitive explanations involving some numerics of why such bounds should exist at all, and [Hogervorst and Rychkov \(2013\)](#) and [Rychkov \(2016a\)](#), Sec. 4.3.3, for an approximate analytic argument. At present, while the existence of bounds can sometimes be understood via such simple means, their actual values can only be precisely computed using the powerful numerical techniques described in the previous sections. Only in a handful of cases, e.g. [Mazac \(2017\)](#) and [Mazac and Paulos \(2018\)](#), have the best possible bounds been proven analytically.

⁹²It is not understood at present how to formulate an algorithm to extract the extremal spectrum along a dimension bound directly from the allowed region in the context of semidefinite programming. The currently used procedure is to sit in the interior of the space allowed by scaling dimension bounds and extremize an OPE coefficient to find an extremal functional.

the initial step of finding an initial extremal solution and can also be used to flow to nonunitary extremal solutions. This idea was shown to work well in $d = 1$ in [Paulos et al. \(2017\)](#) and [El-Showk and Paulos \(2018\)](#).⁹³ It appears very promising and it needs to be further explored and extended, especially into higher dimensions.

E. Truncation method

Finally we turn to an idea introduced by [Gliozzi \(2013\)](#) and explored in a variety of works,⁹⁴ which we call the truncation method. The basic idea is to truncate the bootstrap equations to a finite number of operators $\{\Delta_\sigma, \mathcal{O}_I\}$ with N unknown scaling dimensions. After normalizing by the identity contribution $f_{\Delta_{\mathcal{O}_I}, \ell_{\mathcal{O}_I}}^{\Delta_\sigma}(z, \bar{z}) \equiv F_{\Delta_{\mathcal{O}_I}, \ell_{\mathcal{O}_I}}^{\Delta_\sigma}(z, \bar{z}) / [-F_{0,0}^{\Delta_\sigma}(z, \bar{z})]$, let us write the crossing equations as

$$\begin{aligned} \sum_{\mathcal{O}_I} \lambda_{\sigma\sigma\mathcal{O}_I}^2 f_{\Delta_{\mathcal{O}_I}, \ell_{\mathcal{O}_I}}^{\Delta_\sigma} &= 1, \\ \sum_{\mathcal{O}_I} \lambda_{\sigma\sigma\mathcal{O}_I}^2 \vec{f}_{\Delta_{\mathcal{O}_I}, \ell_{\mathcal{O}_I}}^{\Delta_\sigma} &= 0. \end{aligned} \quad (115)$$

Here the first equation containing

$$f_{\Delta_{\mathcal{O}_I}, \ell_{\mathcal{O}_I}}^{\Delta_\sigma} \equiv f_{\Delta_{\mathcal{O}_I}, \ell_{\mathcal{O}_I}}^{\Delta_\sigma}(1/2, 1/2)$$

is viewed as an “inhomogeneous” equation containing the identity contribution on the right-hand side, and the second “homogeneous” equation contains the vector of derivatives

$$(\vec{f}_{\Delta_{\mathcal{O}_I}, \ell_{\mathcal{O}_I}}^{\Delta_\sigma})^{mn} = \partial_z^m \partial_{\bar{z}}^n f_{\Delta_{\mathcal{O}_I}, \ell_{\mathcal{O}_I}}^{\Delta_\sigma}(z, \bar{z})|_{z=\bar{z}=1/2}.$$

If one keeps M derivatives with $M > N$ then the system becomes overconstrained and has solutions only if all of the minors of order N of the linear system vanish,

$$\det A_i = 0, \quad A_i \subset A = [(\vec{f}_{\Delta_{\mathcal{O}_I}, \ell_{\mathcal{O}_I}}^{\Delta_\sigma})^{mn}]_{N \times M}. \quad (116)$$

Here the “rows” of A would run over different choices of N derivatives mn and the “columns” run over the N unknown scaling dimensions. Note that the set of unknown scaling dimensions will include the external dimension Δ_σ in addition to the \mathcal{O}_I , but may exclude exchanged operators of known dimension, such as the stress tensor of known dimension $\Delta_T = d$. The general strategy is to solve the determinant conditions Eq. (116) to obtain an approximate spectrum of scaling dimensions and then use the system in Eq. (115), including the inhomogeneous equation, in order to fix the OPE coefficients.

An advantage of the truncation approach over the linear and semidefinite programming approaches of the previous

sections is that it does not require unitarity, i.e., it works equally well for any sign of the OPE coefficients. For example, the idea has been successfully applied to the nonunitary Lee-Yang model, as well as to bulk-boundary bootstrap problems where there is no positivity in the coefficients. Another advantage is that it is relatively simple to implement, and the idea can be explored, e.g., using fairly simple MATHEMATICA notebooks.

On the other hand, we also see several disadvantages with this approach in its current incarnation. One is that the resulting spectrum can have a strong sensitivity to the set of included operators (e.g., the choices of spins) and to the set of derivatives included. It is also very difficult to assign reliable errors to the spectrum output from the method.⁹⁵ Thus, it would be desirable to find ways to make the approach more systematic with errors under control. Some steps in this direction were recently taken by [Li \(2017\)](#). Applications to the boundary bootstrap also seem to be less sensitive to these issues ([Gliozzi, 2016](#); [Gliozzi et al., 2015](#)).

Another issue is that simple implementations of numerical studies of the nonlinear determinant conditions (116), such as using the iterative Newton method implemented in MATHEMATICA’s FINDROOT function, do not scale very well with increasing the number of operators and the method likely needs a more efficient numerical implementation in order to push beyond ~ 10 operators.⁹⁶

Note that since we are truncating the spectrum, we cannot generally expect to find exact solutions of Eq. (116). On the other hand, the set of determinant conditions is in fact redundant because of the Plücker relations satisfied by the minors of a matrix; see [Hikami \(2017b\)](#). A cleaner numerical formulation can be obtained by replacing Eq. (116) with the problem of minimizing the smallest singular value of the matrix A ([Esterlis, Liam Fitzpatrick, and Ramirez, 2016](#); [LeClair and Squires, 2018](#)).

Finally, similar to the extremal spectra methods previously mentioned, it is not clear which CFT spectra are “truncable” in the sense that they can be found with this approach.

V. APPLICATIONS IN $d=3$

In this section we turn to applications of the numerical bootstrap techniques to CFTs in $d = 3$ dimensions. Our discussion is organized as follows. We start in Sec. V.A by presenting a general bound on critical versus multicritical behavior in unitary 3D CFTs. In Secs. V.B and V.C we discuss bootstrap bounds which can be derived under the assumption of a \mathbb{Z}_2 or $O(N)$ global symmetry. Applications to the most famous 3D CFTs realizing these symmetries—the critical 3D Ising and $O(N)$ models—will be emphasized.

In Sec. V.D we describe bounds on CFTs with fermionic operators, such as the IR fixed point of the

⁹³The code is implemented as a separate module of JULIBOOTSTRAP ([Paulos, 2014b](#)), available on request from its author.

⁹⁴See [Gliozzi and Rago \(2014\)](#), [Gliozzi et al. \(2015\)](#), [Gliozzi \(2016\)](#), [Esterlis, Liam Fitzpatrick, and Ramirez \(2016\)](#), [Hikami \(2017a, 2017b, 2018\)](#), [Li \(2017, 2018\)](#), and [LeClair and Squires \(2018\)](#).

⁹⁵Comparison with the rigorous results obtained using the linear and semidefinite programming methods, when possible, shows that the published truncation method errors are often underestimated.

⁹⁶One can view the flow method described in Sec. IV.D.1 as a kind of more efficient implementation where additional extremality conditions have been added.

Gross-Neveu-Yukawa models. In Sec. V.E we discuss what the bootstrap currently has to say about CFTs realizable as IR fixed points of 3D QED coupled to matter. In Sec. V.F we discuss recent bootstrap studies which implement crossing symmetry constraints on 4pt functions of stress tensors and conserved currents. These results are very general as they apply to any local 3D CFT. Finally, in Sec. V.G we highlight some targets that may be interesting to look at in future numerical bootstrap studies.

While most of the results will be phrased in a way which is highly model independent and in the language of conformal field theory, we hope that we can emphasize the physical interpretation of the various assumptions that are being made. All of the results summarized in this section have been obtained under the assumption of unitarity. Nonunitary CFTs, which can be studied, e.g., using the truncation method, are discussed separately in Sec. VIII.

Finally, let us remind the reader that all of the numerical results summarized have been obtained using a variety of methods for numerically computing conformal blocks, with different choices of tolerance parameters in linear or semi-definite programs, with different choices of the cutoff Λ on the number of derivatives applied to the crossing relation, etc. To keep our discussion readable, we will in most cases suppress these details, which can be found described in the original studies.

A. Bounds on critical versus multicritical behavior

As discussed in Sec. II.A, two basic structural characteristics of any CFT are the global symmetry group G and the number of relevant scalar operators S which are singlets under G . For this discussion we view discrete spacetime symmetries such as the spatial parity P , if preserved, as a part of G .

The importance of the number S becomes clear when we try to reach the CFT as an IR fixed point of an RG flow starting from a microscopic description, which for this discussion we assume has the full symmetry G . Later in Sec. V.E.3 we will comment on the situation of emergent symmetries which are not present in the microscopic description.

It follows from basic RG theory that the RG flow can reach the IR fixed point without any fine-tuning if and only if $S = 0$. We call such CFTs “self-organized” by loose analogy with what happens in self-organized criticality (Bak, Tang, and Wiesenfeld, 1987). Examples include QED_3 and QCD_4 in the conformal window to be discussed in Secs. V.E and VI.C.

On the other hand, if relevant singlet scalars are present ($S > 0$), then reaching the fixed point requires fine-tuning S parameters in the microscopic Lagrangian. A common case is when $S = 1$, as is realized for the critical Ising model and $O(N)$ models discussed later. Then we say that we have a critical point. Finally, the case $S > 1$ is classified as a multicritical point.⁹⁷

The simplest example of a 3D multicritical point is the free scalar field ϕ . It has a \mathbb{Z}_2 global symmetry acting as $\phi \rightarrow -\phi$,

⁹⁷ In microscopic realizations which do not have the full symmetry G , one must tune a number of parameters equal to the number of relevant singlets under the microscopic symmetry.

with two relevant singlet scalars ϕ^2 and ϕ^4 of dimensions 1 and 2, respectively. A third singlet scalar ϕ^6 has dimension exactly 3 and is marginal (it is actually marginally irrelevant). This CFT describes a tricritical 3D Ising model. Many nontrivial multicritical fixed points can be realized in systems of multiple interacting scalar fields.

Suppose that we know that we have a critical point, but not a multicritical point, i.e., that there is one and only one singlet scalar, call it \mathcal{O}_0 . The OPE of \mathcal{O}_0 with itself has the schematic form

$$\mathcal{O}_0 \times \mathcal{O}_0 \sim 1 + \lambda \mathcal{O}_0 + \lambda' \mathcal{O}'_0 + \dots, \quad (117)$$

where since \mathcal{O}_0 is a singlet it can appear on the rhs, we denote the next singlet scalar as \mathcal{O}'_0 , and \dots stands for all other operators. In this setup, Nakayama and Ohtsuki (2016) used the numerical bootstrap to derive an upper bound on the dimension of \mathcal{O}'_0 as a function of dimension of \mathcal{O}_0 , shown in Fig. 6. From this plot, the requirement $\Delta_{\mathcal{O}'_0} > 3$ translates into the lower bound

$$\Delta_{\mathcal{O}_0} > 1.044 \quad \text{for any critical 3D CFT.} \quad (118)$$

In terms of the critical exponent $\nu = 1/(3 - \Delta_{\mathcal{O}_0})$, this means that $\nu > 0.511$ for any critical (but not multicritical) 3D fixed point described by a unitary CFT.

Among all critical 3D fixed points that we know of, the lowest $\Delta_{\mathcal{O}_0} \approx 1.41$ is realized in the critical Ising model, see later. This satisfies the general bound (118) by a large margin.

B. \mathbb{Z}_2 global symmetry

1. General results

We are not aware of any unitary 3D CFTs which do not possess any global symmetry.⁹⁸ Actually, most 3D CFTs have continuous global symmetries. Here we start by considering the effect of having a discrete \mathbb{Z}_2 ,⁹⁹ which may be a full symmetry as for the 3D Ising model or a subgroup of a larger group.¹⁰⁰

In the CFT context, a \mathbb{Z}_2 symmetry imposes selection rules on the possible operators appearing in different OPE channels. Let us take a \mathbb{Z}_2 -odd scalar operator σ and consider the $\sigma \times \sigma$ OPE. It can contain only \mathbb{Z}_2 -even operators:

⁹⁸ The Lee-Yang model has no global symmetry but is nonunitary; see Sec. VIII. In any CFT with a global symmetry G , the singlet sector is closed under OPE. From the bootstrap point of view the singlet sector can be studied in isolation, the results of Sec. V.A being an example, and would appear as a perfectly consistent CFT with no global symmetry. Dealing only with local operators, we do not consider this construction as defining a complete CFT, as the singlet sector can in principle be extended back by including the other sectors (although it is not known how to decide in practice whether such an extension is possible by looking at the correlators of the singlet sector).

⁹⁹ The bounds described in this section will also hold if the \mathbb{Z}_2 is taken to be a parity or time-reversal symmetry.

¹⁰⁰ Another physically important discrete symmetry is cubic symmetry; see Sec. V.C.4 and footnote 116.

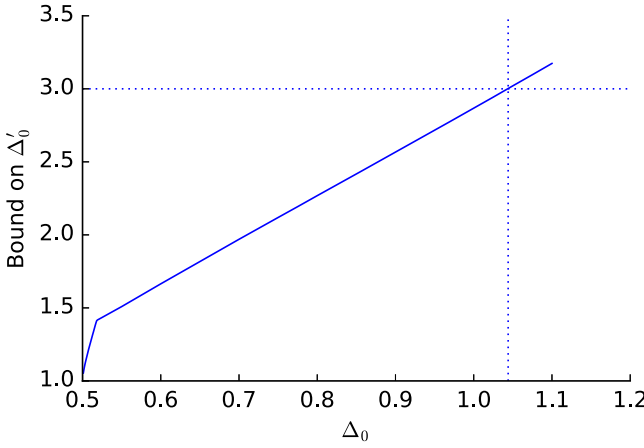


FIG. 6. The upper bound on the dimension of the second singlet scalar \mathcal{O}'_0 as a function of the dimension of the first \mathcal{O}_0 . From Nakayama and Ohtsuki, 2016, Supplementary Material.

$$\sigma \times \sigma \sim 1 + \lambda_{\sigma\sigma\epsilon}\epsilon + \lambda_{\sigma\sigma T}T^{\mu\nu} + \dots \quad (119)$$

Here 1 is the identity operator, ϵ is the leading \mathbb{Z}_2 -even scalar, $T^{\mu\nu}$ is the stress-energy tensor, and so on. In particular, unlike in Eq. (117), σ does not appear in the OPE.

In this setup, we ask what is the maximal allowed value of Δ_ϵ . A numerical bootstrap analysis of the 4pt function $\langle\sigma\sigma\sigma\sigma\rangle$ (via linear or semidefinite programming) produces an upper bound on Δ_ϵ as a function of Δ_σ , shown in Fig. 7.¹⁰¹ The point $\{1/2, 1\}$ corresponds to the theory of a free massless scalar while the point $\sim\{0.518, 1.413\}$, sitting near a discontinuity in the boundary, corresponds to the critical 3D Ising model which we discuss further. Other theories that live in the interior of this region are the critical $O(N)$ models (see Sec. V.C), where we can identify σ with a component of the $O(N)$ fundamental ϕ_i and ϵ with a component of the $O(N)$ symmetric tensor t_{ij} , as well as the line of mean field theory CFTs with $\Delta_\epsilon = 2\Delta_\sigma$ (see Sec. III.I.1).

A particularly physically interesting class of \mathbb{Z}_2 -symmetric CFTs is that with only one relevant \mathbb{Z}_2 -even operator (i.e., they have $S = 1$). If the microscopic realization of the theory preserves the \mathbb{Z}_2 symmetry, then this condition ensures that only one parameter must be tuned in order to reach the critical point. This allowed region in $\{\Delta_\sigma, \Delta_\epsilon\}$ space was also computed by El-Showk *et al.* (2012) from the $\langle\sigma\sigma\sigma\sigma\rangle$ correlator, assuming that all scalars aside from the contribution at Δ_ϵ are irrelevant. This region is shown in Fig. 8, with the assumption having the effect of carving into the allowed region from both the left and the bottom.

Another general result from this 4pt function is a lower bound on the central charge C_T shown in Fig. 9, obtained by computing an upper bound on the coefficient $\lambda_{\sigma\sigma T} \propto \Delta_\sigma / \sqrt{C_T}$ [see Sec. III.H and Eq. (86)]. As $\Delta_\sigma \rightarrow 1/2$, the lower bound on C_T approaches the free scalar value, while near the critical 3D Ising dimension $\Delta_\sigma \sim 0.518$, the lower bound on C_T is

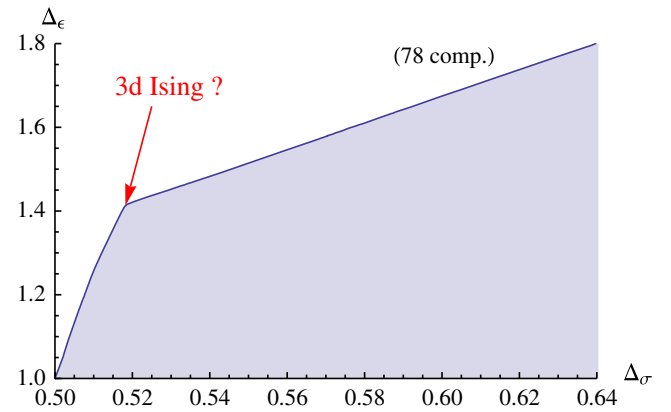


FIG. 7. The upper bound on Δ_ϵ as a function of Δ_σ in 3D CFTs. From El-Showk *et al.*, 2012.

Allowed Region Assuming $\Delta(\epsilon') \geq 3$

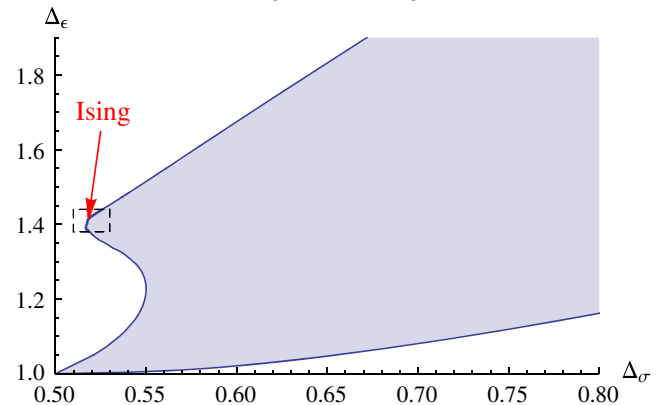


FIG. 8. The allowed region in the $\{\Delta_\sigma, \Delta_\epsilon\}$ plane under the assumption that ϵ is the only relevant scalar. From El-Showk *et al.*, 2012.

seen to have a minimum. This particular bound was computed with the mild assumption $\Delta_\epsilon \geq 1$, so it is applicable to any theory living in the allowed region seen in Fig. 7.

Before we move on to discussing what can be learned from systems of several 4pt functions, we highlight the fact that upper bounds on the leading unknown scaling dimension in other channels can also be computed and are often quite

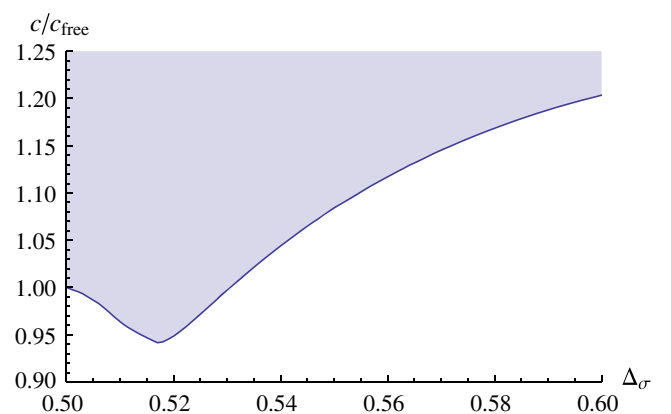


FIG. 9. The lower bound on the central charge as a function of Δ_σ . From El-Showk *et al.*, 2012.

¹⁰¹Nakayama and Ohtsuki (2016) observed empirically that the bounds in Figs. 6 and 7 coincide. *A priori* one may have expected a stronger bound in Fig. 7 due to the extra constraint of not allowing σ on the rhs of the OPE.

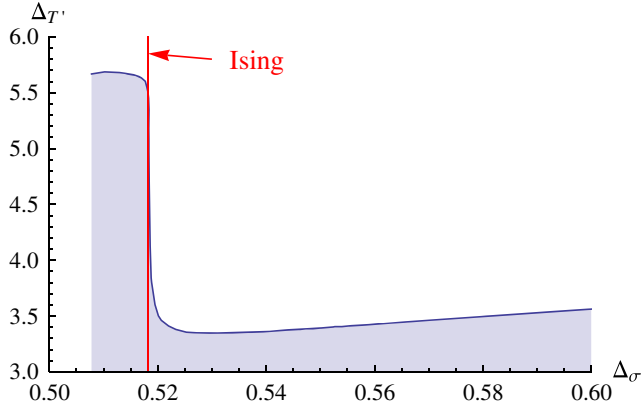


FIG. 10. The upper bound on the dimension $\Delta_{T'}$ of the first \mathbb{Z}_2 -even spin-2 operator after the stress tensor as a function of Δ_σ . From El-Showk *et al.*, 2012.

strong. For example, an upper bound on the leading unknown spin-2 dimension $\Delta_{T'}$ (the first \mathbb{Z}_2 -even spin-2 operator after the stress tensor) is shown in Fig. 10, and an upper bound on the leading spin-4 dimension Δ_C is shown in Fig. 11. The bound on $\Delta_{T'}$ shows a sharp jump near the critical 3D Ising value, while no such transition is seen in the bound on Δ_C (which is close to being saturated by MFT: $\Delta_C = 2\Delta_\sigma + 4$). The jump in $\Delta_{T'}$ shows that it is possible for the low-dimension spin-2 operator present in the spectrum for $\Delta_\sigma \gtrsim 0.52$ to decouple at smaller values of Δ_σ . We discuss operator decoupling phenomena further in Sec. V.B.3.

Next one can ask what is the effect of adding constraints from other 4pt functions. So far the main system that has been studied in the literature is $\{\langle \sigma\sigma\sigma\sigma \rangle, \langle \sigma\sigma\epsilon\epsilon \rangle, \langle \epsilon\epsilon\epsilon\epsilon \rangle\}$, although other systems may also prove interesting. An advantage of including the correlator $\langle \sigma\sigma\epsilon\epsilon \rangle$ is that it allows one to probe the \mathbb{Z}_2 -odd operators appearing in the OPE:

$$\sigma \times \epsilon \sim \lambda_{\sigma\epsilon\sigma}\sigma + \lambda_{\sigma\epsilon\sigma'}\sigma' + \dots \quad (120)$$

Kos, Poland, and Simmons-Duffin (2014a) found that with no assumptions this system leads to an allowed region identical to Fig. 7, while by inputting the assumption of a single relevant \mathbb{Z}_2 -odd operator (i.e., $\Delta_{\sigma'} \geq 3$) it leads to the allowed region shown in Fig. 12. In this plot one can see a detached “island”

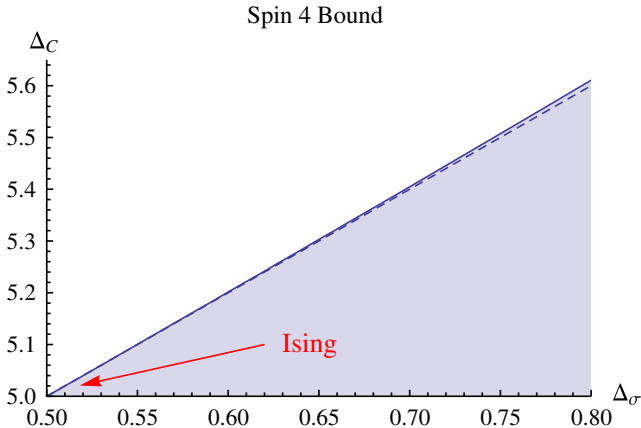


FIG. 11. The upper bound on the dimension of the leading \mathbb{Z}_2 -even spin-4 operator. From El-Showk *et al.*, 2012.

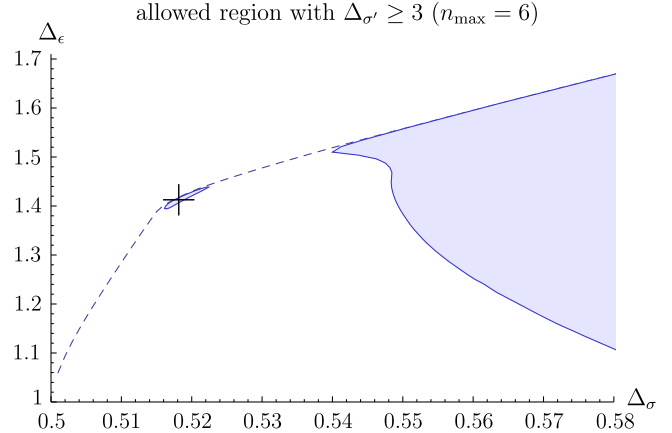


FIG. 12. An allowed region following from the analysis of three 4pt functions assuming $\Delta_{\sigma'} \geq 3$ with no assumption on $\Delta_{\epsilon'}$. From Kos, Poland, and Simmons-Duffin, 2014a.

containing the critical Ising model as well as a “bulk” region further to the right. This bulk region has so far not been systematically explored in the literature: it would be interesting to understand what other CFTs lie inside of it.

In Fig. 13 we also show the difference between assuming $\Delta_{\epsilon'} \geq 3$, $\Delta_{\sigma'} \geq 3$, and both assumptions simultaneously. One can see that the assumption of a gap in the \mathbb{Z}_2 -odd spectrum is primarily responsible for creating the detached region. In the next section we describe the connection to the critical Ising model in more detail, as well as the techniques and additional inputs that can be used to make this detached island as small as possible.

2. Critical Ising model

Perhaps the most well-known 3D CFT is the critical 3D Ising model. The study of this model has a long history (Domb, 1974), in part because it describes critical behavior in uniaxial magnets, liquid-vapor transitions, binary fluid mixtures, the quark-gluon plasma, and more (Pelissetto and Vicari, 2002). While these applications are predominantly for systems in three spatial dimensions at finite temperature, described by a 3D Euclidean CFT, the critical Ising model can

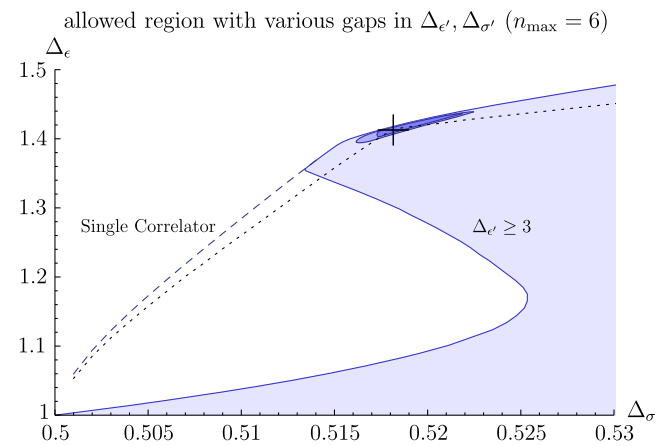


FIG. 13. This plot assumes $\Delta_{\epsilon'} \geq 3$ (light blue), $\Delta_{\sigma'} \geq 3$ (medium blue), or both gaps simultaneously (dark blue). From Kos, Poland, and Simmons-Duffin, 2014a.

also be realized as a Lorentzian $(2+1)$ D quantum critical point (Fradkin and Susskind, 1978; Henkel, 1984). Here we work in the Euclidean signature; the Lorentzian version is obtainable by Wick rotation and has the same set of CFT data.

In its original formulation as a model of ferromagnetism, the 3D Ising model is described using a set of spins $s_i = \pm 1$ on a cubic lattice in \mathbb{R}^3 with nearest neighbor interactions, with the partition function

$$Z = \sum_{\{s_i\}} \exp \left(-J \sum_{\langle ij \rangle} s_i s_j \right). \quad (121)$$

At a critical value of the coupling J , the model becomes a nontrivial CFT at long distances. Note that the lattice model has a manifest \mathbb{Z}_2 symmetry under which $s_i \rightarrow -s_i$. This symmetry is inherited by the CFT, which contains local operators that are either even or odd under its \mathbb{Z}_2 global symmetry.

Another microscopic realization is in terms of a continuous scalar field theory in three dimensions, with action

$$S = \int d^3x \left(\frac{1}{2} (\partial\sigma)^2 + \frac{1}{2} m^2 \sigma^2 + \frac{1}{4!} \lambda \sigma^4 \right), \quad (122)$$

which also has a \mathbb{Z}_2 symmetry under which $\sigma \rightarrow -\sigma$. Because both m^2 and λ describe relevant couplings, this theory is described by a free scalar at short distances but has nontrivial behavior at long distances. At a critical value of the dimensionless ratio m^2/λ^2 the long-distance behavior is described by a CFT, which is the same as for the above lattice model.

From the conformal bootstrap perspective, the Ising CFT has a \mathbb{Z}_2 global symmetry, one relevant \mathbb{Z}_2 -odd scalar operator σ , and one relevant \mathbb{Z}_2 -even scalar operator e . This is evident from experimental realizations, where \mathbb{Z}_2 -preserving microscopic realizations require one tuning (e.g., tuning the temperature in uniaxial magnets) and \mathbb{Z}_2 -breaking microscopic realizations require two tunings (e.g., tuning both temperature and pressure in liquid-vapor transitions).¹⁰² Note that the assumption that the only relevant scaling dimensions are Δ_σ and Δ_e is the same assumption that went into producing the dark blue detached region of Fig. 13.

Kos *et al.* (2016) pursued a numerical analysis of the mixed-correlator bootstrap system containing σ and e to high derivative order. In addition, they studied the impact of scanning over different possible values of the ratio $\lambda_{eee}/\lambda_{\sigma\sigma e}$. This scan effectively inputs the information that there is a single operator in the OPE occurring at the scaling dimension Δ_e , whereas the plot of Fig. 13 allowed for the possibility of multiple degenerate operator contributions at the dimension Δ_e .¹⁰³ This led to the three-dimensional allowed region shown in Fig. 14 and its projection to the

¹⁰²The existence of \mathbb{Z}_2 -breaking liquid-vapor experimental realizations, allowing one to get \mathbb{Z}_2 as an emergent symmetry and predict the total number of relevant scalars, is a nice feature of the Ising model which does not have analogs for the $O(N)$ models.

¹⁰³More precisely, the scan inputs that the outer product of OPE coefficients $(\lambda_{\sigma\sigma e} \lambda_{eee}) \otimes (\lambda_{\sigma\sigma e} \lambda_{eee})$ appearing in Eq. (103) at dimension Δ_e is a rank 1 matrix, rather than the more generic rank 2 possibility which occurs if there are degenerate contributions.

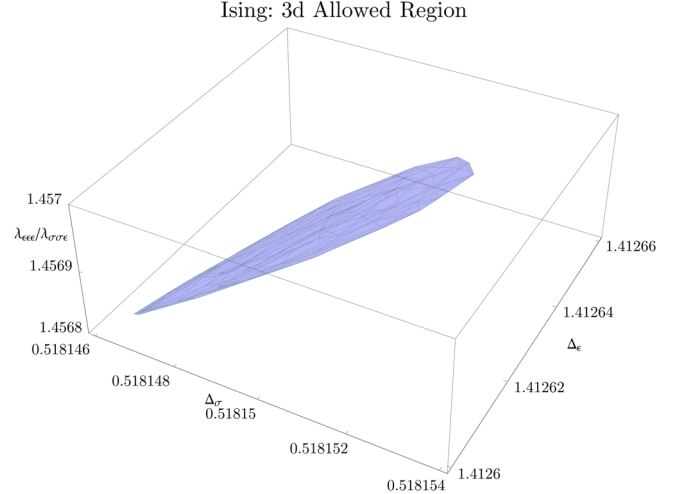


FIG. 14. An allowed region in the $\{\Delta_\sigma, \Delta_e, \lambda_{eee}/\lambda_{\sigma\sigma e}\}$ space obtained by Kos *et al.* (2016).

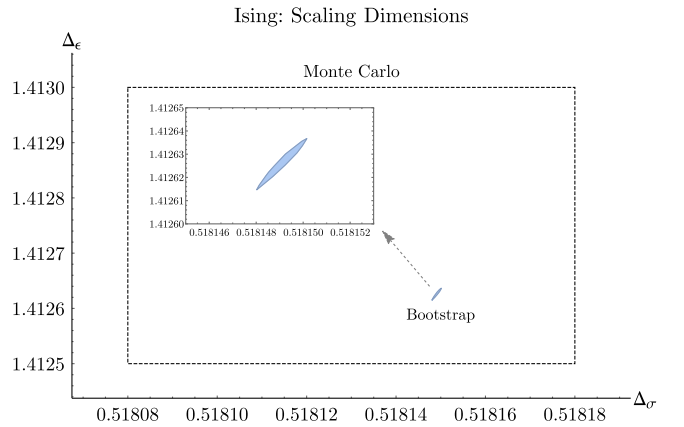


FIG. 15. Projection of the 3D region in Fig. 14 on the $\{\Delta_\sigma, \Delta_e\}$ plane and its comparison with a Monte Carlo prediction for the same quantities. From Kos *et al.*, 2016.

$\{\Delta_\sigma, \Delta_e\}$ plane shown in Fig. 15. In addition, for each point in this region the magnitude of the leading OPE coefficients were also bounded, with the result shown in Fig. 16. These world-record numerical determinations are summarized in Table. II.

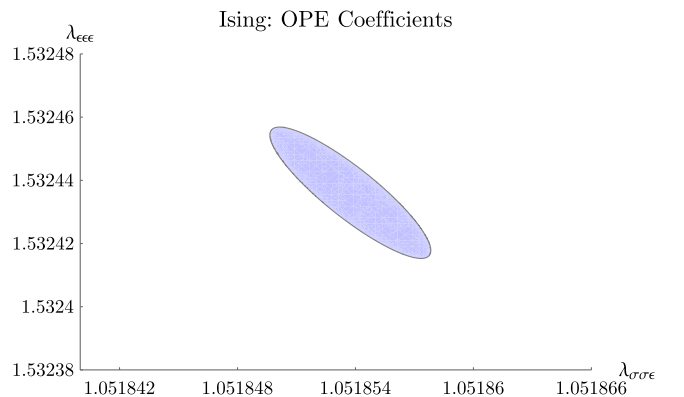


FIG. 16. Variation of λ_{eee} and $\lambda_{\sigma\sigma e}$ within the allowed region in Fig. 14. From Kos *et al.*, 2016.

TABLE II. Stable operators in the critical 3D Ising model with dimensions $\Delta \leq 8$ (Simmons-Duffin, 2017c). Conventional names are shown in the leftmost column when available. Errors in bold are rigorous. All other errors are nonrigorous but, in our opinion, realistic. See Eq. (123) for the central charge prediction from the same study. Because we have chosen a different conformal block normalization convention, the OPE coefficients are related to our convention by $\lambda_{ij\mathcal{O}} = 2^{\ell/2} f_{ij\mathcal{O}}$ (see Table I).

\mathcal{O}	\mathbb{Z}_2	ℓ	Δ	$f_{\sigma\sigma\mathcal{O}}$	$f_{ee\mathcal{O}}$
ϵ	+	0	1.412 625(10)	1.051 8537(41)	1.532 435(19)
ϵ'	+	0	3.829 68(23)	0.053 012(55)	1.536 0(16)
	+	0	6.895 6(43)	0.000 7338(31)	0.127 9(17)
	+	0	7.253 5(51)	0.000 162(12)	0.187 4(31)
$T_{\mu\nu}$	+	2	3	0.326 137 76(45)	0.889 1471(40)
$T'_{\mu\nu}$	+	2	5.509 15(44)	0.010 574 5(42)	0.690 23(49)
	+	2	7.075 8(58)	0.0004 773(62)	0.218 82(73)
$C_{\mu\nu\rho\sigma}$	+	4	5.022 665(28)	0.069 076(43)	0.247 92(20)
	+	4	6.420 65(64)	0.001 955 2(12)	-0.110 247(54)
	+	4	7.385 68(28)	0.002 377 45(44)	0.229 75(10)
	+	6	7.028 488(16)	0.015 741 6(41)	0.066 136(36)
\mathcal{O}	\mathbb{Z}_2	ℓ	Δ	$f_{\sigma e\mathcal{O}}$	
σ	-	0	0.518 148 9(10)	1.051 853 7(41)	
σ'	-	0	5.290 6(11)	0.057 235(20)	
	-	2	4.180 305(18)	0.389 159 41(81)	
	-	2	6.987 3(53)	0.017 413(73)	
	-	3	4.638 04(88)	0.138 5(34)	
	-	4	6.112 674(19)	0.107 705 2(16)	
	-	5	6.709 778(27)	0.041 915 49(88)	

Finally let us mention that recent studies of the conformal bootstrap for stress-tensor 4pt functions have also made contact with the 3D Ising model. In particular, after inputting known values of the leading parity-even spectrum, Dymarsky *et al.* (2018) gave a new bound on the leading parity-odd \mathbb{Z}_2 -even scalar $\Delta_{\text{odd}} < 11.2$ and constrained the independent coefficient in the stress-tensor 3pt function (parametrized by the variable θ) to be in the range $0.01 < \theta < 0.05$ if $\Delta_{\text{odd}} > 3$ and in a tighter range $0.01 < \theta < 0.018$ – 0.019 if Δ_{odd} is close to saturating its bound. We will discuss these constraints in more detail in Sec. V.F.

3. Spectrum extraction and rearrangement

We saw in the previous section the remarkable precision with which the leading scaling dimensions of the critical 3D Ising model can be determined. This raises the immediate question of how well we can extract other operator dimensions and OPE coefficients in the spectrum using bootstrap methods (specifically the strategies described in Sec. IV.D).

Even prior to the mixed-correlator studies already mentioned, El-Showk *et al.* (2014b) extracted the spectrum using the primal simplex method strategy from a solution to crossing for the $\langle\sigma\sigma\sigma\sigma\rangle$ correlator which minimizes the central charge C_T . For example, Fig. 17 shows the scalar operators in the extracted spectrum as a function of Δ_σ near the 3D Ising model. A fascinating feature of these plots is the bifurcation of operators that occurs at the Ising value of Δ_σ , which can be interpreted as a decoupling of one of the operators in the spectrum. This “spectrum rearrangement” phenomenon has yet to be fully understood, but speculatively it could be connected to the nonperturbative equations of motion (i.e., the 3D analog of the relation $\sigma\partial^2\sigma \sim \sigma^4$ at the Wilson-Fisher fixed point) or a higher-dimensional extension

of the null state conditions in the 2D Ising CFT (see also Sec. V.B.4).¹⁰⁴

On the other hand, spectrum extraction using the extremal functional method was applied to the critical 3D Ising model by Komargodski and Simmons-Duffin (2017) and Simmons-Duffin (2017c). In the latter work, for a set of 20 trial points distributed within the island of Fig. 14, C_T minimization was performed and the zeros of the extremal functional were found. While some zeros jump significantly when moving from point to point, many of them are found to be present in all families with tiny variations. About a hundred such “stable zeros” were identified and are believed to represent operators which truly exist in the 3D Ising CFT, providing a remarkable view of the spectrum of this theory. The subset of stable operators with dimensions $\Delta \leq 8$, and their OPE coefficients, are shown in Table II.

This approach, while not fully rigorous, is intuitively justified as a means to extend the reach of rigorous analysis which produced the island in Fig. 14. The errors on stable operator dimensions and OPE coefficients are assigned as standard deviations in the set of trial points. Although these errors are not rigorous, as opposed to rigorous errors implied

¹⁰⁴The 2D analog of Fig. 7 also displays a sharp kink exactly at the location of the 2D Ising model (Rychkov and Vichi, 2009), at which the corresponding extremal solution displays a decoupling of states expected from the null state conditions (El-Showk *et al.*, 2014b). The upper bound to the right of the kink can be interpreted as a one-parameter family of unitary 4pt functions which for a discrete sequence of Δ_σ 's reduce to the 4pt function of the $\phi_{1,2}$ operator in the higher unitary minimal models; see Liendo, Rastelli, and van Rees (2013) and Behan (2017b). While these higher minimal models exhibit further null state conditions, they are not visible in this 4pt function and hence do not lead to kinks in this bound.

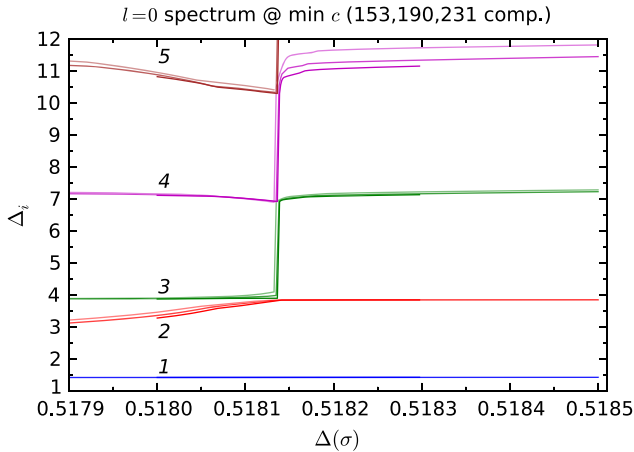


FIG. 17. The spectrum of \mathbb{Z}_2 -even scalar operators appearing in the solution to crossing minimizing C_T near Δ_σ corresponding to the 3D Ising model. Line 1 corresponds to the ϵ operator and shows little variation on the scale of this plot. All other lines exhibit the spectrum rearrangement phenomenon. From El-Showk *et al.*, 2014b.

by Figs. 14, 15, and 16, we believe that they represent realistic estimates. In future studies the error estimates can be further checked by enlarging the set of trial points and by extremizing multiple quantities as opposed to just C_T .

Results of this approach for the leading towers of low-twist operators (of increasing spin) have also been tested against the analytical bootstrap computations in the light cone limit¹⁰⁵ which yield analytical expressions for the large-spin asymptotics. In Fig. 18, the data points extracted from the extremal functional approach show the leading twist ($\tau = \Delta - \ell$) trajectory in the \mathbb{Z}_2 -even sector as a function of $\bar{h} = \ell + \tau/2$, while the curve shows the analytical computation, displaying excellent agreement with the data even down to small spins. Similar good agreement was also found with the extracted OPE coefficients and subleading trajectories as well as in the \mathbb{Z}_2 -odd sector.

We also report here the prediction for the central charge from the above C_T minimization over the 20 points in the island (Simmons-Duffin, 2017a):

$$C_T^{\text{Ising}}/C_T^{\text{free boson}} = 0.946\,538\,9(12), \quad (123)$$

improving the previous C_T -minimization determination by El-Showk *et al.* (2014b).¹⁰⁶

4. Why kink? Why island?

One may be wondering why the 3D Ising model happens to live at a kink in Fig. 7. Plausibly, this has to do with the minimality of the spectrum of exchanged operators required to satisfy the crossing relation. In the interior of the allowed

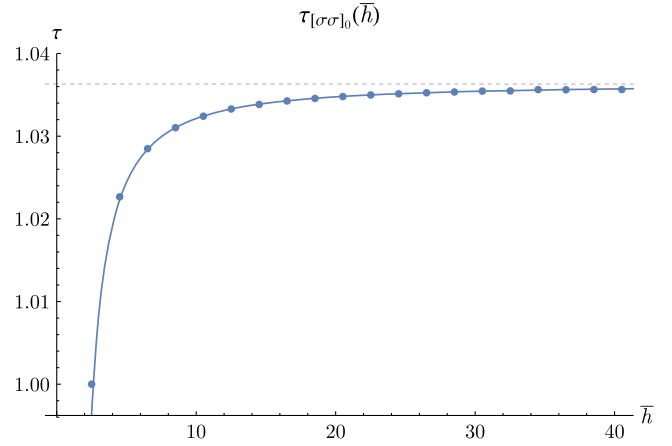


FIG. 18. Comparison of the extremal functional spectrum with the analytic bootstrap; see the text. From Simmons-Duffin, 2017c.

region in Fig. 7, the solution to crossing is not unique. When working numerically, a typical solution contains as many operators as the number of derivatives at $z = \bar{z} = 1/2$ one is keeping in Eqs. (98) and (99). On the other hand, when one approaches the boundary of the allowed region in Fig. 7, the nature of the solution changes in that the operators first organize into pairs with nearby dimensions, and the pairs then merge into single operators at the boundary (El-Showk *et al.*, 2014b). Thus the extremal solutions to crossing are quite economical, containing many fewer operators than the interior solutions, roughly by one-half.¹⁰⁷

Further reduction of the spectrum occurs at the kink. When one approaches the kink moving along the boundary, squared OPE coefficients of certain operators tend to zero. Further analytic continuation of the solution beyond the kink would be inconsistent with unitarity. Thus two different solution branches meet at the kink (El-Showk *et al.*, 2014b), and the spectrum exhibits rearrangement phenomena mentioned in Sec. V.B.3.

To summarize, that the 3D Ising model lives at a kink suggests that it is a CFT with a particularly minimal spectrum of operators. If this idea can be made precise, perhaps it can pave the way to an exact solution.

Leaving the kink aside, let us discuss the island. It is perhaps not surprising that considering crossing for several 4pt functions the allowed region shrinks compared to what was allowed when considering just one 4pt function. It is however altogether unexpected and remarkable that considering only three 4pt functions, plus a physically motivated and

¹⁰⁵See Fitzpatrick *et al.* (2013), Komargodski and Zhiboedov (2013), Alday and Zhiboedov (2017), and Simmons-Duffin (2017c).

¹⁰⁶One can also extract C_T from Table II using $\lambda_{\sigma\sigma T} \propto \Delta_\sigma/\sqrt{C_T}$. While consistent with Eq. (123), this would have a larger error, because the errors on $\lambda_{\sigma\sigma T}$ and Δ_σ are correlated.

¹⁰⁷It is a bit more than half because doubling never occurs for operators which remain at the unitarity bound, such as the stress tensor (if present in the extremal solution), and for operators which saturate the gaps that one is imposing. In general, whether doubling occurs in the bulk of the spectrum depends on how many second-order zeros the extremal functional has. If there are too many zeros, then for some of them, called “singles” by El-Showk and Paulos (2018), doubling will not occur. See also Sec. IV.D.1 for the flow method which uses such considerations to move along the boundary of the allowed region.

robust¹⁰⁸ assumption of only two relevant operators, allows one to produce the tiny island shown in Figs. 12 and 15.

It is not currently understood why this happens. Would the island continue to shrink indefinitely with increasing the number of included derivatives? Or would it stabilize, requiring one to add further correlators to fully fix the CFT? More generally, is it sufficient to include only 4pt functions of relevant operators or are external irrelevant operators also needed to have a unique solution? These are fascinating questions for the future.

We will see many kinks and islands in the subsequent sections of this review, about which similar considerations can be made.

5. Non-Gaussianity

Since the leading spectrum and OPE coefficients of the critical 3D Ising model are now known to a high degree of precision, it is possible to reconstruct the full 4pt function $\langle \sigma\sigma\sigma\sigma \rangle$ over a wide range of cross ratios. One can then probe the question of how much this 4pt function deviates from the “Gaussian,” i.e., fully disconnected, form $\langle \sigma\sigma\sigma\sigma \rangle = \langle \sigma\sigma \rangle \langle \sigma\sigma \rangle + \text{perms}$. This question is also motivated by the fact that the Ising model contains higher-spin operators with dimensions that deviate by a small amount from those of higher-spin currents; see Fig. 18. The first two of these operators are the \mathbb{Z}_2 -even spin-4 and spin-6 operators in Table II, of dimensions close to 5 and 7, respectively.

Rychkov, Simmons-Duffin, and Zan (2017) probed this question quantitatively using bootstrap data to reconstruct the ratio

$$Q(z, \bar{z}) = \frac{g(z, \bar{z})}{1 + (z\bar{z})^{\Delta_\sigma} + [z\bar{z}/(1-z)(1-\bar{z})]^{\Delta_\sigma}}$$

in the critical 3D Ising model, where the denominator corresponds to the Gaussian expectation. A plot of this deviation over a fundamental domain in the complex z plane is shown in Fig. 19. They found, e.g., that $Q < 0.75$ over a wide range of cross-ratio space and that it attains a minimum value of $Q_{\min} \approx 0.683$. Thus, any attempt to explain the small anomalous dimensions of higher-spin operators must account for this significant non-Gaussianity.

6. Boundary and defect bootstrap, nontrivial geometries, off criticality

It is also interesting to study the physics of defects in the 3D Ising model. These include both codimension one defects (e.g., flat 2D boundaries or interfaces) and codimension two defects (i.e., 1D line defects).¹⁰⁹ Here we highlight for the

¹⁰⁸ Islands can also be produced for the Ising and other CFTs using a single 4pt function and reasonable assumptions about gaps in the spin-1 and spin-2 operator spectrum (Li and Su, 2017a). The robustness of these results (i.e., their independence of the numerical values of the assumed gaps in a certain range) needs further investigation.

¹⁰⁹ See Billò *et al.* (2016), Gadde (2016), Lauria, Meineri, and Trevisani (2017), Lemos, Liendo, Meineri, and Sarkar (2017) Rastelli and Zhou (2017), Herzog and Huang (2017), Fukuda, Kobayashi, and Nishioka (2018), and Herzog, Huang, and Jensen (2018) for some recent general discussions of defects in CFT.

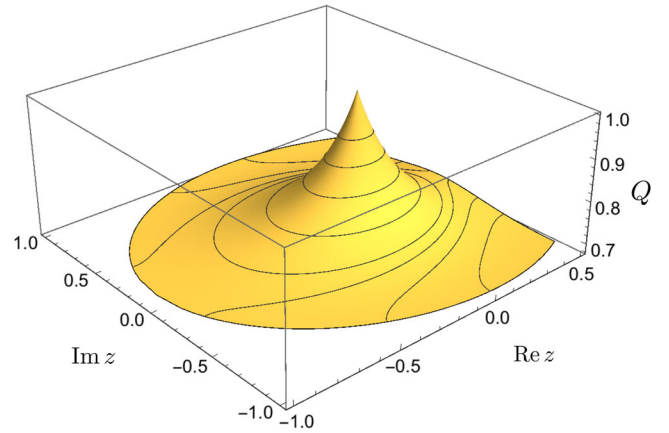


FIG. 19. The non-Gaussianity ratio Q in the critical 3D Ising model. From Rychkov, Simmons-Duffin, and Zan, 2017.

interested reader some recent numerical bootstrap studies of such defects.

Bootstrap constraints in the 3D Ising model in the presence of a flat 2D boundary were first studied using linear programming techniques in Liendo, Rastelli, and van Rees (2013), where a number of rigorous bounds were placed on the scaling dimensions and OPE coefficients of boundary operators for different choices of boundary conditions, corresponding to the “special” and “extraordinary” transitions, assuming positivity of the bulk channel expansion coefficients. Estimates of the leading boundary data using the truncation method were also computed by Gliozzi *et al.* (2015) and Gliozzi (2016), where precise estimates applicable to the boundary condition of the “ordinary” transition could also be made.

Studies have also been performed of the \mathbb{Z}_2 twist line defect in the 3D Ising model, constructed on the lattice by reversing the Ising coupling on a semi-infinite half plane. The 1D boundary of this half plane then yields the twist line defect, which can also be defined in terms of its simple monodromy properties. Local operators living on this defect were studied using both Monte Carlo techniques (Billò *et al.*, 2013) and numerical bootstrap (linear programming) techniques (Gaiotto, Mazac, and Paulos, 2014), with excellent agreement.

A related line of inquiry is to study CFTs such as the critical 3D Ising model on nontrivial geometries, the nontrivial case being manifolds not globally conformally equivalent to infinite flat space.¹¹⁰ This is motivated in part by the search for a higher-dimensional analog of modular invariance. One concrete realization has been to study the 3D Ising model on real projective space (Nakayama, 2016b). In this case the unknown coefficients in one-point functions of scalar primary operators $\langle \mathcal{O} \rangle \propto A_{\mathcal{O}}$ enter into a variant of the bootstrap equations called the cross-cap bootstrap equations. Numerical truncation studies of the cross-cap bootstrap equations in this work have yielded new nontrivial predictions, e.g., $A_\epsilon = 0.667(2)$ and $A_{\epsilon'} = 0.896(5)$ in the critical 3D Ising model on real projective space. Another interesting geometry is

¹¹⁰ CFT correlation functions on manifolds conformally equivalent to flat space, such as the sphere S^d or the “cylinder” $S^{d-1} \times \mathbb{R}$, can be obtained from the flat space correlators via a Weyl transformation.

$S^1 \times \mathbb{R}^{d-1}$, which corresponds to putting the CFT at finite temperature. This was studied for the 3D Ising model and other higher-dimensional CFTs in Iliesiu, Koloğlu *et al.* (2018). Gobeil *et al.* (2018) also discussed a generalization of the conformal block concept relevant for this geometry.

Let us finally mention an interesting study (Caselle, Costagliola, and Magnoli, 2016) which combined the knowledge of the 3D Ising model CFT data acquired by the bootstrap with conformal perturbation theory. They achieved a remarkable agreement with the experimental data describing the 2pt function $\langle \sigma \sigma \rangle$ off criticality, i.e., at temperatures slightly different from the critical temperature, which corresponds to perturbing the CFT by a $\int d^3x \epsilon(x)$ perturbation.

C. $O(N)$ global symmetry

Most known unitary 3D CFTs have a continuous global symmetry, and we now turn to such CFTs. We focus on bootstrap results obtained by assuming $O(N)$ as a full symmetry or as a subgroup.¹¹¹

1. General results

As discussed in Sec. III.G, correlation functions of CFT operators that are in irreducible representations of the global symmetry G can be organized using group theory and decomposed into different G -invariant tensor structures. Section III.I explained how these structures enter the crossing relations. The first numerical analyses of the resulting equations occurred in the context of 4D CFTs,¹¹² but the group theoretic structure is d independent. The bootstrap for $O(N)$ symmetry in 3D was investigated by Kos, Poland, and Simmons-Duffin (2014b), Nakayama and Ohtsuki (2014b), and Kos *et al.* (2015b, 2016).

We start our analysis assuming that the CFT contains an operator $\phi \equiv (\phi_a)_{a=1}^N$ in the fundamental representation of $O(N)$ of dimension Δ_ϕ . Mimicking the discussion in Sec. V.B.1, we want to learn about the operators in the OPE $\phi_a \times \phi_b$. By group theory, operators of even spin ℓ in this OPE will transform as $O(N)$ singlets or symmetric traceless tensors of rank 2, while odd-spin operators will transform in the rank-2 antisymmetric representation.

From the crossing relations for the 4pt function of ϕ one can put upper bounds on the dimensions of various operators. For the lowest dimension scalars ($\ell = 0$) in the singlet (s) and symmetric traceless tensor (t) sector, these bounds are shown in Figs. 20 and 21 as a function of Δ_ϕ for various values of N . The “kinks” in these bounds will be interpreted in the next section.

The $\phi \times \phi$ OPE also contains two interesting operators of spin $\ell \geq 1$: the stress tensor T and the conserved current J . Using the bootstrap one can put lower bounds on their two-point function coefficients C_T and C_J (defined in Sec. III.H) given in Figs. 22 and 23. This is done by bounding from above

¹¹¹All bounds in this section are applicable also under a weaker assumption of $SO(N)$ global symmetry; see Kos *et al.* (2015b), Sec. 2.1.1.

¹¹²See Poland and Simmons-Duffin (2011), Rattazzi, Rychkov, and Vichi (2011a), Vichi (2012), and Poland, Simmons-Duffin, and Vichi (2012).

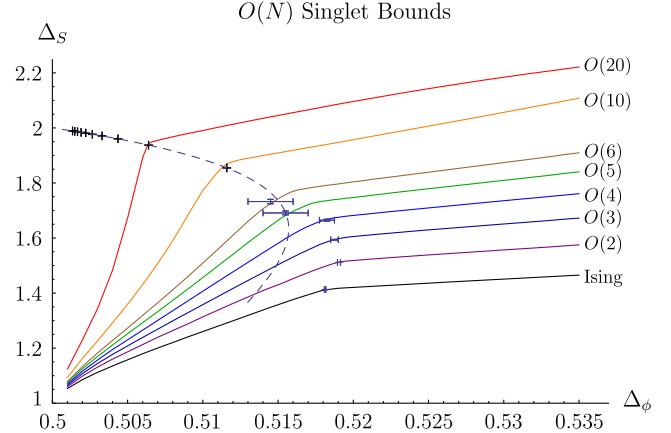


FIG. 20. The upper bound on the dimension of s . From Kos, Poland, and Simmons-Duffin, 2014b.

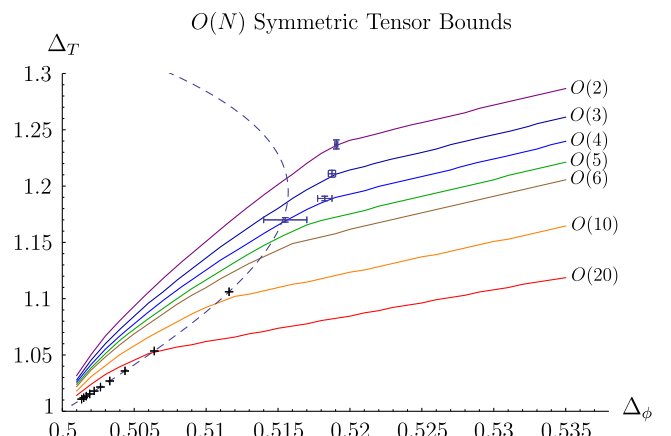


FIG. 21. The upper bound on the dimension of t . From Kos, Poland, and Simmons-Duffin, 2014b.

the OPE coefficients $\lambda_{\phi\phi T} \propto \Delta_\phi / \sqrt{C_T}$ and $\lambda_{\phi\phi J} \propto 1 / \sqrt{C_J}$ [see Eqs. (86) and (90)].

Let us discuss the monotonicity of these bounds with N . Since $O(N+1) \supset O(N)$, the bounds on C_T , C_J , and Δ_t

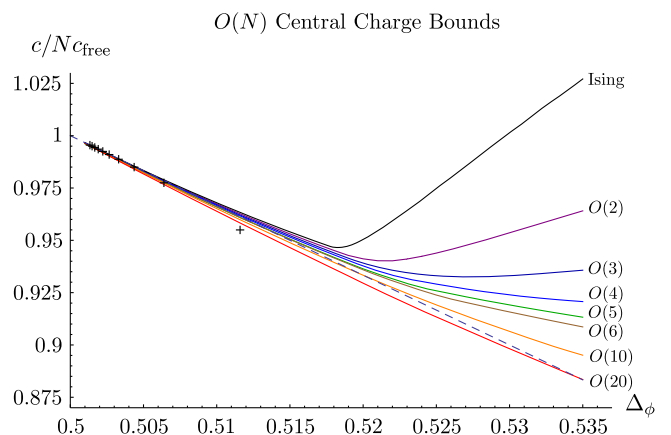


FIG. 22. The lower bound on C_T computed under the assumption $\Delta_s, \Delta_t \geq 1$. From Kos, Poland, and Simmons-Duffin, 2014b.

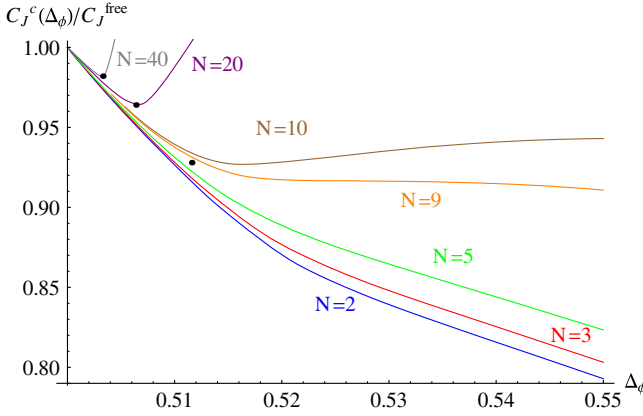


FIG. 23. The Lower bound on C_J . From Nakayama and Ohtsuki, 2014b.

should get stronger with increasing N , and indeed they do (note that C_T is plotted divided by N). Although it may seem counterintuitive that the Δ_s bound gets weaker with N , there is no contradiction. The point is that the symmetric traceless tensor of $O(N+1)$ contains a singlet \tilde{s} when decomposed with respect to $O(N)$. Therefore the only constraint is that the $O(N)$ singlet bound should be weaker than the $O(N+1)$ symmetric traceless bound, which is satisfied by inspection.

Note also that the scaling of the C_T, C_J bounds with N close to $\Delta_\phi = 1/2$ is consistent with the fact that in the theory of N free scalars, C_T grows linearly with N while C_J is constant.

2. Critical $O(N)$ model

The most famous 3D CFT with $O(N)$ symmetry is the critical point of the $O(N)$ lattice model, which is the generalization of Eq. (121) to N -component spins satisfying the constraint $|\vec{s}| = 1$. This CFT is also known as the Wilson-Fisher fixed point, being an IR fixed point of the $O(N)$ symmetric scalar field theory with quartic interaction (Wilson and Fisher, 1972). For any integer N this 3D CFT is unitary, given that the microscopic realizations are unitary.¹¹³

It is natural to ask where the critical $O(N)$ models lie in the parameter space of $O(N)$ symmetric CFTs allowed by the general bounds from the previous section. In the Wilson-Fisher description, ϕ_a is the fundamental scalar field appearing in the Lagrangian, $s = \phi^2$, and t is the traceless part of $\phi_a\phi_b$. Dimensions of these fields have been previously estimated using RG methods (in particular, the ϵ expansion and the large N expansion), Monte Carlo studies, and experiments. Comparing the s and t bounds and these prior determinations, marked with crosses in Figs. 20 and 21, one is led to conjecture that the critical $O(N)$ models correspond to the kinks. Similar kinklike features are visible

in the lower bounds on C_J and C_T . In the latter case the kinks can be made sharper by imposing that the S operator saturate the gap; see Fig. 5 in Kos, Poland, and Simmons-Duffin (2014b). This conjecture can be used to extract values of the ϕ, s, t dimensions and of C_T , given in Table 3 of Kos, Poland, and Simmons-Duffin (2014b).

We now discuss how to isolate the critical $O(N)$ models without relying on the kink conjecture. The idea is to exploit the crucial physical feature of these CFTs—that they possess robust gaps in the operator spectrum. The singlet scalar s corresponds to the temperature deformation of the critical point and is relevant. The next singlet scalar s' must necessarily be irrelevant (otherwise the critical point would be multicritical), implying the gap $\Delta_{s'} \geq 3$ in the singlet scalar sector. We also expect a gap in the fundamental representation scalar sector. The order parameter ϕ_a belongs to this sector and is relevant, while most likely the next fundamental scalar is irrelevant: $\Delta_{\phi'} \geq 3$. This can be also deduced using the Wilson-Fisher description, using a nonrigorous but suggestive equation of motion argument (Kos et al., 2015b).

Kos et al. (2015b) studied bootstrap constraints for the system of three correlators $\{\langle \phi_a \phi_b \phi_c \phi_d \rangle, \langle \phi_a \phi_b s s \rangle, \langle s s s s \rangle\}$. Imposing the assumptions $\Delta_{s'} \geq 3$ and $\Delta_{\phi'} \geq 3$, they found small allowed regions (“islands”) shown in Fig. 24. Improved versions of these islands for $O(2)$ and $O(3)$, discussed in the next sections, were subsequently obtained by Kos et al. (2016). It is important to stress that, as in Fig. 12 for the Ising model, there are disconnected allowed regions outside the shown part of the parameter space; see, e.g., Fig. 25 for the $O(2)$ case. These regions are practically unexplored and they might contain other interesting CFTs.

3. $O(2)$ global symmetry

We finally discuss separately specific values of N starting with $O(2) \supset U(1)$. There are many physically interesting 3D CFTs possessing $O(2)$ or $U(1)$ symmetry. The most famous of these is the critical $O(N)$ model for $N = 2$, also known as the critical XY model. It describes, in particular, the Curie point of easy-plane ferromagnets, and of easy-plane antiferromagnets on bipartite lattices. Here the $O(2)$ symmetry arises as the symmetry of local magnetic moment interactions.

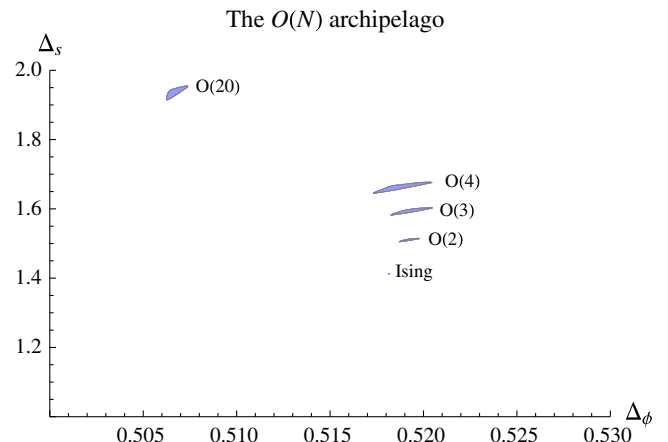


FIG. 24. The $O(N)$ archipelago. From Kos et al., 2015b.

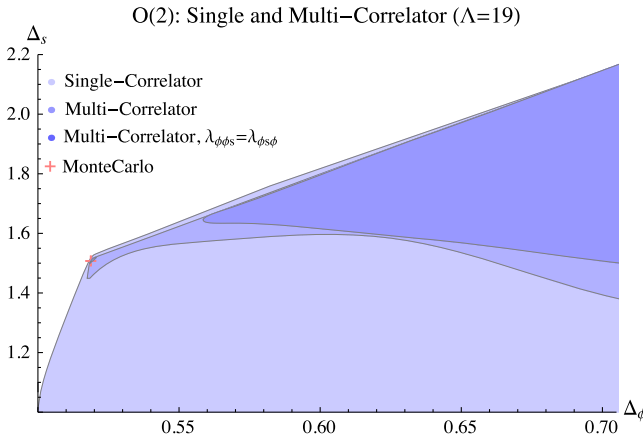


FIG. 25. Allowed regions in the parameter space of $O(2)$ or $U(1)$ symmetric CFTs. The strongest constraint (dark blue) has been obtained from the analysis of three correlators $\{\langle \phi\phi\phi\phi \rangle, \langle \phi\phi ss \rangle, \langle ssss \rangle\}$, assuming that s and ϕ are the only two relevant scalars of charge 0 and 1, and imposing the OPE coefficient relation $\lambda_{\phi\phi s} = \lambda_{\phi s\phi}$. From Kos *et al.*, 2015b.

Another frequent appearance of $U(1)$ symmetry in condensed matter physics is as particle number conservation. The most famous such $U(1)$ transition is the superfluid transition in ${}^4\text{He}$. Another example is the superfluid-insulator quantum phase transition in the $(2+1)\text{D}$ Bose-Hubbard model at integer particle density (Fisher *et al.*, 1989). Both these transitions are also described by the critical $O(2)$ model.

A wide class of CFTs with $U(1)$ global symmetry are IR fixed points of theories which at the microscopic level contain $U(1)$ gauge fields coupled to fermion or scalar matter. The global $U(1)$ symmetry in these theories is topological in origin, and the local operators charged under it are monopoles of the gauge field. These CFTs often appear in condensed matter applications; they will be discussed in more detail in Sec. V.E.

Here we discuss general constraints from the multiple correlator bootstrap for $U(1)$ symmetric CFTs, which have been pursued further than in the general $O(N)$ case previously discussed.

Operators in $U(1)$ theories are classified by their $U(1)$ charge, with s, ϕ, t of the previous section¹¹⁴ having charge 0, 1, and 2. Imposing the constraints that there is a unique relevant charge 1 and a unique relevant charge 0 scalar, one gets the allowed region shown in dark blue in Fig. 25. Note that this region consists of a detached island to which the critical $O(2)$ model belongs, and a further region on the right, similar to Fig. 12 for the Ising model.

The island containing the critical $O(2)$ model has been studied more accurately by Kos *et al.* (2016) by increasing the derivative order and performing a scan over the OPE coefficient ratio $\lambda_{sss}/\lambda_{\phi\phi s}$. This led to the improved constraints

¹¹⁴Instead of vectors and tensors of $O(2)$ here we use, as is customary, complex fields charged under $U(1) \subset O(2)$. In the bootstrap studies we describe the distinction between $U(1) = SO(2)$ and $O(2)$ is unimportant, so the constraints will apply to either symmetry (see footnote 111).

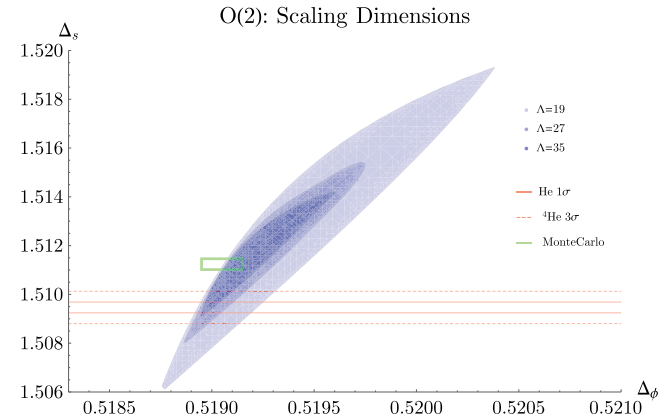


FIG. 26. Allowed islands in the mixed correlator analysis of $O(2)$ or $U(1)$ symmetric CFTs after performing a scan over the OPE coefficient ratio $\lambda_{sss}/\lambda_{\phi\phi s}$. From Kos *et al.*, 2016.

shown in Fig. 26. The resulting dimensions and OPE coefficients are given in Table III.

In Table III we give the determinations of Δ_t and C_J obtained by Kos *et al.* (2015b) by scanning over the allowed island in the $\{\Delta_\phi, \Delta_s\}$ plane, under the respective assumptions that $\Delta'_t \geq 3$ and $\Delta'_{J'} \geq 3$.¹¹⁵

These results are compatible but somewhat less precise in the case of Δ_ϕ , Δ_s , and Δ_t than other available determinations by lattice and RG methods; see Kos *et al.* (2015b, 2016) for references. In particular, a further increase in precision is required to resolve the discrepancy between the experimental and theoretical determinations of Δ_s shown in Fig. 26. This is an important problem for the future. On the other hand, the bootstrap is currently the only source of information about the OPE coefficients $\lambda_{\phi\phi s}$ and λ_{sss} . The central charge C_J is related to the zero-temperature (or high-frequency) conductivity of the quantum critical points described by the critical $O(2)$ model. Although not yet experimentally measured, this parameter has been extensively studied theoretically and numerically in the condensed matter literature. As discussed by Kos *et al.* (2015b), the bootstrap currently provides the best determination of C_J .

4. $O(3)$ global symmetry

We now specialize to the case of $O(3)$ global symmetry, focusing on the most famous such CFT which is the critical $O(3)$ model. Apart from describing the critical point of isotropic ferromagnets, the same CFT also describes the $(2+1)\text{D}$ quantum critical point in coupled dimer antiferromagnets; see Sachdev (2004) and references therein.

The bootstrap analysis of this theory mimics the $U(1)$ case from the previous section. Under the assumption that ϕ_a and s are the only two relevant scalars transforming in the fundamental and trivial representation of $O(3)$, Kos *et al.* (2016) found an island allowed by the bootstrap constraints shown in

¹¹⁵As before, we denote by a prime the subleading operator with the same quantum numbers. So t' is the next traceless symmetric scalar after t , and J' is the next vector after the conserved current J_μ , transforming in the antisymmetric $SO(N)$ representation.

TABLE III. Bootstrap results for the operator dimensions and OPE coefficients in the critical $O(2)$ and $O(3)$ models (see Secs. V.C.3 and V.C.4).

	$O(2)$	$O(3)$
Δ_ϕ	0.519 26(32)	0.519 28(62)
Δ_s	1.511 7(25)	1.595 7(55)
$\lambda_{sss}/\lambda_{\phi\phi s}$	1.205(9)	0.953(25)
$\lambda_{\phi\phi s}$	0.687 26(65)	0.524 4(11)
λ_{sss}	0.828 6(60)	0.499(12)
Δ_t	1.235 7(33)	1.210(6)
$C_J/C_{J\text{free}}$	0.905 0(16)	0.906 5(27)

Fig. 27. The bootstrap determinations of the scaling dimensions and OPE coefficients following from this analysis are given in Table III. As for the $U(1)$ case, the scaling dimension determinations are compatible but somewhat less precise than the best available Monte Carlo and RG results.

One long-standing question about the critical $O(3)$ model concerns its stability with respect to perturbations which may potentially lead to two different CFTs, the so-called cubic and biconical fixed points, which have symmetries $B_3 = S_3 \rtimes (\mathbb{Z}_2)^3$ and $O(2) \times \mathbb{Z}_2$, respectively. These perturbations take the form $K^{ijkl}\Phi_{ijkl}$, where Φ is a scalar operator transforming in the rank-4 symmetric traceless representation of $O(3)$, and K is a constant tensor breaking $O(3)$ to one or the other subgroup. RG calculations indicate that the $O(3)$ fixed point is unstable while the cubic and biconical fixed points are stable, with the correction to scaling critical exponents $\omega_{O(3)} = -0.013(6)$ and $\omega_{B_3} = 0.010(4)$ or 0.015(2) according to two calculations; see Pelissetto and Vicari (2002) Secs. 11.3 and 11.7, and references therein. This would imply that $\Delta_\Phi = 3 + \omega_{O(3)}$ is very weakly relevant. From the bootstrap point of view, Φ appears in the OPE $t \times t$, and its dimension could be determined by an analysis involving correlators of t . This is an interesting problem for the future.¹¹⁶

Let us mention another 3D CFT with an $O(3)$ global symmetry—the critical Gross-Neveu-Heisenberg (GNH) model (Herbut, Juricic, and Vafeck, 2009), realized as the IR fixed point of a microscopic Lagrangian with Yukawa and quartic couplings

$$g\bar{\Psi}\sigma^i\phi_i\Psi + \lambda(\phi_i^2)^2, \quad (124)$$

where ϕ_i is a three-component scalar order parameter, and Ψ is a two-component multiplet of massless Dirac fermions. This CFT is believed to describe the continuum limit of the Hubbard model on the honeycomb and π -flux lattices (Sachdev, 2010). While clearly distinct from the critical $O(3)$ model, the scalar sector of this theory would be subject

¹¹⁶Preliminary investigations of the $\langle tttt \rangle$ bootstrap have produced bounds that still allow Φ to be irrelevant (Kos *et al.*, 2015a; Nakayama and Ohtsuki, 2016). See also Rong and Su (2017) and Stergiou (2018) for recent bootstrap studies of 3D CFTs assuming cubic and related discrete symmetries. The latter finds evidence that there may be two different critical 3D theories with cubic symmetry, one of which is related to the physics of magnets, while the other may describe structural phase transitions in perovskites.

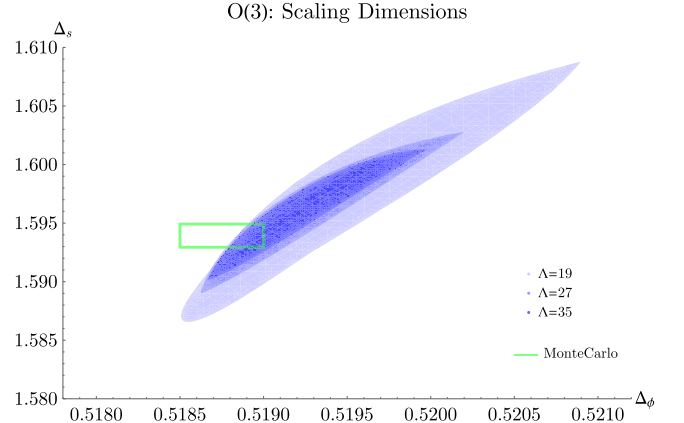


FIG. 27. The $O(3)$ analog of Fig. 26. From Kos *et al.*, 2016.

to the general $O(3)$ bounds shown in Figs. 20–23. However, the expected value of $\Delta_\phi \approx 0.85$ (Parisen Toldin *et al.*, 2015) [Eq. (25)] puts it outside of the region explored so far. The fermionic sector of this theory could be constrained by methods from the next section.

D. CFTs with fermion operators

1. Models

The preceding sections discussed constraints from crossing relations for 4pt functions of scalar operators. Many 3D or $(2+1)$ D CFTs of theoretical and experimental interest also contain fermionic operators, and here we discuss what the bootstrap has so far been able to say about them.

Perhaps the simplest example is the family of CFTs described by the Gross-Neveu model at criticality (Gross and Neveu, 1974).¹¹⁷ While the critical theory is often described as the UV fixed point in a theory of fermions with 4-fermi interactions $\mathcal{L} \sim (\bar{\psi}\psi)^2$, a better nonperturbative definition is as an IR fixed point in a theory with a scalar field coupled to fermions via Yukawa interactions. The latter Gross-Neveu-Yukawa (GNY) model contains a scalar ϕ and N Majorana fermions ψ_i :

$$\mathcal{L}_{\text{GNY}} = \frac{1}{2} \sum_{i=1}^N \bar{\psi}_i (\partial^\mu + g\phi)\psi_i + \frac{1}{2} \partial^\mu \phi \partial_\mu \phi + \frac{1}{2} m^2 \phi^2 + \lambda \phi^4. \quad (125)$$

This model has an $O(N)$ symmetry rotating the fermions. A fixed point can be established perturbatively at large N in a $1/N$ expansion; see, e.g., Gracey (1992, 1994) and Derkachov

¹¹⁷This model and its variations are frequently invoked to describe quantum phase transitions in condensed matter systems with emergent Lorentz symmetry in $(2+1)$ D. Some examples of its applications include models for phase transitions in graphene (Herbut, 2006; Herbut, Juricic, and Vafeck, 2009), the Hubbard model on the honeycomb and π -flux lattice (Parisen Toldin *et al.*, 2015), models of time-reversal symmetry breaking in d -wave superconductors (Vojta, Zhang, and Sachdev, 2000; Vojta, 2003), and models of three-dimensional gapless semiconductors (Moon *et al.*, 2013; Herbut and Janssen, 2014).

et al. (1993). This model has also been studied extensively from the perspective of the ϵ expansion, with recent results by Fei *et al.* (2016), Mihaila *et al.* (2017), and Zerf *et al.* (2017).

An interesting special case is $N = 1$ (a single Majorana fermion coupled to a real scalar). It is expected (Fei *et al.*, 2016) that this model may contain a fixed point with $\mathcal{N} = 1$ supersymmetry. This supersymmetric fixed point has been proposed to describe a critical point on the boundary of topological superconductors (Grover, Sheng, and Vishwanath, 2014).

There are variations of this model containing multiple scalar order parameters. One notable example is the $\mathcal{N} = 2$ supersymmetric critical Wess-Zumino model, containing a complex scalar related to a 3D Dirac fermion by supersymmetry.¹¹⁸ This theory has been proposed to describe a critical point on the surface of topological insulators (Grover, Sheng, and Vishwanath, 2014; Ponte and Lee, 2014), and a superconducting critical point in $(2 + 1)$ D Dirac semimetals with an attractive Hubbard interaction (Li *et al.*, 2017). Another important example is the Gross-Neveu-Heisenberg model, described in Sec. V.C.4.

2. General results

We first discuss general results following from the existence of fermionic operators. Specialized bounds where the critical GNY and other models are featured more prominently will be discussed later.

A bootstrap analysis of 4pt functions of identical Majorana fermions $\langle \psi\psi\psi\psi \rangle$ was performed by Iliesiu *et al.* (2016a) and extended to 4pt functions $\langle \psi_i\psi_j\psi_k\psi_l \rangle$ containing fermions that are vectors under an $O(N)$ symmetry by Iliesiu, Kos *et al.* (2018). These studies both assumed a general $(2 + 1)$ D CFT with parity symmetry. Tensor structures and conformal blocks for 4pt functions were derived using a spinorial embedding-space formalism also developed by Iliesiu *et al.* (2016a), similar in logic to the vectorial embedding space reviewed in the Appendix.

In Fig. 28 we show general upper bounds on the leading parity-odd and parity-even scalars in the $\psi \times \psi$ OPE, called σ and ϵ , respectively. The bound on σ is nearly saturated by the MFT line $\Delta_\sigma = 2\Delta_\psi$, at least at small values of Δ_σ . As $\Delta_\psi \rightarrow 1$ the bound approaches the free theory value $\Delta_\sigma = 2$, where we can identify $\sigma = \bar{\psi}\psi$. On the other hand, there is an abrupt discontinuity in the bound around $\Delta_\psi \sim 1.27$ occurring when Δ_σ approaches 3. This jump also coincides with a kink in the bound on Δ_ϵ . The interpretation of these features is currently an open question—it is tempting to speculate that a CFT may live at the top of the jump in the bound on Δ_σ and in the kink in the bound on Δ_ϵ but no concrete candidate CFTs have yet been identified. If it exists, this CFT would appear to have an unusual property of not possessing any relevant scalar deformations.¹¹⁹

¹¹⁸We describe some of the implications of supersymmetry and a bootstrap analysis connecting to this model later in Sec. VII.

¹¹⁹Hypothetical theories with this property were recently named “dead-end” CFTs by Nakayama (2015a). They should be distinguished from “self-organized” CFTs which do not have any relevant singlet scalars as defined in Sec. V.A.

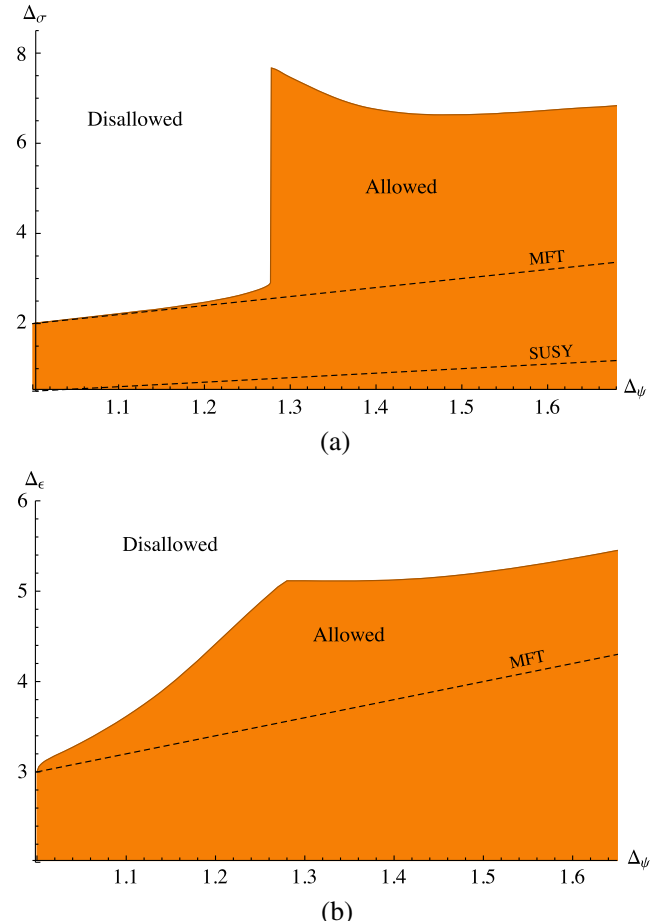


FIG. 28. The upper bounds on the dimension of (a) the first parity-odd scalar σ and (b) the first parity-even scalar ϵ in the OPE $\psi \times \psi$ as a function of Δ_ψ . Here ψ is a Majorana fermion primary operator in a 3D parity-invariant unitary CFT. From Iliesiu *et al.*, 2016a.

In Fig. 29 we also show the general lower bounds on the central charge C_T (normalized to its value in the theory of a free Majorana fermion), obtained by bounding the coefficient of the stress-tensor conformal block. These lower bounds approach the free values as $\Delta_\psi \rightarrow 1$ and disappear completely for $\Delta_\psi \gtrsim 1.47$. In the case of $O(N)$ symmetry they can be seen to grow linearly with N and are compatible with values computed in the $1/N$ expansion of the GNY model. Generalizations to the current central charge C_J for fermions charged under $O(N)$ symmetry were also computed by Iliesiu, Kos *et al.* (2018).

3. Gross-Neveu-Yukawa models

In the critical GNY model at large N , ψ_i has dimension $1 + 4/(3\pi^2 N) + \dots$, while the leading parity-odd scalars in the $\psi_i \times \psi_j$ OPE are the $O(N)$ singlet ϕ with dimension $1 - 32/(3\pi^2 N) + \dots$ and the $O(N)$ symmetric tensor $\bar{\psi}_i\psi_j$ with dimension $2 + 32/(3\pi^2 N) + \dots$ (Iliesiu, Kos *et al.*, 2018, Table 1). The accumulation point $(\Delta_\psi, \Delta_\sigma) \rightarrow (1, 1)$ sits well in the interior of Fig. 28(a), but by imposing a gap until the second parity-odd scalar, $\Delta_{\sigma'} \geq 2 + \delta$ for different positive

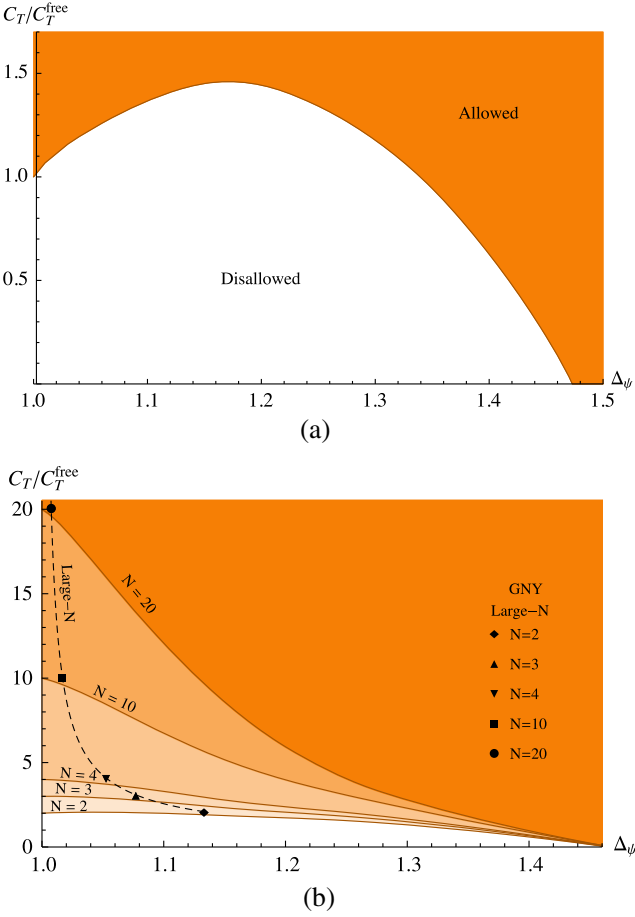


FIG. 29. The lower bounds on C_T as a function of Δ_ψ , where ψ is (a) a Majorana fermion or (b) a multiplet of Majorana fermions in the fundamental representation of an $O(N)$ global symmetry group. From Iliesiu *et al.*, 2016a and Iliesiu, Kos *et al.*, 2018.

values of δ , we have the possibility of obtaining an allowed region that rules out critical GNY models with N sufficiently large.

This is realized in Fig. 30, where the effects of gaps ranging from $\Delta_{\sigma'} \geq 2.01$ to $\Delta_{\sigma'} \geq 2.9$ are shown. At very small values of δ the lower bounds of the allowed regions possess a kink whose location matches very well to the large- N GNY model prediction. At larger values of δ , the precise map between δ and N is not known but it is plausible that the kinks continue to match to the GNY model even at small values of N . However, starting around $\Delta_{\sigma'} \geq 2.3$, a second lower feature also appears in these curves, where they all intersect and have an additional kink at a point near $(1.08, 0.565)$.

This structure of an “upper” and a “lower” kink can be seen clearly in Fig. 31, specialized to the case $\Delta_{\sigma'} \geq 3$. In fact, in this case the line $\Delta_\psi = \Delta_\sigma + 1/2$ expected for theories with supersymmetry comes very close to (but just misses) the upper kink. Thus, it is tempting to conjecture that the $\mathcal{N} = 1$ supersymmetric Gross-Neveu-Yukawa model (see Sec. V.D.1) may sit in this feature and has $\Delta_{\sigma'}$ slightly smaller than 3. This picture seems consistent with estimate $\Delta_{\sigma'} \approx 0.59$ from a Padé extrapolation of the ϵ expansion (Fei *et al.*, 2016), as well as with the rigorous lower bound $\Delta_{\sigma'} \geq 0.565$ (Bashkirov, 2013).

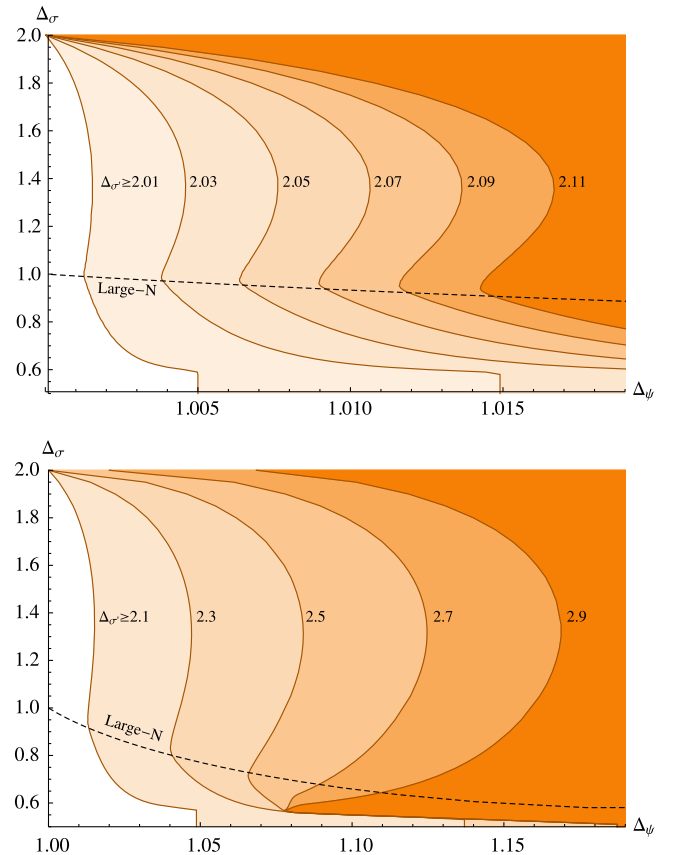


FIG. 30. The effect of imposing a gap until the second pseudoscalar σ' on the parameter space of 3D parity-invariant CFTs. From Iliesiu *et al.*, 2016a.

which follows using another supersymmetric relation $\Delta_e = \Delta_\sigma + 1$ together with the bootstrap bound in Fig. 7, applicable with parity playing the role of a \mathbb{Z}_2 symmetry.¹²⁰ An additional speculation is that the lower feature may coincide with a nonsupersymmetric fixed point, called GNY* by Iliesiu, Kos *et al.* (2018), which is seen in the ϵ expansion as a nonunitary fixed point at large N , but whose fate at small N and $\epsilon \rightarrow 1$ is not known.

Additional evidence for this picture comes from the generalization of the bounds to $O(N)$ symmetry (Iliesiu, Kos *et al.*, 2018), where one can place independent bounds on different $O(N)$ representations. In Fig. 32 we show computed bounds on the leading singlet dimension Δ_σ , assuming that the next singlet is irrelevant, $\Delta_{\sigma'} \geq 3$. These bounds also show both an upper and a lower kink, which appear not too far from the ϵ -expansion estimates for the GNY and GNY* models. In Fig. 33 we also highlight the bounds on the leading $O(N)$ symmetric tensor σ_T , which display

¹²⁰Further progress on this CFT was made very recently by Rong and Su (2018) and Atanasov, Hillman, and Poland (2018), where it was understood how to obtain an island in the scalar mixed-correlator bootstrap around $\Delta_\sigma = 0.584\,444(30)$. In these studies in addition to relations between scaling dimensions it is important to incorporate nontrivial 3D $\mathcal{N} = 1$ superconformal blocks.

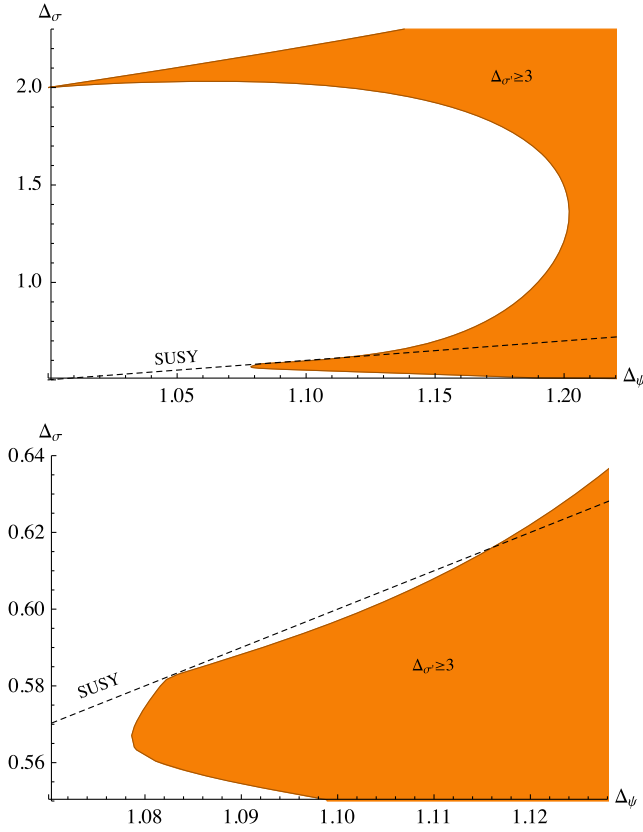


FIG. 31. The effect of imposing that there is only one relevant pseudoscalar $\Delta_{\sigma'} \geq 3$ in 3D parity-invariant CFTs. From Iliesiu *et al.*, 2016a.

mysterious and unexplained jumps when Δ_{σ_T} reaches marginality and at smaller values of Δ_{ψ_i} show a series of kinks which match to the large- N GNY models. Understanding the mechanism behind these jumps is an important open problem, which may be related to the spectrum rearrangement phenomena from Sec. V.B.3.

E. QED₃

Continuing our survey of physically important 3D CFTs, another class of theories are those defined by coupling 3D gauge or Chern-Simons fields to matter. One of the simplest examples is 3D quantum electrodynamics (QED₃), containing a $U(1)$ gauge field coupled to N_f two-component massless Dirac fermions ψ_i . This theory is known to flow to a nontrivial CFT at large N_f , which can be studied in the $1/N_f$ expansion (Appelquist, Nash, and Wijewardhana, 1988; Nash, 1989). There has been a long-standing question of whether there is a critical value of N_f below which the theory undergoes spontaneous breaking of the $SU(N_f)$ global symmetry. Numerous estimates of the critical value of N_f have been made over the years; see, e.g., Gukov (2017), Table 5.

It would be interesting to shed light on these theories and the question of the conformal window using bootstrap techniques. One starting point would be to study the bootstrap for 4pt functions of the gauge-invariant fermion bilinears

$\bar{\psi}_i \psi_j$.¹²¹ Basic bootstrap bounds on scalar 4pt functions, of the type discussed in Secs. V.B and V.C, would apply to this operator, but it is not *a priori* clear how to isolate QED₃ as compared to other theories with similar scalar operators such as QCD₃. However, this is an underexplored direction and in future studies it may be useful to combine the bootstrap for $SU(N_f)$ adjoints and singlets with additional gap assumptions and bootstrap constraints for other operators.

1. Monopole bootstrap for QED₃

An alternate approach, pursued by Chester and Pufu (2016) and Chester *et al.* (2017), is to focus on monopole operators. When dealing with a compact $U(1)$ gauge field, these operators create topologically nontrivial configurations of the gauge field having magnetic flux emerging from a spacetime point.¹²² Such operators are charged under a topological $U(1)_T$ global symmetry with symmetry current $J_T^\mu = (1/8\pi)\epsilon^{\mu\nu\rho}F_{\nu\rho}$. Taking the monopole operators to have charge $q \in \mathbb{Z}/2$, the scalar monopoles transform in representations of $SU(N_f)$ corresponding to fully rectangular Young diagrams with $N_f/2$ rows and $2|q|$ columns (Dyer, Mezei, and Pufu, 2013). Thus, the lightest scalar monopoles $M_{\pm 1/2}^I$ are expected to be in $SU(N_f)$ representations with $N_f/2$ fully antisymmetric indices.¹²³

The bootstrap for 4pt functions of $M_{\pm 1/2}^I$ was studied by Chester and Pufu (2016) for $N_f = 2, 4$, and 6 , where they focused on placing bounds on the dimension of the second monopole operator Δ_{M_1} , making various assumptions about gaps in the uncharged ($q = 0$) sector. These bounds are shown in Figs. 34 and 35, where for $N_f = 4$ and 6 they can be compared with the large N_f estimate (black cross). Intriguingly, there is a kinklike discontinuity in the bound which comes close to the large N_f estimate for certain values of the gap in the uncharged sector for operators in the same $SU(N_f)$ representation. By increasing the gap above M_1 , the allowed region could also be turned into a peninsula around the kink. Similar bounds for the lightest spinning monopoles in the case $N_f = 4$, along with a comparison to the large N_f predictions, were presented by Chester *et al.* (2017).

While these results are not definitive, they seem promising and show that the bootstrap for QED₃ has a reasonable chance to be successful, perhaps after a few more ingredients are added. Some possible directions would be to consider a multiple correlator bootstrap involving $M_{\pm 1/2}$, $M_{\pm 1}$, and/or $\bar{\psi}_i \psi_j$. It may also be fruitful to combine these with constraints from 4pt functions containing the $U(1)_T$ current, the $SU(N_f)$ current, or the stress tensor.

¹²¹Because of gauge symmetry, a single fermion field is unphysical in QED₃ and it would not be legitimate to consider its 4pt functions, unlike in GNY models in Sec. V.D, where ψ was physical.

¹²²Thus they could also be called instantons, but the common terminology refers to them as monopoles.

¹²³Monopoles with spin transform in other nontrivial flavor representations; see Chester *et al.* (2017).

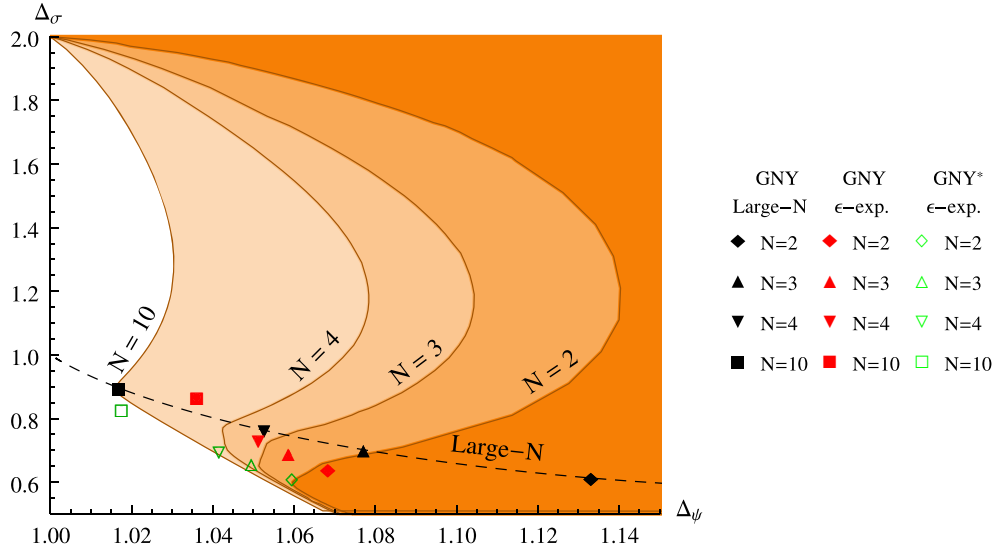


FIG. 32. The effect of imposing a gap $\Delta_{\sigma'} \geq 3$ in the singlet pseudoscalar sector of $O(N)$ -symmetric fermionic CFTs. The kinks at low N may perhaps be identified with the GNY and GNY* CFTs. From Iliesiu, Kos *et al.*, 2018.

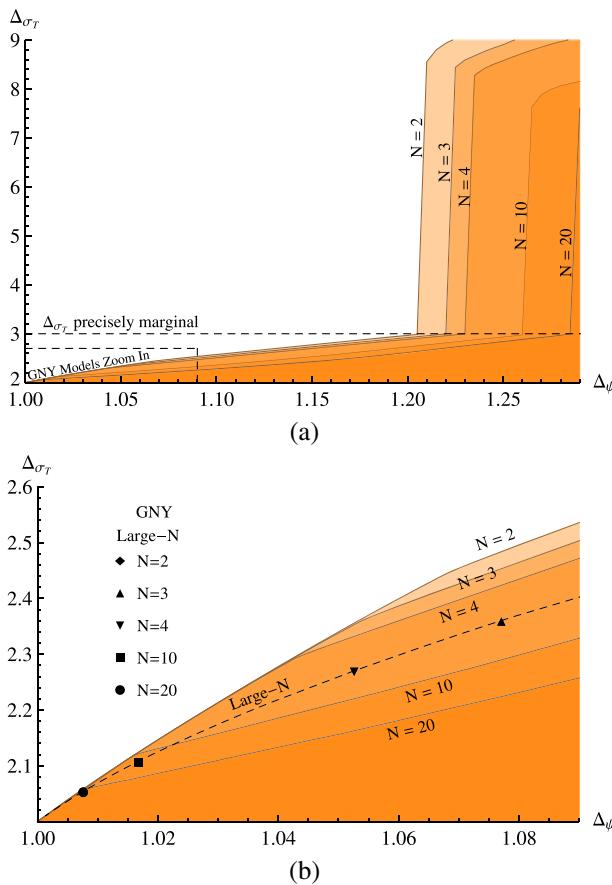


FIG. 33. The upper bounds on the dimension of the symmetric traceless pseudoscalar σ_T in the OPE $\psi_i \times \psi_j$ in $O(N)$ -symmetric fermionic CFTs. Notice the mysterious jumps in the wide view of the bounds (a) when they cross marginality. (b) A zoom on the small Δ_ψ region, where the bounds exhibit kinks, in agreement with the GNY dimensions at large N . From Iliesiu, Kos *et al.*, 2018.

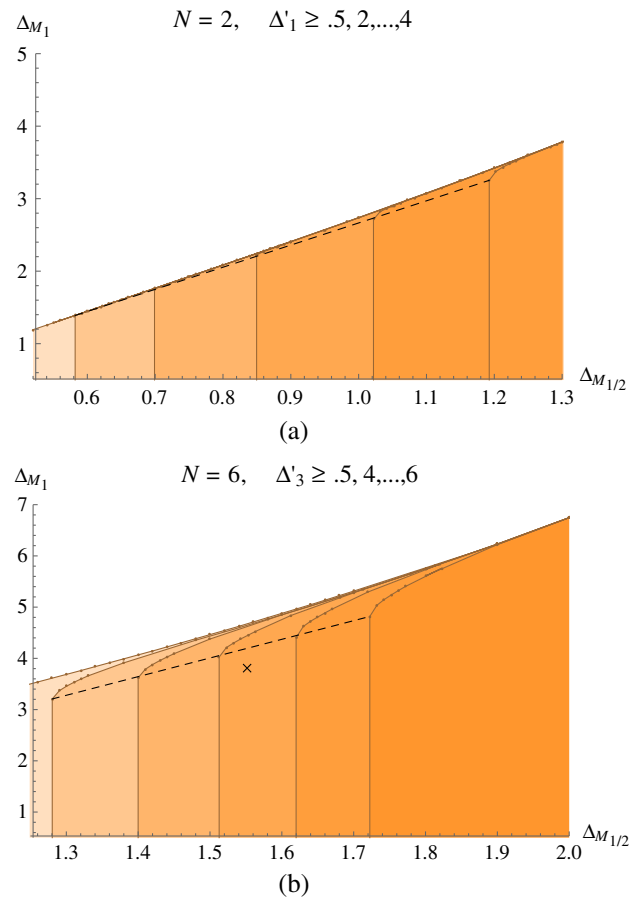


FIG. 34. Bounds on (a) Δ_{M_1} in terms of $\Delta_{M_{1/2}}$ in $d = 3$ for $N_f = 2$ and 6, and (b) with various assumptions on the gaps in the uncharged sector in the same $SU(N_f)$ representation as M_1 . From Chester and Pufu, 2016.

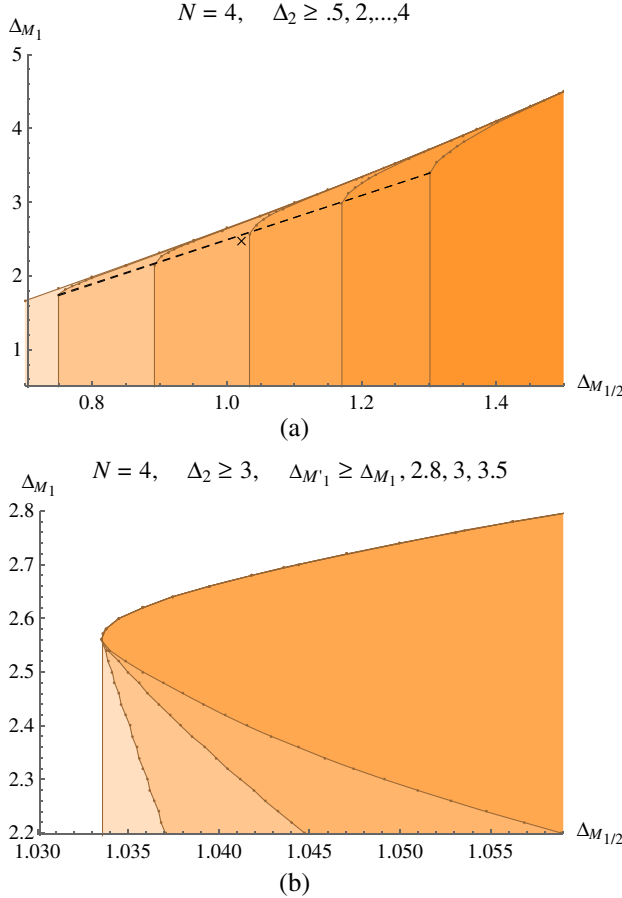


FIG. 35. (a) The analog of Fig. 34 for $N_f = 4$. (b) Starting from the $\Delta_2 \geq 3$ case of (a) and showing that placing an additional gap $\Delta_{M'_1}$ above Δ_{M_1} turns the kink into a peninsula. From Chester and Pufu, 2016.

2. Bosonic QED₃ and deconfined quantum critical points

Finally we review the rich physics of bosonic QED₃, where some bootstrap insights have recently been obtained. Bosonic QED₃ is obtained by coupling the $U(1)$ gauge field to N complex scalars ϕ_i with an $SU(N)$ invariant potential $m^2|\phi|^2 + \lambda(|\phi|^2)^2$. This is also known as the N -component Abelian Higgs model and is believed to flow to a CFT for large enough N . Unlike for fermions, the boson mass term preserves all the symmetries and has to be fine-tuned to reach the fixed point.

This model has been much discussed in the condensed matter literature as the ‘‘noncompact CP ^{$N-1$} model’’ (NCCP ^{$N-1$}) in connection with the phenomenon of ‘‘deconfined criticality’’ (Senthil *et al.*, 2004). To briefly review this connection, the physical systems of interest are certain quantum anti-ferromagnets in $2+1$ dimensions, which have a quantum phase transition between Néel and valence-bond-solid (VBS) phases.¹²⁴ The transition can be described by the $O(3)$ nonlinear

¹²⁴The absence of a disordered phase in such transitions can be understood using ‘t Hooft anomalies; see Komargodski, Sharon *et al.* (2017). This perspective also gives insight into the rich physics of interfaces in these theories (Komargodski, Sulejmanpasic, and Ünsal, 2018).

sigma model (NLSM) for the Néel order parameter, modified by the inclusion of Berry phase effects which suppress topological defects (hedgehogs), which will play an important role below.

The $O(3)$ NLSM can be written as the CP^1 model, which has two complex vectors $\mathbf{z} = (z_1, z_2)$ subject to the constraint $|z_1|^2 + |z_2|^2 = 1$ and a $U(1)$ gauge invariance $\mathbf{z} \sim e^{i\phi}\mathbf{z}$. This explains the emergence of the gauge field. Replacing the constraint by a quartic potential and adding a Maxwell kinetic term for the gauge field (expected to be generated by the RG flow), one obtains bosonic QED₃ with $N = 2$.

In the language of QED₃, the above-mentioned topological defects are the monopole operators of quantized charge, similar to the ones in Sec. V.E.1. Of course the dimensions of monopole operators differ in bosonic and fermionic QED. Also here we normalize the topological charge to be integer $q \in \mathbb{Z}$.

If a monopole of charge q appears in the action, it breaks the global topological $U(1)_T$ symmetry to the \mathbb{Z}_q subgroup. Microscopic descriptions of quantum antiferromagnets may realize a discrete subgroup of $U(1)_T$ at the lattice level. On cubic lattices, a \mathbb{Z}_{q_0} with $q_0 = 4$ is preserved, while for the hexagonal and rectangular lattices we have $q_0 = 3$ and 2. The \mathbb{Z}_{q_0} symmetry is also visible in the VBS phase where it permutes the vacua. This microscopic symmetry means that only monopoles with charges multiple of q_0 appear. Monopoles with different charges have their fugacity killed by the above-mentioned Berry phases (Read and Sachdev, 1990).

In light of the above discussion, the analysis of the critical behavior of QED₃ can be split into two parts. First, does bosonic QED₃, with all monopoles suppressed, have a fixed point? If the answer is yes, then one can ask: can this fixed point be reached provided that one allows monopoles with charges in multiples of q_0 ? For this to happen, the monopole of charge q_0 has to be irrelevant.

One can study these questions analytically at large N : one finds a fixed point and computes the critical exponents in the $1/N$ expansion.¹²⁵ At small N one resorts to Monte Carlo simulations. The bootstrap at present cannot by itself resolve the question of the fixed point existence. However, it can provide valuable consistency checks on the other studies. Suppose that a certain Monte Carlo simulation is done on a lattice preserving a \mathbb{Z}_{q_0} subgroup, finds a second-order phase transition, and measures the scaling dimensions Δ_q of monopole operators M_q for a subset of charges q (we denote by M_0 the relevant singlet scalar driving the transition). We have the following OPE algebra in the scalar sector, omitting the OPE coefficients ($M_{-q} = M_q^\dagger$):

$$M_q \times M_{q'} \sim \delta_{q+q'} \mathbb{1} + M_{q+q'} + \dots \quad (126)$$

From the previous discussion, the operator M_{q_0} has to be irrelevant, as well as the higher charge monopoles. We can use the bootstrap to study the consistency of this algebra given the measured operator dimensions.

¹²⁵See Murthy and Sachdev (1990), Kaul and Sachdev (2008), Metlitski *et al.* (2008), and Dyer *et al.* (2015).

3. Aside: Constraints on symmetry enhancement

What we just presented is an instance of a more general question: under which conditions can the global symmetry of the fixed point G be larger than the microscopically realized symmetry H ? The case of interest for the previous section is $G = U(1)$ and $H = \mathbb{Z}_{q_0}$. For the symmetry enhancement to happen, operators which break G to H must be irrelevant. The bootstrap is a powerful tool to study whether this irrelevance assumption is consistent with conformal symmetry and with other information which may be available about the fixed point. We will see further applications of this philosophy in Secs. VI.B and VI.C.

We now describe bootstrap constraints on the symmetry enhancement from \mathbb{Z}_{q_0} to $U(1)$ derived by Nakayama and Ohtsuki (2016). Enhancement from \mathbb{Z}_2 requires that M_2 is irrelevant. Since $M_1 \times M_1 \sim M_2$, one can bound Δ_2 given Δ_1 , by studying the 4pt function $\langle M_1 M_1^\dagger M_1 M_1^\dagger \rangle$. The resulting bound is given in Fig. 36. Imposing $\Delta_2 > 3$, one gets a necessary condition $\Delta_1 > 1.08$ for enhancement from \mathbb{Z}_2 to $U(1)$.

The same plot in Fig. 36 can be used to derive rough necessary conditions on the enhancement from \mathbb{Z}_4 to $U(1)$. Indeed, the bound also applies to $M_2 \times M_2 \sim M_4$. If M_4 is irrelevant, then we must have $\Delta_2 > 1.08$, which in turn implies $\Delta_1 > 0.504$.

To study enhancement from \mathbb{Z}_3 , one analyzes simultaneously three 4pt functions $\langle M_1 M_1^\dagger M_1 M_1^\dagger \rangle$, $\langle M_1 M_1^\dagger M_2 M_2^\dagger \rangle$, and $\langle M_2 M_2^\dagger M_2 M_2^\dagger \rangle$. It is reasonable to assume that M_4 is irrelevant (as would be the case if M_3 is irrelevant and Δ_q is monotonic in q), and to impose $\Delta_0 > 1.044$ (which follows from an assumption that the fixed point is critical and not multicritical; see Sec. V.A). Under these assumptions, the upper bound on Δ_3 as a function of $\{\Delta_1, \Delta_2\}$ is shown in Fig. 37. From this bound, irrelevance of M_3 requires $\Delta_1 > 0.585$.

4. Back to deconfined criticality: Is the transition second order?

The necessary conditions described in the previous section have been compared with available Monte Carlo and large- N

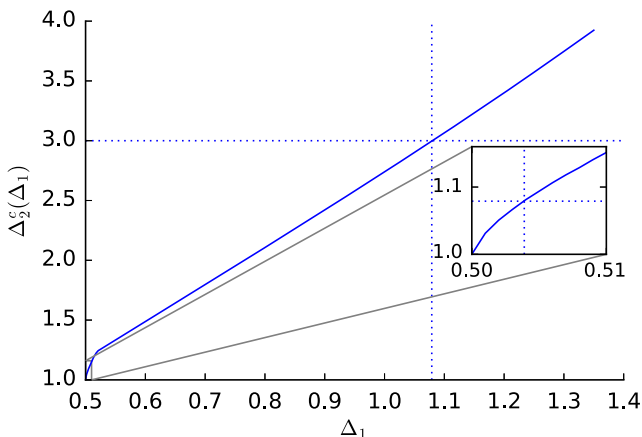


FIG. 36. The 3D upper bound on Δ_2 as a function of Δ_1 . It may be possible to improve this bound if Δ_0 is known. The same bound applies to $M_2 \times M_2 \sim M_4$. From Nakayama and Ohtsuki, 2016.

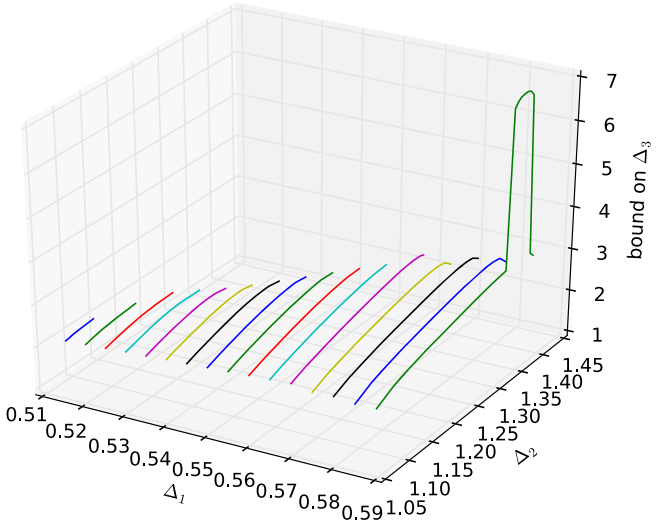


FIG. 37. An upper bound on Δ_3 as a function of $\{\Delta_1, \Delta_2\}$ under the assumptions that $\Delta_0 > 1.044$, $\Delta_4 > 3$. It follows from Fig. 36 that the range of Δ_2 is restricted by the latter assumption from below, and, for fixed Δ_1 , from above. From Nakayama and Ohtsuki, 2016.

data on the Néel VBS transition which claim to see a second-order transition and measure some critical exponents. For square and hexagonal lattices, there is nice consistency, as for rectangular lattices for $N \leq 4$ and $N \geq 6$, while some $N = 5$ simulations are inconsistent with the bootstrap. The conclusion is that there must either be an error in the $N = 5$ Monte Carlo measurement or in the assumption that the transition is second order. See Nakayama and Ohtsuki (2016) for this survey and for further details.

It should be emphasized that while the bootstrap results may point out an inconsistency in Monte Carlo simulations, they cannot, at present, validate them and prove that the phase transition is indeed second order. It is still possible that even in the above cases when there is a nice agreement between Monte Carlo results and the bootstrap necessary conditions, the transition is still very weakly first order and not second order.

Let us focus on the case $N = 2$ which presents a controversy. Large-scale Monte Carlo simulations for $N = 2$ were performed by Nahum, Chalker *et al.* (2015), using a loop model on a cubic lattice which is in the same universality class as NCCP¹ and has monopole suppression up to $q_0 = 4$, and going up to very large lattices of linear size up to $L = 640$.¹²⁶ While they have not seen signs of a finite correlation length or a conventional first-order transition, and observed scaling behavior of correlation functions at distances $1 \ll r \ll L$, they have seen scaling violation for observables at larger distances $r \sim L$, inconsistent with a conventional second-order transition.

So, is the transition second order or weakly first order? Assuming a second-order transition, Nahum, Chalker *et al.*

¹²⁶See also Harada *et al.* (2013) and Sreejith, Powell, and Nahum (2018) for simulations of other microscopic models in the same universality class.

(2015) extracted the scaling dimension of the monopole operator $\Delta_1 = 0.625(15)$, which is consistent with the bootstrap condition $\Delta_1 > 0.504$ necessary for the enhancement from \mathbb{Z}_4 to $U(1)$. However, there is an extra piece of information which allows one to set up an even more stringent bootstrap test: further symmetry enhancement at the transition from $SO(3) \times U(1)$ to $SO(5)$. Here $SO(3)$ acts on the Néel order parameter $N_a = \mathbf{z}^\dagger \sigma_a \mathbf{z}$. Empirically, the scaling dimension of N is very close to Δ_1 (Nahum, Chalker *et al.*, 2015) and, moreover, the joint probability distribution of (N, M_1) is very close to the spherical one after a rescaling (Nahum, Serna *et al.*, 2015), which can be explained if N and M_1 belong to a vector multiplet Φ of $SO(5)$ of dimension $\Delta_\Phi = \Delta_1$.

In this description, the relevant scalar which drives the transition is a component of the symmetric traceless tensor (roughly $\Phi_A \Phi_B - \text{trace}$).¹²⁷ For the $SO(5)$ enhancement to happen, any other scalar which breaks $SO(5)$ back to $SO(3) \times U(1)$ must be irrelevant. In addition, the $SO(5)$ singlet S (roughly $\Phi_A \Phi^A$) must be irrelevant for the transition to be second order, since otherwise the fixed point will not be reached; see Wang *et al.* (2017) for further discussion. Given the dimension $\Delta_\Phi = \Delta_1$ as above, it is straightforward to compute an upper bound on the dimension of S which occurs in the OPE $\Phi \times \Phi$. This is the same bound as for $N = 5$ in Fig. 21 except the plot has to be extended to larger Δ_Φ . Nakayama and Ohtsuki (2016) and Simmons-Duffin (2016b) performed this analysis and reported that $\Delta_S > 3$ is excluded for Δ_Φ as above. In fact $\Delta_S > 3$ requires $\Delta_\Phi > 0.76$ (Nakayama, 2016a).

To summarize, the bootstrap excludes a second-order phase transition described by a unitary 3D CFT with symmetry enhanced to $SO(5)$ and the order parameter scaling dimension taking the above value suggested by the Monte Carlo simulations. In our opinion, the most compelling interpretation of available data is a weakly first-order transition due to walking RG behavior which ensues when the RG flow has no fixed points for a real value of the coupling but two complex conjugate fixed points with small imaginary parts. This is the same mechanism as for the weakly first-order transition in the 2D Potts model with $Q \gtrsim 4$. As discussed by Nahum, Chalker *et al.* (2015), this scenario may resolve the observed scaling violations at distances $r \sim L$. It can also accommodate the enhancement to $SO(5)$ (Wang *et al.*, 2017). In this scenario, there is no unitary 3D CFT (the complex fixed points being nonunitary), and the bootstrap bounds do not apply, resolving the contradiction.

Finally, let us note that a similar analysis can constrain another scenario outlined by Wang *et al.* (2017), in which a variant called the easy-plane NCCP¹ model is conjectured to have a fixed point with enhanced $O(4)$ symmetry and be dual to $N_f = 2$ fermionic QED₃. In this scenario, the conjectured fixed point cannot contain any fully $O(4)$ -invariant scalar perturbations. However, recent Monte Carlo simulations (Qin *et al.*, 2017) point to a dimension for the $O(4)$ vector order parameter $\Delta_\Phi = 0.565(15)$ which seems incompatible with the bootstrap bound assuming irrelevance of the $O(4)$ singlet

(Fig. 20 extended further to the right), which requires $\Delta_\Phi > 0.868$ (Poland, 2017). In the future it will be interesting to further study the fate of these models using both bootstrap and Monte Carlo data.

F. Current and stress-tensor bootstrap

In the previous sections we discussed results following from 4pt functions of scalars and fermions. Here we discuss interesting results which have recently been obtained from 4pt functions of tensor operators, specifically of conserved currents and stress tensors. Namely, a number of numerical bounds on scaling dimensions and OPE coefficients from such correlators in parity-preserving 3D CFTs were recently computed by Dymarsky *et al.* (2017, 2018), building on important analytical developments for spinning correlators as reviewed in Sec. III.F.7.¹²⁸ Such studies are well motivated because they probe the general space of local CFTs and may even lead to the discovery of new theories.

A concrete application of these constraints is to study bounds on current and stress-tensor 3pt function coefficients under various assumptions. These coefficients are known to satisfy various analytical bounds following from the averaged null energy condition (see Sec. III.E.3), as was originally argued in the context of conformal collider physics by Hofman and Maldacena (2008), with 3D bounds worked out by Buchel *et al.* (2010) and Chowdhury *et al.* (2013). One application of the numerical bootstrap is to study how the conformal collider bounds change as a function of gaps. Another application is to determine these coefficients in various CFTs, e.g., the critical 3D Ising and $O(N)$ models. These studies also allow one to probe parity-odd operators in the spectrum which have previously been inaccessible from the perspective of scalar 4pt functions (although they could be accessed from the fermionic correlators in Sec. V.D).

In Fig. 38 we show general lower bounds on the central charge (in units of the free boson central charge C_B) from the bootstrap applied to $\langle TTTT \rangle$, as a function of the independent parity-preserving $\langle TTT \rangle$ 3pt function coefficient which is parametrized by the variable θ .¹²⁹ In this notation the conformal collider bound is $0 \leq \theta \leq \pi/2$, where a free scalar has $\theta = 0$ and free Majorana fermion has $\theta = \pi/2$. It can be readily seen that the numerical bootstrap is able to reproduce this constraint in addition to giving general lower bounds on C_T . A similar set of bounds from the $\langle JJJJ \rangle$ bootstrap is shown in Fig. 39, where in this plot C_T is normalized to the central charge of a free *complex* scalar C_T^{free} and the

¹²⁸See also Dymarsky (2015) for a discussion about the general properties of these correlation functions.

¹²⁹In fact, Figs. 38 and 39 should also apply to parity-violating theories since all needed conformal blocks have been included (e.g., contributions from parity-violating $\langle TTT \rangle$ or $\langle JJJ \rangle$ couplings are accounted for by allowing parity-odd spin-2 contributions at the unitarity bound). This also holds for bounds where identical gaps have been imposed in a given parity-even and parity-odd sector simultaneously (e.g., Fig. 45 along the diagonal). Stronger bounds may hold in parity-violating theories after adding crossing relations from parity-violating 4pt structures and assuming nonzero values of parity-violating coefficients.

¹²⁷Nahum, Serna *et al.* (2015) measured its scaling dimension to be ~ 1.5 .

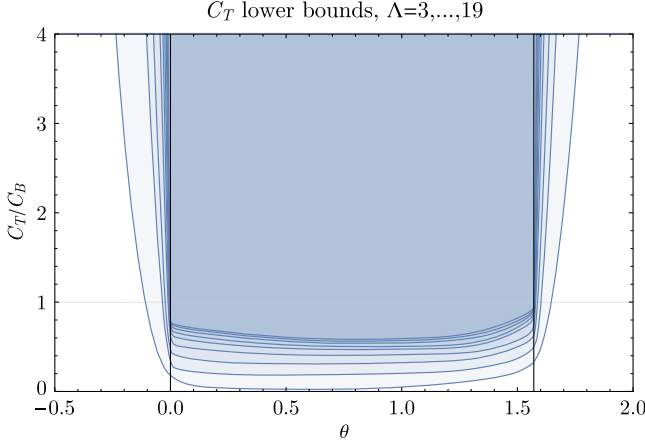


FIG. 38. Bounds on C_T as a function of the $\langle TTT \rangle$ 3pt function parameter θ . From Dymarsky *et al.*, 2018.

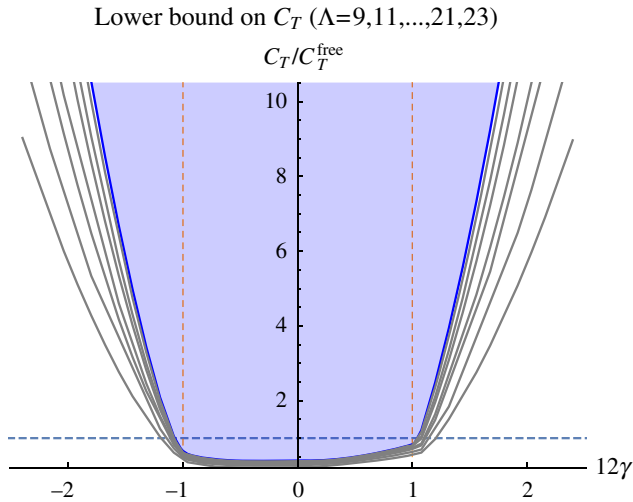


FIG. 39. Bounds on C_T as a function of the $\langle JJJ \rangle$ 3pt function parameter γ . From Dymarsky *et al.*, 2017.

independent parity-preserving $\langle JJJ \rangle$ coupling is parametrized by γ , where the conformal collider bound is given by $-1/12 \leq \gamma \leq 1/12$. In this case the free complex scalar has $\gamma = -1/12$ while the free Dirac fermion has $\gamma = 1/12$.

As mentioned, the advantage of the numerical bootstrap is that it can readily probe how constraints on these couplings depend on gaps in the spectrum. For example, in Fig. 40 we show how the lower bound on C_T as a function of θ in the $\langle TTTT \rangle$ bootstrap varies as one increases the gap in the parity-odd scalar sector Δ_{odd} from 2 to 8. It can be seen that increasing the parity-odd gap forbids the “fermion” end of the range for θ but allows the “scalar” end. This is consistent with the fact that the free scalar has a very large parity-odd gap $\Delta_{\text{odd}} = 11$, while the free Majorana fermion has a small gap $\Delta_{\text{odd}} = 2$.

Similarly, imposing a parity-even gap forbids the scalar end. In Fig. 41 we illustrate this by showing what happens when the leading parity-even scalar is irrelevant, corresponding to “self-organized” CFTs (see Sec. V.A). This lower central charge bound applies for instance to fermionic QED₃

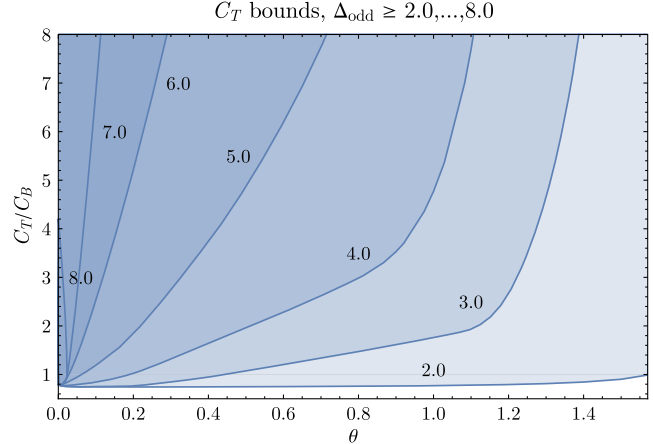


FIG. 40. Bounds on C_T as a function of the $\langle TTT \rangle$ 3pt function parameter θ for different values of the parity-odd scalar gap Δ_{odd} . From Dymarsky *et al.*, 2018.

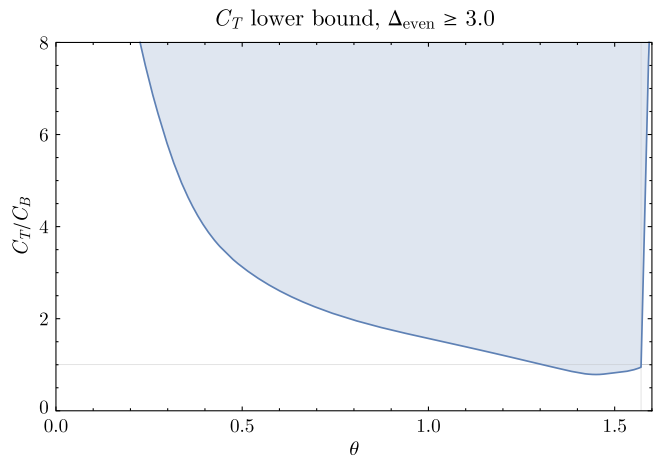


FIG. 41. Bounds on C_T as a function of the $\langle TT \rangle$ 3pt function parameter θ assuming that the leading parity-even scalar is irrelevant. From Dymarsky *et al.*, 2018.

in the conformal window from Sec. V.E, with N_f even for parity invariance.

Furthermore, imposing gaps on both parity-even and parity-odd scalars forces one to live with intermediate values of θ , at least for moderately small values of the central charge. These and other bounds with different gap assumptions (including upper bounds on C_T for gaps excluding large- N theories) can be found by Dymarsky *et al.* (2018).

A similar story holds for bounds from the $\langle JJJJ \rangle$ bootstrap, where Fig. 42 shows how the lower bound on C_T changes when either parity-even or parity-odd scalars are irrelevant (dashed blue lines), or when both are irrelevant (solid blue line). These bounds are consistent with the gaps for a free complex scalar ($\Delta_0^+ = 2$, $\Delta_0^- = 7$) and free Dirac fermion ($\Delta_0^+ = 4$, $\Delta_0^- = 2$). Similar bounds with different gap assumptions have been found by Dymarsky *et al.* (2017). In the future, by generalizing this analysis to $SU(N_f)$ [or $SU(N_f) \times U(1)$] global symmetry one may be able to place interesting bounds on the fermionic QED₃ central charge using the same argument as the one based on Fig. 41.

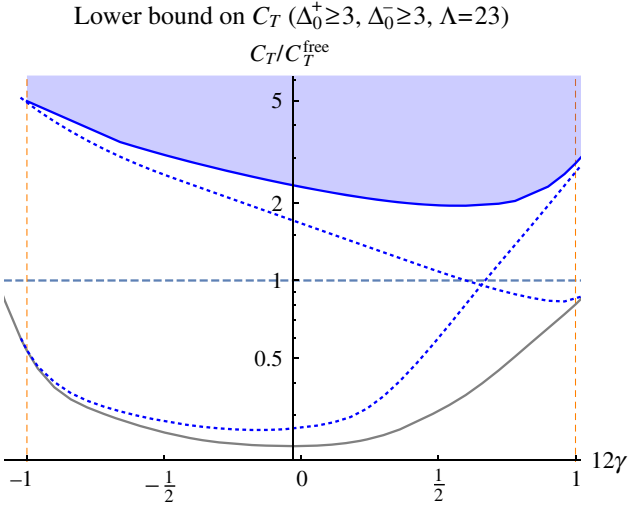


FIG. 42. Bounds on C_T as a function of the $\langle JJJ \rangle$ 3pt function parameter γ with no assumptions (lower solid curve), parity-odd scalars irrelevant (lower dashed curve), parity-even scalars irrelevant (upper dashed curve), and all scalars irrelevant (upper solid curve). From Dymarsky *et al.*, 2017.

It is interesting to ask if one can use these general bootstrap constraints to determine θ or γ in some CFTs of interest, e.g., the Ising or $O(2)$ models. In the case of the Ising model, it is a plausible assumption (e.g., from the ϵ expansion) that its leading parity-odd (but \mathbb{Z}_2 -even) operator has a very large dimension as in the free scalar theory. Using known parity-even data the $\langle TTTT \rangle$ bootstrap yields an upper bound $\Delta_{\text{odd}}^{\text{Ising}} < 11.2$, and one can obtain small closed regions in the $\{\theta, C_T\}$ plane that are consistent with the known Ising central charge, Eq. (123). These regions, shown in Fig. 43, yield the determination $0.01 < \theta < 0.018$ – 0.019 if Δ_{odd} is close to saturating its bound. Note that if one makes the weaker assumption of irrelevance $\Delta_{\text{odd}} > 3$, then there is still a reasonably tight range $0.01 < \theta < 0.05$ consistent with C_T^{Ising} .

In the case of the $\langle JJJJ \rangle$ bootstrap, one can similarly try to determine γ for the $O(2)$ model. In this case after inputting the

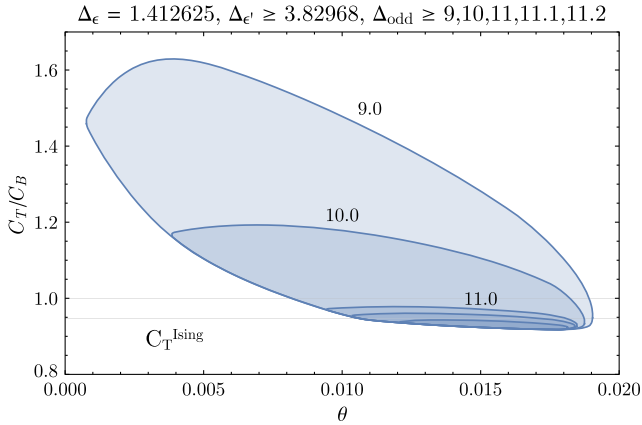


FIG. 43. Bounds on C_T as a function of the $\langle TTT \rangle$ 3pt function parameter θ with gap assumptions plausible for the Ising model. From Dymarsky *et al.*, 2018.

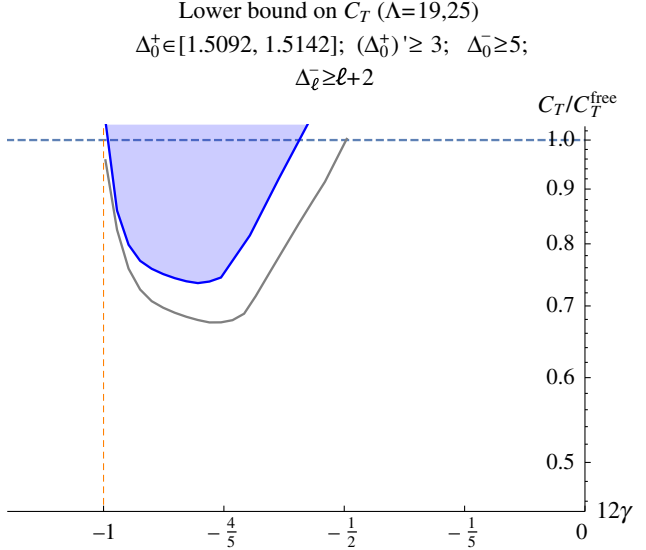


FIG. 44. Bounds on C_T as a function of the $\langle JJJ \rangle$ 3pt function parameter γ with gap assumptions plausible for the critical $O(2)$ model. From Dymarsky *et al.*, 2017.

known dimension of the leading $O(2)$ parity-even singlet, irrelevance of the second $O(2)$ parity-even singlet, and the plausible parity-odd gaps $\Delta_0^- \geq 5$ and $\Delta_\ell^- \geq \ell + 2$, Fig. 44 yields the range $-0.0824 < \gamma < -0.0494$. Based on a linear extrapolation, Dymarsky *et al.* (2017) also estimated the more restrictive range $-0.080 < \gamma < -0.061$. A negative value of γ in the $O(2)$ model also appears to be favored by the results of quantum Monte Carlo simulations (Katz *et al.*, 2014). In future work it will be interesting to find ways to improve these determinations, extend them to other $O(N)$ models, and perhaps connect the smallness of the deviations of θ and γ from their free values to the existence of approximate higher-spin currents in these theories.

Finally, in Fig. 45 we show a more global picture of the allowed region of parity-odd and parity-even scalar gaps from both the $\langle TTTT \rangle$ and $\langle JJJJ \rangle$ bootstrap, making no additional assumptions. These regions satisfy a number of consistency checks, e.g., being consistent with known gaps in free theories, MFTs, and critical $O(N)$ models. They additionally show fairly sharp features near the scaling dimensions in the Ising and $O(2)$ models. It will be interesting to improve these maps in future studies and identify the locations of other CFTs of interest. The lower “scalar exclusion” regions of these plots are ruled out from 4pt functions of the leading parity-odd scalar (assuming the parity-even scalar appears in both OPEs as would be generically expected), an example of how the scalar and the stress-tensor and current bootstraps can yield complementary information.

There are a number of directions for future work, which include considering mixed systems containing stress tensors and currents together with scalars, studying the implications of parity violation (see footnote 129), studying in more detail the conditions for large N and holographic theories, and generalizing these studies to other dimensions. Recent progress on how to compute spinning conformal blocks in

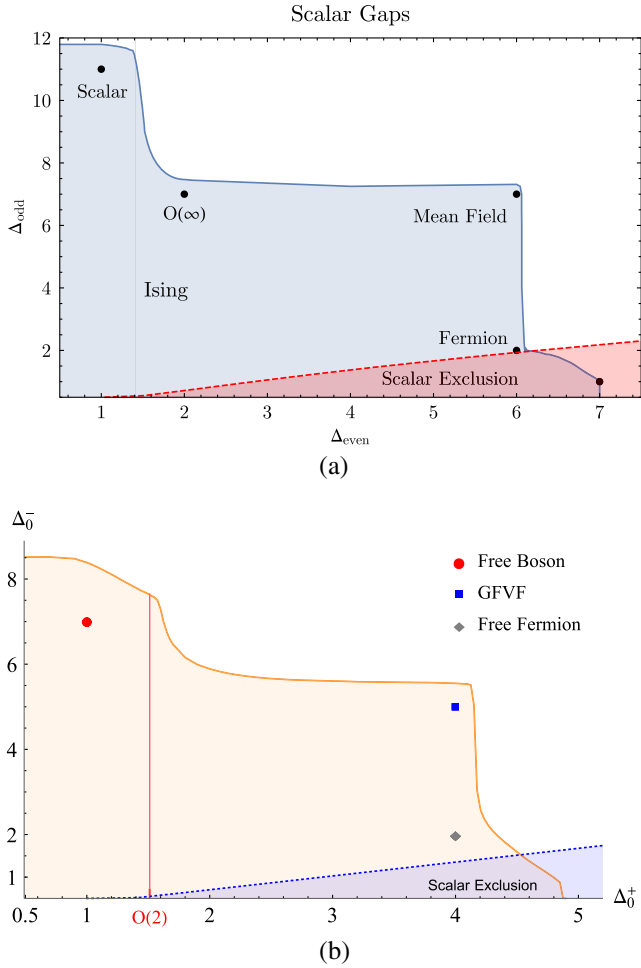


FIG. 45. Allowed region for parity-even and parity-odd scalar gaps from (a) the $\langle TTTT \rangle$ bootstrap. From Dymarsky *et al.*, 2018. (b) The $\langle JJJJ \rangle$ bootstrap. From Dymarsky *et al.*, 2017.

4D and in general dimensions¹³⁰ should make these analyses tractable in the future outside of 3D. Current and stress-tensor multiplets can also be considered in superconformal theories, where the bootstrap analysis can be simplified using the fact that they reside in multiplets with operators of lower spin.¹³¹

G. Future targets

In this section we collect some additional 3D models which in our opinion represent interesting future targets for the bootstrap.

1. Multifield Landau-Ginzburg models

There exists rich phenomenology of fixed points arising from Lagrangians with multiple scalar fields transforming under product group symmetries, e.g., $SO(n) \times SO(m)$. One can consider Lagrangians involving two coupled scalar multiplets, one transforming in the fundamental of $SO(n)$ and another of $SO(m)$. Alternatively, one can consider a field

¹³⁰See Secs. III.C.2 and III.F.7 for a summary.

¹³¹However, to do this requires knowledge of the superconformal blocks. Some studies where this has been pursued are mentioned in Secs. VII and IX.

transforming in the bifundamental of $SO(n) \times SO(m)$. Such Lagrangians have been invoked to describe phase transitions in many physical systems; see Vicari (2007) for further details.

When studying these fixed points using the RG, a recurrent feature is that many of them do not exist in the $4 - \epsilon$ expansion and have to be studied directly in 3D. Since such computations lack a manifestly small expansion parameter, there seems to be no consensus about the existence of these fixed points. So this appears to be a perfect target for a nonperturbative approach such as the bootstrap. Some preliminary bootstrap studies of 3D CFTs with $SO(n) \times SO(m)$ were carried out by Nakayama and Ohtsuki (2014a, 2015), but in our opinion more work is needed before firm conclusions can be drawn.

2. Projective space models

An interesting 3D lattice model is the CP^n model, where microscopic lattice variables belong to CP^n and have ferromagnetic interactions preserving the symmetry (see below for the antiferromagnetic case). Recall that CP^n can be realized by starting with $(n + 1)$ -dimensional complex vectors $\mathbf{z} = (z_1, \dots, z_{n+1})$ and imposing the constraint $\mathbf{z}^\dagger \cdot \mathbf{z} = 1$, preserved up to the equivalence $\mathbf{z} \sim e^{i\phi} \mathbf{z}$. A simple lattice Hamiltonian is

$$H = -J \sum_{\langle ij \rangle} |\mathbf{z}_i^\dagger \cdot \mathbf{z}_j|^2, \quad (127)$$

with $J > 0$ in the considered ferromagnetic case. The physics of this model is influenced by defects (hedgehogs), which are possible because $\pi_2(CP^n) = \mathbb{Z}$. Here we consider the CP^n model with defects allowed. It should be distinguished from the ‘‘noncompact CP^n model’’ which results when defects are suppressed; see Sec. V.E.2.

The CP^1 model is equivalent to the $O(3)$ model, with the order parameter $N_a = \mathbf{z}^\dagger \sigma_a \mathbf{z}$, and it has a second-order phase transition described by the same CFT.

The CP^2 model has an internal symmetry $SU(3)$ (modulo global issues), with traceless Hermitian matrix $Q_{ab} = z_a \bar{z}_b - \delta_{ab}$ as an order parameter. The Landau-Ginzburg description contains a cubic invariant $\text{Tr}(Q^3)$ and would suggest a first-order transition, but Monte Carlo simulations (Nahum *et al.*, 2013) indicate that the phase transition is continuous. This is similar to what happens for the three-state Potts model in 2D and can be explained as an effect of fluctuations. Monte Carlo results for the critical exponents are $\eta = 0.23(2)$ and $\nu = 0.536(13)$, translating into the dimensions of Q and of the relevant singlet scalar. Can this model be isolated using the numerical bootstrap?

One can also consider antiferromagnetic projective space models, taking $J < 0$ in the above Hamiltonian. Antiferromagnetic CP^n models (Delfino, Pelissetto, and Vicari, 2015) do not give rise to new universality classes.¹³² On

¹³²The ACP^1 model on a cubic lattice is equivalent to the ferromagnetic model and, as the latter, has a phase transition in the $O(3)$ universality class. For higher n there is no equivalence between the antiferromagnetic and ferromagnetic models. The ACP^2 model has a second-order transition which belongs to the $O(8)$ universality class (and so is different from CP^2). For still higher n the transition is first order.

the other hand, a new class is observed for the antiferromagnetic RP^4 model [Pelissetto, Tripodo, and Vicari \(2018\)](#), and it could constitute a target for the bootstrap.¹³³

3. Non-Abelian gauge and Chern-Simons matter theories

While we focused our attention on QED_3 , there is a whole landscape of 3D gauge theories coupled to various types of matter. An interesting case is QCD_3 with a simple gauge group G coupled to N_f fundamental fermions. Such theories may, for example, play a role in the physics of cuprate superconductors ([Chowdhury and Sachdev, 2014, 2015](#)). A fixed point can be established and the properties studied at large N_f ([Appelquist and Nash, 1990](#)). For example, [Dyer, Mezei, and Pufu \(2013\)](#) performed a systematic study of monopole operators in such theories, allowing for estimates of the bottom of the conformal window for different choices of G by imposing irrelevance of the monopole operators ([Dyer, Mezei, and Pufu, 2013, Table 4](#)). QCD_3 coupled to both fermions and scalars was also proposed to describe the critical point of the “orthogonal semimetal” confinement transition in [Gazit *et al.* \(2018\)](#), with critical exponents extracted in quantum Monte Carlo simulations. It would be interesting to understand how to isolate these theories using bootstrap techniques and test these estimates.

Another natural set of targets consists of Chern-Simons gauge fields coupled to matter. Such theories are known to have conformal fixed points and sit in an intricate web of dualities.¹³⁴ Some possible experimental realizations of these theories as transitions between fractional quantum Hall states were proposed by [Lee *et al.* \(2018\)](#). A hallmark of these theories is the existence of parity violation; it would be interesting to see if they can be found after introducing parity-violating couplings into the bootstrap. Monopole operators in these theories were also recently studied by [Chester *et al.* \(2017\)](#) and would constitute natural targets for the bootstrap.

4. Other models

Another theory briefly mentioned in Sec. [V.C.4](#) is the GNH model, a variant of the GN models with a three-component scalar order parameter. For a pedagogical review of the model,

¹³³The RP^n models are versions of $O(n)$ models with a gauged \mathbb{Z}_2 symmetry. Their second-order phase transitions for $n = 2$ and 3 belong to the $O(2)$ and $O(5)$ classes, respectively, but the $n = 4$ class is mysterious.

¹³⁴See, for example, [Aharony \(2016\)](#), [Seiberg *et al.* \(2016\)](#), [Hsin and Seiberg \(2016\)](#), [Aharony, Benini *et al.* \(2017\)](#), [Benini, Hsin, and Seiberg \(2017\)](#), and [Gomis, Komargodski, and Seiberg \(2017\)](#). Duality means that two different microscopic descriptions lead to the same IR CFT (perhaps after tuning some parameters). Why should dualities exist? One reason may be the paucity of CFTs. If so, some dualities may perhaps be explained by the bootstrap, providing evidence that there is a single CFT satisfying certain constraints (symmetry, the number of relevant operators, etc.). Then any microscopic theory satisfying these constraints should flow to this CFT at criticality. In this sense, the results of Sec. [V.C.3](#) provide an explanation for the particle-vortex duality of the Abelian Higgs model, originally proposed by [Peskin \(1978\)](#) and [Dasgupta and Halperin \(1981\)](#).

its applications, and its connection to the lattice Hubbard model, see [Sachdev \(2010\)](#). This constitutes another interesting target for the bootstrap.

A 3D CFT with $SU(4)$ global symmetry and an order parameter in the symmetric tensor representation was considered by [Basile, Pelissetto, and Vicari \(2005, 2006\)](#). It was proposed to describe a continuous chiral phase transition in 4D $SU(N)$ gauge theory coupled to $N_f = 2$ massless quarks in the adjoint representation at finite temperature. The existence of this CFT and some information about critical exponents was found using RG methods; it would be interesting to explore it using the bootstrap.

VI. APPLICATIONS IN $d=4$

In this section we now turn to numerical bootstrap applications in unitary 4D CFTs. We first present general constraints in Sec. [VI.A](#) and then discuss more specific physical applications. In Sec. [VI.B](#) we review applications to high-energy physics beyond the standard model (SM). Applications to 4D conformal gauge theories will be discussed in Sec. [VI.C](#). Supersymmetric 4D CFTs will be presented in the next section.

A. General results

This section will follow the same logic as Secs. [V.B.1](#) and [V.C.1](#) devoted to 3D CFTs. Historically, however, the first attempt to study crossing relations using numerical techniques focused on 4D CFTs. This analysis, pioneered by [Rattazzi *et al.* \(2008\)](#) and then refined by [Rychkov and Vichi \(2009\)](#), was spurred by high-energy physics motivations which will be reviewed in Sec. [VI.B](#). But first let us discuss general conformal bootstrap results for 4D CFTs with various global symmetries.

Consider first the simple case of a 4D CFT containing a scalar operator ϕ with dimension Δ_ϕ . We further assume that it is charged under a global symmetry (e.g., a \mathbb{Z}_2 symmetry) so that the OPE $\phi \times \phi$ does not contain ϕ . Then it is interesting to ask how high can one push the dimension of the first scalar operator in this OPE. It is also interesting to ask how large the OPE coefficient of the stress tensor $\lambda_{\phi\phi T} \propto \Delta_\phi / \sqrt{C_T}$ is allowed to be ([Poland and Simmons-Duffin, 2011](#); [Rattazzi, Rychkov, and Vichi, 2011b](#)), which translates into a lower bound on the central charge C_T . The best bounds to date were computed by [Poland, Simmons-Duffin, and Vichi \(2012\)](#) and are shown in Fig. 46.¹³⁵ When Δ_ϕ approaches the unitarity bound, both bounds approach the free theory value for Δ_{ϕ^2} and C_T . This is consistent with the fact that a scalar with dimension $(d-2)/2$ satisfies $\partial^2 \phi = 0$ whenever inserted in a correlation function and must therefore be a free scalar.

Analogous bounds have been obtained for CFTs assuming various continuous global symmetries. [Poland, Simmons-Duffin, and Vichi \(2012\)](#) studied the 4pt functions of a scalar ϕ transforming in the fundamental representation of $SO(N)$ or $SU(N)$, deriving an upper bound on the dimension of the lowest singlet scalar in the OPEs $\phi_i \times \phi_j$ [or $\phi^{\dagger i} \times \phi_j$] in the

¹³⁵The bound on C_T can be somewhat strengthened by incorporating the assumption that ϕ is the lowest dimension scalar, as in [Rattazzi, Rychkov, and Vichi \(2011b\)](#).

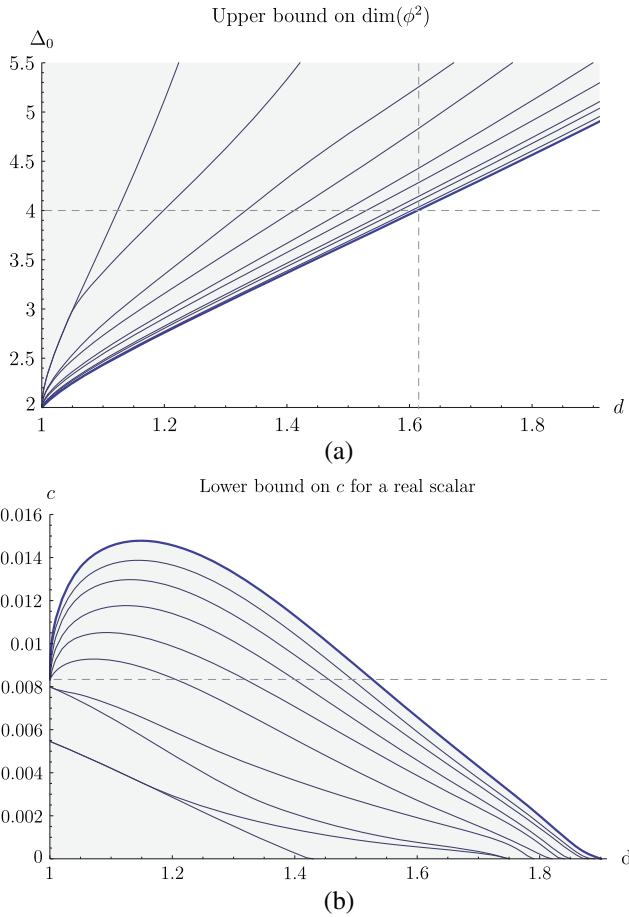


FIG. 46. (a) The upper bound on the dimension of the first scalar in the $\phi \times \phi$ OPE as a function of Δ_ϕ in 4D unitary CFTs; (b) the lower bound on the central charge C_T , computed by maximizing the OPE coefficient $\lambda_{\phi\phi T}$. From Poland, Simmons-Duffin, and Vichi, 2012.

case of $SU(N)$], as well as a lower bound on the central charge, shown in Fig. 47.¹³⁶ As expected, the bounds scale with N , the size of the fundamental representation, at least when the dimension of the external scalar approaches the free value. It should be possible to extend this analysis to obtain upper bounds on the dimensions of operators transforming in other representations. For scalars in the symmetric traceless representation of $SO(4)$ this was done by Poland, Simmons-Duffin, and Vichi (2012).

It is also possible to place upper bounds on the OPE coefficients of conserved vectors of dimension 3 in the OPE of ϕ with its conjugate. This class of operators includes the conserved currents of the considered global symmetry $G = SO(N)$ or $SU(N)$, transforming in the adjoint representation of G . The upper bounds on their OPE coefficients translate into the lower bounds on the central charges C_J . These bounds

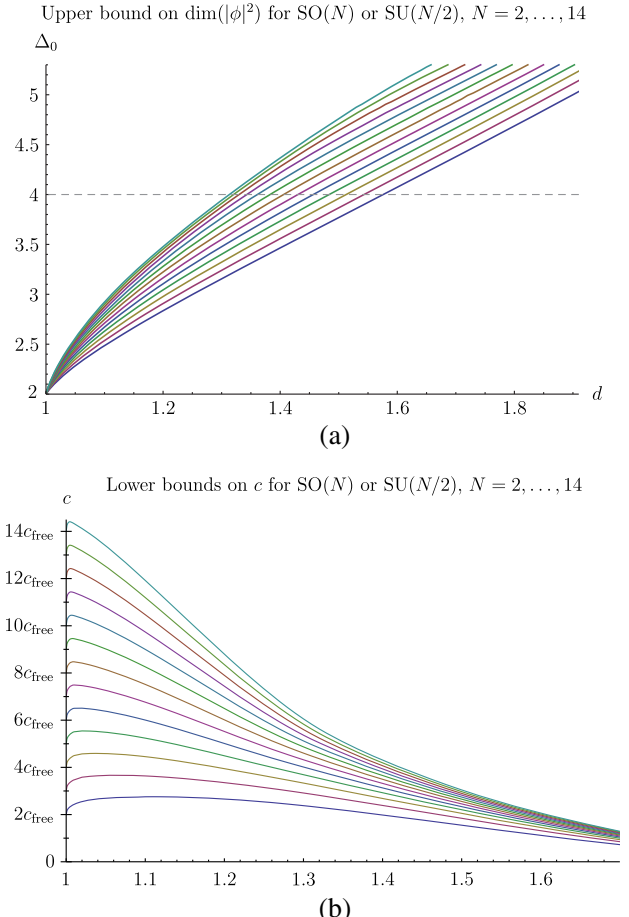


FIG. 47. (a) The upper bounds on the singlet scalar dimension in $SO(N)$ and $SU(N)$ symmetric 4D CFTs, as a function of Δ_ϕ in the fundamental; (b) the lower bounds on C_T in the same theories. From Poland, Simmons-Duffin, and Vichi, 2012.

are shown in Fig. 48. Once again the $SU(N/2)$ bounds coincide with $SO(N)$ ones (Caracciolo *et al.*, 2014). For Δ_ϕ close to the free value, these bounds smoothly approach the free $SO(N)$ value.

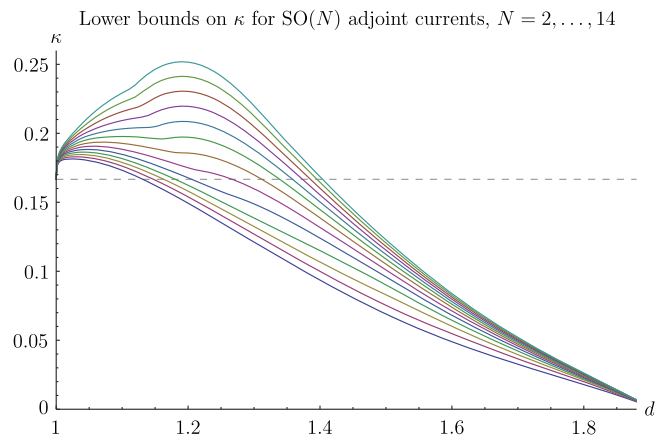


FIG. 48. The lower bounds on C_J in $SO(N)$ -symmetric unitary 4D CFTs as a function of the dimension of a scalar in the fundamental (Poland, Simmons-Duffin, and Vichi, 2012). $SU(N/2)$ adjoint currents satisfy the same bound (Caracciolo *et al.*, 2014).

In addition, for $G = SU(N)$ the OPE $\phi^{\dagger i} \times \phi_j$ may also contain conserved currents of some other global symmetry which may exist in the theory, which are singlets under G . The lower bound on their inverse-square OPE coefficient is given in Fig. 49. Close to the free theory dimension, these bounds approach the value corresponding to the theory of N massless complex scalar fields, whose full symmetry $SO(2N)$ is indeed larger than $SU(N)$.

Additionally, Caracciolo *et al.* (2014) derived lower bounds on C_J in the presence of a gap in the scalar singlet sector, as well as for extended global symmetries $SO(N) \times SO(M)$ and $SO(N) \times SU(M)$.

Unlike in 3D, most of the 4D bounds computed so far do not display any prominent kink or other dramatic feature, suggesting that existing 4D CFTs may lie inside the allowed regions and not on the boundary. Note however that some unexplained features are visible in the C_J lower bounds in Fig. 48, as well as in the bounds on supersymmetric CFTs discussed in Sec. VII.

The bounds discussed in this section have been obtained by studying a 4pt function $\langle \phi_i \phi_j \phi_k \phi_l \rangle$ or $\langle \phi_i \phi^{\dagger j} \phi_k \phi^{\dagger l} \rangle$, where ϕ_i is a single primary operator or a global symmetry multiplet of primary operators. As far as we are aware, a systematic study of numerical bootstrap constraints from mixed correlators in 4D CFTs has not yet been performed outside of the supersymmetric context (Lemos and Liendo, 2016a; Li, Meltzer, and Stergiou, 2017). It will be important to do so in the future and to study the impact on such bounds of assuming only a limited set of relevant operators.

B. Applications to the hierarchy problem

Next we review some bootstrap results which shed light on the attempts to alleviate the hierarchy problem of the SM of particle physics, which historically was one of the motivations for the development of the numerical bootstrap in 4D.

For our discussion, the hierarchy problem can be briefly summarized as follows. The SM is certainly not the complete description of fundamental interactions, as it does not account for dark matter, baryogenesis, neutrino masses, and gravity.

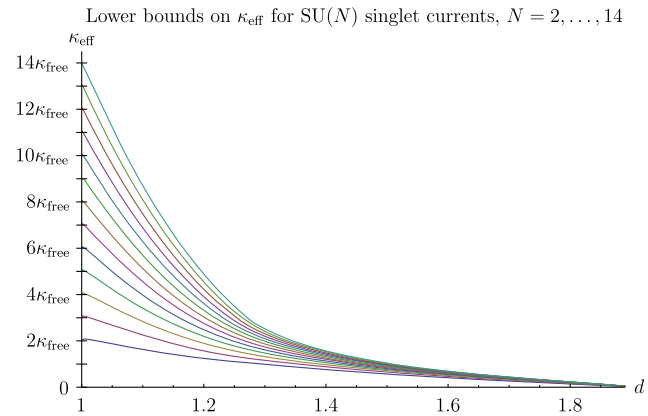


FIG. 49. The lower bounds on the inverse-square OPE coefficient of a singlet current in $SU(N)$ -symmetric unitary 4D CFTs as a function of dimension of a scalar in the fundamental. From Poland, Simmons-Duffin, and Vichi, 2012.

Instead it can be regarded as an effective description, valid at least up to the electroweak scale, where it has been extensively tested, including at the ongoing Large Hadron Collider (LHC) experiments. According to the effective field theory paradigm, the leading effects in this description are captured by the relevant and marginal operators, while all higher-dimensional operators correspond to subleading effects and are suppressed by powers of the electroweak scale ($\Lambda_{\text{IR}} \sim 100$ GeV) over the scale of new physics (Λ_{UV}). The incredible success of the SM in precisely describing all phenomena observed so far is explained by simply pushing the scale of new physics to high values. In particular, electroweak precision tests and more importantly bounds from flavor physics (in particular, from $K-\bar{K}$ mixing) generically require $\Lambda_{\text{UV}} \gtrsim 10^5$ TeV.

This simple assumption creates however a tension (called the hierarchy problem) with the other energy scale in the theory, namely, the scale associated with the only relevant operator present in the SM—the Higgs mass term $H^\dagger H$. Indeed, whenever a relevant deformation exists, it is generically expected to be generated at the fundamental scale with order one strength, unless some symmetry prevents this from happening. The contrary is usually considered an unnatural tuning of the model, similarly to how, in condensed matter systems, one typically needs to adjust a control parameter to approach a critical point.

The quest for a solution to the hierarchy problem has been and remains an important goal in theoretical high-energy physics. Strategies for solving it can be broadly divided into two categories: the first makes use of an additional symmetry that prevents the Higgs mass term from appearing, and then slightly breaks it in order to generate a scale parametrically smaller than Λ_{UV} . The second strategy instead removes altogether the dangerous relevant deformation by increasing the scaling dimension of the Higgs mass term. An example of the first strategy is low-energy supersymmetry, while the second one is realized in technicolor, which replaces the Higgs field with a fermion bilinear operator, of scaling dimension close to 3.

While technicolor solves the hierarchy problem by making the Higgs mass term irrelevant, it also raises the SM Yukawa operator dimensions from 4 to 6. To generate heavy quark masses of needed size, these operators need to originate at an energy scale not much above Λ_{IR} . This leads to a tension with flavor observables, due to four-fermion operators expected to originate at about the same scale unless yet additional structure is added. To solve this problem, Luty and Okui (2006) proposed the “conformal technicolor” scenario, in which the Higgs field has a scaling dimension close to the free value, while the Higgs mass term is close to marginality or irrelevant.

More precisely, to realize this scenario one would need a unitary CFT which contains a scalar operator H replacing the SM Higgs field. To preserve the SM custodial symmetry, the CFT must have an $SO(4)$ global symmetry, with H transforming in the fundamental. The scaling dimension requirements are as follows: Δ_H has to be close to 1, while $\Delta_S \gtrsim 4$, where S is the first scalar $SO(4)$ -singlet operator in the OPE $H^\dagger \times H$, playing the role of the Higgs mass term in this setup. Given the scaling dimension requirements, this hypothetical CFT must necessarily be strongly coupled, while its coupling to the rest of the SM (gauge fields and fermions) can be treated as a small perturbation.

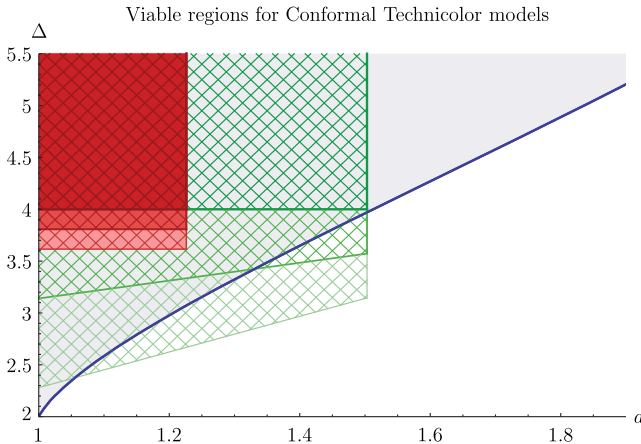


FIG. 50. Viable regions in the $\{\Delta_H, \Delta_S\}$ plane for conformal technicolor models in the flavor-generic (red) and flavor-optimistic (cross-hatched green) cases, superimposed with the $SO(4)$ bound. Regions for no tuning, 10%, and 1% tuning are shown in successively lighter shades of each color, with the largest region corresponding to 1% tuning in each case. Flavor-generic models are ruled out. From [Poland, Simmons-Duffin, and Vichi, 2012](#).

The 4D numerical bootstrap grew out from the attempts to show that the most optimistic requirements $\Delta_H \rightarrow 1$, $\Delta_S > 4$ are impossible to realize. A proof of this theorem about unitary 4D CFTs is visible in the upper bound on Δ_S provided by the $N = 4$ curve in Fig. 47, which approaches 2 for $\Delta_H \rightarrow 1$.

It is phenomenologically acceptable to have Δ_H slightly deviate from 1 without violating flavor constraints, and to allow Δ_S somewhat below 4 at the price of some moderate tuning ([Luty and Okui, 2006](#); [Rattazzi *et al.*, 2008](#); [Rychkov, 2011](#)). Although this freedom helps to alleviate bootstrap constraints, some tension remains. Figure 50 from [Poland, Simmons-Duffin, and Vichi \(2012\)](#) shows the regions of $\{\Delta_H, \Delta_S\}$ allowed under different degrees of tuning and different assumptions about the structure of the flavor sector. The conclusion is that compatibility with the bootstrap bound can be achieved only under optimistic flavor assumptions and with a moderate tuning.

An additional phenomenological constraint on conformal technicolor comes from the existence of the Higgs boson particle. While a SM-like Higgs boson may appear in conformal technicolor as a resonance of the strong dynamics at the electroweak scale associated with breaking of conformal invariance ([Luty and Okui, 2006](#)), it is expected to be somewhat heavier than the experimentally observed value 125 GeV and to have some deviations in its coupling to the top quark, which were not seen so far. This further reduces the likelihood that the conformal technicolor scenario is realized in nature. Still, the above analysis, performed prior to the Higgs boson discovery, remains an example of how theoretical investigations can lead to first-principles constraints on strongly coupled scenarios for particle physics beyond the SM.

C. Constraints on the QCD₄ conformal window

Perhaps the most famous class of unitary 4D CFTs is the IR fixed points of asymptotically free non-Abelian gauge theories coupled to massless fermions, often referred to as Banks-Zaks

fixed points ([Banks and Zaks, 1982](#)) although they were first considered by [Caswell \(1974\)](#) and [Belavin and Migdal \(1974\)](#). Depending on the number of fermion representations N , this IR conformal behavior is realized in an interval of N called the “conformal window.” These CFTs are of great interest theoretically and historically have also been discussed because of their relation to walking technicolor models of electroweak symmetry breaking.¹³⁷ Close to the upper end of the conformal window these theories can be studied perturbatively; see, e.g., [Ryttov and Shrock \(2017\)](#). They have also been studied actively using lattice Monte Carlo techniques; see [Nogradi and Patella \(2016\)](#) and [Svetitsky \(2018\)](#) for recent reviews.

Here we describe what the bootstrap so far has to say about these CFTs. For concreteness we provide our discussion for a QCD-like theory with N massless Dirac fermions in the fundamental representation (\square) of an $SU(N_c)$ gauge group, with $N_c \geq 3$, although the results will also apply to the case $N_c = 2$. The global symmetry G of this theory is

$$G = U(1)_V \times H, \quad H = SU(N)_L \times SU(N)_R, \quad (128)$$

where H rotates left and right Weyl components ψ_L and ψ_R of the fermions separately, while the vectorial $U(1)_V$ rotates them simultaneously; its axial counterpart is instead anomalous. The theory also preserves P and C , which interchange left and right fermions.

If an IR fixed point is reached, the above global symmetry remains unbroken. This implies that all operators of the would-be CFT must organize in irreducible representation of G . We are interested, in particular, in gauge-invariant scalar operators (“mesons”) which are fermion bilinears:

$$\Phi_i^k = \bar{\psi}_L^k \psi_{Ri}, \quad (129)$$

which transform in $\bar{\square} \times \square$ under H . The mesons are not charged under the $U(1)_V$, which will play no role below. Parity maps Φ into its complex conjugate $\bar{\Phi}$. The scaling dimension of Φ is an interesting observable, often expressed in terms of the anomalous dimension $\gamma_\Phi = 3 - \Delta_\Phi$; see [Giedt \(2016\)](#) for a review of lattice measurements of γ_Φ . The bootstrap will give lower bounds on Δ_Φ , translating into upper bounds on γ_Φ .

[Nakayama \(2016c\)](#) carried out a bootstrap analysis of the 4pt function $\langle \Phi \bar{\Phi} \bar{\Phi} \bar{\Phi} \rangle$ using the global symmetry H .¹³⁸ Of particular interest is an upper bound on the dimension of the lowest scalar in the OPE $\Phi \times \bar{\Phi}$ which is a singlet under H , shown in Fig. 51 for $N = 8$. Such scalars are parity even, with an example being $\text{Tr}[F_{\mu\nu} F^{\mu\nu}]$, where $F_{\mu\nu}$ is the Yang-Mills

¹³⁷Walking behavior is expected to be realized for N just below the lower end of the conformal window ([Kaplan *et al.*, 2009](#)), but detailed discussion of this physics is beyond our scope. See [Gorbenko, Rychkov, and Zan \(2018a, 2018b\)](#) for a recent CFT perspective and [Appelquist, Ingoldby, and Piai \(2017, 2018\)](#) for a recent lattice perspective using effective field theory.

¹³⁸In his notation Φ was a bifundamental of H under a different (but equivalent) convention for the transformation of left-handed fermions.

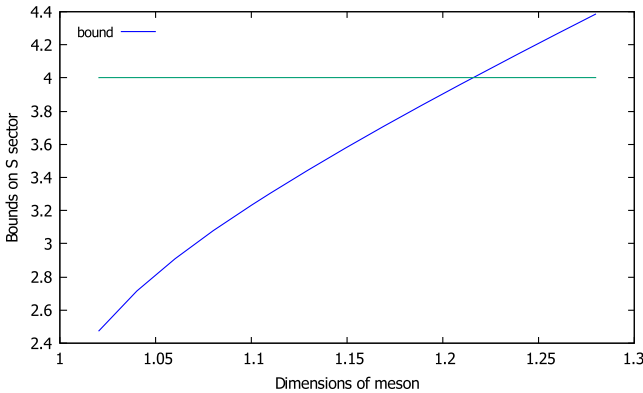


FIG. 51. The upper bound on the dimension of the first singlet operator appearing in the OPE $\Phi \times \bar{\Phi}$ for $N = 8$ as a function of Δ_Φ . From Nakayama, 2016c.

field strength.¹³⁹ A necessary condition for reaching a fixed point is that all such scalars must be irrelevant. Indeed, the Banks-Zaks fixed point is an example of a “self-organized” CFT in the terminology of Sec. V.A. Using this crucial observation and the bound in Fig. 51, we conclude that if $N = 8$ belongs to the conformal window, then necessarily

$$\Delta_\Phi > 1.21 \quad (N = 8). \quad (130)$$

For $N = 16$ the analogous bound is $\Delta_\Phi > 1.71$ (Nakayama, 2016c), and for other N the bounds can be derived analogously but have not been published.

Nakayama (2016c) also derived, under the same assumptions, upper bounds on the lowest scalars in $\Phi \times \bar{\Phi}$ which transform as TT or AA under H , where T/A stands for the symmetric or antisymmetric traceless tensor representation. See Fig. 52 for the bound at $N = 8$. From an idea of Iha, Makino, and Suzuki (2016),¹⁴⁰ such bounds constrain possible global symmetry enhancements, in parallel with Sec. V.E.3. Namely, imagine that we are trying to reach the CFT describing the Banks-Zaks fixed point in an RG flow from a microscopic description which at short distances preserves only a subgroup H' of H , as well as parity. For example, this would be true for lattice studies with Wilson or domain wall fermions, which only realize the diagonal subgroup

$$H'_{\text{Wilson}} = SU(N)_V, \quad (131)$$

as in Ishikawa *et al.* (2014, 2015). A second example is furnished by staggered fermions, another lattice fermion realization commonly used to study the QCD₄ conformal window. Being defined for N a multiple of 4, these preserve microscopically a subgroup

¹³⁹On the other hand, the instanton density operator $\text{Tr}[F_{\mu\nu}\tilde{F}^{\mu\nu}]$ is parity odd and does not appear in the OPE $\Phi \times \bar{\Phi}$. We note that this operator is also expected to be irrelevant, since at the fixed point it becomes a descendant of the anomalous axial current: $\partial^\mu J_\mu^A \sim \text{Tr}[F_{\mu\nu}\tilde{F}^{\mu\nu}]$.

¹⁴⁰See also Hasenfratz, Rebbi, and Witzel (2017, 2018) for a lattice perspective.

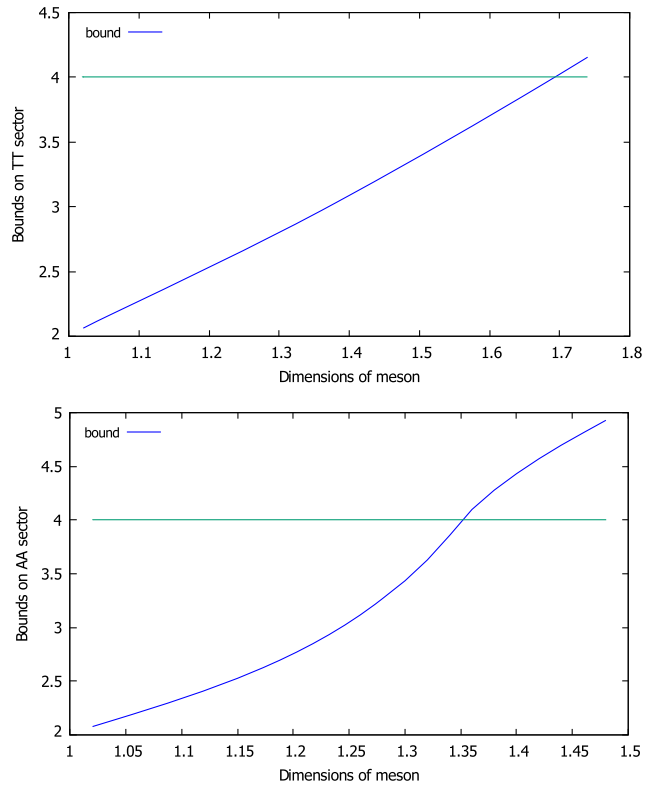


FIG. 52. The upper bounds on the dimensions of the first TT and AA operators appearing in the OPE $\Phi \times \bar{\Phi}$ for $N = 8$ as a function of Δ_Φ . From Nakayama, 2016c.

$$H'_{\text{staggered}} = SU(N/4) \times SU(N/4). \quad (132)$$

Observing the Banks-Zaks fixed point in a lattice Monte Carlo simulation using a fermion realization with a reduced symmetry implies a symmetry enhancement. For this to be possible, all parity-even scalar operators which are singlets under H' (but not necessarily under H) must be irrelevant. Since the TT and AA representations of H contain a singlet when reduced under either Eq. (131) or (132), we obtain a necessary condition that the TT and AA scalars must be irrelevant in both cases. So, from the TT bound in Fig. 52, enhancement from H'_{Wilson} or $H'_{\text{staggered}}$ requires

$$\text{Wilson or staggered} \Rightarrow \Delta_\Phi > 1.69 \quad (N = 8). \quad (133)$$

Compared to Nakayama (2016c), the earlier analysis of symmetry enhancement bounds for lattice QCD by Iha, Makino, and Suzuki (2016) did not use the full symmetry H but only the vectorial subgroup $SU(N)_V$, grouping the operators (129) into the irreducible representations of $SU(N)_V \times P$,

$$S = \sum_{j=1}^N \bar{\psi}^j \psi_j, \quad S_i^k = \bar{\psi}^k \psi_i - \frac{1}{N} \delta_i^k S, \\ \phi = \sum_{j=1}^N \bar{\psi}^j \gamma_5 \psi_j, \quad \phi_i^k = \bar{\psi}^k \gamma_5 \psi_i - \frac{1}{N} \delta_i^k \phi, \quad (134)$$

which transform as singlets or adjoints under $SU(N)_V$ and have $P = \pm$. This simplifies the analysis, as the system of crossing relations for representations of $SU(N)_V$ is easier than for the full H . Of course, by not using the full symmetry one loses information, although this can be partially remedied by imposing by hand the constraint that all operators in Eq. (134) have the same dimension.

In this setup Iha, Makino, and Suzuki (2016) could extract bounds from the symmetry enhancement for staggered fermions (but not for Wilson fermions). To do this they analyzed the 4pt function of the adjoint pseudoscalar ϕ_i^k for $N = 8, 12$, and 16. They derived upper bounds on the lowest dimension scalar in the $\phi \times \phi$ OPE transforming in the representation $[N-1, N-1, 1, 1]$ ¹⁴¹ of $SU(N)_V$. They argued that symmetry enhancement requires that this scalar be irrelevant.

To illustrate this more clearly, using results of Lee and Sharpe (1999) they identified explicitly some four-fermion operators which are singlets under Eq. (132) and which have nonzero overlap with $[N-1, N-1, 1, 1]$ when the symmetry is reduced to $SU(N)_V$. The resulting necessary condition for staggered fermion enhancement is

$$\text{Staggered} \Rightarrow \Delta_\Phi > 1.67, 1.71, 1.71 \quad (N=8, 12, 16). \quad (135)$$

The fact that for $N = 8$ this bound is somewhat weaker than Eq. (133) is explained partly by not using the full symmetry and partly by working at a lower derivative order.

It should be mentioned that most studies of the QCD conformal window by lattice Monte Carlo or RG methods point to rather small anomalous dimensions γ_Φ . Hence the above bootstrap bounds on Δ_Φ are probably not optimal. Finding better bootstrap constraints on the QCD conformal window is an interesting open problem. Some possibilities to make further progress are to pursue mixed correlator studies, to include global symmetry currents and the stress-tensor in the bootstrap (whose 3pt functions contain known anomaly coefficients), and/or to study baryon operators.

VII. APPLICATIONS TO SUPERCONFORMAL THEORIES

Conformal symmetry admits a supersymmetric extension into a superalgebra containing the standard anticommuting supercharges $\{\mathcal{Q}, \bar{\mathcal{Q}}\} \sim P$ as well as R -symmetry generators and the anticommuting analog of SCTs $\{\mathcal{S}, \bar{\mathcal{S}}\} \sim K$ (called special superconformal transformations). Superconformal field theories (SCFTs) are extraordinarily rich and have been studied intensively from many viewpoints. In the last decades the variety of known theories has grown in size: new constructions have been made, including many Lagrangian models, but remarkably also many theories that appear to admit no such description have been found. Also, a great number of strongly coupled SCFTs are known to exist, in different dimensions and with different number of supercharges, some of which can be understood using field theory or holographic dualities.

¹⁴¹The notation gives a list of the number of boxes in each successive column of the Young tableau.

SCFTs represent an important playground to test our understanding of CFTs and the effectiveness of bootstrap techniques. The presence of supersymmetry allows one to exactly compute some interesting CFT data, even in a strongly interacting regime, which in turn can be compared with bootstrap predictions.

From the point of view of the conformal bootstrap, supersymmetry has essentially three consequences: (1) relating the OPE coefficients and dimensions of operators belonging to the same supersymmetric multiplet, creating superconformal blocks; (2) acting as a selection rule for the operators entering a given OPE and imposing stronger constraints from unitarity; and (3) fixing the dimensions of certain short multiplets. By virtue of these constraints, crossing symmetry is expected to be more effective in SCFTs.

A. Theories with 4D $\mathcal{N}=1$ supersymmetry

Before discussing the numerical bootstrap results, let us say a few words on the structure of representations of the superconformal algebra. For concreteness we provide this discussion for SCFTs with 4D $\mathcal{N}=1$ supersymmetry.¹⁴² Superconformal primary operators (annihilated by the special superconformal generators $\mathcal{S}, \bar{\mathcal{S}}$) are labeled by four numbers $(q, \bar{q}, \ell, \bar{\ell})$, where $\ell, \bar{\ell}$ are the usual Lorentz quantum numbers and q, \bar{q} are related to the scaling dimension Δ and R charge of the superconformal primary operator:

$$\Delta = q + \bar{q}, \quad R = \frac{2}{3}(q - \bar{q}). \quad (136)$$

Unitarity bounds on these operators were worked out by Flato and Frønsdal (1984) and Dobrev and Petkova (1985), taking the form

$$\begin{aligned} q \geq \frac{1}{2}\ell + 1, \quad \bar{q} \geq \frac{1}{2}\bar{\ell} + 1 & \quad (\ell\bar{\ell} \neq 0), \\ q \geq \frac{1}{2}\ell + 1 & \quad (\bar{q} = \bar{\ell} = 0), \\ \bar{q} \geq \frac{1}{2}\bar{\ell} + 1 & \quad (q = \ell = 0). \end{aligned} \quad (137)$$

The second and third lines in the above expression identify chiral ($\Phi_{\alpha_1 \dots \alpha_\ell}$) or antichiral ($\bar{\Phi}_{\dot{\alpha}_1 \dots \dot{\alpha}_{\bar{\ell}}}$) operators, which are annihilated by the supercharge $\bar{\mathcal{Q}}$ or \mathcal{Q} , respectively.

Finally, we mention a few theoretical results for superconformal blocks present in the literature, focusing on those relevant for the 4D $\mathcal{N}=1$ bootstrap. Superconformal blocks for correlation function of scalar superconformal primaries can be expressed in terms of finite linear combinations of ordinary scalar conformal blocks with suitable dimensions and spin; however, computing these coefficients can be a challenging task. The work of Poland and Simmons-Duffin (2011) and Vichi (2012) obtained the superconformal blocks for 4pt functions of a scalar chiral supermultiplet Φ . Shortly after, Fortin, Intriligator, and Stergiou (2011) computed

¹⁴²For similar results in other dimensions or with extended supersymmetry see Minwalla (1998) and the summary of recent progress in Sec. IX. Many results described here can also be treated in a uniform way across dimensions for algebras with the same number of supercharges; see Bobev *et al.* (2015a).

superconformal blocks for 4pt functions of the multiplet associated with global symmetry conserved currents, whose lowest component is again a scalar field.¹⁴³ A similar analysis applicable to 4pt functions of R -current multiplets (containing the stress tensor) was also recently carried out by [Manenti, Stergiou, and Vichi \(2018\)](#). The general approach in these works was to classify the possible three-point functions in superspace using the formalism of [Osborn \(1999\)](#) and then expand in the Grassmann variables θ_i to compute relations between OPE coefficients of conformal primaries. In this approach one must also carefully compute the norm of each conformal primary in the multiplet.¹⁴⁴

The work of [Fitzpatrick et al. \(2014\)](#) developed alternate techniques based on either solving the super-Casimir equation or writing the blocks as superconformal integrals using a superembedding formalism. The latter approach was employed by [Khandker et al. \(2014\)](#) to find the blocks appearing in the more general correlation function $\langle \Phi_1 \bar{\Phi}_2 \Psi_1 \bar{\Psi}_2 \rangle$, where Φ_i and Ψ_i are scalar superconformal primary operators with arbitrary dimension and R charge,¹⁴⁵ with the restriction that the exchanged operator is neutral under R symmetry. This analysis was later extended by [Li and Su \(2016\)](#) to the more general case of four distinct scalar superconformal primary operators with arbitrary scaling dimensions and R charges, with no restriction on the exchanged operators besides those imposed by superconformal symmetry. However, this analysis was missing a particular class of superconformal blocks, associated with exchanged primaries in representations of the Lorentz group with $\ell \neq \bar{\ell}$. In this case the corresponding superconformal primary does not enter the OPE of the external operators, but some of its superconformal descendants do. This issue was fixed by [Li, Meltzer, and Stergiou \(2017\)](#).

1. Bounds without global symmetries

Now we summarize numerical results for correlation functions involving scalar chiral superfields. The first numerical studies, starting with [Poland and Simmons-Duffin \(2011\)](#) and improved by [Vichi \(2012\)](#) and [Poland, Simmons-Duffin, and Vichi \(2012\)](#), focused on 4pt functions containing a single scalar chiral supermultiplet $\langle \Phi \bar{\Phi} \Phi \bar{\Phi} \rangle$. Crossing symmetry for this correlation function involves two OPE channels. Because of the chirality conditions, the $\Phi \times \bar{\Phi}$ OPE receives contributions only from traceless symmetric tensor superconformal primaries together with their $\mathcal{Q}\bar{\mathcal{Q}}$ and $\mathcal{Q}^2\bar{\mathcal{Q}}^2$ superdescendants, giving rise to the superconformal blocks described above. The $\Phi \times \Phi$ OPE, on the other hand, is more subtle and can receive three different contributions: (1) the chiral superfield Φ^2 , (2) $\bar{\mathcal{Q}}$ descendants of semishort multiplets, and (3) $\bar{\mathcal{Q}}^2$ descendants of generic (long) multiplets. As a

¹⁴³Some incorrect coefficients and missing blocks were later pointed out by [Berkooz, Yacoby, and Zait \(2014\)](#) and [Khandker et al. \(2014\)](#).

¹⁴⁴Such norms were worked out for general multiplets by [Li and Stergiou \(2014\)](#).

¹⁴⁵The first and second pairs have the same conformal weights q and \bar{q} , hence the notation.

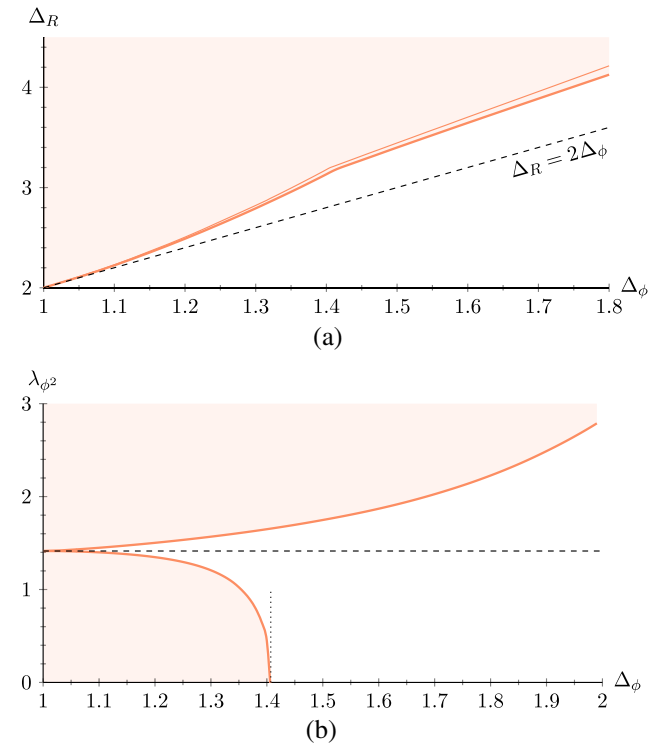


FIG. 53. (a) The upper bound on the dimension of the operator \mathcal{R} as a function of Δ_Φ . The shaded area is excluded. The dashed line at $\Delta_R = 2\Delta_\Phi$ corresponds to generalized free theories. From [Li, Meltzer, and Stergiou, 2017](#) and [Poland, Simmons-Duffin, and Vichi, 2012](#). (b) The lower and upper bounds on the OPE coefficient of the chiral operator Φ^2 entering the $\Phi \times \Phi$ OPE. The vertical dotted line is at $\Delta_\Phi = 1.407$ and the horizontal dashed line is at the free theory value $\lambda_{\Phi\Phi\Phi^2} \equiv \lambda_\phi^2 = \sqrt{2}$. From [Poland and Stergiou, 2015](#).

result, this channel allows conformal blocks of even spin $\ell = \bar{\ell}$ either at the protected dimensions $\Delta = 2\Delta_\Phi + \ell$ or at unprotected dimensions satisfying the unitarity bound $\Delta \geq |2\Delta_\Phi - 3| + \ell + 3$.

In Fig. 53 we show an upper bound on the dimension of the first real scalar supermultiplet \mathcal{R} entering the OPE $\Phi \times \bar{\Phi}$. A first important consequence of this result is that in any perturbative SCFT, the combination $2\Delta_\Phi - \Delta_R$ must be positive (or very suppressed) to satisfy the bound. Secondly, one can observe a minor kinklike feature on the boundary of the allowed region. The same feature appears in the lower bound on the central charge, Fig. 54, and it also coincides with the minimal value of Δ_Φ consistent with the absence of the chiral operator Φ^2 , as shown in the bottom panel of Fig. 53.

In light of this, it is tempting to conjecture the existence of a “minimal SCFT” that realizes the chiral ring relation $\Phi^2 = 0$ and saturates these bounds. This conjecture has been seriously addressed by [Poland and Stergiou \(2015\)](#) and [Li, Meltzer, and Stergiou \(2017\)](#), who studied the properties of this hypothetical theory. Note that the minimal value of Δ_Φ consistent with the chiral ring assumption, let us call it Δ_Φ^{mSCFT} , represents an extremal solution, and it is therefore uniquely determined. In addition, to coincide with the kinks it should agree with the

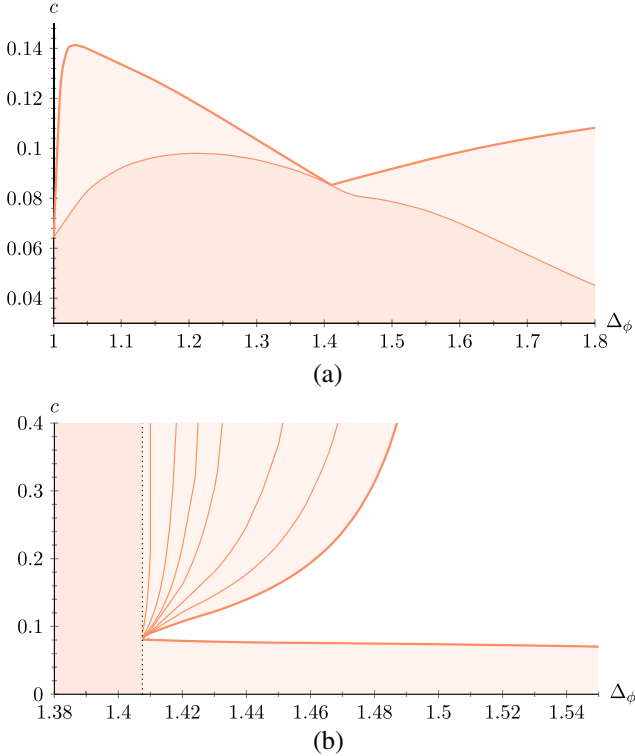


FIG. 54. (a) The lower bound on the central charge as a function of Δ_Φ assuming that $\Delta_{\mathcal{R}}$ is consistent with the unitarity bound (thin line) or it saturates the upper bound in Fig. 53 (thick line). The shaded area is excluded. From Li, Meltzer, and Stergiou, 2017. (b) The lower and upper bounds on the central charge as a function of Δ_Φ , with the assumption that there is no Φ^2 operator. The upper bounds correspond to different gaps until the second spin-1 superconformal primary $\Delta_{\ell=1} \geq 3.1, 3.3, 3.5, 3.7, 3.9, 4, 4.1$ (from left to right). The shaded area is excluded. From Poland and Stergiou, 2015.

solution obtained from maximizing the dimension of the first neutral unprotected operator and the solution obtained from minimizing the central charge at the same value of Δ_Φ .

Figure 54(a) shows that the two extremization procedures generically lead to two different solutions, except at $\Delta_\Phi^{\text{mSCFT}}$. This confirms our expectation of a unique solution coinciding with the kinks. Furthermore, by inputting a gap between the stress-tensor multiplet [whose lowest component is the spin-1 $U(1)_R$ current] and the next spin-1 supermultiplet, one is able to extract an upper bound on the central charge. While this bound is gap dependent at generic Δ_Φ , it almost coincides with the lower bound at $\Delta_\Phi^{\text{mSCFT}}$, as shown in Fig. 54(b). By extrapolating these results at large Λ , Poland and Stergiou (2015) obtained the prediction $\Delta_\Phi^{\text{mSCFT}} \approx 1.428$, $c \approx 0.111$, perhaps consistent with $\Delta_\Phi^{\text{mSCFT}} = 10/7$, $c = 1/9$.

Recently a few theories have been proposed as mSCFT candidates (Buican and Nishinaka, 2016; Xie and Yonekura, 2016), which implement the chiral ring condition $\Phi^2 = 0$; however, they do not quite match the bootstrap predictions presented here. In particular, the central charge is much larger than $1/9$.

It is also worth noting that, in any solution saturating the dimension bound of Fig. 53, the chiral operator Φ is not

charged under any global symmetry. If it was, in fact, the solution would contain a spin-1 conserved current, which in $\mathcal{N} = 1$ SUSY happens to be the superdescendant of a dimension-2 real scalar which would appear in the $\Phi \times \bar{\Phi}$ OPE.

To conclude this section, let us mention that the work of Li, Meltzer, and Stergiou (2017) who also performed a bootstrap study of a system of mixed correlators involving a scalar chiral superfield Φ and a long real scalar superfield \mathcal{R} , identified with the first scalar operator appearing in the $\Phi \times \bar{\Phi}$ OPE. Unlike in 3D, this analysis did not seem to allow one to easily isolate a closed region. A preliminary inspection of the extremal solution does not reveal any obvious low-lying operators decoupling from the spectrum, but rather it involves a rearrangement of higher-dimensional operators (Stergiou, 2017). It will be interesting to study this rearrangement further and understand how to robustly isolate the conjectured mSCFT in future work.

2. Bounds with global symmetries

As mentioned in the previous section, conserved currents of global symmetries j_μ^a sit in real supermultiplets \mathcal{J}^a whose lowest component is a dimension-2 scalar J^a . In addition, the multiplet satisfies the conservation condition $D^2 \mathcal{J}^a = \bar{D}^2 \mathcal{J}^a = 0$. Bootstrapping correlation functions of the scalars J^a allow one access to the space of local SCFTs with a given global symmetry. Hence, due to supersymmetry, one can apply the same machinery encountered so far, with no need to deal with spinning conformal blocks.

Bounds on OPE coefficients of $SU(N)$ currents were explored by Berkooz, Yacoby, and Zait (2014) and dimension bounds (and coefficient bounds assuming gaps) from single 4pt functions $\langle JJJJ \rangle$ were explored by Li, Meltzer, and Stergiou (2017). The latter work also studied the case of mixed correlators involving J and a chiral field Φ charged under the global symmetry. Note that this charge necessarily differs from the R symmetry, which instead is part of the conformal algebra: the conserved current associated with the latter is the lowest component of the Ferrara-Zumino multiplet which contains the stress tensor and supercurrents.

A key result, shown in Fig. 55, shows that any local SCFT with a continuous global symmetry must contain a real scalar multiplet \mathcal{O} with dimension $\Delta_{\mathcal{O}} \leq 5.246$. The same figure also shows upper bounds on the OPE coefficient associated with J itself as well as the one associated with the stress-tensor multiplet, denoted as V . Interestingly, both bounds on c_J and c_V show plateaus for small values of the gap in the scalar sector. These are perhaps consistent with the existence of SCFT solutions shaping the bounds. On the other hand, the values extracted from Fig. 55 are much smaller than the limits one obtains by inspecting the correlation functions of chiral superfields. For instance, the relation between c_V and Fig. 54 is $c_V^2 = 1/(90c)$, making the bound on the central charge very weak.¹⁴⁶

¹⁴⁶The OPE coefficient bounds obtained by Berkooz, Yacoby, and Zait (2014) for $SU(N)$ current 4pt functions were also relatively weak.

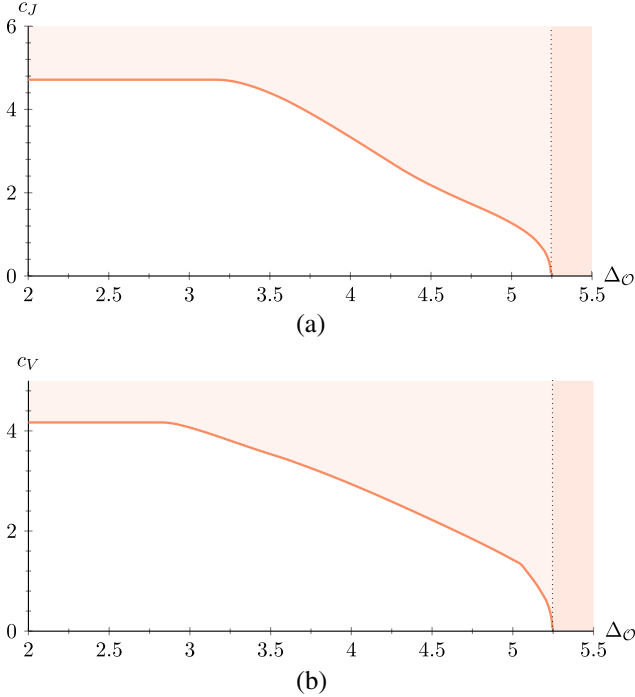


FIG. 55. The upper bounds on the OPE coefficients $c_{\mathcal{O}} \equiv 2^{-\ell/2} \lambda_{J\mathcal{O}}$ appearing in the $J \times J$ OPE arising from (a) J itself or (b) the stress-tensor supermultiplet V , as a function of the dimension of the first unprotected scalar \mathcal{O} in the $J \times J$ OPE. The region to the right of the dotted vertical line at $\Delta_{\mathcal{O}} = 5.246$ is not allowed. From Li, Meltzer, and Stergiou, 2017.

An alternative method to study SCFTs with global symmetries is to consider external scalar operators in nontrivial representations of the symmetry. An important target is to make contact with supersymmetric QCD (SQCD) theories, e.g., supersymmetric gauge theories with gauge group $SU(N_c)$ and N_f flavors of quarks $Q_i, \bar{Q}^{\bar{j}}$, with N_f in the conformal window $3N_c/2 \leq N_f \leq 3N_c$ (Seiberg, 1995). The simplest gauge-invariant operators are the mesons $M_i^{\bar{j}} = Q_i \bar{Q}^{\bar{j}}$, which transform as bifundamentals of $SU(N_f)_L \times SU(N_f)_R$ and have dimension $\Delta_M = 3(1 - N_c/N_f)$. Because of supersymmetry, both the central charge and current central charge can be exactly computed due to their relation to anomaly coefficients.

A partial bootstrap analysis applicable to meson 4pt functions was performed by Poland, Simmons-Duffin, and Vichi (2012), which considered chiral scalar multiplets transforming in the fundamental representation of $SU(N)$ and obtained bounds on the OPE coefficients associated with conserved currents transforming in both the singlet and the adjoint representations of $SU(N)$. As can be seen in Fig. 56, these bounds are still somewhat far from the exact results of SQCD, most likely because this study did not utilize the full symmetry. It will be interesting in future work to extend these analyses of chiral 4pt functions to use the whole SQCD global symmetry, together with mixed correlators containing the $SU(N_f)_{L/R}$ current multiplets and/or the stress-tensor multiplet.

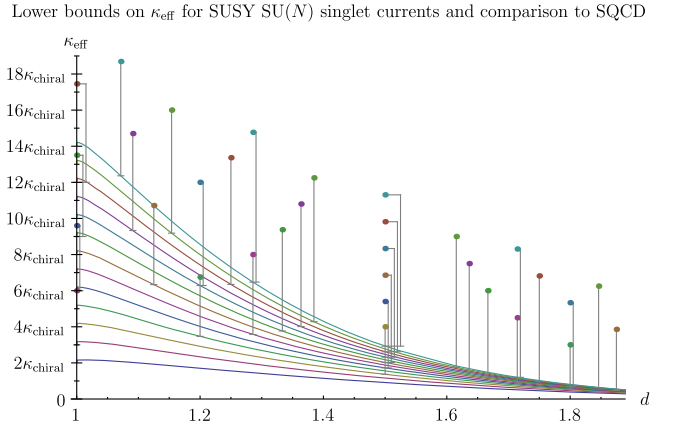


FIG. 56. The lower bounds on the effective 2pt function coefficient $\kappa_{\text{eff}} = 1/\lambda_{\Phi\Phi}^2$ of $SU(N)$ singlet currents appearing in $\Phi \times \bar{\Phi}$, where Φ is a chiral scalar of dimension d in the fundamental of $SU(N)$, for $N = 2, \dots, 14$. The bounds are normalized to the value κ_{chiral} corresponding to a free chiral superfield. Each dot connected to a bound corresponds to the exact value in an SQCD theory with the same symmetry. From Poland, Simmons-Duffin, and Vichi, 2012.

B. Theories with 3D $\mathcal{N}=2$ supersymmetry

Another interesting set of targets for the conformal bootstrap are the 3D CFTs with $\mathcal{N} = 1$ or 2 supersymmetry. We initially discussed the former in Sec. V.D.3, where there were no constraints from supersymmetry used other than relations between scaling dimensions (see, however, footnote 120). The superconformal representation theory of the latter has a similar structure to that of 4D $\mathcal{N} = 1$ SCFTs; for details see Minwalla (1998) and Bobev *et al.* (2015a). Perhaps the simplest such theory is the $\mathcal{N} = 2$ supersymmetric Wess-Zumino model described in Sec. V.D.1. This CFT can be thought of as the IR fixed point of a theory of a single chiral superfield $\Phi = \phi + \psi\theta + F\theta^2$ and superpotential $W = \lambda\Phi^3$. The fixed point has a $U(1)_R$ symmetry under which Φ has charge $2/3$, implying exact dimensions for the complex scalar ϕ and the Dirac fermion ψ : $\Delta_\phi = q_\phi = 2/3$, $\Delta_\psi = \Delta_\phi + 1/2 = 7/6$.

Applying the numerical bootstrap to the 4pt function $\langle \Phi \bar{\Phi} \Phi \bar{\Phi} \rangle$ and incorporating the unitarity bounds and superconformal blocks of $\mathcal{N} = 2$ superconformal symmetry, Bobev *et al.* (2015a, 2015b) and Li and Su (2017a) studied general bounds on the dimension of the leading unprotected scalar operator $\Phi \bar{\Phi}$, with the basic result shown in Fig. 57. Curiously, the resulting bound has three distinct features, the first of which occurs at a scaling dimension $\Delta_\Phi \approx 2/3$. This gives a sharp upper bound $\Delta_{\Phi\bar{\Phi}} < 1.91$ for the $\mathcal{N} = 2$ supersymmetric Wess-Zumino model and a plausible conjecture that the model saturates the optimal version of this bound. Further analysis of the extremal spectrum of this kink can be found in Bobev *et al.* (2015a, 2015b), while Li and Su (2017a) found that an isolated island around $\{\Delta_\Phi, \Delta_{\Phi\bar{\Phi}}\} = \{0.6678(13), 1.903(10)\}$ could be obtained by assuming a modest gap in the spectrum of spin-1 superconformal primaries $\Delta_{J'} \geq 3.5$.

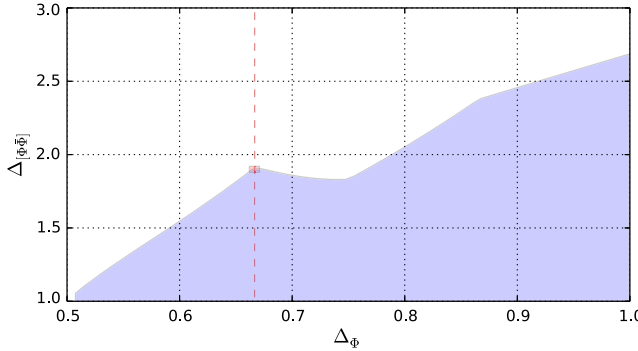


FIG. 57. The bound on the dimension of the first unprotected scalar $\Phi\bar{\Phi}$ in the $\Phi \times \bar{\Phi}$ OPE in 3D SCFTs with $\mathcal{N} = 2$ supersymmetry. From Bobev *et al.*, 2015b.

The middle kink occurs near $\Delta_\Phi = 3/4$ and coincides with a kinematic threshold beyond which superconformal descendants of antichiral operators $Q^2\bar{\Psi}$ can no longer appear in the $\Phi \times \Phi$ OPE. It is not yet clear if any CFT sits at this kink. The rightmost kink, occurring near $\Delta_\Phi \sim 0.86$, also still lacks a clear interpretation, but seems to interpolate to the kink in the 4D $\mathcal{N} = 1$ bounds discussed above. Notably, the extremal spectrum of this kink seems to satisfy the chiral ring relation $\Phi^2 = 0$ (Bobev *et al.*, 2015a) and an island around the point can also be isolated using a set of gap assumptions (Li and Su, 2017a), making it a plausible candidate for a new CFT. Finally let us mention that this analysis was also extended to 3D $\mathcal{N} = 2$ supersymmetric CFTs with $O(N)$ global symmetry by Chester, Giombi *et al.* (2016) and Chester, Iliesiu *et al.* (2016), who found similar features at each value of N . A related 3D $\mathcal{N} = 2$ theory with multiple interacting chiral superfields and a conformal manifold was also recently studied using bootstrap methods by Baggio *et al.* (2018).

VIII. APPLICATIONS TO NONUNITARY MODELS

The majority of numerical conformal bootstrap applications considered to date have concerned unitary CFTs. This limitation was mainly due to the fact that the main two rigorous numerical bootstrap methods, linear programming and semidefinite programming (Sec. IV), require positivity of the squares of OPE coefficients or positive definiteness of the matrices made of their pairwise products, which hold only in unitary theories. Nevertheless there have been some promising attempts to apply conformal bootstrap methods to nonunitary theories, which we briefly describe here.

One naturally occurring class of nonunitary CFTs is theories analytically continued from integer to noninteger space dimensions d , the prime example being the Wilson-Fisher family of fixed points in $2 \leq d < 4$. It was understood only recently that these CFTs are nonunitary for noninteger d ¹⁴⁷

Fortunately, the violation of unitarity in these theories seems to be rather mild as the negative-norm operators have

¹⁴⁷ See Hogervorst, Rychkov, and van Rees (2015, 2016) for the original observation and Di Pietro and Stamou (2018) for further work.

rather high dimension (Hogervorst, Rychkov, and van Rees, 2016). As a result it is believed that the standard linear and semidefinite programming methods, while nonrigorous in this context, should still give reasonable results. This explains the success of El-Showk *et al.* (2014a) who found good agreement between the numerical bootstrap and the ϵ expansion in the entire range $2 \leq d < 4$ using the 4pt function $\langle \sigma\sigma\sigma\sigma \rangle$ and analytically continuing conformal blocks to noninteger d . Similarly, Behan (2017a) generalized to noninteger d the multiple-correlator analysis leading to the 3D Ising model island in Fig. 13. A related successful study by Bobev *et al.* (2015a) analyzed the analytic continuation to $2 \leq d \leq 4$ of theories with four supercharges, which for $d = 3$ reduces to the $\mathcal{N} = 2$ Wess-Zumino model from Sec. VII.B.¹⁴⁸

Leaving aside the physical interpretation, the \mathbb{Z}_2 -invariant Wilson-Fisher fixed points can actually be analytically continued even below $d = 2$ and perhaps all the way to $d = 1^+$ (Holovatch, 1993). Interestingly, the analytic continuation seems to no longer be reproduced by the linear programming bootstrap in $d < 2$, likely because violations of unitarity are stronger in this case than for $d \geq 2$ (Golden and Paulos, 2015). This serves as a warning to keep in mind when applying the linear and semidefinite methods to nonunitary theories.

As described in Sec. IV.E, the truncation method should in principle be more suitable for analyzing nonunitary theories. Gliozzi (2013) and Gliozzi and Rago (2014)¹⁴⁹ successfully applied the truncation method to the Lee-Yang CFT, which is a nonunitary CFT describing the IR fixed point of the ϕ^3 scalar theory in $2 \leq d < 6$ dimensions (Fisher, 1978). Truncating the $\phi \times \phi$ OPE to the identity operator, ϕ itself, the stress tensor, and two more operators, estimates of Δ_ϕ were obtained in good agreement with RG and lattice predictions and with the exact solution available for $d = 2$.

Finally we mention that bootstrap methods can also be straightforwardly applied to nonunitary CFTs if a reasonable conjecture for the spectrum is available as happens in the case of 2D percolation (Picco, Ribault, and Santachiara, 2016). In this special situation, one simply solves crossing relations for the squares of OPE coefficients, with no restriction on sign.

IX. OTHER APPLICATIONS

We finish our review by briefly describing some of the many related topics that we have not been able to cover. Many of these topics have also seen significant recent progress and would merit their own reviews. We hope that we can at a minimum give the interested reader some useful entry points into the literature.

¹⁴⁸ See also Chester, Pufu, and Yacobi (2015), Chester, Giombi *et al.* (2016), Chester, Iliesiu *et al.* (2016), and Pang, Rong, and Su (2016) for related studies.

¹⁴⁹ See also Hikami (2017b). Other nonunitary models of interest to statistical physics tackled by the truncation method include the self-avoiding walk, branched polymers, random field Ising model, and percolation (Hikami, 2017a, 2018; LeClair and Squires, 2018). The analytic continuation of the $O(N)$ model to noninteger N was also studied using the linear programming method by Shimada and Hikami (2016), but the unitarity violation effects may not be sufficiently small to allow this (see footnote 113).

A traditional approach to learning about CFTs has been to use perturbation theory, often in the context of ϵ expansions or $1/N$ expansions. There is older literature about using bootstraplike techniques to reproduce $1/N$ expansions [see, e.g., Lang and Ruhl (1992) and Petkou (1996)], involving setting up self-consistency equations using a sum over dressed Feynman diagrams sometimes called a “skeleton expansion.” More recently, there have been a number of recent works which use more modern analytical bootstrap techniques to study perturbative expansions, e.g., studying bootstrap equations in a $1/N$ expansion,¹⁵⁰ using conformal invariance and the appearance of null states to reproduce ϵ expansions,¹⁵¹ and using a formulation of the bootstrap in Mellin space¹⁵² to reproduce ϵ and large- N expansions by reviving an old idea by Polyakov (1974) to make crossing symmetry manifest and impose unitarity.¹⁵³

A related analytical approach has been to study bootstrap equations in various Lorentzian limits. One such limit is the light cone limit developed by Fitzpatrick *et al.* (2013) and Komargodski and Zhiboedov (2013), which has allowed for a systematic study of CFT data in a large spin expansion¹⁵⁴ or with slightly broken higher-spin symmetry in the works (Alday and Zhiboedov, 2016; Alday, 2017b). Another limit where recent progress has been made is the Regge limit.¹⁵⁵ Both of these limits can be connected to constraints from Lorentzian causality, where nontrivial bounds and sum rules can be derived,¹⁵⁶ yielding new arguments for the conformal

¹⁵⁰See Heemskerk *et al.* (2009), Heemskerk and Sully (2010), Alday, Bissi, and Lukowski (2015b), and Aharony, Alday *et al.* (2017).

¹⁵¹See Rychkov and Tan (2015), Basu and Krishnan (2015), Ghosh *et al.* (2016), Raju (2016), Roumpedakis (2016), Gliozzi *et al.* (2017a, 2017b), Liendo (2017), and Gliozzi (2018).

¹⁵²The Mellin transformation of CFT correlation functions was introduced by Mack (2009), Penedones (2011), Paulos (2011), and Fitzpatrick *et al.* (2011) and developed in many subsequent works. While it is not yet known if and how it can be used for the numerical bootstrap, this formalism can be used to study many related questions. For example, Sleight and Taronna (2017, 2018b) constructed spinning CPWs in Mellin space for external traceless symmetric tensors in general d (see Sec. III.F.7 for the discussion in real space).

¹⁵³See Sen and Sinha (2016), Gopakumar *et al.* (2017a, 2017b), Dey, Kaviraj, and Sinha (2017), Dey, Ghosh, and Sinha (2018), and Dey and Kaviraj (2018).

¹⁵⁴See Fitzpatrick, Kaplan, and Walters (2014), Kaviraj, Sen, and Sinha (2015a, 2015b), Alday, Bissi, and Lukowski (2015a), Dey, Kaviraj, and Sen (2016), Hofman *et al.* (2016), Li, Meltzer, and Poland (2016a, 2016b), Alday (2017a), Alday and Bissi (2017), Alday and Zhiboedov (2017), Elkhidir and Karateev (2017), Simmons-Duffin (2017c), Dey, Ghosh, and Sinha (2018), van Loon (2018), and Henriksson and Loon (2018).

¹⁵⁵See Li, Meltzer, and Poland (2017), Costa, Hansen, and Penedones (2017), Meltzer and Perlmutter (2017), Alday, Bissi, and Perlmutter (2017), and Kulaxizi, Parnachev, and Zhiboedov (2017), which built on earlier work developing conformal Regge theory by Brower *et al.* (2007), Cornalba (2007), Cornalba, Costa, and Penedones (2007), Cornalba *et al.* (2007a, 2007b), and Costa, Goncalves, and Penedones (2012).

¹⁵⁶See Hartman, Jain, and Kundu (2016a, 2016b), Hofman *et al.* (2016), Hartman, Kundu, and Tajdini (2017), and Afkhami-Jeddi *et al.* (2017a, 2017b).

collider bounds of Hofman and Maldacena (2008), Buchel *et al.* (2010), and Chowdhury *et al.* (2013), as well as the more stringent constraints of Camanho *et al.* (2016) in holographic theories. Finally we should mention the recent development of a powerful Lorentzian inversion formula¹⁵⁷ as well as related work on higher-dimensional crossing kernels,¹⁵⁸ which are another promising route for further analytical progress.

The conformal bootstrap in two dimensions has a long history, for example, the seminal applications to rational CFTs in Belavin, Polyakov, and Zamolodchikov (1984).¹⁵⁹ The modern numerical bootstrap has been reapplied to 2D CFTs in a number of works.¹⁶⁰ A related direction is the modular bootstrap, which sets up consistency conditions arising from modular invariance. A number of recent studies¹⁶¹ have also looked at these constraints using modern numerical bootstrap techniques. A proper summary of these results and related analytical progress in the context of both the history of the 2D bootstrap and holography would merit its own review; see, e.g., Yin (2017).

One can also study the conformal bootstrap in more than four dimensions or with extended supersymmetry. One application of the numerical bootstrap has, e.g., been to the 6D (2,0) SCFT (Beem, Lemos, Rastelli, and van Rees, 2016), interesting in part because of its non-Lagrangian nature and ability to teach us about new dualities. Another application in $d > 4$ has been to probe the existence of $O(N)$ vector models in 5D.¹⁶² Progress has also been made placing constraints on a variety of other 5D and 6D SCFTs,¹⁶³ 4D $\mathcal{N} = 2$ and $\mathcal{N} = 3$ SCFTs,¹⁶⁴ 4D $\mathcal{N} = 4$ supersymmetric Yang-Mills

¹⁵⁷See Caron-Huot (2017), Simmons-Duffin, Stanford, and Witten (2017), Cardona (2018), Kravchuk and Simmons-Duffin (2018b), and Cardona and Sen (2018).

¹⁵⁸See Gadde (2017), Hogervorst (2017), Hogervorst and van Rees (2017), Karateev, Kravchuk, and Simmons-Duffin (2018), Sleight and Taronna (2018a, 2018b), and Liu *et al.* (2018).

¹⁵⁹See also Knizhnik and Zamolodchikov (1984), Gepner and Witten (1986), and Bouwknegt and Schoutens (1993).

¹⁶⁰See Rattazzi *et al.* (2008), Rychkov and Vichi (2009), Vichi (2011), Liendo, Rastelli, and van Rees (2013), El-Showk and Paulos (2013), Gliozzi (2013), Gliozzi and Rago (2014), El-Showk *et al.* (2014b), Bobev *et al.* (2015a), Esterlis, Liam Fitzpatrick, and Ramirez (2016), Behan (2017b), Hongbin Chen *et al.* (2017), Collier *et al.* (2017), Cornagliotto, Lemos, and Schomerus (2017), Li (2017, 2018), Lin, Shao, Simmons-Duffin *et al.* (2017), and Lin, Shao, Wang, and Yin (2017).

¹⁶¹See Hellerman (2011), Hellerman and Schmidt-Colinet (2011), Friedan and Keller (2013), Qualls and Shapere (2014), Hartman, Keller, and Stoica (2014), Keller and Maloney (2015), Qualls (2015b, 2015c), Chang and Lin (2016), Kim, Kravchuk, and Ooguri (2016), Benjamin *et al.* (2016), Collier, Lin, and Yin (2016), Apolo (2017), Bae, Lee, and Song (2017), Collier *et al.* (2017), Cho, Collier, and Yin (2017), Cardy, Maloney, and Maxfield (2017), Keller, Mathys, and Zadeh (2017), Dyer, Liam Fitzpatrick, and Xin (2018), and Anous, Mahajan, and Shaghoulian (2018).

¹⁶²See Nakayama and Ohtsuki (2014b), Bae and Rey (2014), Chester, Pufu, and Yacoby (2015), and Li and Su (2017b).

¹⁶³See Pang, Rong, and Su (2016), Nakayama (2017), Chang and Lin (2017), and Chang *et al.* (2018).

¹⁶⁴See Beem, Lemos *et al.* (2016), Lemos and Liendo (2016a), Lemos, Liendo, Meneghelli, and Mitev (2017), Cornagliotto, Lemos, and Schomerus (2017), and Cornagliotto, Lemos, and Liendo (2018).

theory,¹⁶⁵ and 3D $\mathcal{N} = 8$ SCFTs (Chester *et al.*, 2014) including ones inspired by M theory (Agmon, Chester, and Pufu, 2017b). Related analytical progress at solving subsectors of SCFTs with extended supersymmetry was also made by Beem, Lemos *et al.* (2015), Beem, Rastelli, and van Rees (2015), and Chester *et al.* (2015) and used in a number of follow-up studies.¹⁶⁶

Work on the superconformal bootstrap (particularly with extended supersymmetry) is not possible without analytical computations of superconformal blocks, which have been developed in a number of works using both superembedding space methods and by solving the superconformal Casimir equation.¹⁶⁷

Another intriguing line of research is the development of a direct relation between conformal blocks and the wave functions of integrable Hamiltonians.¹⁶⁸ Finally, while we cannot review here all of the interesting developments in the AdS/CFT correspondence, it is worth mentioning that there has been an abundance of activity in connecting both global blocks¹⁶⁹ and semiclassical Virasoro blocks¹⁷⁰ to geodesics in AdS and bulk semiclassical physics.

¹⁶⁵See Beem, Rastelli, and van Rees (2013, 2017), Alday and Bissi (2014, 2015), and Liendo and Meneghelli (2017).

¹⁶⁶See and Beem, Peelaers *et al.* (2015), Lemos and Peelaers (2015), Beem, Lemos *et al.* (2016), Liendo, Ramirez, and Seo (2016), Lemos and Liendo (2016b), Nishinaka and Tachikawa (2016), Xie, Yan, and Yau (2016), Agmon, Chester, and Pufu (2017a), Beem, Peelaers, and Rastelli (2017), Beem and Rastelli (2017), Cordova, Gaiotto, and Shao (2017), Creutzig (2017), Fluder and Song (2017), Liendo, Meneghelli, and Mitev (2017), Song (2017), Dedushenko, Pufu, and Yacoby (2018), Dedushenko *et al.* (2018), Fredrickson *et al.* (2018), and Pan and Peelaers (2018).

¹⁶⁷See Dolan and Osborn (2002, 2006), Dolan, Gallot, and Sokatchev (2004), Poland and Simmons-Duffin (2011), Fortin, Intriligator, and Stergiou (2011), Goldberger, Skiba, and Son (2012), Khandker and Li (2012), Goldberger *et al.* (2013), Fitzpatrick *et al.* (2014), Khandker *et al.* (2014), Li and Stergiou (2014), Bobev *et al.* (2015a), Doobary and Heslop (2015), Beem, Lemos *et al.* (2016), Beem, Lemos, Rastelli, and van Rees (2016), Bissi and Lukowski (2016), Li and Su (2016), Liendo, Ramirez, and Seo (2016), Ramírez (2016), Bobev, Lauria, and Mazac (2017), Chang and Lin (2017), Cornagliotto, Lemos, and Schomerus (2017), Lemos, Liendo, Meneghelli, and Mitev (2017), Li, Meltzer, and Stergiou (2017), Rong and Su (2018), and Zhijin Li (2018).

¹⁶⁸See Isachenkov and Schomerus (2016, 2017), Chen and Qualls (2017), Schomerus, Sobko, and Isachenkov (2017), and Schomerus and Sobko (2018).

¹⁶⁹See Hijano *et al.* (2016), Bhatta, Raman, and Suryanarayana (2016), Dyer, Freedman, and Sully (2017), Castro, Llabrs, and Rejon-Barrera (2017), Chen, Kuo, and Kyono (2017), Nishida and Tamaoka (2017), Sleight and Taronna (2017), and Tamaoka (2017).

¹⁷⁰See Fitzpatrick, Kaplan, and Walters (2014, 2015), Alkalaev and Belavin (2015, 2016a, 2016b, 2016c, 2017), Hijano *et al.* (2015), Hijano, Kraus, and Snively (2015), Alkalaev (2016), Banerjee, Datta, and Sinha (2016), Besken *et al.* (2016), Fitzpatrick and Kaplan (2016, 2017), Fitzpatrick, Kaplan, Li, and Wang (2016), Fitzpatrick, Kaplan, Walters, and Wang (2016), Alkalaev, Geiko, and Rappoport (2017), Belavin and Geiko (2017), Hongbin Chen *et al.* (2017), Fitzpatrick *et al.* (2017), Hulk, Prochzka, and Raeymaekers (2017), Kraus *et al.* (2017), Lencsés and Novaes (2017), and Maloney, Maxfield, and Ng (2017).

All of the conformal bootstrap constraints and numerical bounds we have considered in this review have applied to either Euclidean CFT or relativistic Lorentzian CFT. It is also of interest to learn about nonrelativistic conformal field theories due to their many experimental realizations, e.g., to ultracold atomic gases near the unitary limit. While nonrelativistic conformal symmetries are inherently less constraining, some important theoretical groundwork on correlation functions and the OPE has been laid for systems governed by the nonrelativistic Schrödinger algebra,¹⁷¹ which is a necessary precursor to any bootstrap analysis.

Another interesting situation that we have not discussed is systems governed by logarithmic CFTs, a class of nonunitary CFTs describing, e.g., models of percolation, self-avoiding random walks, and systems with quenched disorder. While such theories have been considered for a long time in two dimensions [see Creutzig and Ridout (2013) for a review], logarithmic CFTs in higher dimensions have received less attention. A general theoretical analysis of correlation functions in such theories was recently developed by Hogervorst, Paulos, and Vichi (2017), building on earlier work (Ghezelbash and Karimipour, 1997). Attempts to apply direct numerical bootstrap to such theories have been mentioned in Sec. VIII.¹⁷² Let us also mention the study by Komargodski and Simmons-Duffin (2017) of the Ising model with quenched disorder which made extensive use of bootstrap data to develop an approach based on conformal perturbation theory.

X. OUTLOOK

The conformal bootstrap is still in its infancy and there remains much low-hanging fruit to pick along with many important open questions. For instance, can we use the bootstrap to fully classify the space of critical CFTs with a given symmetry, placing universality on a rigorous footing? Can the bootstrap solve the conformal windows of QED₃ and QCD₄? Can it be used as a discovery tool to find new, perhaps non-Lagrangian CFTs? Is there an analytical understanding of the kinks in numerical bounds or why certain CFTs such as the 3D Ising model live in them? Which CFTs can be found using extremal spectrum or truncation methods? And is there a fruitful way to incorporate developments in the analytical bootstrap with rigorous numerical methods?

For newcomers to the numerical bootstrap who want to quickly get started, after learning CFT basics we recommend becoming familiar with the available software tools,¹⁷³ particularly SDPB which is under active development, along with one of the efficient methods to compute conformal blocks in the dimension of interest as described in Sec. III.F. Then one can start reproducing numerical bounds and thinking about

¹⁷¹See Nishida and Son (2007), Golkar and Son (2014), Goldberger, Khandker, and Prabhu (2015), Gubler *et al.* (2015), and Pal (2018).

¹⁷²It should be kept in mind that the conformal blocks in logarithmic theories are in general more complicated than in usual CFTs (Hogervorst, Paulos, and Vichi, 2017, Sec. 5.2.2).

¹⁷³Many of the currently available tools have been collected at <http://bootstrapcollaboration.com/activities/>.

how they can be generalized to say something new about situations of physical interest. For this purpose it is also helpful to get used to restating the physical properties of critical systems using symmetries and the spectrum of scaling dimensions, so questions can be sharply rephrased in the language of the bootstrap.

ACKNOWLEDGMENTS

We would like to thank Connor Behan, John Chalker, Shai Chester, Subham Dutta Chowdhury, Luigi Del Debbio, Mykola Dedushenko, Yin-Chen He, Kuo-Wei Huang, Denis Karateev, Zohar Komargodski, Petr Kravchuk, Adam Nahum, Yu Nakayama, Miguel Paulos, Silvius Pufu, Leonardo Rastelli, Subir Sachdev, David Simmons-Duffin, Andreas Stergiou, Tin Sulejmanpasic, Senthil Todadri, Emilio Trevisani, Ettore Vicari, and William Witczak-Krempa for useful discussions and comments. D. P. is supported by the NSF Grant No. PHY-1350180 and the Simons Foundation Grant No. 488651 (Simons Collaboration on the Nonperturbative Bootstrap). S. R. is supported by the Simons Foundation Grant No. 488655 (Simons Collaboration on the Nonperturbative Bootstrap), and by Mitsubishi Heavy Industries as an ENS-MHI Chair holder. A. V. is supported by the Swiss National Science Foundation under Grant No. PP00P2-163670 and by the European Research Council Starting Grant under No. 758903.

APPENDIX: EMBEDDING FORMALISM

As we saw in Sec. III.A, the conformal group is isomorphic to $SO(d+1, 1)$. This suggests that we can avoid complications due to the SCTs acting nonlinearly on \mathbb{R}^d by embedding this space into $\mathbb{R}^{d+1,1}$, where the whole conformal group will act linearly. This main idea of the embedding formalism (also called the projective null cone formalism) goes back to Dirac (1936). Here we review only the main logic and a few fundamental results; see Costa *et al.* (2011b) for details and Rychkov (2016b) for a pedagogical introduction.

We denote points in the “embedding space” $\mathbb{R}^{d+1,1}$ by P^A , and use the light cone coordinates

$$\begin{aligned} P^A &= (P^+, P^-, P^\mu), \quad P^\pm = P^{d+2} \pm P^{d+1}, \\ P^2 &= P^\mu P_\mu - P^+ P^- . \end{aligned} \quad (\text{A1})$$

In this space we consider the “null cone” defined by $P^2 = 0$. The physical space \mathbb{R}^d is identified with the “Poincaré section” of the cone given by

$$P^A = (1, x^2, x^\mu), \quad x^\mu \in \mathbb{R}^d. \quad (\text{A2})$$

This identification is natural because, as is easy to check, the flat Minkowski metric in $\mathbb{R}^{d+1,1}$ induces a flat d -dimensional metric on the Poincaré section (see Fig. 58).

$SO(d+1, 1)$ acts naturally on the null rays forming the null cone, and this defines an action on the Poincaré section by picking the intersection point. One can verify that this action realizes a conformal transformation of \mathbb{R}^d .

Similarly, operators in d dimensions can be lifted to the embedding space. Focusing on traceless symmetric tensors,

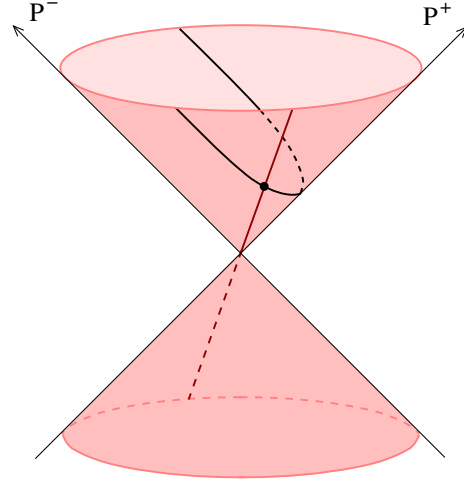


FIG. 58. The light cone in the embedding space; light rays are in one-to-one correspondence with points of \mathbb{R}^d . The Poincaré section of the cone is also shown. From Costa *et al.*, 2011b.

$\mathcal{O}_{\Delta, \ell}^{\mu_1 \dots \mu_\ell}(x)$ is promoted to a traceless symmetric tensor $\hat{\mathcal{O}}_{\Delta, \ell}^{A_1 \dots A_\ell}(P)$, transforming linearly under $SO(d+1, 1)$. The latter operator is required to be homogeneous of degree $-\Delta$:

$$\hat{\mathcal{O}}_{\Delta, \ell}^{A_1 \dots A_\ell}(\lambda P) = \lambda^{-\Delta} \hat{\mathcal{O}}_{\Delta, \ell}^{A_1 \dots A_\ell}(P). \quad (\text{A3})$$

The relation between the two operators is obtained by the projection

$$\mathcal{O}_{\Delta, \ell}^{\mu_1 \dots \mu_\ell}(x) = \frac{\partial P_{A_1}}{\partial x_{\mu_1}} \dots \frac{\partial P_{A_\ell}}{\partial x_{\mu_\ell}} \hat{\mathcal{O}}_{\Delta, \ell}^{A_1 \dots A_\ell}(P), \quad (\text{A4})$$

where P is restricted to the Poincaré section so that

$$\frac{\partial P_A}{\partial x_\mu} = (0, 2x_\mu, \delta_\mu^\alpha).$$

This is consistent with the symmetric traceless condition. Note as well that two embedding space tensors which differ by anything proportional to P^A project to the same physical space tensor, because $P^A \partial P_A / \partial x_\mu = 0$. This is sometimes referred to as “gauge freedom,” and it ensures that both representations have the same number of physical components.

The main advantage of this formalism is that the embedding space operators transform linearly under the conformal group. Thus, the problem of classifying correlation functions in embedding space is reduced to finding covariant tensors of $SO(d+1, 1)$. In the index free notation, this is equivalent to constructing invariant polynomials depending on the position vectors P_A and the polarization vectors Z_A , with the correct homogeneity properties (A3). For traceless tensors it is enough to work with null polarization vectors $Z^2 = 0$. Due to the above-mentioned gauge freedom, it is also enough to restrict to transverse polarizations: $Z \cdot P = 0$. In these conventions, all correlation functions can be built from the basic building blocks (Costa *et al.*, 2011b)

$$H_{ij} \equiv \frac{(Z_i \cdot Z_j)(P_i \cdot P_j) - (Z_i \cdot P_j)(Z_j \cdot P_i)}{(P_i \cdot P_j)},$$

$$V_{i,jk} \equiv \frac{(Z_i \cdot P_j)(P_i \cdot P_k) - (Z_i \cdot P_k)(P_i \cdot P_j)}{\sqrt{-2(P_i \cdot P_j)(P_i \cdot P_k)(P_j \cdot P_k)}}. \quad (\text{A5})$$

In particular, we have ($P_{ij} \equiv -2P_i \cdot P_j$),

$$\langle \hat{O}_{\Delta,\ell}(P_1, Z_1) \hat{O}_{\Delta,\ell}(P_2, Z_2) \rangle = \frac{(H_{12})^\ell}{P_{12}^\Delta}, \quad (\text{A6})$$

$$\langle \hat{O}_{\Delta_1}(P_1) \hat{O}_{\Delta_2}(P_2) \hat{O}_{\Delta_3}(P_3, Z_3) \rangle = \lambda_{123} \frac{(V_{3,12})^\ell}{P_{12}^{h_{123}+\ell} P_{13}^{h_{132}-\ell} P_{23}^{h_{231}-\ell}}. \quad (\text{A7})$$

Projecting to \mathbb{R}^d gives Eqs. (22) and (23).

Operators transforming in other $SO(d)$ representations can also be lifted to the embedding space; see, e.g., Costa and Hansen (2015) for mixed-symmetry tensors. One can also construct other types of embedding spaces which may be more convenient for dealing with fermions, for supersymmetric CFTs, or in specific d .¹⁷⁴

¹⁷⁴For some examples, see Weinberg (2010), Goldberger, Skiba, and Son (2012), Khandker and Li (2012), Siegel (2012), Goldberger *et al.* (2013), Fitzpatrick *et al.* (2014), Simmons-Duffin (2014a), Elkhidir, Karateev, and Serone (2015), and Iliesiu *et al.* (2016a).

REFERENCES

- Afkhami-Jeddi, Nima, Thomas Hartman, Sandipan Kundu, and Amirhossein Tajdini, 2017a, “Einstein gravity 3-point functions from conformal field theory,” *J. High Energy Phys.* **12**, 049.
- Afkhami-Jeddi, Nima, Thomas Hartman, Sandipan Kundu, and Amirhossein Tajdini, 2017b, “Shockwaves from the Operator Product Expansion,” [arXiv:1709.03597](#).
- Agmon, Nathan B., Shai M. Chester, and Silviu S. Pufu, 2017a, “A New Duality Between $\mathcal{N} = 8$ Superconformal Field Theories in Three Dimensions,” [arXiv:1708.07861](#).
- Agmon, Nathan B., Shai M. Chester, and Silviu S. Pufu, 2017b, “Solving M-theory with the Conformal Bootstrap,” [arXiv:1711.07343](#).
- Aharony, Ofer, 2016, “Baryons, monopoles and dualities in Chern-Simons-matter theories,” *J. High Energy Phys.* **02**, 093.
- Aharony, Ofer, Luis F. Alday, Agnese Bissi, and Eric Perlmutter, 2017, “Loops in AdS from Conformal Field Theory,” *J. High Energy Phys.* **07**, 036.
- Aharony, Ofer, Francesco Benini, Po-Shen Hsin, and Nathan Seiberg, 2017, “Chern-Simons-matter dualities with SO and USp gauge groups,” *J. High Energy Phys.* **02**, 072.
- Alba, Vasyl, and Kenan Diab, 2016, “Constraining conformal field theories with a higher spin symmetry in $d = 4$,” *J. High Energy Phys.* **03**, 044.
- Alday, Luis F., 2017a, “Large Spin Perturbation Theory for Conformal Field Theories,” *Phys. Rev. Lett.* **119**, 111601.
- Alday, Luis F., 2017b, “Solving CFTs with Weakly Broken Higher Spin Symmetry,” *J. High Energy Phys.* **10**, 161.
- Alday, Luis F., and Agnese Bissi, 2014, “The superconformal bootstrap for structure constants,” *J. High Energy Phys.* **09**, 144.
- Alday, Luis F., and Agnese Bissi, 2015, “Generalized bootstrap equations for $\mathcal{N} = 4$ SCFT,” *J. High Energy Phys.* **02**, 101.
- Alday, Luis F., and Agnese Bissi, 2017, “Crossing symmetry and Higher spin towers,” *J. High Energy Phys.* **12**, 118.
- Alday, Luis F., Agnese Bissi, and Tomasz Lukowski, 2015a, “Large spin systematics in CFT,” *J. High Energy Phys.* **11**, 101.
- Alday, Luis F., Agnese Bissi, and Tomasz Lukowski, 2015b, “Lessons from crossing symmetry at large N ,” *J. High Energy Phys.* **06**, 074.
- Alday, Luis F., Agnese Bissi, and Eric Perlmutter, 2017, “Holographic Reconstruction of AdS Exchanges from Crossing Symmetry,” *J. High Energy Phys.* **08**, 147.
- Alday, Luis F., and Alexander Zhiboedov, 2016, “Conformal Bootstrap With Slightly Broken Higher Spin Symmetry,” *J. High Energy Phys.* **06**, 091.
- Alday, Luis F., and Alexander Zhiboedov, 2017, “An Algebraic Approach to the Analytic Bootstrap,” *J. High Energy Phys.* **04**, 157.
- Alkalaev, K. B., 2016, “Many-point classical conformal blocks and geodesic networks on the hyperbolic plane,” *J. High Energy Phys.* **12**, 070.
- Alkalaev, K. B., and V. A. Belavin, 2015, “Classical conformal blocks via AdS/CFT correspondence,” *J. High Energy Phys.* **08**, 049.
- Alkalaev, K. B., and V. A. Belavin, 2016a, “From global to heavy-light: 5-point conformal blocks,” *J. High Energy Phys.* **03**, 184.
- Alkalaev, K. B., and V. A. Belavin, 2016b, “Holographic interpretation of 1-point toroidal block in the semiclassical limit,” *J. High Energy Phys.* **06**, 183.
- Alkalaev, K. B., and V. A. Belavin, 2016c, “Monodromic vs geodesic computation of Virasoro classical conformal blocks,” *Nucl. Phys. B* **904**, 367–385.
- Alkalaev, K. B., and V. A. Belavin, 2017, “Holographic duals of large- c torus conformal blocks,” *J. High Energy Phys.* **10**, 140.
- Alkalaev, K. B., R. V. Geiko, and V. A. Rapoport, 2017, “Various semiclassical limits of torus conformal blocks,” *J. High Energy Phys.* **04**, 070.
- Andrews, Thomas, 1869, “The Bakerian Lecture: On the Continuity of the Gaseous and Liquid States of Matter,” *Phil. Trans. R. Soc. London* **159**, 575–590.
- Anous, Tarek, Raghu Mahajan, and Edgar Shaghoulian, 2018, “Parity and the modular bootstrap,” [arXiv:1803.04938](#).
- Apolo, Luis, 2017, “Bounds on CFTs with \mathcal{W}_3 algebras and AdS_3 higher spin theories,” *Phys. Rev. D* **96**, 086003.
- Appelquist, Thomas, James Ingoldby, and Maurizio Piai, 2017, “Dilaton EFT Framework For Lattice Data,” *J. High Energy Phys.* **07**, 035.
- Appelquist, Thomas, James Ingoldby, and Maurizio Piai, 2018, “Analysis of a Dilaton EFT for Lattice Data,” *J. High Energy Phys.* **03**, 039.
- Appelquist, Thomas, and Daniel Nash, 1990, “Critical Behavior in (2+1)-dimensional QCD,” *Phys. Rev. Lett.* **64**, 721.
- Appelquist, Thomas, Daniel Nash, and L. C. R. Wijewardhana, 1988, “Critical Behavior in (2+1)-Dimensional QED,” *Phys. Rev. Lett.* **60**, 2575.
- Atanasov, Alexander, Aaron Hillman, and David Poland, 2018, “Bootstrapping the Minimal 3D SCFT,” [arXiv:1807.05702](#).
- Bae, Jin-Beom, Sungjay Lee, and Jaewon Song, 2017, “Modular Constraints on Conformal Field Theories with Currents,” *J. High Energy Phys.* **12**, 045.
- Bae, Jin-Beom, and Soo-Jong Rey, 2014, “Conformal Bootstrap Approach to O(N) Fixed Points in Five Dimensions,” [arXiv:1412.6549](#).

- Baggio, Marco, Nikolay Bobev, Shai M. Chester, Edoardo Lauria, and Silvius S. Pufu, 2018, “Decoding a Three-Dimensional Conformal Manifold,” *J. High Energy Phys.* **02**, 062.
- Bak, Per, Chao Tang, and Kurt Wiesenfeld, 1987, “Self-organized criticality: An explanation of the 1/f noise,” *Phys. Rev. Lett.* **59**, 381–384.
- Banerjee, Pinaki, Shouvik Datta, and Ritam Sinha, 2016, “Higher-point conformal blocks and entanglement entropy in heavy states,” *J. High Energy Phys.* **05**, 127.
- Banks, Tom, and A. Zaks, 1982, “On the Phase Structure of Vector-Like Gauge Theories with Massless Fermions,” *Nucl. Phys. B* **196**, 189–204.
- Bashkirov, Denis, 2013, “Bootstrapping the $\mathcal{N} = 1$ SCFT in three dimensions,” [arXiv:1310.8255](https://arxiv.org/abs/1310.8255).
- Basile, Francesco, Andrea Pelissetto, and Ettore Vicari, 2005, “The Finite-temperature chiral transition in QCD with adjoint fermions,” *J. High Energy Phys.* **02**, 044.
- Basile, Francesco, Andrea Pelissetto, and Ettore Vicari, 2006, “Finite-temperature chiral transition in QCD with quarks in the fundamental and adjoint representation,” Proceedings of the 23rd International Symposium on Lattice field theory (Lattice 2005), *Proc. Sci.*, LAT2005, 199.
- Basu, Pallab, and Chethan Krishnan, 2015, “ ϵ -expansions near three dimensions from conformal field theory,” *J. High Energy Phys.* **11**, 040.
- Bateman, H., 1910, “The transformation of the electrodynamic equations,” *Proc. London Math. Soc.* **s2-8**, 223–264.
- Baxter, R. J., 1989, *Exactly solved models in statistical mechanics* (Academic Press, New York).
- Beem, Christopher, Madalena Lemos, Pedro Liendo, Wolfgang Peelaers, Leonardo Rastelli, and Balt C. van Rees, 2015, “Infinite Chiral Symmetry in Four Dimensions,” *Commun. Math. Phys.* **336**, 1359–1433.
- Beem, Christopher, Madalena Lemos, Pedro Liendo, Leonardo Rastelli, and Balt C. van Rees, 2016, “The $\mathcal{N} = 2$ superconformal bootstrap,” *J. High Energy Phys.* **03**, 183.
- Beem, Christopher, Madalena Lemos, Leonardo Rastelli, and Balt C. van Rees, 2016, “The $(2, 0)$ superconformal bootstrap,” *Phys. Rev. D* **93**, 025016.
- Beem, Christopher, Wolfgang Peelaers, and Leonardo Rastelli, 2017, “Deformation quantization and superconformal symmetry in three dimensions,” *Commun. Math. Phys.* **354**, 345–392.
- Beem, Christopher, Wolfgang Peelaers, Leonardo Rastelli, and Balt C. van Rees, 2015, “Chiral algebras of class S,” *J. High Energy Phys.* **05**, 020.
- Beem, Christopher, and Leonardo Rastelli, 2017, “Vertex operator algebras, Higgs branches, and modular differential equations,” [arXiv:1707.07679](https://arxiv.org/abs/1707.07679).
- Beem, Christopher, Leonardo Rastelli, and Balt C. van Rees, 2013, “The $\mathcal{N} = 4$ Superconformal Bootstrap,” *Phys. Rev. Lett.* **111**, 071601.
- Beem, Christopher, Leonardo Rastelli, and Balt C. van Rees, 2015, “ \mathcal{W} symmetry in six dimensions,” *J. High Energy Phys.* **05**, 017.
- Beem, Christopher, Leonardo Rastelli, and Balt C. van Rees, 2017, “More $\mathcal{N} = 4$ superconformal bootstrap,” *Phys. Rev. D* **96**, 046014.
- Behan, Connor, 2017a, “PyCFTBoot: A flexible interface for the conformal bootstrap,” *Commun. Comput. Phys.* **22**, 1–38.
- Behan, Connor, 2017b, “The unitary subsector of generalized minimal models,” [arXiv:1712.06622](https://arxiv.org/abs/1712.06622).
- Behan, Connor, Leonardo Rastelli, Slava Rychkov, and Bernardo Zan, 2017a, “A scaling theory for the long-range to short-range crossover and an infrared duality,” *J. Phys. A* **50**, 354002.
- Behan, Connor, Leonardo Rastelli, Slava Rychkov, and Bernardo Zan, 2017b, “Long-range critical exponents near the short-range crossover,” *Phys. Rev. Lett.* **118**, 241601.
- Belavin, A. A., and A. A. Migdal, 1974, “Calculation of anomalous dimensions in non-abelian gauge field theories,” *Pis'ma Zh. Eksp. Teor. Fiz.* **19**, 317–320 [JETP Lett. **19**, 181–182 (1974), http://www.jetpletters.ac.ru/ps/1774/article_27000.pdf].
- Belavin, A. A., Alexander M. Polyakov, and A. B. Zamolodchikov, 1984, “Infinite conformal symmetry in two-dimensional quantum field theory,” *Nucl. Phys. B* **241**, 333–380.
- Belavin, V. A., and R. V. Geiko, 2017, “Geodesic description of Heavy-Light Virasoro blocks,” *J. High Energy Phys.* **08**, 125.
- Benini, Francesco, Po-Shen Hsin, and Nathan Seiberg, 2017, “Comments on global symmetries, anomalies, and duality in $(2 + 1)d$,” *J. High Energy Phys.* **04**, 135.
- Benjamin, Nathan, Ethan Dyer, A. Liam Fitzpatrick, and Shamit Kachru, 2016, “Universal Bounds on Charged States in 2d CFT and 3d Gravity,” *J. High Energy Phys.* **08**, 041.
- Berkooz, Micha, Ran Yacoby, and Amir Zait, 2014, “Bounds on $\mathcal{N} = 1$ superconformal theories with global symmetries,” *J. High Energy Phys.* **08**, 008.
- Besken, Mert, Ashwin Hegde, Eliot Hijano, and Per Kraus, 2016, “Holographic conformal blocks from interacting Wilson lines,” *J. High Energy Phys.* **08**, 099.
- Bhatta, Atanu, Prashanth Raman, and Nemani V. Suryanarayana, 2016, “Holographic Conformal Partial Waves as Gravitational Open Wilson Networks,” *J. High Energy Phys.* **06**, 119.
- Billò, M., M. Caselle, D. Gaiotto, F. Gliozzi, M. Meineri, and R. Pellegrini, 2013, “Line defects in the 3d Ising model,” *J. High Energy Phys.* **07**, 055.
- Billò, Marco, Vasco Gonçalves, Edoardo Lauria, and Marco Meineri, 2016, “Defects in conformal field theory,” *J. High Energy Phys.* **04**, 091.
- Bissi, Agnese, and Tomasz Lukowski, 2016, “Revisiting $\mathcal{N} = 4$ superconformal blocks,” *J. High Energy Phys.* **02**, 115.
- Bobev, Nikolay, Sheer El-Showk, Dalimil Mazac, and Miguel F. Paulos, 2015a, “Bootstrapping SCFTs with Four Supercharges,” *J. High Energy Phys.* **08**, 142.
- Bobev, Nikolay, Sheer El-Showk, Dalimil Mazac, and Miguel F. Paulos, 2015b, “Bootstrapping the Three-Dimensional Supersymmetric Ising Model,” *Phys. Rev. Lett.* **115**, 051601.
- Bobev, Nikolay, Edoardo Lauria, and Dalimil Mazac, 2017, “Superconformal Blocks for SCFTs with Eight Supercharges,” *J. High Energy Phys.* **07**, 061.
- Bourget, Antoine, and Jan Troost, 2018, “The Conformal Characters,” *J. High Energy Phys.* **04**, 055.
- Bouwknegt, Peter, and Kareljan Schoutens, 1993, “ \mathcal{W} symmetry in conformal field theory,” *Phys. Rep.* **223**, 183–276.
- Brower, Richard C., Joseph Polchinski, Matthew J. Strassler, and Chung-I Tan, 2007, “The Pomeron and gauge/string duality,” *J. High Energy Phys.* **12**, 005.
- Buchel, Alex, Jorge Escobedo, Robert C. Myers, Miguel F. Paulos, Aninda Sinha, and Michael Smolkin, 2010, “Holographic GB gravity in arbitrary dimensions,” *J. High Energy Phys.* **03**, 111.
- Buican, Matthew, and Takahiro Nishinaka, 2016, “Small deformation of a simple $\mathcal{N} = 2$ superconformal theory,” *Phys. Rev. D* **94**, 125002.
- Camanho, Xian O., Jose D. Edelstein, Juan Maldacena, and Alexander Zhiboedov, 2016, “Causality Constraints on Corrections to the Graviton Three-Point Coupling,” *J. High Energy Phys.* **02**, 020.

- Caracciolo, Francesco, Alejandro Castedo Echeverri, Benedict von Harling, and Marco Serone, 2014, “Bounds on OPE Coefficients in 4D Conformal Field Theories,” *J. High Energy Phys.* **10**, 20.
- Caracciolo, Francesco, and Vyacheslav S. Rychkov, 2010, “Rigorous Limits on the Interaction Strength in Quantum Field Theory,” *Phys. Rev. D* **81**, 085037.
- Cardona, Carlos, 2018, “OPE inversion in Mellin space,” [arXiv: 1803.05086](#).
- Cardona, Carlos, and Kallol Sen, 2018, “Anomalous dimensions at finite conformal spin from OPE inversion,” [arXiv:1806.10919](#).
- Cardy, John, 1990, “Conformal Invariance and Statistical Mechanics,” in *Fields, Strings and Critical Phenomena (Les Houches 1988, Session 49)*, edited by E. Brézin and J. Zinn-Justin (North-Holland, Amsterdam).
- Cardy, John, Alexander Maloney, and Henry Maxfield, 2017, “A new handle on three-point coefficients: OPE asymptotics from genus two modular invariance,” *J. High Energy Phys.* **10**, 136.
- Cardy, John L., 1987, “Conformal Invariance,” in *Phase Transitions and Critical Phenonema*, Vol. 11, edited by L. Domb and J. L. Lebowitz (Academic Press, New York), pp. 55–126.
- Cardy, John L., 1988, “Is There a c Theorem in Four-Dimensions?” *Phys. Lett. B* **215**, 749–752.
- Cardy, John L., 1996, *Scaling and renormalization in statistical physics*, Cambridge Lecture Notes in Physics: 3 (Cambridge University Press, Cambridge, United Kingdom), p. 238.
- Caron-Huot, Simon, 2017, “Analyticity in Spin in Conformal Theories,” *J. High Energy Phys.* **09**, 078.
- Caselle, Michele, Gianluca Costagliola, and Nicodemo Magnoli, 2016, “Conformal perturbation of off-critical correlators in the 3D Ising universality class,” *Phys. Rev. D* **94**, 026005.
- Casini, H., and Marina Huerta, 2012, “On the RG running of the entanglement entropy of a circle,” *Phys. Rev. D* **85**, 125016.
- Castedo Echeverri, Alejandro, Emtinan Elkhidir, Denis Karateev, and Marco Serone, 2016, “Seed Conformal Blocks in 4D CFT,” *J. High Energy Phys.* **02**, 183.
- Castedo Echeverri, Alejandro, Benedict von Harling, and Marco Serone, 2016, “The Effective Bootstrap,” *J. High Energy Phys.* **09**, 097.
- Castro, Alejandra, Eva Llabrs, and Fernando Rejon-Barrera, 2017, “Geodesic Diagrams, Gravitational Interactions & OPE Structures,” *J. High Energy Phys.* **06**, 099.
- Caswell, William E., 1974, “Asymptotic Behavior of Nonabelian Gauge Theories to Two Loop Order,” *Phys. Rev. Lett.* **33**, 244.
- Chang, Chi-Ming, Martin Fluder, Ying-Hsuan Lin, and Yifan Wang, 2018, “Spheres, Charges, Instantons, and Bootstrap: A Five-Dimensional Odyssey,” *J. High Energy Phys.* **03**, 123.
- Chang, Chi-Ming, and Ying-Hsuan Lin, 2016, “Bootstrapping 2D CFTs in the Semiclassical Limit,” *J. High Energy Phys.* **08**, 056.
- Chang, Chi-Ming, and Ying-Hsuan Lin, 2017, “Carving Out the End of the World or (Superconformal Bootstrap in Six Dimensions),” *J. High Energy Phys.* **08**, 128.
- Chen, Heng-Yu, En-Jui Kuo, and Hideki Kyono, 2017, “Anatomy of Geodesic Witten Diagrams,” *J. High Energy Phys.* **05**, 070.
- Chen, Heng-Yu, and Joshua D. Qualls, 2017, “Quantum Integrable Systems from Conformal Blocks,” *Phys. Rev. D* **95**, 106011.
- Chen, Hongbin, Charles Hussong, Jared Kaplan, and Daliang Li, 2017, “A Numerical Approach to Virasoro Blocks and the Information Paradox,” *J. High Energy Phys.* **09**, 102.
- Chester, Shai M., Simone Giombi, Luca V. Iliesiu, Igor R. Klebanov, Silviu S. Pufu, and Ran Yacoby, 2016, “Accidental Symmetries and the Conformal Bootstrap,” *J. High Energy Phys.* **01**, 110.
- Chester, Shai M., Luca V. Iliesiu, Mark Mezei, and Silviu S. Pufu, 2017, “Monopole Operators in $U(1)$ Chern-Simons-Matter Theories,” [arXiv:1710.00654](#).
- Chester, Shai M., Luca V. Iliesiu, Silviu S. Pufu, and Ran Yacoby, 2016, “Bootstrapping $O(N)$ Vector Models with Four Supercharges in $3 \leq d \leq 4$,” *J. High Energy Phys.* **05**, 103.
- Chester, Shai M., Jaehoon Lee, Silviu S. Pufu, and Ran Yacoby, 2014, “The $\mathcal{N} = 8$ superconformal bootstrap in three dimensions,” *J. High Energy Phys.* **09**, 143.
- Chester, Shai M., Jaehoon Lee, Silviu S. Pufu, and Ran Yacoby, 2015, “Exact Correlators of BPS Operators from the 3d Superconformal Bootstrap,” *J. High Energy Phys.* **03**, 130.
- Chester, Shai M., and Silviu S. Pufu, 2016, “Towards bootstrapping QED_3 ,” *J. High Energy Phys.* **08**, 019.
- Chester, Shai M., Silviu S. Pufu, and Ran Yacoby, 2015, “Bootstrapping $O(N)$ vector models in $4 < d < 6$,” *Phys. Rev. D* **91**, 086014.
- Cho, Minjae, Scott Collier, and Xi Yin, 2017, “Genus Two Modular Bootstrap,” [arXiv:1705.05865](#).
- Chowdhury, Debanjan, Suvrat Raju, Subir Sachdev, Ajay Singh, and Philipp Strack, 2013, “Multipoint correlators of conformal field theories: implications for quantum critical transport,” *Phys. Rev. B* **87**, 085138.
- Chowdhury, Debanjan, and Subir Sachdev, 2014, “The enigma of the pseudogap phase of the cuprate superconductors,” [arXiv:1501.00002](#).
- Chowdhury, Debanjan, and Subir Sachdev, 2015, “Higgs criticality in a two-dimensional metal,” *Phys. Rev. B* **91**, 115123.
- Chowdhury, Subham Dutta, 2017, “Shear sum rule in higher derivative gravity theories,” *J. High Energy Phys.* **12**, 156.
- Chowdhury, Subham Dutta, Justin R. David, and Shiroman Prakash, 2017a, “Constraints on parity violating conformal field theories in $d = 3$,” *J. High Energy Phys.* **11**, 171.
- Chowdhury, Subham Dutta, Justin R. David, and Shiroman Prakash, 2017b, “Spectral sum rules for conformal field theories in arbitrary dimensions,” *J. High Energy Phys.* **07**, 119.
- Collier, Scott, Petr Kravchuk, Ying-Hsuan Lin, and Xi Yin, 2017, “Bootstrapping the Spectral Function: On the Uniqueness of Liouville and the Universality of BTZ,” [arXiv:1702.00423](#).
- Collier, Scott, Ying-Hsuan Lin, and Xi Yin, 2016, “Modular Bootstrap Revisited,” [arXiv:1608.06241](#).
- Cordova, Clay, and Kenan Diab, 2018, “Universal Bounds on Operator Dimensions from the Average Null Energy Condition,” *J. High Energy Phys.* **02**, 131.
- Cordova, Clay, Davide Gaiotto, and Shu-Heng Shao, 2017, “Surface Defects and Chiral Algebras,” *J. High Energy Phys.* **05**, 140.
- Cordova, Clay, Juan Maldacena, and Gustavo J. Turiaci, 2017, “Bounds on OPE Coefficients from Interference Effects in the Conformal Collider,” *J. High Energy Phys.* **11**, 032.
- Cornagliotto, Martina, Madalena Lemos, and Pedro Liendo, 2018, “Bootstrapping the (A_1, A_2) Argyres-Douglas theory,” *J. High Energy Phys.* **03**, 033.
- Cornagliotto, Martina, Madalena Lemos, and Volker Schomerus, 2017, “Long Multiplet Bootstrap,” *J. High Energy Phys.* **10**, 119.
- Cornalba, Lorenzo, 2007, “Eikonal methods in AdS/CFT: Regge theory and multi-reggeon exchange,” [arXiv:0710.5480](#).
- Cornalba, Lorenzo, Miguel S. Costa, and Joao Penedones, 2007, “Eikonal approximation in AdS/CFT: Resumming the gravitational loop expansion,” *J. High Energy Phys.* **09**, 037.
- Cornalba, Lorenzo, Miguel S. Costa, Joao Penedones, and Ricardo Schiappa, 2007a, “Eikonal Approximation in AdS/CFT: Conformal Partial Waves and Finite N Four-Point Functions,” *Nucl. Phys. B* **767**, 327–351.

- Cornalba, Lorenzo, Miguel S. Costa, Joao Penedones, and Ricardo Schiappa, 2007b, “Eikonal Approximation in AdS/CFT: From Shock Waves to Four-Point Functions,” *J. High Energy Phys.* **08**, 019.
- Costa, Miguel S., Vasco Goncalves, and Joao Penedones, 2012, “Conformal Regge theory,” *J. High Energy Phys.* **12**, 091.
- Costa, Miguel S., and Tobias Hansen, 2015, “Conformal correlators of mixed-symmetry tensors,” *J. High Energy Phys.* **02**, 151.
- Costa, Miguel S., Tobias Hansen, and Joo Penedones, 2017, “Bounds for OPE coefficients on the Regge trajectory,” *J. High Energy Phys.* **10**, 197.
- Costa, Miguel S., Tobias Hansen, Joo Penedones, and Emilio Trevisani, 2016a, “Projectors and seed conformal blocks for traceless mixed-symmetry tensors,” *J. High Energy Phys.* **07**, 018.
- Costa, Miguel S., Tobias Hansen, Joo Penedones, and Emilio Trevisani, 2016b, “Radial expansion for spinning conformal blocks,” *J. High Energy Phys.* **07**, 057.
- Costa, Miguel S., Joao Penedones, David Poland, and Slava Rychkov, 2011a, “Spinning Conformal Blocks,” *J. High Energy Phys.* **11**, 154.
- Costa, Miguel S., Joao Penedones, David Poland, and Slava Rychkov, 2011b, “Spinning Conformal Correlators,” *J. High Energy Phys.* **11**, 071.
- Creutzig, Thomas, 2017, “W-algebras for Argyres-Douglas theories,” [arXiv:1701.05926](https://arxiv.org/abs/1701.05926).
- Creutzig, Thomas, and David Ridout, 2013, “Logarithmic Conformal Field Theory: Beyond an Introduction,” *J. Phys. A* **46**, 494006.
- Cunningham, E., 1910, “The principle of relativity in electrodynamics and an extension thereof,” *Proc. London Math. Soc.* **s2-8**, 77–98.
- Cuomo, Gabriel Francisco, Denis Karateev, and Petr Kravchuk, 2018, “General Bootstrap Equations in 4D CFTs,” *J. High Energy Phys.* **01**, 130.
- Dasgupta, C., and B. I. Halperin, 1981, “Phase Transition in a Lattice Model of Superconductivity,” *Phys. Rev. Lett.* **47**, 1556–1560.
- Dedushenko, Mykola, Yale Fan, Silviu S. Pufu, and Ran Yacoby, 2018, “Coulomb Branch Operators and Mirror Symmetry in Three Dimensions,” *J. High Energy Phys.* **04**, 037.
- Dedushenko, Mykola, Silviu S. Pufu, and Ran Yacoby, 2018, “A one-dimensional theory for Higgs branch operators,” *J. High Energy Phys.* **03**, 138.
- Delfino, Francesco, Andrea Pelissetto, and Ettore Vicari, 2015, “Three-dimensional antiferromagnetic CP^{N-1} models,” *Phys. Rev. E* **91**, 052109.
- Derkachov, Sergey E., N. A. Kivel, A. S. Stepanenko, and A. N. Vasiliev, 1993, “On calculation in $1/n$ expansions of critical exponents in the Gross-Neveu model with the conformal technique,” [arXiv:hep-th/9302034](https://arxiv.org/abs/hep-th/9302034).
- Dey, Parijat, Kausik Ghosh, and Aninda Sinha, 2018, “Simplifying large spin bootstrap in Mellin space,” *J. High Energy Phys.* **01**, 152.
- Dey, Parijat, and Apratim Kaviraj, 2018, “Towards a Bootstrap approach to higher orders of epsilon expansion,” *J. High Energy Phys.* **02**, 153.
- Dey, Parijat, Apratim Kaviraj, and Kallol Sen, 2016, “More on analytic bootstrap for O(N) models,” *J. High Energy Phys.* **06**, 136.
- Dey, Parijat, Apratim Kaviraj, and Aninda Sinha, 2017, “Mellin space bootstrap for global symmetry,” *J. High Energy Phys.* **07**, 019.
- Di Francesco, P., P. Mathieu, and D. Senechal, 1997, *Conformal Field Theory, Graduate Texts in Contemporary Physics* (Springer-Verlag, New York).
- Di Pietro, Lorenzo, and Emmanuel Stamou, 2018, “Operator mixing in the ϵ -expansion: Scheme and evanescent-operator independence,” *Phys. Rev. D* **97**, 065007.
- Dirac, Paul A. M., 1936, “Wave equations in conformal space,” *Ann. Math.* **37**, 429–442.
- Dobrev, V. K., G. Mack, V. B. Petkova, S. G. Petrova, and I. T. Todorov, 1977, “Harmonic Analysis on the n-Dimensional Lorentz Group and Its Application to Conformal Quantum Field Theory,” *Lect. Notes Phys.* **63**, 1–280.
- Dobrev, V. K., and V. B. Petkova, 1985, “All Positive Energy Unitary Irreducible Representations of Extended Conformal Supersymmetry,” *Phys. Lett. B* **162**, 127–132.
- Dobrev, V. K., V. B. Petkova, S. G. Petrova, and I. T. Todorov, 1976, “Dynamical Derivation of Vacuum Operator Product Expansion in Euclidean Conformal Quantum Field Theory,” *Phys. Rev. D* **13**, 887.
- Dolan, F. A., and H. Osborn, 2001, “Conformal four point functions and the operator product expansion,” *Nucl. Phys. B* **599**, 459–496.
- Dolan, F. A., and H. Osborn, 2002, “Superconformal symmetry, correlation functions and the operator product expansion,” *Nucl. Phys. B* **629**, 3–73.
- Dolan, F. A., and H. Osborn, 2004, “Conformal partial waves and the operator product expansion,” *Nucl. Phys. B* **678**, 491–507.
- Dolan, F. A., and H. Osborn, 2006, “Conformal partial wave expansions for $\mathcal{N} = 4$ chiral four point functions,” *Ann. Phys. (Amsterdam)* **321**, 581–626.
- Dolan, F. A., and H. Osborn, 2011, “Conformal Partial Waves: Further Mathematical Results,” [arXiv:1108.6194v2](https://arxiv.org/abs/1108.6194v2).
- Dolan, Francis A., Laurent Gallot, and Emery Sokatchev, 2004, “On four-point functions of 1/2-BPS operators in general dimensions,” *J. High Energy Phys.* **09**, 056.
- Domb, C. M., 1974, “Ising model,” in *Phase Transitions and Critical Phenomena*, Vol. 3, edited by C. M. Domb and M. S. Green (Academic Press, New York), pp. 357–484.
- Doobary, Reza, and Paul Heslop, 2015, “Superconformal partial waves in Grassmannian field theories,” *J. High Energy Phys.* **12**, 159.
- Dyer, Ethan, Daniel Z. Freedman, and James Sully, 2017, “Spinning Geodesic Witten Diagrams,” *J. High Energy Phys.* **11**, 060.
- Dyer, Ethan, A. Liam Fitzpatrick, and Yuan Xin, 2018, “Constraints on Flavored 2d CFT Partition Functions,” *J. High Energy Phys.* **02**, 148.
- Dyer, Ethan, Márk Mezei, and Silviu S. Pufu, 2013, “Monopole Taxonomy in Three-Dimensional Conformal Field Theories,” [arXiv:1309.1160](https://arxiv.org/abs/1309.1160).
- Dyer, Ethan, Márk Mezei, Silviu S. Pufu, and Subir Sachdev, 2015, “Scaling dimensions of monopole operators in the \mathbb{CP}^{N_b-1} theory in 2 + 1 dimensions,” *J. High Energy Phys.* **06**, 037.
- Dymarsky, Anatoly, 2015, “On the four-point function of the stress-energy tensors in a CFT,” *J. High Energy Phys.* **10**, 075.
- Dymarsky, Anatoly, Filip Kos, Petr Kravchuk, David Poland, and David Simmons-Duffin, 2018, “The 3d Stress-Tensor Bootstrap,” *J. High Energy Phys.* **02**, 164.
- Dymarsky, Anatoly, Joao Penedones, Emilio Trevisani, and Alessandro Vichi, 2017, “Charting the space of 3D CFTs with a continuous global symmetry,” [arXiv:1705.04278](https://arxiv.org/abs/1705.04278).
- Echeverri, Alejandro Castedo, Emtinan Elkhidir, Denis Karateev, and Marco Serone, 2015, “Deconstructing Conformal Blocks in 4D CFT,” *J. High Energy Phys.* **08**, 101.
- Elkhidir, Emtinan, and Denis Karateev, 2017, “Scalar-Fermion Analytic Bootstrap in 4D,” [arXiv:1712.01554](https://arxiv.org/abs/1712.01554).
- Elkhidir, Emtinan, Denis Karateev, and Marco Serone, 2015, “General Three-Point Functions in 4D CFT,” *J. High Energy Phys.* **01**, 133.

- El-Showk, Sheer, and Kyriakos Papadodimas, 2012, “Emergent Spacetime and Holographic CFTs,” *J. High Energy Phys.* **10**, 106.
- El-Showk, Sheer, and Miguel F. Paulos, 2013, “Bootstrapping Conformal Field Theories with the Extremal Functional Method,” *Phys. Rev. Lett.* **111**, 241601.
- El-Showk, Sheer, and Miguel F. Paulos, 2018, “Extremal bootstrapping: go with the flow,” *J. High Energy Phys.* **03**, 148.
- El-Showk, Sheer, Miguel F. Paulos, David Poland, Slava Rychkov, David Simmons-Duffin, and Alessandro Vichi, 2012, “Solving the 3D Ising Model with the Conformal Bootstrap,” *Phys. Rev. D* **86**, 025022.
- El-Showk, Sheer, Miguel Paulos, David Poland, Slava Rychkov, David Simmons-Duffin, and Alessandro Vichi, 2014a, “Conformal field theories in fractional dimensions,” *Phys. Rev. Lett.* **112**, 141601.
- El-Showk, Sheer, Miguel F. Paulos, David Poland, Slava Rychkov, David Simmons-Duffin, and Alessandro Vichi, 2014b, “Solving the 3d Ising Model with the Conformal Bootstrap II. c -Minimization and Precise Critical Exponents,” *J. Stat. Phys.* **157**, 869.
- El-Showk, Sheer, and Slava Rychkov, 2014, “A Python/Cython continuous linear programming solver for the conformal bootstrap,” available on request from the authors.
- Esterlis, Ilya, A. Liam Fitzpatrick, and David Ramirez, 2016, “Closure of the Operator Product Expansion in the Non-Unitary Bootstrap,” *J. High Energy Phys.* **11**, 030.
- Evans, N. T., 1967, “Discrete series for the universal covering group of the $3+2$ de sitter group,” *J. Math. Phys. (N.Y.)* **8**, 170–184.
- Faulkner, Thomas, Robert G. Leigh, Onkar Parrikar, and Huajia Wang, 2016, “Modular Hamiltonians for Deformed Half-Spaces and the Averaged Null Energy Condition,” *J. High Energy Phys.* **09**, 038.
- Fei, Lin, Simone Giombi, Igor R. Klebanov, and Grigory Tarnopolsky, 2016, “Yukawa CFTs and Emergent Supersymmetry,” *Prog. Theor. Exp. Phys.* **2016**, 12C105.
- Ferrara, S, R. Gatto, and A. F. Grillo, 1973, “Conformal algebra in space-time and operator product expansion,” *Springer Tracts Mod. Phys.* **67**, 1–64.
- Ferrara, S, Raoul Gatto, and A. F. Grillo, 1974, “Positivity Restrictions on Anomalous Dimensions,” *Phys. Rev. D* **9**, 3564.
- Ferrara, S, Raoul Gatto, and A. F. Grillo, 1975, “Properties of Partial Wave Amplitudes in Conformal Invariant Field Theories,” *Nuovo Cimento A* **26**, 226.
- Ferrara, S, A. F. Grillo, and R. Gatto, 1971, “Manifestly conformal covariant operator-product expansion,” *Lett. Nuovo Cimento* **2**, 1363–1369.
- Ferrara, S, A. F. Grillo, and R. Gatto, 1973, “Tensor representations of conformal algebra and conformally covariant operator product expansion,” *Ann. Phys. (N.Y.)* **76**, 161–188.
- Ferrara, S, A. F. Grillo, R. Gatto, and G. Parisi, 1974, “Analyticity Properties and Asymptotic Expansions of Conformal Covariant Green’s Functions,” *Nuovo Cimento A* **19**, 667–695.
- Ferrara, S, A. F. Grillo, G. Parisi, and Raoul Gatto, 1972, “Covariant expansion of the conformal four-point function,” *Nucl. Phys. B* **49**, 77–98.
- Fisher, M. E., 1978, “Yang-Lee Edge Singularity and ϕ^3 Field Theory,” *Phys. Rev. Lett.* **40**, 1610–1613.
- Fisher, Matthew P. A., Peter B. Weichman, G. Grinstein, and Daniel S. Fisher, 1989, “Boson localization and the superfluid-insulator transition,” *Phys. Rev. B* **40**, 546–570.
- Fitzpatrick, A. Liam, and Jared Kaplan, 2012, “Unitarity and the Holographic S-Matrix,” *J. High Energy Phys.* **10**, 032.
- Fitzpatrick, A. Liam, and Jared Kaplan, 2016, “Conformal Blocks Beyond the Semi-Classical Limit,” *J. High Energy Phys.* **05**, 075.
- Fitzpatrick, A. Liam, and Jared Kaplan, 2017, “On the Late-Time Behavior of Virasoro Blocks and a Classification of Semiclassical Saddles,” *J. High Energy Phys.* **04**, 072.
- Fitzpatrick, A. Liam, Jared Kaplan, Zuhair U. Khandker, Daliang Li, David Poland, and David Simmons-Duffin, 2014, “Covariant Approaches to Superconformal Blocks,” *J. High Energy Phys.* **08**, 129.
- Fitzpatrick, A. Liam, Jared Kaplan, Daliang Li, and Junpu Wang, 2016, “On information loss in AdS_3/CFT_2 ,” *J. High Energy Phys.* **05**, 109.
- Fitzpatrick, A. Liam, Jared Kaplan, Daliang Li, and Junpu Wang, 2017, “Exact Virasoro Blocks from Wilson Lines and Background-Independent Operators,” *J. High Energy Phys.* **07**, 092.
- Fitzpatrick, A. Liam, Jared Kaplan, Joao Penedones, Suvrat Raju, and Balt C. van Rees, 2011, “A Natural Language for AdS/CFT Correlators,” *J. High Energy Phys.* **11**, 095.
- Fitzpatrick, A. Liam, Jared Kaplan, David Poland, and David Simmons-Duffin, 2013, “The Analytic Bootstrap and AdS Superhorizon Locality,” *J. High Energy Phys.* **12**, 004.
- Fitzpatrick, A. Liam, Jared Kaplan, and Matthew T. Walters, 2014, “Universality of Long-Distance AdS Physics from the CFT Bootstrap,” *J. High Energy Phys.* **08**, 145.
- Fitzpatrick, A. Liam, Jared Kaplan, and Matthew T. Walters, 2015, “Virasoro Conformal Blocks and Thermality from Classical Background Fields,” *J. High Energy Phys.* **11**, 200.
- Fitzpatrick, A. Liam, Jared Kaplan, Matthew T. Walters, and Junpu Wang, 2016, “Hawking from Catalan,” *J. High Energy Phys.* **05**, 069.
- Flato, Moshe, and Christian Fronsdal, 1984, “Representations of Conformal Supersymmetry,” *Lett. Math. Phys.* **8**, 159.
- Fluder, Martin, and Jaewon Song, 2017, “Four-dimensional Lens Space Index from Two-dimensional Chiral Algebra,” *arXiv:1710.06029*.
- Fortin, Jean-Francois, Kenneth Intriligator, and Andreas Stergiou, 2011, “Current OPEs in Superconformal Theories,” *J. High Energy Phys.* **09**, 071.
- Fortin, Jean-Francois, and Witold Skiba, 2016a, “Conformal Bootstrap in Embedding Space,” *Phys. Rev. D* **93**, 105047.
- Fortin, Jean-Francois, and Witold Skiba, 2016b, “Conformal Differential Operator in Embedding Space and its Applications,” *arXiv:1612.08672*.
- Fradkin, E. S., and M. Ya. Palchik, 1996, *Conformal Quantum Field Theory in D-dimensions*, Mathematics and its Applications Vol. 376 (Kluwer, Dordrecht, Netherlands), p. 461.
- Fradkin, Eduardo, and Leonard Susskind, 1978, “Order and disorder in gauge systems and magnets,” *Phys. Rev. D* **17**, 2637–2658.
- Fredrickson, Laura, Du Pei, Wenbin Yan, and Ke Ye, 2018, “Argyres-Douglas Theories, Chiral Algebras and Wild Hitchin Characters,” *J. High Energy Phys.* **01**, 150.
- Friedan, Daniel, and Christoph A. Keller, 2013, “Constraints on 2d CFT partition functions,” *J. High Energy Phys.* **10**, 180.
- Fukuda, Masayuki, Nozomu Kobayashi, and Tatsuma Nishioka, 2018, “Operator product expansion for conformal defects,” *J. High Energy Phys.* **01**, 013.
- Gadde, Abhijit, 2016, “Conformal constraints on defects,” *arXiv: 1602.06354*.
- Gadde, Abhijit, 2017, “In search of conformal theories,” *arXiv:1702.07362*.
- Gaiotto, Davide, Dalimil Mazac, and Miguel F. Paulos, 2014, “Bootstrapping the 3d Ising twist defect,” *J. High Energy Phys.* **03**, 100.
- Gazit, S., F. F. Assaad, S. Sachdev, A. Vishwanath, and C. Wang, 2018, “Confinement transition of \mathbb{Z}_2 gauge theories coupled to

- massless fermions: emergent QCD₃ and $SO(5)$ symmetry,” [arXiv:1804.01095](#).
- Gepner, Doron, and Edward Witten, 1986, “String Theory on Group Manifolds,” *Nucl. Phys. B* **278**, 493–549.
- Ghezelbash, A. M., and V. Karimipour, 1997, “Global conformal invariance in d-dimensions and logarithmic correlation functions,” *Phys. Lett. B* **402**, 282–289.
- Ghosh, Sudip, Rajesh Kumar Gupta, Kasi Jaswin, and Amin A. Nizami, 2016, “ ϵ -Expansion in the Gross-Neveu model from conformal field theory,” *J. High Energy Phys.* **03**, 174.
- Giedt, Joel, 2016, “Anomalous dimensions on the lattice,” *Int. J. Mod. Phys. A* **31**, 1630011.
- Gillioz, Marc, Xiaochuan Lu, and Markus A. Luty, 2017, “Scale Anomalies, States, and Rates in Conformal Field Theory,” *J. High Energy Phys.* **04**, 171.
- Gillioz, Marc, Xiaochuan Lu, and Markus A. Luty, 2018, “Graviton Scattering and a Sum Rule for the c Anomaly in 4D CFT,” [arXiv:1801.05807](#).
- Ginsparg, Paul, 1990, “Applied Conformal Field Theory,” in *Fields, Strings and Critical Phenomena*, Les Houches 1988, Session 49, edited by E. Brézin and J. Zinn-Justin (North-Holland, Amsterdam).
- Giombi, Simone, Shiroman Prakash, and Xi Yin, 2013, “A Note on CFT Correlators in Three Dimensions,” *J. High Energy Phys.* **07**, 105.
- Gliozzi, Ferdinando, 2013, “More constraining conformal bootstrap,” *Phys. Rev. Lett.* **111**, 161602.
- Gliozzi, Ferdinando, 2016, “Truncatable bootstrap equations in algebraic form and critical surface exponents,” *J. High Energy Phys.* **10**, 037.
- Gliozzi, Ferdinando, 2018, “Anomalous dimensions of spinning operators from conformal symmetry,” *J. High Energy Phys.* **01**, 113.
- Gliozzi, Ferdinando, Andrea Guerrieri, Anastasios C. Petkou, and Congkao Wen, 2017a, “Generalized Wilson-Fisher Critical Points from the Conformal Operator Product Expansion,” *Phys. Rev. Lett.* **118**, 061601.
- Gliozzi, Ferdinando, Andrea L. Guerrieri, Anastasios C. Petkou, and Congkao Wen, 2017b, “The analytic structure of conformal blocks and the generalized Wilson-Fisher fixed points,” *J. High Energy Phys.* **04**, 056.
- Gliozzi, Ferdinando, Pedro Liendo, Marco Meineri, and Antonio Rago, 2015, “Boundary and Interface CFTs from the Conformal Bootstrap,” *J. High Energy Phys.* **05**, 036.
- Gliozzi, Ferdinando, and Antonio Rago, 2014, “Critical exponents of the 3d Ising and related models from Conformal Bootstrap,” *J. High Energy Phys.* **10**, 042.
- Gobeil, Yan, Alexander Maloney, Gim Seng Ng, and Jie-qiang Wu, 2018, “Thermal Conformal Blocks,” [arXiv:1802.10537](#).
- Goldberger, Walter D., Zuhair U. Khandker, Daliang Li, and Witold Skiba, 2013, “Superembedding Methods for Current Superfields,” *Phys. Rev. D* **88**, 125010.
- Goldberger, Walter D., Zuhair U. Khandker, and Siddharth Prabhu, 2015, “OPE convergence in non-relativistic conformal field theories,” *J. High Energy Phys.* **12**, 1.
- Goldberger, Walter D., Witold Skiba, and Minho Son, 2012, “Superembedding Methods for 4d $N = 1$ SCFTs,” *Phys. Rev. D* **86**, 025019.
- Golden, John, and Miguel F. Paulos, 2015, “No unitary bootstrap for the fractal Ising model,” *J. High Energy Phys.* **03**, 167.
- Golkar, Siavash, and Dam T. Son, 2014, “Operator Product Expansion and Conservation Laws in Non-Relativistic Conformal Field Theories,” *J. High Energy Phys.* **12**, 063.
- Gomis, Jaume, Zohar Komargodski, and Nathan Seiberg, 2017, “Phases Of Adjoint QCD₃ And Dualities,” [arXiv:1710.03258](#).
- Gopakumar, Rajesh, Apratim Kaviraj, Kallool Sen, and Aninda Sinha, 2017a, “A Mellin space approach to the conformal bootstrap,” *J. High Energy Phys.* **05**, 027.
- Gopakumar, Rajesh, Apratim Kaviraj, Kallool Sen, and Aninda Sinha, 2017b, “Conformal Bootstrap in Mellin Space,” *Phys. Rev. Lett.* **118**, 081601.
- Gorbenko, Victor, Slava Rychkov, and Bernardo Zan, 2018a, “Walking, Weak first-order transitions, and Complex CFTs,” [arXiv:1807.11512](#).
- Gorbenko, Victor, Slava Rychkov, and Bernardo Zan, 2018b, “Walking, Weak first-order transitions, and Complex CFTs II. Two-dimensional Potts model at $Q > 4$,” [arXiv:1808.04380](#).
- Grabner, David, Nikolay Gromov, Vladimir Kazakov, and Gregory Korchemsky, 2018, “Strongly γ -Deformed $\mathcal{N} = 4$ Supersymmetric Yang-Mills Theory as an Integrable Conformal Field Theory,” *Phys. Rev. Lett.* **120**, 111601.
- Gracey, J. A., 1992, “Anomalous mass dimension at $O(1/N^2)$ in the $O(N)$ Gross-Neveu model,” *Phys. Lett. B* **297**, 293–297.
- Gracey, J. A., 1994, “Computation of critical exponent eta at $O(1/N^3)$ in the four Fermi model in arbitrary dimensions,” *Int. J. Mod. Phys. A* **09**, 727–744.
- Grinstein, Benjamin, Kenneth A. Intriligator, and Ira Z. Rothstein, 2008, “Comments on Unparticles,” *Phys. Lett. B* **662**, 367–374.
- Gross, David J., and Andre Neveu, 1974, “Dynamical Symmetry Breaking in Asymptotically Free Field Theories,” *Phys. Rev. D* **10**, 3235.
- Grover, Tarun, D. N. Sheng, and Ashvin Vishwanath, 2014, “Emergent Space-Time Supersymmetry at the Boundary of a Topological Phase,” *Science* **344**, 280–283.
- Gubler, Philipp, Naoki Yamamoto, Tetsuo Hatsuda, and Yusuke Nishida, 2015, “Single-particle spectral density of the unitary Fermi gas: Novel approach based on the operator product expansion, sum rules and the maximum entropy method,” *Ann. Phys. (Amsterdam)* **356**, 467–497.
- Gukov, Sergei, 2017, “RG Flows and Bifurcations,” *Nucl. Phys. B* **919**, 583–638.
- Gürdoğan, Ömer, and Vladimir Kazakov, 2016, “New Integrable 4D Quantum Field Theories from Strongly Deformed Planar $\mathcal{N} = 4$ Supersymmetric Yang-Mills Theory,” *Phys. Rev. Lett.* **117**, 201602.
- Harada, K., T. Suzuki, T. Okubo, H. Matsuo, J. Lou, H. Watanabe, S. Todo, and N. Kawashima, 2013, “Possibility of deconfined criticality in $SU(N)$ Heisenberg models at small N ,” *Phys. Rev. B* **88**, 220408.
- Hartman, Thomas, Sachin Jain, and Sandipan Kundu, 2016a, “A New Spin on Causality Constraints,” *J. High Energy Phys.* **10**, 141.
- Hartman, Thomas, Sachin Jain, and Sandipan Kundu, 2016b, “Causality Constraints in Conformal Field Theory,” *J. High Energy Phys.* **05**, 099.
- Hartman, Thomas, Christoph A. Keller, and Bogdan Stoica, 2014, “Universal Spectrum of 2d Conformal Field Theory in the Large c Limit,” *J. High Energy Phys.* **09**, 118.
- Hartman, Thomas, Sandipan Kundu, and Amirhossein Tajdini, 2017, “Averaged Null Energy Condition from Causality,” *J. High Energy Phys.* **07**, 066.
- Hasenfratz, A., C. Rebbi, and O. Witzel, 2017, “Violation of Fermion Universality at a Conformal Fixed Point,” [arXiv:1710.11578](#).
- Hasenfratz, Anna, Claudio Rebbi, and Oliver Witzel, 2018, “Testing Fermion Universality at a Conformal Fixed Point,” *EPJ Web Conf.* **175**, 03006.

- Heemskerk, Idse, Joao Penedones, Joseph Polchinski, and James Sully, 2009, “Holography from Conformal Field Theory,” *J. High Energy Phys.* **10**, 079.
- Heemskerk, Idse, and James Sully, 2010, “More Holography from Conformal Field Theory,” *J. High Energy Phys.* **09**, 099.
- Hellerman, Simeon, 2011, “A Universal Inequality for CFT and Quantum Gravity,” *J. High Energy Phys.* **08**, 130.
- Hellerman, Simeon, and Cornelius Schmidt-Colinet, 2011, “Bounds for State Degeneracies in 2D Conformal Field Theory,” *J. High Energy Phys.* **08**, 127.
- Henkel, M., 1984, “Statistical mechanics of the 2d quantum xy model in a transverse field,” *J. Phys. A* **17**, L795.
- Henkel, Malte, 1999, *Conformal Invariance and Critical Phenomena* (Springer, New York).
- Henriksson, Johan, and Mark van Loon, 2018, “Critical O(N) model to order ϵ^4 from analytic bootstrap,” [arXiv:1801.03512](#).
- Herbut, Igor F., 2006, “Interactions and phase transitions on graphene’s honeycomb lattice,” *Phys. Rev. Lett.* **97**, 146401.
- Herbut, Igor F., and Lukas Janssen, 2014, “Topological Mott insulator in three-dimensional systems with quadratic band touching,” *Phys. Rev. Lett.* **113**, 106401.
- Herbut, Igor F., Vladimir Juricic, and Oskar Vafek, 2009, “Relativistic Mott criticality in graphene,” *Phys. Rev. B* **80**, 075432.
- Herzog, Christopher, Kuo-Wei Huang, and Kristan Jensen , 2018, “Displacement Operators and Constraints on Boundary Central Charges,” *Phys. Rev. Lett.* **120**, 021601.
- Herzog, Christopher P., and Kuo-Wei Huang, 2017, “Boundary Conformal Field Theory and a Boundary Central Charge,” *J. High Energy Phys.* **10**, 189.
- Hijano, Eliot, Per Kraus, Eric Perlmutter, and River Snively, 2015, “Semiclassical Virasoro blocks from AdS_3 gravity,” *J. High Energy Phys.* **12**, 077.
- Hijano, Eliot, Per Kraus, Eric Perlmutter, and River Snively, 2016, “Witten Diagrams Revisited: The AdS Geometry of Conformal Blocks,” *J. High Energy Phys.* **01**, 146.
- Hijano, Eliot, Per Kraus, and River Snively, 2015, “Worldline approach to semi-classical conformal blocks,” *J. High Energy Phys.* **07**, 131.
- Hikami, S., 2017a, “Conformal Bootstrap Analysis for Single and Branched Polymers,” [arXiv:1708.03072](#).
- Hikami, S., 2017b, “Conformal Bootstrap Analysis for Yang-Lee Edge Singularity,” [arXiv:1707.04813](#).
- Hikami, Shinobu, 2018, “Dimensional Reduction by Conformal Bbootstrap,” [arXiv:1801.09052](#).
- Hilbert, David, 1888, “Über die Darstellung definiter Formen als Summe von Formenquadraten,” *Math. Ann.* **32**, 342–350.
- Hofman, Diego M., Daliang Li, David Meltzer, David Poland, and Fernando Rejon-Barrera, 2016, “A Proof of the Conformal Collider Bounds,” *J. High Energy Phys.* **06**, 111.
- Hofman, Diego M., and Juan Maldacena, 2008, “Conformal collider physics: Energy and charge correlations,” *J. High Energy Phys.* **05**, 012.
- Hogervorst, Matthijs, 2017, “Crossing Kernels for Boundary and Crosscap CFTs,” [arXiv:1703.08159](#).
- Hogervorst, Matthijs, Hugh Osborn, and Slava Rychkov, 2013, “Diagonal Limit for Conformal Blocks in d Dimensions,” *J. High Energy Phys.* **08**, 014.
- Hogervorst, Matthijs, Miguel Paulos, and Alessandro Vichi, 2017, “The ABC (in any D) of Logarithmic CFT,” *J. High Energy Phys.* **10**, 201.
- Hogervorst, Matthijs, and Slava Rychkov, 2013, “Radial Coordinates for Conformal Blocks,” *Phys. Rev. D* **87**, 106004.
- Hogervorst, Matthijs, Slava Rychkov, and Balt C. van Rees, 2015, “Truncated conformal space approach in d dimensions: A cheap alternative to lattice field theory?,” *Phys. Rev. D* **91**, 025005.
- Hogervorst, Matthijs, Slava Rychkov, and Balt C. van Rees, 2016, “Unitarity violation at the Wilson-Fisher fixed point in $4-\epsilon$ dimensions,” *Phys. Rev. D* **93**, 125025.
- Hogervorst, Matthijs, and Balt C. van Rees, 2017, “Crossing symmetry in alpha space,” *J. High Energy Phys.* **11**, 193.
- Holovatch, Yu, 1993, “Critical exponents of Ising like systems in general dimensions,” *Theor. Math. Phys.* **96**, 1099–1110.
- Hsin, Po-Shen, and Nathan Seiberg, 2016, “Level/rank Duality and Chern-Simons-Matter Theories,” *J. High Energy Phys.* **09**, 095.
- Hulk, Ondrej, Tom Prochzka, and Joris Raeymaekers, 2017, “Multi-centered AdS_3 solutions from Virasoro conformal blocks,” *J. High Energy Phys.* **03**, 129.
- Iha, Hisashi, Hiroki Makino, and Hiroshi Suzuki, 2016, “Upper bound on the mass anomalous dimension in many-flavor gauge theories: a conformal bootstrap approach,” *Prog. Theor. Exp. Phys.* **2016**, 053B03.
- Iliesiu, Luca, Murat Koloğlu, Raghu Mahajan, Eric Perlmutter, and David Simmons-Duffin, 2018, “The Conformal Bootstrap at Finite Temperature,” [arXiv:1802.10266](#).
- Iliesiu, Luca, Filip Kos, David Poland, Silviu S. Pufu, and David Simmons-Duffin, 2018, “Bootstrapping 3D Fermions with Global Symmetries,” *J. High Energy Phys.* **01**, 036.
- Iliesiu, Luca, Filip Kos, David Poland, Silviu S. Pufu, David Simmons-Duffin, and Ran Yacoby, 2016a, “Bootstrapping 3D Fermions,” *J. High Energy Phys.* **03**, 120.
- Iliesiu, Luca, Filip Kos, David Poland, Silviu S. Pufu, David Simmons-Duffin, and Ran Yacoby, 2016b, “Fermion-scalar conformal blocks,” *J. High Energy Phys.* **04**, 074.
- Isachenkov, Mikhail, and Volker Schomerus, 2016, “Superintegrability of d -dimensional Conformal Blocks,” *Phys. Rev. Lett.* **117**, 071602.
- Isachenkov, Mikhail, and Volker Schomerus, 2017, “Integrability of Conformal Blocks I: Calogero-Sutherland Scattering Theory,” [arXiv:1711.06609](#).
- Ishikawa, K. I., Y. Iwasaki, Yu Nakayama, and T. Yoshie, 2014, “Global Structure of Conformal Theories in the $SU(3)$ Gauge Theory,” *Phys. Rev. D* **89**, 114503.
- Ishikawa, K. I., Y. Iwasaki, Yu Nakayama, and T. Yoshie, 2015, “IR fixed points in $SU(3)$ gauge Theories,” *Phys. Lett. B* **748**, 289–294.
- Isono, Hiroshi, 2017, “On conformal correlators and blocks with spinors in general dimensions,” *Phys. Rev. D* **96**, 065011.
- Jack, I., and H. Osborn, 1990, “Analogs for the c Theorem for Four-dimensional Renormalizable Field Theories,” *Nucl. Phys. B* **343**, 647–688.
- Jafferis, Daniel L., Igor R. Klebanov, Silviu S. Pufu, and Benjamin R. Safdi, 2011, “Towards the F-Theorem: $N = 2$ Field Theories on the Three-Sphere,” *J. High Energy Phys.* **06**, 102.
- Jantzen, Jens C., 1977, “Kontravariante Formen auf induzierten Darstellungen halbeinfacher Lie-Algebren,” *Math. Ann.* **226**, 53–65.
- Kadanoff, Leo P., 1969, “Operator Algebra and the Determination of Critical Indices,” *Phys. Rev. Lett.* **23**, 1430–1433.
- Kaplan, David B., Jong-Wan Lee, Dam T. Son, and Mikhail A. Stephanov, 2009, “Conformality Lost,” *Phys. Rev. D* **80**, 125005.
- Karateev, Denis, Petr Kravchuk, and David Simmons-Duffin, 2018, “Weight Shifting Operators and Conformal Blocks,” *J. High Energy Phys.* **02**, 081.
- Kastrup, H. A., 2008, “On the Advancements of Conformal Transformations and their Associated Symmetries in Geometry and Theoretical Physics,” *Ann. Phys. (Berlin)* **17**, 631–690.

- Katz, Emanuel, Subir Sachdev, Erik S. Sørensen, and William Witczak-Krempa, 2014, “Conformal field theories at nonzero temperature: Operator product expansions, Monte Carlo, and holography,” *Phys. Rev. B* **90**, 245109.
- Kaul, Ribhu K., and Subir Sachdev, 2008, “Quantum criticality of $U(1)$ gauge theories with fermionic and bosonic matter in two spatial dimensions,” *Phys. Rev. B* **77**, 155105.
- Kaviraj, Apratim, Kallol Sen, and Aninda Sinha, 2015a, “Analytic bootstrap at large spin,” *J. High Energy Phys.* **11**, 083.
- Kaviraj, Apratim, Kallol Sen, and Aninda Sinha, 2015b, “Universal anomalous dimensions at large spin and large twist,” *J. High Energy Phys.* **07**, 026.
- Kazakov, Vladimir, and Enrico Olivucci, 2018, “Bi-scalar integrable CFT at any dimension,” [arXiv:1801.09844](https://arxiv.org/abs/1801.09844).
- Keller, Christoph A., and Alexander Maloney, 2015, “Poincaré Series, 3D Gravity and CFT Spectroscopy,” *J. High Energy Phys.* **02**, 080.
- Keller, Christoph A., Gregoire Mathys, and Ida G. Zadeh, 2017, “Bootstrapping Chiral CFTs at Genus Two,” [arXiv:1705.05862](https://arxiv.org/abs/1705.05862).
- Khandker, Zuhair U., and Daliang Li, 2012, “Superembedding Formalism and Supertwistors,” [arXiv:1212.0242](https://arxiv.org/abs/1212.0242).
- Khandker, Zuhair U., Daliang Li, David Poland, and David Simmons-Duffin, 2014, “ $\mathcal{N} = 1$ superconformal blocks for general scalar operators,” *J. High Energy Phys.* **08**, 049.
- Kim, Hyungrok, Petr Kravchuk, and Hirosi Ooguri, 2016, “Reflections on Conformal Spectra,” *J. High Energy Phys.* **04**, 184.
- Klebanov, Igor R., Silviu S. Pufu, and Benjamin R. Safdi, 2011, “F-Theorem without Supersymmetry,” *J. High Energy Phys.* **10**, 038.
- Klinkhammer, G., 1991, “Averaged energy conditions for free scalar fields in flat space-times,” *Phys. Rev. D* **43**, 2542–2548.
- Knizhnik, V. G., and A. B. Zamolodchikov, 1984, “Current Algebra and Wess-Zumino Model in Two-Dimensions,” *Nucl. Phys. B* **247**, 83–103.
- Komargodski, Zohar, 2012, “The Constraints of Conformal Symmetry on RG Flows,” *J. High Energy Phys.* **07**, 069.
- Komargodski, Zohar, Manuela Kulaxizi, Andrei Parnachev, and Alexander Zhiboedov, 2017, “Conformal Field Theories and Deep Inelastic Scattering,” *Phys. Rev. D* **95**, 065011.
- Komargodski, Zohar, and Adam Schwimmer, 2011, “On Renormalization Group Flows in Four Dimensions,” *J. High Energy Phys.* **12**, 099.
- Komargodski, Zohar, Adar Sharon, Ryan Thorngren, and Xinan Zhou, 2017, “Comments on Abelian Higgs Models and Persistent Order,” [arXiv:1705.04786](https://arxiv.org/abs/1705.04786).
- Komargodski, Zohar, and David Simmons-Duffin, 2017, “The Random-Bond Ising Model in 2.01 and 3 Dimensions,” *J. Phys. A* **50**, 154001.
- Komargodski, Zohar, Tin Sulejmanpasic, and Mithat Ünsal, 2018, “Walls, anomalies, and deconfinement in quantum antiferromagnets,” *Phys. Rev. B* **97**, 054418.
- Komargodski, Zohar, and Alexander Zhiboedov, 2013, “Convexity and Liberation at Large Spin,” *J. High Energy Phys.* **11**, 140.
- Kos, Filip, David Poland, and David Simmons-Duffin, 2014a, “Bootstrapping Mixed Correlators in the 3D Ising Model,” *J. High Energy Phys.* **11**, 109.
- Kos, Filip, David Poland, and David Simmons-Duffin, 2014b, “Bootstrapping the $O(N)$ vector models,” *J. High Energy Phys.* **06**, 091.
- Kos, Filip, David Poland, David Simmons-Duffin, and Alessandro Vichi, 2015a, unpublished.
- Kos, Filip, David Poland, David Simmons-Duffin, and Alessandro Vichi, 2015b, “Bootstrapping the $O(N)$ Archipelago,” *J. High Energy Phys.* **11**, 106.
- Kos, Filip, David Poland, David Simmons-Duffin, and Alessandro Vichi, 2016, “Precision Islands in the Ising and $O(N)$ Models,” *J. High Energy Phys.* **08**, 036.
- Kraus, Per, Alexander Maloney, Henry Maxfield, Gim Seng Ng, and Jie-qiang Wu, 2017, “Witten Diagrams for Torus Conformal Blocks,” *J. High Energy Phys.* **09**, 149.
- Kravchuk, Petr, 2018, “Casimir recursion relations for general conformal blocks,” *J. High Energy Phys.* **02**, 011.
- Kravchuk, Petr, and David Simmons-Duffin, 2018a, “Counting Conformal Correlators,” *J. High Energy Phys.* **02**, 096.
- Kravchuk, Petr, and David Simmons-Duffin, 2018b, “Light-ray operators in conformal field theory,” [arXiv:1805.00098](https://arxiv.org/abs/1805.00098).
- Kulaxizi, Manuela, Andrei Parnachev, and Alexander Zhiboedov, 2017, “Bulk Phase Shift, CFT Regge Limit and Einstein Gravity,” [arXiv:1705.02934](https://arxiv.org/abs/1705.02934).
- Lang, K., and W. Ruhl, 1992, “The Critical $O(N)$ Sigma Model at Dimension $2 < D < 4$ and Order $1/N^2$: Operator Product Expansions and Renormalization,” *Nucl. Phys. B* **377**, 371–404.
- Lauria, Edoardo, Marco Meineri, and Emilio Trevisani, 2017, “Radial coordinates for defect CFTs,” [arXiv:1712.07668](https://arxiv.org/abs/1712.07668).
- LeClair, Andre, and Joshua Squires, 2018, “Conformal bootstrap for percolation and polymers,” [arXiv:1802.08911](https://arxiv.org/abs/1802.08911).
- Lee, Jong Yeon, Chong Wang, Michael P. Zaletel, Ashvin Vishwanath, and Yin-Chen He, 2018, “Emergent Multi-flavor QED3 at the Plateau Transition between Fractional Chern Insulators: Applications to graphene heterostructures,” [arXiv:1802.09538](https://arxiv.org/abs/1802.09538).
- Lee, Weon-Jong, and Stephen R. Sharpe, 1999, “Partial flavor symmetry restoration for chiral staggered fermions,” *Phys. Rev. D* **60**, 114503.
- Lemos, Madalena, and Pedro Liendo, 2016a, “Bootstrapping $\mathcal{N} = 2$ chiral correlators,” *J. High Energy Phys.* **01**, 025.
- Lemos, Madalena, and Pedro Liendo, 2016b, “ $\mathcal{N} = 2$ central charge bounds from 2d chiral algebras,” *J. High Energy Phys.* **04**, 004.
- Lemos, Madalena, Pedro Liendo, Marco Meineri, and Sourav Sarkar, 2017, “Universality at large transverse spin in defect CFT,” [arXiv:1712.08185](https://arxiv.org/abs/1712.08185).
- Lemos, Madalena, Pedro Liendo, Carlo Meneghelli, and Vladimir Mitev, 2017, “Bootstrapping $\mathcal{N} = 3$ superconformal theories,” *J. High Energy Phys.* **04**, 032.
- Lemos, Madalena, and Wolfgang Peelaers, 2015, “Chiral Algebras for Trinion Theories,” *J. High Energy Phys.* **02**, 113.
- Lencsés, Máté, and Fábio Novaes, 2017, “Classical Conformal Blocks and Accessory Parameters from Isomonodromic Deformations,” [arXiv:1709.03476](https://arxiv.org/abs/1709.03476).
- Levy, Tom, and Yaron Oz, 2018, “Liouville Conformal Field Theories in Higher Dimensions,” [arXiv:1804.02283](https://arxiv.org/abs/1804.02283).
- Li, Daliang, David Meltzer, and David Poland, 2016a, “Conformal Collider Physics from the Lightcone Bootstrap,” *J. High Energy Phys.* **02**, 143.
- Li, Daliang, David Meltzer, and David Poland, 2016b, “Non-Abelian Binding Energies from the Lightcone Bootstrap,” *J. High Energy Phys.* **02**, 149.
- Li, Daliang, David Meltzer, and David Poland, 2017, “Conformal Bootstrap in the Regge Limit,” *J. High Energy Phys.* **12**, 013.
- Li, Daliang, David Meltzer, and Andreas Stergiou, 2017, “Bootstrapping mixed correlators in 4D $\mathcal{N} = 1$ SCFTs,” *J. High Energy Phys.* **07**, 029.

- Li, Daliang, and Andreas Stergiou, 2014, “Two-point functions of conformal primary operators in $\mathcal{N} = 1$ superconformal theories,” *J. High Energy Phys.* **10**, 37.
- Li, Wenliang, 2017, “New method for the conformal bootstrap with OPE truncations,” [arXiv:1711.09075](#).
- Li, Wenliang, 2018, “Inverse Bootstrapping Conformal Field Theories,” *J. High Energy Phys.* **01**, 077.
- Li, Zhijin, 2018, “Superconformal Partial Waves for Stress-tensor Multiplet Correlator in 4D $\mathcal{N} = 2$ SCFTs,” [arXiv:1806.11550](#).
- Li, Zhijin, and Ning Su, 2016, “The Most General 4D $\mathcal{N} = 1$ Superconformal Blocks for Scalar Operators,” *J. High Energy Phys.* **05**, 163.
- Li, Zhijin, and Ning Su, 2017a, “3D CFT Archipelago from Single Correlator Bootstrap,” [arXiv:1706.06960](#).
- Li, Zhijin, and Ning Su, 2017b, “Bootstrapping Mixed Correlators in the Five Dimensional Critical O(N) Models,” *J. High Energy Phys.* **04**, 098.
- Li, Zi-Xiang, Abolhassan Vaezi, Christian B. Mendl, and Hong Yao, 2017, “Observation of Emergent Spacetime Supersymmetry at Superconducting Quantum Criticality,” [arXiv:1711.04772](#).
- Liendo, Pedro, 2017, “Revisiting the dilatation operator of the Wilson-Fisher fixed point,” *Nucl. Phys. B* **920**, 368–384.
- Liendo, Pedro, and Carlo Meneghelli, 2017, “Bootstrap equations for $\mathcal{N} = 4$ SYM with defects,” *J. High Energy Phys.* **01**, 122.
- Liendo, Pedro, Carlo Meneghelli, and Vladimir Mitev, 2017, “On Correlation Functions of BPS Operators in 3d $\mathcal{N} = 6$ Superconformal Theories,” *Commun. Math. Phys.* **350**, 387–419.
- Liendo, Pedro, Israel Ramirez, and Jihye Seo, 2016, “Stress-tensor OPE in $\mathcal{N} = 2$ superconformal theories,” *J. High Energy Phys.* **02**, 019.
- Liendo, Pedro, Leonardo Rastelli, and Balt C. van Rees, 2013, “The Bootstrap Program for Boundary CFT_d,” *J. High Energy Phys.* **07**, 113.
- Lin, Ying-Hsuan, Shu-Heng Shao, David Simmons-Duffin, Yifan Wang, and Xi Yin, 2017, “ $\mathcal{N} = 4$ superconformal bootstrap of the K3 CFT,” *J. High Energy Phys.* **05**, 126.
- Lin, Ying-Hsuan, Shu-Heng Shao, Yifan Wang, and Xi Yin, 2017, “(2, 2) superconformal bootstrap in two dimensions,” *J. High Energy Phys.* **05**, 112.
- Liu, Junyu, Eric Perlmutter, Vladimir Rosenhaus, and David Simmons-Duffin, 2018, “ d -dimensional SYK, AdS Loops, and 6j Symbols,” [arXiv:1808.00612](#).
- Luty, Markus A., and Takemichi Okui, 2006, “Conformal technicolor,” *J. High Energy Phys.* **09**, 070.
- Mack, G., 1977a, “All Unitary Ray Representations of the Conformal Group $SU(2, 2)$ with Positive Energy,” *Commun. Math. Phys.* **55**, 1.
- Mack, G., 1977b, “Convergence of Operator Product Expansions on the Vacuum in Conformal Invariant Quantum Field Theory,” *Commun. Math. Phys.* **53**, 155.
- Mack, G., 1977c, “Duality in Quantum Field Theory,” *Nucl. Phys. B* **118**, 445.
- Mack, G., and Abdus Salam, 1969, “Finite component field representations of the conformal group,” *Ann. Phys. (N.Y.)* **53**, 174–202.
- Mack, Gerhard, 2009, “D-independent representation of Conformal Field Theories in D dimensions via transformation to auxiliary Dual Resonance Models. Scalar amplitudes,” [arXiv:0907.2407](#).
- Maldacena, Juan, and Alexander Zhiboedov, 2013, “Constraining Conformal Field Theories with A Higher Spin Symmetry,” *J. Phys. A* **46**, 214011.
- Maloney, Alexander, Henry Maxfield, and Gim Seng Ng, 2017, “A conformal block Farey tail,” *J. High Energy Phys.* **06**, 117.
- Manenti, Andrea, Andreas Stergiou, and Alessandro Vichi, 2018, “R-current three-point functions in 4d $\mathcal{N} = 1$ superconformal theories,” [arXiv:1804.09717](#).
- Mazac, Dalimil, 2017, “Analytic bounds and emergence of AdS₂ physics from the conformal bootstrap,” *J. High Energy Phys.* **04**, 146.
- Mazac, Dalimil, and Miguel F. Paulos, 2018, “The Analytic Functional Bootstrap I: 1D CFTs and 2D S-Matrices,” [arXiv:1803.10233](#).
- Meltzer, David, and Eric Perlmutter, 2017, “Beyond $a = c$: Gravitational Couplings to Matter and the Stress Tensor OPE,” [arXiv:1712.04861](#).
- Metlitski, Max A., Michael Hermele, T. Senthil, and Matthew P. A. Fisher, 2008, “Monopoles in CP^{N-1} model via the state-operator correspondence,” *Phys. Rev. B* **78**, 214418.
- Migdal, Alexander A., 1971, “Conformal invariance and bootstrap,” *Phys. Lett. B* **37**, 386–388.
- Mihaila, Luminita N., Nikolai Zerf, Bernhard Ihrig, Igor F. Herbut, and Michael M. Scherer, 2017, “Gross-Neveu-Yukawa model at three loops and Ising critical behavior of Dirac systems,” *Phys. Rev. B* **96**, 165133.
- Minwalla, Shiraz, 1998, “Restrictions Imposed by Superconformal Invariance on Quantum Field Theories,” *Adv. Theor. Math. Phys.* **2**, 783.
- Monge, Gaspard, 1850, *Application de l’analyse à la géométrie* (Bachelier, Paris); see pp. 609–616 for Liouville’s theorem.
- Moon, Eun-Gook, Cenke Xu, Yong Baek Kim, and Leon Balents, 2013, “Non-Fermi liquid and topological states with strong spin-orbit coupling,” *Phys. Rev. Lett.* **111**, 206401.
- Moshe, Moshe, and Jean Zinn-Justin, 2003, “Quantum field theory in the large N limit: A Review,” *Phys. Rep.* **385**, 69–228.
- Murthy, Ganpathy, and Subir Sachdev, 1990, “Action of Hedgehog Instantons in the Disordered Phase of the (2 + 1)-dimensional CP^{N-1} Model,” *Nucl. Phys. B* **344**, 557–595.
- Nahum, Adam, J. T. Chalker, P. Serna, M. Ortúñoz, and A. M. Somoza, 2013, “Phase transitions in three-dimensional loop models and the CP^{n-1} sigma model,” *Phys. Rev. B* **88**, 134411.
- Nahum, Adam, J. T. Chalker, P. Serna, M. Ortúñoz, and A. M. Somoza, 2015, “Deconfined Quantum Criticality, Scaling Violations, and Classical Loop Models,” *Phys. Rev. X* **5**, 041048.
- Nahum, Adam, P. Serna, J. T. Chalker, M. Ortúñoz, and A. M. Somoza, 2015, “Emergent $SO(5)$ Symmetry at the Néel to Valence-Bond-Solid Transition,” *Phys. Rev. Lett.* **115**, 267203.
- Nakata, M., 2010, “A numerical evaluation of highly accurate multiple-precision arithmetic version of semidefinite programming solver: Sdpa-gmp, -qd and -dd,” in *IEEE International Symposium on Computer-Aided Control System Design (CACSD)* (IEEE, New York), pp. 29–34.
- Nakayama, Yu, 2015a, “Perturbative search for dead-end CFTs,” *J. High Energy Phys.* **05**, 046.
- Nakayama, Yu, 2015b, “Scale invariance vs conformal invariance,” *Phys. Rep.* **569**, 1–93.
- Nakayama, Yu, 2016a, private communication.
- Nakayama, Yu, 2016b, “Bootstrapping critical Ising model on three-dimensional real projective space,” *Phys. Rev. Lett.* **116**, 141602.
- Nakayama, Yu, 2016c, “Bootstrap bound for conformal multi-flavor QCD on lattice,” *J. High Energy Phys.* **07**, 038.
- Nakayama, Yu, 2017, “Bootstrap experiments on higher dimensional CFTs,” [arXiv:1705.02744](#).
- Nakayama, Yu, and Tomoki Ohtsuki, 2014a, “Approaching the conformal window of $O(n) \times O(m)$ symmetric Landau-Ginzburg models using the conformal bootstrap,” *Phys. Rev. D* **89**, 126009.

- Nakayama, Yu, and Tomoki Ohtsuki, 2014b, “Five dimensional $O(N)$ -symmetric CFTs from conformal bootstrap,” *Phys. Lett. B* **734**, 193–197.
- Nakayama, Yu, and Tomoki Ohtsuki, 2015, “Bootstrapping phase transitions in QCD and frustrated spin systems,” *Phys. Rev. D* **91**, 021901.
- Nakayama, Yu, and Tomoki Ohtsuki, 2016, “Necessary Condition for Emergent Symmetry from the Conformal Bootstrap,” *Phys. Rev. Lett.* **117**, 131601.
- Nash, Daniel, 1989, “Higher Order Corrections in (2+1)-Dimensional QED,” *Phys. Rev. Lett.* **62**, 3024.
- Nishida, Mitsuhiro, and Kotaro Tamaoka, 2017, “Geodesic Witten diagrams with an external spinning field,” *Prog. Theor. Exp. Phys.* **2017**, 053B06.
- Nishida, Yusuke, and Dam T. Son, 2007, “Nonrelativistic conformal field theories,” *Phys. Rev. D* **76**, 086004.
- Nishinaka, Takahiro, and Yuji Tachikawa, 2016, “On 4d rank-one $\mathcal{N} = 3$ superconformal field theories,” *J. High Energy Phys.* **09**, 116.
- Nogradi, Daniel, and Agostino Patella, 2016, “Strong dynamics, composite Higgs and the conformal window,” *Int. J. Mod. Phys. A* **31**, 1643003.
- Ohtsuki, Tomoki, 2016, “CBoot: A sage module to create (convolved) conformal block table,” <https://github.com/tohsky/cboot>.
- Onsager, Lars, 1944, “Crystal Statistics. I. A Two-Dimensional Model with an Order-Disorder Transition,” *Phys. Rev.* **65**, 117–149.
- Osborn, H., 1989, “Derivation of a Four-dimensional c Theorem,” *Phys. Lett. B* **222**, 97–102.
- Osborn, H., 2012, “Conformal Blocks for Arbitrary Spins in Two Dimensions,” *Phys. Lett. B* **718**, 169–172.
- Osborn, H., and A. C. Petkou, 1994, “Implications of conformal invariance in field theories for general dimensions,” *Ann. Phys. (N.Y.)* **231**, 311–362.
- Osborn, Hugh, 1999, “ $\mathcal{N} = 1$ superconformal symmetry in four-dimensional quantum field theory,” *Ann. Phys. (N.Y.)* **272**, 243–294.
- Osborn, Hugh, 2018, “Lectures on Conformal Field Theories in more than two dimensions,” lecture notes available online.
- Pal, Sridip, 2018, “Unitarity and Universality in non relativistic Conformal Field theory,” [arXiv:1802.02262](https://arxiv.org/abs/1802.02262).
- Pan, Yiwen, and Wolfgang Peelaers, 2018, “Chiral Algebras, Localization and Surface Defects,” *J. High Energy Phys.* **02**, 138.
- Pang, Yi, Junchen Rong, and Ning Su, 2016, “ ϕ^3 theory with F_4 flavor symmetry in $6 - 2\epsilon$ dimensions: 3-loop renormalization and conformal bootstrap,” *J. High Energy Phys.* **12**, 057.
- Pappadopulo, Duccio, Slava Rychkov, Johnny Espin, and Riccardo Rattazzi, 2012, “OPE Convergence in Conformal Field Theory,” *Phys. Rev. D* **86**, 105043.
- Parisen Toldin, Francesco, Martin Hohenadler, Fakher F. Assaad, and Igor F. Herbut, 2015, “Fermionic quantum criticality in honeycomb and π -flux Hubbard models: Finite-size scaling of renormalization-group-invariant observables from quantum Monte Carlo,” *Phys. Rev. B* **91**, 165108.
- Parisi, G., 1972, “On self-consistency conditions in conformal covariant field theory,” *Lett. Nuovo Cimento* **4**, 777–780.
- Paulos, Miguel, 2014a, “JuliBoots: A Julia-based package for performing numerical conformal bootstrap computations,” <https://github.com/mfpaulos/JuliBoots>.
- Paulos, Miguel F., 2014b, “JuliBootS: a hands-on guide to the conformal bootstrap,” [arXiv:1412.4127](https://arxiv.org/abs/1412.4127).
- Paulos, Miguel F., 2011, “Towards Feynman rules for Mellin amplitudes,” *J. High Energy Phys.* **10**, 074.
- Paulos, Miguel F., Joao Penedones, Jonathan Toledo, Balt C. van Rees, and Pedro Vieira, 2017, “The S-matrix bootstrap. Part I: QFT in AdS,” *J. High Energy Phys.* **11**, 133.
- Paulos, Miguel F., Slava Rychkov, Balt C. van Rees, and Bernardo Zan, 2016, “Conformal Invariance in the Long-Range Ising Model,” *Nucl. Phys. B* **902**, 246–291.
- Pelissetto, Andrea, Antonio Tripodo, and Ettore Vicari, 2018, “Criticality of $O(N)$ symmetric models in the presence of discrete gauge symmetries,” *Phys. Rev. E* **97**, 012123.
- Pelissetto, Andrea, and Ettore Vicari, 2002, “Critical phenomena and renormalization-group theory,” *Phys. Rep.* **368**, 549–727.
- Penedones, Joao, 2011, “Writing CFT correlation functions as AdS scattering amplitudes,” *J. High Energy Phys.* **03**, 025.
- Penedones, João, Emilio Trevisani, and Masahito Yamazaki, 2016, “Recursion Relations for Conformal Blocks,” *J. High Energy Phys.* **09**, 070.
- Peskin, Michael E., 1978, “Mandelstam ’t Hooft Duality in Abelian Lattice Models,” *Ann. Phys. (N.Y.)* **113**, 122.
- Petkou, Anastasios, 1996, “Conserved Currents, Consistency Relations, and Operator Product Expansions in the Conformally Invariant $O(N)$ Vector Model,” *Ann. Phys. (N.Y.)* **249**, 180–221.
- Picco, Marco, Sylvain Ribault, and Raoul Santachiara, 2016, “A conformal bootstrap approach to critical percolation in two dimensions,” *SciPost Phys.* **1**, 009.
- Poland, David, 2017, unpublished.
- Poland, David, and David Simmons-Duffin, 2011, “Bounds on 4D Conformal and Superconformal Field Theories,” *J. High Energy Phys.* **05**, 017.
- Poland, David, and David Simmons-Duffin, 2016, “The conformal bootstrap,” *Nat. Phys.* **12**, 535–539.
- Poland, David, David Simmons-Duffin, and Alessandro Vichi, 2012, “Carving Out the Space of 4D CFTs,” *J. High Energy Phys.* **05**, 110.
- Poland, David, and Andreas Stergiou, 2015, “Exploring the Minimal 4D $\mathcal{N} = 1$ SCFT,” *J. High Energy Phys.* **12**, 121.
- Polchinski, Joseph, 1988, “Scale and Conformal Invariance in Quantum Field Theory,” *Nucl. Phys. B* **303**, 226.
- Polyakov, A. M., 1974, “Nonhamiltonian approach to conformal quantum field theory,” *Zh. Eksp. Teor. Fiz.* **66**, 23–42 [Sov. Phys. JETP **39**, 10–18 (1974), http://www.jetp.ac.ru/cgi-bin/dn/e_039_01_0010.pdf].
- Polyakov, Alexander M., 1970, “Conformal symmetry of critical fluctuations,” *JETP Lett.* **12**, 381–383 [http://www.jetletters.ac.ru/ps/1737/article_26381.pdf].
- Ponte, Pedro, and Sung-Sik Lee, 2014, “Emergence of supersymmetry on the surface of three dimensional topological insulators,” *New J. Phys.* **16**, 013044.
- Qin, Yan Qi, Yuan-Yao He, Yi-Zhuang You, Zhong-Yi Lu, Arnab Sen, Anders W. Sandvik, Cenke Xu, and Zi Yang Meng, 2017, “Duality between the deconfined quantum-critical point and the bosonic topological transition,” *Phys. Rev. X* **7**, 031052.
- Qualls, Joshua D., 2015a, “Lectures on Conformal Field Theory,” [arXiv:1511.04074](https://arxiv.org/abs/1511.04074).
- Qualls, Joshua D., 2015b, “Universal Bounds on Operator Dimensions in General 2D Conformal Field Theories,” [arXiv:1508.00548](https://arxiv.org/abs/1508.00548).
- Qualls, Joshua D., 2015c, “Universal Bounds in Even-Spin CFTs,” *J. High Energy Phys.* **12**, 001.
- Qualls, Joshua D., and Alfred D. Shapere, 2014, “Bounds on Operator Dimensions in 2D Conformal Field Theories,” *J. High Energy Phys.* **05**, 091.
- Raju, Avinash, 2016, “ ϵ -Expansion in the Gross-Neveu CFT,” *J. High Energy Phys.* **10**, 097.
- Ramírez, Israel A., 2016, “Mixed OPEs in $\mathcal{N} = 2$ superconformal theories,” *J. High Energy Phys.* **05**, 043.

- Rastelli, Leonardo, and Xian Zhou, 2017, “The Mellin Formalism for Boundary CFT_d,” *J. High Energy Phys.* **10**, 146.
- Rattazzi, Riccardo, Slava Rychkov, and Alessandro Vichi, 2011a, “Bounds in 4D Conformal Field Theories with Global Symmetry,” *J. Phys. A* **44**, 035402.
- Rattazzi, Riccardo, Slava Rychkov, and Alessandro Vichi, 2011b, “Central Charge Bounds in 4D Conformal Field Theory,” *Phys. Rev. D* **83**, 046011.
- Rattazzi, Riccardo, Vyacheslav S. Rychkov, Erik Tonni, and Alessandro Vichi, 2008, “Bounding scalar operator dimensions in 4D CFT,” *J. High Energy Phys.* **12**, 031.
- Read, N., and Subir Sachdev, 1990, “Spin-peierls, valence-bond solid, and n  l   ground states of low-dimensional quantum antiferromagnets,” *Phys. Rev. B* **42**, 4568–4589.
- Reemtsen, Rembert, and Stephan G  rner, 1998, “Numerical methods for semi-infinite programming: A survey,” in *Semi-Infinite Programming*, edited by Rembert Reemtsen and Jan-J. R  ckmann (Springer, New York), pp. 195–275.
- Rejon-Barrera, Fernando, and Daniel Robbins, 2016, “Scalar-Vector Bootstrap,” *J. High Energy Phys.* **01**, 139.
- Riva, Valentina, and John L. Cardy, 2005, “Scale and conformal invariance in field theory: A Physical counterexample,” *Phys. Lett. B* **622**, 339–342.
- Rong, Junchen, and Ning Su, 2017, “Scalar CFTs and Their Large N Limits,” [arXiv:1712.00985](https://arxiv.org/abs/1712.00985).
- Rong, Junchen, and Ning Su, 2018, “Bootstrapping minimal $\mathcal{N}=1$ superconformal field theory in three dimensions,” [arXiv:1807.04434](https://arxiv.org/abs/1807.04434).
- Roumpedakis, Konstantinos, 2016, “Leading Order Anomalous Dimensions at the Wilson-Fisher Fixed Point from CFT,” [arXiv:1612.08115](https://arxiv.org/abs/1612.08115).
- Rychkov, Slava, 2011, “Is Conformal Technicolor Plausible?,” Talk at Planck 2011.
- Rychkov, Slava, 2016a, “Conformal bootstrap,” *Lectures at the 10th Asian Winter School on Strings, Particles and Cosmology* (OIST, Okinawa).
- Rychkov, Slava, 2016b, “EPFL Lectures on Conformal Field Theory in $D \geq 3$ Dimensions,” SpringerBriefs in Physics, [arXiv:1601.05000](https://arxiv.org/abs/1601.05000).
- Rychkov, Slava, David Simmons-Duffin, and Bernardo Zan, 2017, “Non-gaussianity of the critical 3d Ising model,” *SciPost Phys.* **2**, 001.
- Rychkov, Slava, and Zhong Ming Tan, 2015, “The ϵ -expansion from conformal field theory,” *J. Phys. A* **48**, 29FT01.
- Rychkov, Slava, and Pierre Yvernay, 2016, “Remarks on the Convergence Properties of the Conformal Block Expansion,” *Phys. Lett. B* **753**, 682–686.
- Rychkov, Vyacheslav S., and Alessandro Vichi, 2009, “Universal Constraints on Conformal Operator Dimensions,” *Phys. Rev. D* **80**, 045006.
- Ryttov, Thomas A., and Robert Shrock, 2017, “Higher-order scheme-independent series expansions of $\gamma_{\bar{\psi}\psi,IR}$ and β'_{IR} in conformal field theories,” *Phys. Rev. D* **95**, 105004.
- Sachdev, S., 2004, “Quantum Phases and Phase Transitions of Mott Insulators,” in *Quantum Magnetism*, Lecture Notes in Physics (Springer-Verlag, Berlin), Vol. 645, p. 381.
- Sachdev, Subir, 2010, “The landscape of the Hubbard model,” in *Proceedings, Theoretical Advanced Study Institute in Elementary Particle Physics (TASI 2010). String Theory and Its Applications: From meV to the Planck Scale* (World Scientific, Singapore), pp. 559–620.
- Schomerus, Volker, and Evgeny Sobko, 2018, “From Spinning Conformal Blocks to Matrix Calogero-Sutherland Models,” *J. High Energy Phys.* **04**, 052.
- Schomerus, Volker, Evgeny Sobko, and Mikhail Isachenkov, 2017, “Harmony of Spinning Conformal Blocks,” *J. High Energy Phys.* **03**, 085.
- Seiberg, N., 1995, “Electric—magnetic duality in supersymmetric nonAbelian gauge theories,” *Nucl. Phys. B* **435**, 129–146.
- Seiberg, Nathan, T. Senthil, Chong Wang, and Edward Witten, 2016, “A Duality Web in 2+1 Dimensions and Condensed Matter Physics,” *Ann. Phys. (Amsterdam)* **374**, 395–433.
- Sen, Kallol, and Aninda Sinha, 2016, “On critical exponents without Feynman diagrams,” *J. Phys. A* **49**, 445401.
- Senthil, T., Leon Balents, Subir Sachdev, Ashvin Vishwanath, and Matthew P. A. Fisher, 2004, “Quantum criticality beyond the Landau-Ginzburg-Wilson paradigm,” *Phys. Rev. B* **70**, 144407.
- Shimada, Hirohiko, and Shinobu Hikami, 2016, “Fractal dimensions of self-avoiding walks and Ising high-temperature graphs in 3D conformal bootstrap,” *J. Stat. Phys.* **165**, 1006.
- Siegel, W., 2012, “Embedding versus 6D twistors,” [arXiv:1204.5679](https://arxiv.org/abs/1204.5679).
- Simmons-Duffin, David, 2014a, “Projectors, Shadows, and Conformal Blocks,” *J. High Energy Phys.* **04**, 146.
- Simmons-Duffin, David, 2014b, “SIPSSolver: A semi-infinite program solver based on a custom simplex method,” <https://gitlab.com/bootstrapcollaboration/SIPSSolver>.
- Simmons-Duffin, David, 2015a, “A Semidefinite Program Solver for the Conformal Bootstrap,” *J. High Energy Phys.* **06**, 174.
- Simmons-Duffin, David, 2015b, “Blocks-Recursion.m: Mathematica code for generating tables of derivatives of conformal blocks,” [https://gitlab.com/bootstrapcollaboration\(blocks-mathematica](https://gitlab.com/bootstrapcollaboration(blocks-mathematica).
- Simmons-Duffin, David, 2016a, <https://gitlab.com/bootstrapcollaboration/spectrum-extraction>.
- Simmons-Duffin, David, 2016b, private communication.
- Simmons-Duffin, David, 2017a, private communication.
- Simmons-Duffin, David, 2017b, “The Conformal Bootstrap,” in *Proceedings, Theoretical Advanced Study Institute in Elementary Particle Physics: New Frontiers in Fields and Strings (TASI 2015)* (World Scientific, Singapore), pp. 1–74.
- Simmons-Duffin, David, 2017c, “The Lightcone Bootstrap and the Spectrum of the 3d Ising CFT,” *J. High Energy Phys.* **03**, 086.
- Simmons-Duffin, David, Douglas Stanford, and Edward Witten, 2017, “A spacetime derivation of the Lorentzian OPE inversion formula,” [arXiv:1711.03816](https://arxiv.org/abs/1711.03816).
- Sleight, Charlotte, and Massimo Taronna, 2018a, “A Note on Anomalous Dimensions from Crossing Kernels,” [arXiv:1807.05941](https://arxiv.org/abs/1807.05941).
- Sleight, Charlotte, and Massimo Taronna, 2018b, “Spinning Mellin Bootstrap: Conformal Partial Waves, Crossing Kernels and Applications,” [arXiv:1804.09334](https://arxiv.org/abs/1804.09334).
- Sleight, Charlotte, and Massimo Taronna, 2017, “Spinning Witten Diagrams,” *J. High Energy Phys.* **06**, 100.
- Smoluchowski, Marian, 1908, “Molekular-kinetische Theorie der Opaleszenz von Gasen im kritischen Zustande, sowie einiger verwandter Erscheinungen,” *Ann. Phys. (Berlin)* **330**, 205–226.
- Song, Jaewon, 2017, “Macdonald Index and Chiral Algebra,” *J. High Energy Phys.* **08**, 044.
- Sreejith, G. J., Stephen Powell, and Adam Nahum, 2018, “Emergent $SO(5)$ symmetry at the columnar ordering transition in the classical cubic dimer model,” [arXiv:1803.11218](https://arxiv.org/abs/1803.11218).
- Stergiou, Andreas, 2017, private communication.
- Stergiou, Andreas, 2018, “Bootstrapping hypercubic and hyper-tetrahedral theories in three dimensions,” [arXiv:1801.07127](https://arxiv.org/abs/1801.07127).
- Svetitsky, Benjamin, 2018, “Looking behind the Standard Model with lattice gauge theory,” *EPJ Web Conf.* **175**, 01017.
- Tamaoka, Kotaro, 2017, “Geodesic Witten diagrams with antisymmetric tensor exchange,” *Phys. Rev. D* **96**, 086007.

- van Loon, Mark, 2018, “The Analytic Bootstrap in Fermionic CFTs,” *J. High Energy Phys.* **01**, 104.
- Vicari, Ettore, 2007, “Critical phenomena and renormalization-group flow of multi-parameter Φ^4 field theories,” in Proceedings of the 25th International Symposium on Lattice field theory (Lattice 2007), *Proc. Sci.*, LATTICE2007, 023.
- Vichi, Alessandro, 2011, “A New Method to Explore Conformal Field Theories in Any Dimension,” Ph.D. thesis (EPFL, Lausanne, LPPC).
- Vichi, Alessandro, 2012, “Improved bounds for CFT’s with global symmetries,” *J. High Energy Phys.* **01**, 162.
- Vojta, Matthias, 2003, “Quantum phase transitions,” *Rep. Prog. Phys.* **66**, 2069.
- Vojta, Matthias, Ying Zhang, and Subir Sachdev, 2000, “Quantum Phase Transitions in d-Wave Superconductors,” *Phys. Rev. Lett.* **85**, 4940–4943.
- Wang, Chong, Adam Nahum, Max A. Metlitski, Cenke Xu, and T. Senthil, 2017, “Deconfined quantum critical points: symmetries and dualities,” *Phys. Rev. X* **7**, 031051.
- Weinberg, Steven, 2010, “Six-dimensional Methods for Four-dimensional Conformal Field Theories,” *Phys. Rev. D* **82**, 045031.
- Weinberg, Steven, and Edward Witten, 1980, “Limits on Massless Particles,” *Phys. Lett. B* **96**, 59–62.
- Wilson, K. G., 1983, “The renormalization group and critical phenomena,” *Rev. Mod. Phys.* **55**, 583–600.
- Wilson, K. G., and John B. Kogut, 1974, “The Renormalization group and the epsilon expansion,” *Phys. Rep.* **12**, 75–200.
- Wilson, Kenneth G., 1969, “Nonlagrangian models of current algebra,” *Phys. Rev.* **179**, 1499–1512.
- Wilson, Kenneth G., and Michael E. Fisher, 1972, “Critical exponents in 3.99 dimensions,” *Phys. Rev. Lett.* **28**, 240–243.
- Witczak-Krempa, William, 2015, “Constraining Quantum Critical Dynamics: (2 + 1)D Ising Model and Beyond,” *Phys. Rev. Lett.* **114**, 177201.
- Xie, Dan, Wenbin Yan, and Shing-Tung Yau, 2016, “Chiral algebra of Argyres-Douglas theory from M5 brane,” [arXiv:1604.02155](https://arxiv.org/abs/1604.02155).
- Xie, Dan, and Kazuya Yonekura, 2016, “Search for a Minimal $N = 1$ Superconformal Field Theory in 4D,” *Phys. Rev. Lett.* **117**, 011604.
- Yamashita, M., K. Fujisawa, M. Fukuda, K. Nakata, and M. Nakata, 2010, “A high-performance software package for semidefinite programs: SDPA 7,” Research Report B-463, Dept. of Mathematical and Computing, Science, Tokyo Institute of Technology, Tokyo, Japan.
- Yamazaki, Masahito, 2016, “Comments on Determinant Formulas for General CFTs,” *J. High Energy Phys.* **10**, 035.
- Yin, Xi, 2017, “Aspects of Two-Dimensional Conformal Field Theories,” in *Proceedings of Theoretical Advanced Study Institute Summer School (TASI 2017) “Physics at the Fundamental Frontier* [<https://pos.sissa.it/305/>].
- Zamolodchikov, A. B., 1986, “Irreversibility of the Flux of the Renormalization Group in a 2D Field Theory,” *JETP Lett.* **43**, 730–732 [http://www.jetpletters.ac.ru/ps/1413/article_21504.pdf].
- Zamolodchikov, Al B., 1984, “Conformal Symmetry in Two-Dimensions: an Explicit Recurrence Formula for the Conformal Partial Wave Amplitude,” *Commun. Math. Phys.* **96**, 419–422.
- Zamolodchikov, Al B., 1987, “Conformal symmetry in two-dimensional space: Recursion representation of conformal block,” *Theor. Math. Phys.* **73**, 1088–1093.
- Zerf, Nikolai, Luminita N. Mihaila, Peter Marquard, Igor F. Herbut, and Michael M. Scherer, 2017, “Four-loop critical exponents for the Gross-Neveu-Yukawa models,” *Phys. Rev. D* **96**, 096010.